Phenotypic Consequences of Mutations in Homologous Recombination Repair Genes in Colorectal Cancer Cells

A thesis submitted to the University of Sheffield for the degree of Doctor of Philosophy

Jennifer Susan Scorah

Institute for Cancer Studies

University of Sheffield Medical School

October 2003

I hereby declare that no part of this thesis has previously been submitted for any degree or qualification of this, or any other, University or Institute of learning.

Acknowledgements

I wish to thank my supervisor Mark Meuth and my advisor Simon Cross for guidance and inspiration throughout my PhD. I am indebted to Anil Ganesh, Dave Hammond and Angie Cox for the discussions and patient explanations that have pointed me in the right direction along the way. I am additionally grateful to Yorkshire Cancer Research and MWG Biotech for funding this study.

I would like to thank all the technicians at I.C.S, not only for their help in the lab but also for the cryptic crosswords and tearoom chats that have helped keep me sane!

Of course, this PhD would not have been possible without my wonderful family and fantastic husband, Nick. I sincerely appreciate their continued support and encouragement.

Summary

The DNA damage response is important for maintaining genomic integrity following introduction of double-strand breaks (DSB) since illegitimate or incorrect repair of a DSB could promote malignant transformation. Mismatch-repair (MMR) deficient tumour cell lines are acutely sensitive to thymidine treatment and fail to activate homologous recombination (HR) repair following a DSB (Mohindra et al., 2002). Therefore, it was hypothesised that loss of HR repair may occur as a downstream event in tumours already deficient in MMR. The primary aim was to determine whether there were somatic mutations in candidate HR genes that were associated with colorectal cancer development and to examine the phenotypic consequences of such mutations.

Analysis of the candidate HR genes, *XRCC2*, *XRCC3* and *Mus81* in a random collection of primary colorectal cancers and in a specific MMR-deficient tumour population revealed no tumour-specific mutations.

Analysis of the *MRE11*, *NBS1* and *Rad50* genes revealed a frameshift mutation in an intronic T_{11} tract of *MRE11* that gave rise to alternative splicing of the gene. This mutation was present in >85% of MSI^+ colorectal tumours suggesting that alteration of *MRE11* occurs at a high frequency in tumours already deficient in MMR.

The phenotypic consequences of MRE11 dysfunction were investigated by expressing splice variants of MRE11 in MMR-proficient human cells. Cells expressing an MRE11 variant with a compromised nuclease domain, failed to activate wild-type MRE11 following DNA damage, were dramatically more sensitive to thymidine and failed to activate HR repair following thymidine treatment.

The novel results obtained here suggest that a functional MRE11 is essential for the HR repair-mediated rescue of DNA replication forks impaired by thymidine. Furthermore, it was speculated that a functional MRE11 may be essential to resolve the recombinogenic substrate specifically produced by thymidine. Given that this DNA damage response pathway appears to be disrupted in >85% of MSI^+ colorectal tumours, these finding have important implications for treatment strategies directed against this subset of tumours.

Abbreviations

aa	Amino Acid
APC	Adenomatous Polyposis Coli
APS	Ammonium Persulphate
ATP	Adenosine Triphosphate
ATPase	Adenosine Triphosphotase
A-T	Ataxia-Telangiectasia
A-TLD	Ataxia-Telangiectasia Like Disorder
ATM	Ataxia-Telangiectasia Mutated
ATR	ATM and Rad3 Related
BASC	BRCA1-Associated Genome Surveillance Complex
BCDX2	Rad51B- Rad51C- Rad51D-XRCC2 Complex
bp	Base Pair
BRCA1	Breast Cancer Associated 1
BRCT	BRCA1 Carboxy-Terminal Domain
BSA	Bovine Serum Albumin
CHO	Chinese Hamster Ovary
CRC	Colorectal Cancer
CPT	Camptothecin
Da	Daltons
dATP	Deoxyadenosine Triphosphate
dCTP	Deoxycytidine Triphosphate
dGTP	Deoxyguanosine Triphosphate
dTTP	Deoxythymidine Triphosphate
dNTP	Deoxynucleotide Triphosphate
ddNTP	Dideoxynucleotide Triphosphate
DMEM	Dulbecco's Modified Eagle Medium
DMSO	Dimethyl Sulphoxide
DNA	Deoxyribonucleic acid
cDNA	Complementary DNA
dsDNA	Double-Strand DNA
ssDNA	Single-Strand DNA
DSB	Double-Strand Break

E. coli	*Escherichia coli*
EDTA	Ethylene Diamine Tetra-acetic Acid
FAP	Familial Adenomatous Polyposis
FHA	Forkhead Associated Domain
G_1	Gap Phase 1
G_2	Gap Phase 2
GFP	Green Fluorescent Protein
HJ	Holliday Junction
HNPCC	Hereditary Non-Polyposis Colorectal Cancer
HR	Homologous Recombination
HU	Hydroxyurea
IR	Ionising Radiation
IRD	Infrared Dye
kb	Kilobase
kDa	Kilo-Dalton
LOH	Loss of Heterozygosity
M-phase	Mitosis Phase
MMC	Mitomycin C
MMR	Mismatch Repair
MRE11	Meiotic Recombination 11 Homologue A (*S.cerevisiae*)
MSI	Microsatellite Instability
MSI-H	High Microsatellite Instability
MSI-L	Low Microsatellite Instability
MSS	Microsatellite Stable
NBS	Nijmegen Breakage Syndrome
neo	Neomycin Phosphotransferase
NHEJ	Non-Homologous End-Joining
nt	Nucleotide
PAGE	Polyacrylamide Gel Electrophoresis
PBS	Phosphate Buffered Saline
PCNA	Proliferating Cell Nuclear Antigen
PCR	Polymerase Chain Reaction
PFGE	Pulsed Field Gel Electrophoresis
PIKK	Phosphatidyl-inositol-3-kinase-like Protein Kinase

PMSF	Phenyl Methyl Sulphonyl Fluoride
RDS	Radio-resistant DNA Synthesis
RNA	Ribonucleic Acid
RNase	Ribonuclease
mRNA	Messenger RNA
RTase	Reverse transcriptase
RT-PCR	Reverse-transcription PCR
S-phase	DNA Synthesis Phase
S. cerevisiae	*Saccharomyces cerevisiae*
SMC	Structural Maintenance of Chromosomes
S. pombe	*Saccharomyces pombe*
SSCP	Single-strand Conformation Polymorphism
TdR	Thymidine
TEMED	N,N,N′,N′ Tetramethylethylenediamine
TGFβRII	Transforming Growth Factor β Receptor II
SDS	Sodium Dodecyl Sulphate
v/v	Volume:Volume Ratio
w/v	Weight:Volume Ratio
UV	Ultraviolet
XRCC2	X-ray Cross-Complementing 2
XRCC3	X-ray Cross-Complementing 3

Amino Acid Abbreviations:

3 letter code	*1 letter code*	*Amino Acid*
Ala	A	Alanine
Arg	R	Arginine
Asp	D	Aspartic Acid
Asn	N	Asparagine
Cys	C	Cysteine
Gln	Q	Glutamine
Glu	E	Glutamic Acid
Gly	G	Glycine
His	H	Histidine
Iso	I	Isoleucine
Leu	L	Leucine
Lys	K	Lysine
Met	M	Methionine
Phe	F	Phenylalanine
Pro	P	Proline
Ser	S	Serine
Thr	T	Threonine
Trp	W	Tryptophan
Tyr	Y	Tyrosine
Val	V	Valine

CONTENTS

CHAPTER 1

Introduction

1.1 Colorectal Cancer

The colon is divided into the cecum and the ascending, transverse, descending and sigmoid colon. The colon and rectum are host to more primary neoplasms than any other organ of the body (Cotran et al., 1999). Colorectal cancers (CRC) are usually adenocarcinoma and the lifetime risk to the general population is 6% (McCormick et al., 2002). One of the risk factors for CRC is increasing age with the peak incidence of CRC being 60-79 years of age and less than 20% of all cases occurring before age 50 (Cotran et al., 1999, McCormick et al., 2002). Other risk factors include family history, a high fat, low fibre diet, physical inactivity and long standing inflammatory bowel disease (Price, 2002).

Up to 15% of all CRCs are inherited in an autosomal dominant manner (Kinzler and Vogelstein, 1996). The two best defined familial forms are familial adenomatous polyposis (FAP) and hereditary non-polyposis colorectal cancer (HNPCC). Patients with FAP develop multiple benign colonic adenomas at an early age and malignant progression of these polyps usually occurs by age 40-50 (Lynch and de la Chapelle, 2003). FAP is caused by truncating germ-line mutations of the adenomatous polyposis coli (*APC*) gene, located on chromosome 5q21 and penetrance of FAP approaches 100% (Lynch and de la Chapelle, 2003). HNPCC is associated with an 80% lifetime risk of CRC that develops at an average age of 45 years (Aaltonen et al., 1998). The majority of cancers in HNPCC develop on the right-side of the colon, are poorly differentiated, mucinous and primarily show a diploid karyotype (Cotran et al., 1999, Chung, 2000, Burt, 2000). HNPCC accounts for only 1-3% of all colorectal cancers and is also commonly associated with endometrial, gastric and ovarian cancers (Burt, 2000, Chung and Rustgi, 2003).

CRC can remain asymptomatic for years and diagnosis then only occurs at late stage where prognosis is grave. When the disease is diagnosed at an early stage the 5-year

survival rate is estimated to be >90% whereas CRC diagnosed at late stages when metastases are present has a 5-year survival rate of only 7-9% (Burt, 2000, McCormick et al., 2002). For this reason it is important to identify new tumour markers for the molecular staging and therapy of colorectal cancer.

The accumulation of multiple mutations is necessary for colorectal cancer development and it was proposed that each mutation drives the malignant process (Vogelstein and Kinzler, 1993). However, the mutation rate in normal human cells, even after exposure to carcinogens, may not be sufficient to account for these multiple alterations. It was therefore proposed that an early step in tumour progression is one that induces a "mutator" phenotype (Loeb, 1991). Mechanisms that maintain genomic integrity, such as high fidelity DNA replication and various processes that recognise and repair DNA damage or eliminate damaged cells, are highly conserved in normal cells (Coleman and Tsongalis, 1999). A mutator phenotype could be caused by loss of one or more of these mechanisms that preserve genomic integrity. Evidence to support this hypothesis arose from studies of HNPCC where the underlying molecular defect was defined as a mismatch-repair (MMR) deficiency (Kinzler and Vogelstein, 1996).

1.2 Mismatch Repair (MMR)

Studies of the bacterial and yeast mismatch repair genes provided clues as to how the analogous human MMR system functions (Miller, 1998, Kolodner, 1995, Fishel and Kolodner, 1995). The human MMR proteins involved in mitotic processes include hMLH1, hMSH2, hMSH3, hMSH6, hPMS1 and hPMS2. These MMR proteins function to repair post-replicative DNA damage and to inhibit recombination between divergent sequences (Toft and Arends, 1998).

hMSH2, in a heterodimeric complex with either hMSH6 or hMSH3, recognises and binds directly to mismatched DNA (Acharya et al., 1996). The hMSH2-hMSH6 complex binds base-pair mismatches and small insertion/deletion loops created by primer-template slippage whereas hMSH2-hMSH3 binds only these insertion/deletion loops in the DNA (Raschle et al., 1999). The redundancy between hMSH3 and hMSH6 is reflected in yeast studies where msh3 and msh6 must both be mutated to demonstrate the same repair defect as an msh2 single mutant (Acharya et al., 1996). A second heterodimeric complex of hMLH1 and hPMS2 is then thought to be recruited to the mismatch to coordinate the interplay between the mismatch recognition complex and other proteins necessary for excision of the mismatched DNA (Kolodner, 1995, Chung and Rustgi, 2003). hMLH1 can also form a complex with hMLH3 and hPMS1 but the function of these heterodimers is currently unknown (Raschle et al., 1999).

In addition to its functions in DNA repair and recombination the MMR system may also have role in the DNA damage response as these proteins form part of the BRCA1-associated genome surveillance complex (BASC) that recognises DNA damage (Wang et al., 2000).

Loss of post-replicative MMR was found to increase mutation rates 200- to 600-fold above normal levels and therefore induce a mutator phenotype (Bhattacharyya et al., 1994). This mutator phenotype becomes most apparent in repetitive elements throughout the genome known as microsatellites. These iterative loci are normally relatively stable but DNA polymerase is prone to slip on these elements during replication. The resulting small loops in the template or nascent strand are usually repaired by the MMR system (Fishel and Kolodner, 1995). In MMR-deficient cells the loops persist and alleles of different sizes are produced in subsequent rounds of replication. This phenomenon is known as microsatellite instability (MSI) and is

defined as a change in length in a microsatellite due to the insertion or deletion of repeating units, within tumour DNA compared to normal DNA (Boland et al., 1998). The classification of tumours according to MSI status is important as it may enhance prognostic information since CRC prognosis is correlated with MSI (Chung and Rustgi, 2003) and it might also define distinct subsets of tumours that respond better to specific types of therapy.

The increased genetic instability caused by loss of MMR can promote tumour development and mutations in the two main MMR genes, *hMLH1* and *hMSH2*, are present in almost 90% of HNPCC cases (Burt, 2000, Lynch and de la Chapelle, 2003). MMR deficiency has also been shown to be associated with sporadic colorectal, endometrial and gastric cancer (Liu et al., 1995, Fornasarig et al., 2000, Umar et al., 1994, Fleisher et al., 1999). However, sporadic and hereditary MMR-deficient CRCs develop through different molecular pathways as the majority of sporadic MSI^+ tumours do not have mutations in the MMR genes (Katabuchi et al., 1995, Umar et al., 1994). Epigenetic changes primarily cause MMR-deficiency in sporadic tumours as over 80% of sporadic MSI^+ CRC have *hMLH1* promoter hypermethylation which acts to silence the gene by decreasing transcription and ultimately reducing hMLH1 protein expression (Leunig et al., 1999, Kane et al., 1997, Chung, 2000, Veigl et al., 1998).

Loss of MMR alone is not sufficient for malignant transformation and is likely to be an early event in tumour development that is essential for the sequential mutations that drive the neoplastic processes (Lengauer et al., 1998). Genes that function to protect genomic integrity, such as the MMR genes, were collectively labelled as 'caretaker genes' and it was proposed that mutation of such caretakers does not directly promote tumour initiation (Kinzler and Vogelstein, 1997). Instead, inactivation of the MMR

caretakers promotes microsatellite instability which means all mononucleotide runs, including those in coding regions, become hotspots for mutation (Jiricny, 1996, Baross-Francis et al., 1998, Bhattacharyya et al., 1994).

Growth controlling genes with repetitive coding elements are known to be mutated in MSI^+ CRC. TGFβ*RII* has an A_{10} mononucleotide run that is mutated in up to 83% of HNPCC cases and up to 90% of sporadic MSI^+ CRC (Chung, 2000). TGFβ inhibits growth of multiple epithelial cell types and loss of this negative regulation is thought to contribute to tumour development (Markowitz et al., 1995). One of the mechanisms by which human CRC cells lose responsiveness to TGFβ is by inactivation of the TGFβ*RII* receptor.

Other coding mononucleotide runs that are frequently mutated in MSI^+ CRC are the G_8 tract of the apoptosis regulator BAX, the G_8 run of the IGF2R growth factor and the A_8 and C_8 runs of MSH3 and MSH6, respectively. Further mutation of the MMR genes may act as a positive feedback loop to enhance the MSI phenotype and thereby promote the acquisition of more traits that increase the likelihood of tumour progression (Chung, 2000). Mutations in repetitive elements of the DNA repair genes ATR, Chk1 and Cdc25C have also been detected in MSI^+ but not MSS endometrial cancers (Vassileva et al., 2002). However, whilst this analysis suggests that certain genes might be more susceptible to alterations in MSI^+ rather than MSS cells, the majority of these mutations are heterozygous and it is not clear whether they contribute to tumour development. Further investigation is needed to establish whether mutations in genes involved in key cellular pathways, such as cell-cycle checkpoints and DNA repair, contribute to tumour progression in MMR-deficient cells.

1.3 The DNA Damage Response

The DNA damage response includes triggering checkpoints that slow or arrest cell-cycle progression to allow time for repair, changing chromatin structure at the site of damage and the recruitment and activation of various proteins involved in DNA repair (Rouse and Jackson, 2002). All of these processes are essential for maintaining genomic stability and cellular viability following DNA damage. In humans, defects in many of the DNA damage responses are generally associated with cancer predisposition (Hoeijmakers, 2001, Jackson, 2002).

Of the many types of DNA damage that can occur in the cell probably the most dangerous are DNA double-strand breaks (DSB) that occur spontaneously or are induced by DNA damaging agents (Khanna and Jackson, 2001).

As few as four DSBs appear to be sufficient to activate the checkpoint signalling cascade and repair mechanisms (Bakkenist and Kastan, 2003), showing that DNA damage responses are extremely sensitive and must efficiently amplify the initial stimulus (D'Amours and Jackson, 2002).

A member of the phosphatidyl-inositol-3-kinase-like protein kinase (PIKK) family, ATM (Ataxia-Telangiectasia Mutated) is a component of the cell signalling pathway that responds primarily to DSBs (Rouse and Jackson, 2002). Once a DSB has been sensed the signal is transduced through ATM to downstream effectors to induce cell-cycle arrest, DNA repair and in some cases, apoptosis (Petrini and Stracker, 2003). Perturbations of the DNA damage response following a DSB may lead to improperly or illegitimately repaired DSBs that might promote malignant transformation (Pastink and Lohman, 1999).

1.3.1 DNA Damage-Dependent Checkpoints

The cell-cycle consists of successive rounds of DNA replication and segregation of replicated chromosomes into two separate daughter cells. Mitosis (M-phase) involves nuclear division and the first gap phase G_1, where the cell prepares for DNA synthesis, subsequently takes place (Vermeulen et al., 2003). DNA replication occurs during the ensuing S-phase and this is followed by the second gap phase G_2 where the cell again prepares for mitosis (Vermeulen et al., 2003).

Checkpoints ensure an orderly sequence of events during the cell-cycle and DNA damage-dependent checkpoints, as discussed here, delay or arrest the cell-cycle after DNA insults to allow time for repair. Therefore, cell-cycle checkpoint control is critical for preventing genomic instability after DNA damage (Seo et al., 2003). Recent findings relating to a group of cancer predisposition syndromes suggest that several recombination repair proteins also have a role in DNA-damage dependent cell-cycle regulation (Petrini, 2000a). This implies that DNA repair processes and the checkpoint response are tightly coordinated.

DNA damage sustained in G_1 triggers the G_1-checkpoint to delay entry to S-phase and therefore prevent replication of a damaged DNA template. Cells in G_1 have only one copy of the genome available and the options for repair of specific types of DNA damage are limited (McGowan, 2002). DNA damage present during S-phase elicits an intra-S-phase checkpoint response to provide maximal inhibition of DNA synthesis and slow the progression through the S-phase. A third checkpoint, the G_2-M checkpoint, allows time for repair of damaged chromatids prior to segregation in mitosis (Figure 1.3.1.1).

Figure 1.3.1.1 Schematic diagram of the phases of the cell-cycle and cell-cycle checkpoints.

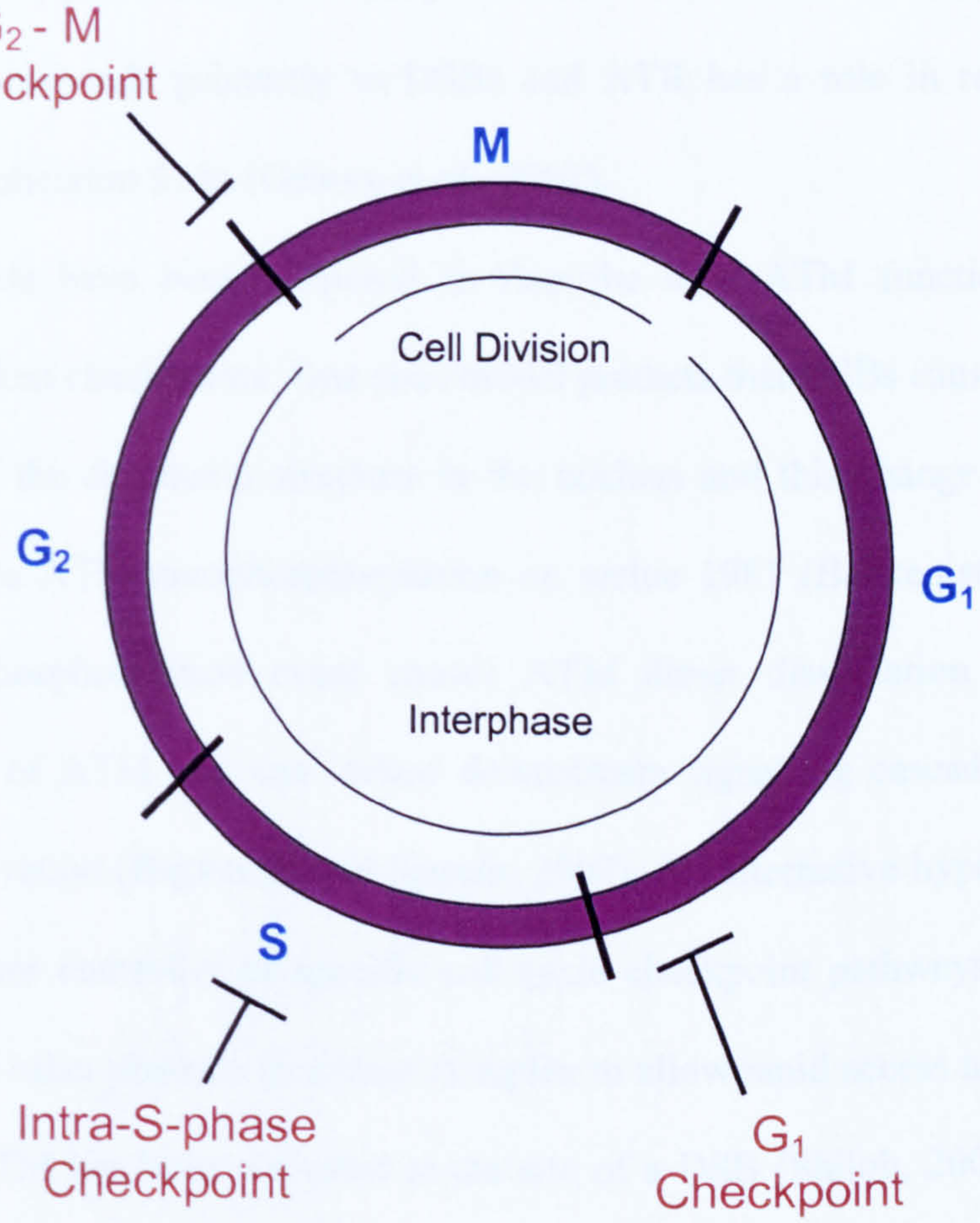

Activation of cell-cycle checkpoints, by sensors that detect damaged or unreplicated DNA, initiates a signal transduction pathway that results in the phosphorylation of several proteins and transcription of a number of genes (Myung and Kolodner, 2002). All checkpoints require the PIKK family members ATM and ATR (ATM and Rad3 related). ATM responds primarily to DSBs and ATR has a role in recognition of stalled DNA replication forks (Osborn et al., 2002).

Different models have been proposed to describe how ATM functions in DNA damage-dependent checkpoints. One such model predicts that DSBs cause a change in some aspect of the chromatin structure in the nucleus and this change is sensed by ATM leading to ATM autophosphorylation on serine 1981 (Bakkenist and Kastan, 2003). This phosphorylation event causes ATM dimer dissociation releasing an activated form of ATM that can induce downstream signalling cascades leading to checkpoint activation (Bakkenist and Kastan, 2003). An alternative hypothesis is that ATM is a master controller of specific cell-cycle checkpoint pathways and may be associated with other proteins in a large complex to allow rapid access to downstream targets once ATM has been activated at the site of a DSB (Shiloh, 2001). Whatever activation mechanism occurs following DNA damage ATM is a guardian of genomic stability (Shiloh, 2003) and once activated ATM phosphorylates several downstream target proteins such as NBS1, Chk2 and p53 that have different effects on DNA repair, cell-cycle progression and apoptosis. ATR phosphorylates an overlapping set of targets to ATM, but responds to a distinct spectrum of lesions (Jackson, 2002).

Following induction of a DSB in S-phase ATM activates two parallel branches of the S-phase checkpoint response in mammalian cells to inhibit DNA replication (Falck et al., 2002). On one arm the protein kinase Chk2 is recruited to sites of DSBs for its ATM-dependent phosphorylation on Thr-68. Phospho-Chk2 then disperses throughout the nucleus to reach its physiological targets (Lukas et al., 2003), in this case Cdc25A

phosphotase. Chk2-mediated phosphorylation of Cdc25A on Ser123 targets it for polyubiquitination-mediated proteolysis thereby preventing the activation of both the S-phase promoting cyclin E/Cdk2 and the loading of Cdc45, an essential replication factor, onto replication origins (Falck et al., 2002).

The second branch of the pathway involves ATM-mediated phosphorylation of NBS1 on Ser343 to activate the MRE11/NBS1/Rad50 complex (Figure 1.3.1.2). How this complex mediates S-phase arrest is not clear as its downstream targets are unknown. However, the importance of this complex is apparent as mutations in MRE11 or NBS1 can cause loss of the S-phase checkpoint and cancer predisposition (Stewart et al., 1999, Varon et al., 1998).

Figure 1.3.1.2 Overview of the two parallel branches of the S-phase checkpoint response initiated by ATM after a DSB [adapted from (Falck et al., 2002)].

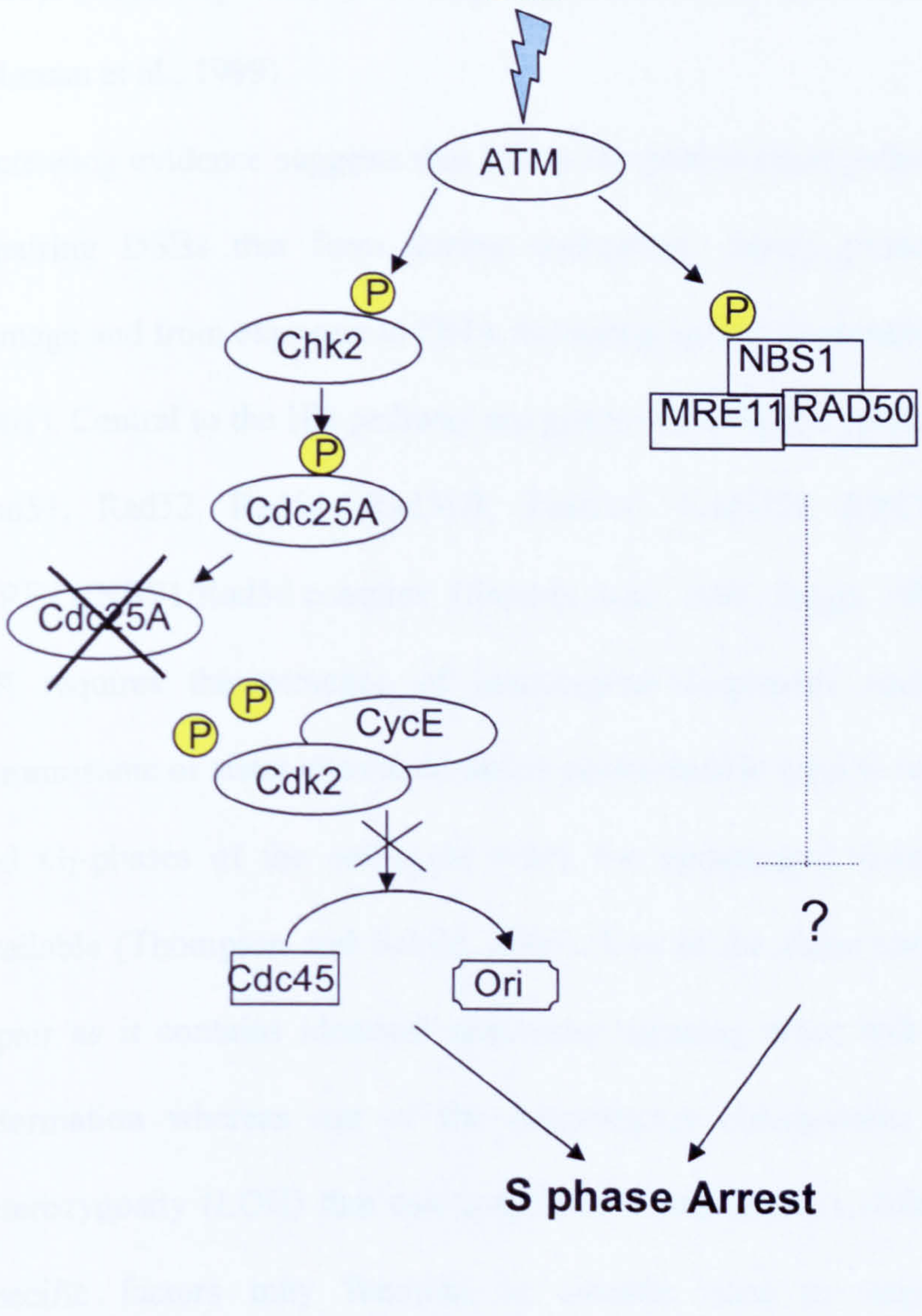

1.3.2 Homologous Recombination Repair

In response to a DSB the cell may also activate repair mechanisms. The two main pathways for DSB repair in mammalian cells are homologous recombination (HR) and non-homologous end-joining (NHEJ). DSB repair by HR requires homologous duplex DNA in the genome and occurs with high fidelity (Thompson and Schild, 2001). NHEJ requires little, if any, sequence homology and is potentially mutagenic (Moreau et al., 1999).

Increasing evidence suggests that HR is the predominant pathway in mitotic cells for repairing DSBs that form during replication, during processing of spontaneous damage and from exposure to DNA damaging agents (Symington, 2002, Sonoda et al., 2001). Central to the HR pathway are genes of the Rad52 epistasis group that includes Rad51, Rad52, Rad54, Rad51B, Rad51C, Rad51D, XRCC2, XRCC3 and the MRE11/NBS1/Rad50 complex (Sonoda et al., 2001, Jeggo, 1998).

HR requires the presence of homologous sequences such as the homologous chromosome or sister chromatid and is preferentially used to repair DSB in the late S- and G_2-phases of the cell-cycle when the undamaged sister chromatid is readily available (Thompson and Schild, 2001). Use of the sister chromatid is preferable in repair as it contains identical sequences meaning there will be no loss of genetic information whereas use of the homologous chromosome may lead to loss of heterozygosity (LOH) that can contribute to malignancy (Johnson and Jasin, 2001). Specific factors may function in somatic cells to impede interchromosomal recombination and prevent LOH (Pastink and Lohman, 1999).

Following induction of a DSB a 5′-3′ exonuclease is recruited to resect the DSB ends and expose 3′ single-strand DNA (ssDNA) tails (Thompson and Schild, 2001). The identity of the nuclease responsible for the 5′-3′ resection of DSBs in HR is unknown. The MRE11/NBS1/Rad50 complex was originally proposed to be a candidate for this

processing because yeast mutants lacking components of the complex show a delay in or loss of 5′-3′ resection of mitotic DSBs (Ivanov et al., 1994, Tsubouchi and Ogawa, 1998, Lee et al., 2002). However, it is now considered unlikely that the MRE11 complex assumes this role because MRE11 possesses only 3′-5′ exonuclease activity and therefore the polarity of the nuclease activity is incompatible with resection (Paull and Gellert, 1998). A more likely role for the MRE11 complex is in recruiting or facilitating a 5′-3′ exonuclease *in vivo* (Paull and Gellert, 1999, Bressan et al., 1999) to create 3′ ssDNA tails. The ssDNA tails are then bound by RPA and Rad51 forming a nucleoprotein filament. Rad51 interacts with Rad52, Rad54 and the Rad51 paralogs (Rad51B, Rad51C, Rad51D, XRCC2 and XRCC3) that assist strand transfer activity and the search for homologous sequences within the genome (Khanna and Jackson, 2001). Once homologous sequences are found the nucleoprotein filament invades the undamaged DNA duplex displacing one strand as a D-loop (Jackson, 2002). The 3′ terminus of the damaged DNA molecule is extended by DNA polymerase using sequences of the homologous chromosome/sister chromatid as a template. Ligation and migration of the DNA ends creates a secondary cross-over structure known as a Holliday junction. Resolution of the Holliday junction, possibly by Mus81, results in cross-over if both strands are cleaved in opposite senses or results in gene conversion with no cross-over when cleavage occurs in the same sense (Chen et al., 2001).

Cells that are compromised for HR repair functions would have to rely on the more error prone NHEJ in S- and G_2-phases of the cell-cycle leading to an increase in genomic instability and promotion of tumorigenesis (Thompson and Schild, 2001). Reflecting this fundamental role in maintaining chromosome stability the HR repair genes have been proposed to be candidate tumour suppressor genes or oncogenes (Thompson and Schild, 1999, Johnson and Jasin, 2001).

Figure 1.3.2.1 Overview of the main stages of the HR repair pathway and the genes predicted to have a role in various stages of HR.

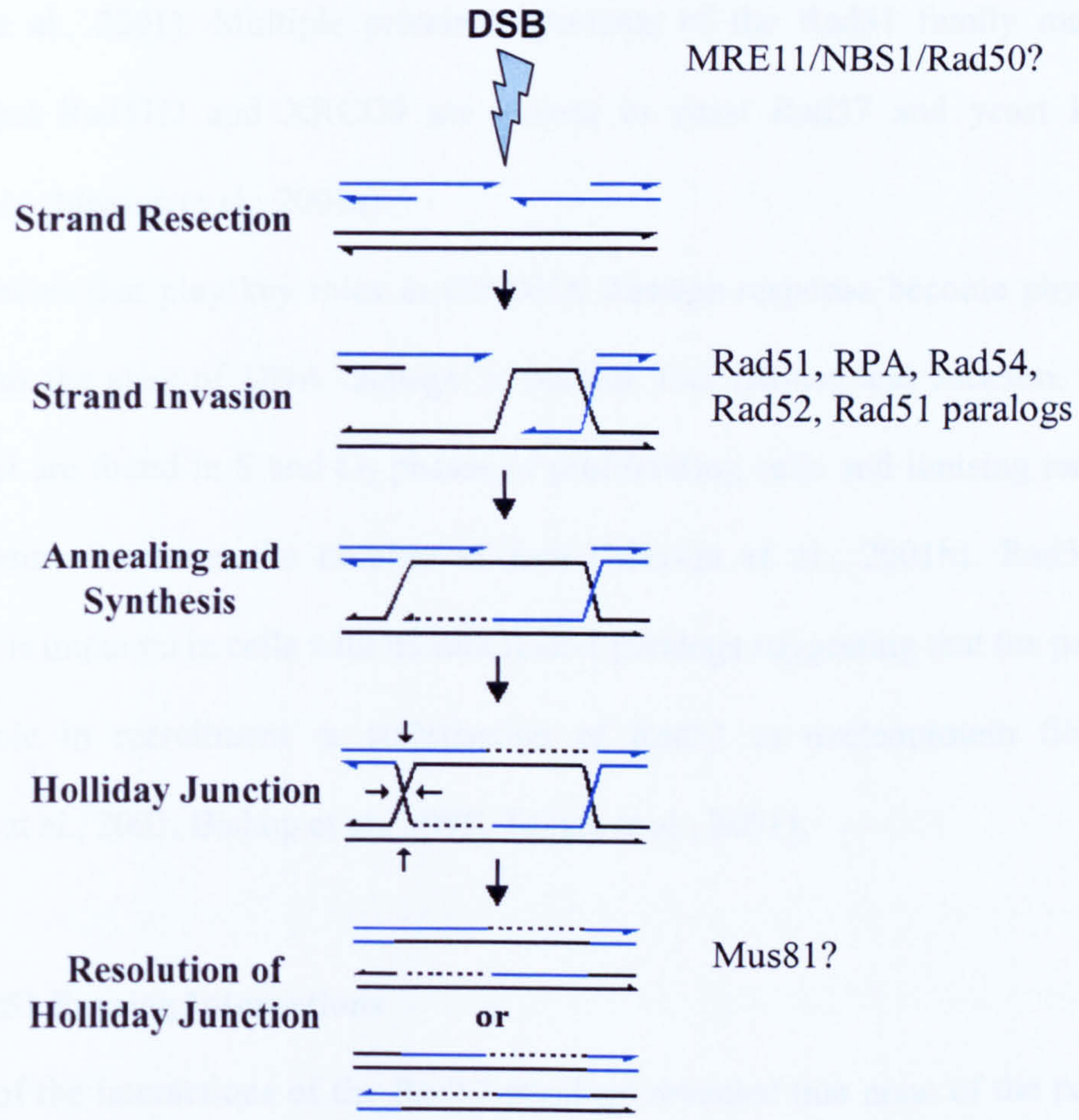

1.4 Rad51 Paralogs

Both mitotic and meiotic cells express the Rad51 paralogs XRCC2, XRCC3, Rad51B, Rad51C and Rad51D. The five human paralogs have 20-30% identity with Rad51 and show <30% identity with each other and with the yeast paralogs Rad55 and Rad57 (Takata et al., 2001). Multiple protein alignments of the Rad51 family members suggest that Rad51D and XRCC3 are closest to yeast Rad57 and yeast Rad55, respectively (Masson et al., 2001a).

Many proteins that play key roles in the DNA damage response become physically localised to the sites of DNA damage in nuclear foci (Rouse and Jackson, 2002). Rad51 foci are found in S and G_2 phases of proliferating cells and ionising radiation (IR) exposure increases the number of foci (Masson et al., 2001b). Rad51 foci formation is impaired in cells with mutant Rad51 paralogs suggesting that the paralogs have a role in recruitment or stabilisation of Rad51 to nucleoprotein filaments (O'Regan et al., 2001, Bishop et al., 1998, Takata et al., 2001).

1.4.1 Rad51 Paralog Interactions

Analysis of the interactions of the Rad51 paralogs revealed that none of the paralogs interacts with itself but each paralog has a unique set of interactions with other paralogs suggesting they are not functionally redundant (Schild et al., 2000).

Rad51B and Rad51D interact with each other indirectly via their interactions with Rad51C (Schild et al., 2000, Liu et al., 2002). XRCC2 and Rad51D interact to form nucleoprotein filaments in the presence of ssDNA (Kurumizaka et al., 2002) and Rad51C also binds XRCC3 in a stable complex (Masson et al., 2001a).

It was initially suggested that the paralogs participate in a single multi-protein complex through their simultaneous interactions (Schild et al., 2000). However, it now seems likely that at least two distinct complexes exist in the cell, the first including

XRCC3-Rad51C and the second having Rad51B-Rad51C-Rad51D-XRCC2 (BCDX2) in a 1:1:1:1 stoichiometry (Masson et al., 2001b). Rad51C binds Rad51D and XRCC3 separately not simultaneously and so Rad51C may be partitioned between the two complexes in the cell (Liu et al., 2002). Interaction between the paralogs is likely to be dynamic and it is possible that other stable complexes are formed in a transient manner.

The paralog associations do not require the presence of DNA and protein interactions are not affected by DNA damage, suggesting that complex formation is not induced by the presence of DNA DSBs (Wiese et al., 2002). No interaction between the complexes and Rad51 was observed suggesting that Rad51 association perhaps does require the presence of a DSB (Miller et al., 2002). Alternatively the interaction between the paralogs and Rad51 could be weak or transient (Wiese et al., 2002).

Both the BCDX2 and XRCC3-Rad51C complexes preferentially bind ssDNA in an ATP-independent manner to promote DNA aggregation (Masson et al., 2001a). This aggregation may facilitate DNA-DNA contacts during the search for homologous sequences on the sister chromatid or homologous chromosome. The specificity of the ssDNA binding activity of each of the complexes is potentially important for initiation of recombination repair as DSBs are resected to expose ssDNA tails (Masson et al., 2001b).

Therefore the Rad51 paralogs seemingly do not have overlapping roles but may act in a functional unit to promote the assembly of the Rad51 nucleoprotein filament (Thompson and Schild, 2001, Takata et al., 2001, Johnson and Jasin, 2001).

1.4.2 XRCC2 and XRCC3

Chinese hamster ovary (CHO) cell lines *irs1* and *irs1SF* cells show an extreme (60- to 100-fold) sensitivity to DNA cross-linking agents such as mitomycin-C (MMC), a mild (~2-fold) sensitivity to IR and high levels of chromosome aberrations relative to wild type cells (Masson et al., 2001b). XRCC2 and XRCC3 were initially identified by their ability to complement the DNA-damage sensitivity and chromosomal instability of *irs1* and *irs1SF*, respectively (Tebbs et al., 1995, Tambini et al., 1997). Xrcc2 null mutations are embryonic lethal in mice (Deans et al., 2000) suggesting that XRCC2 is an essential gene. The relatively mild growth defect in *irs1* cells may reflect species differences but more likely suggests that Xrcc2 is not completely inactive in CHO cells.

XRCC3 was localised to chromosome 14q32.3 and found to encode a 2.5kb transcript (Tebbs et al., 1995). XRCC2 was mapped to chromosome 7q36.1 and found to encode a 1.8kb transcript that is expressed relatively abundantly in the brain and testis and at low levels in most other tissues (Cartwright et al., 1998). The XRCC2 and XRCC3 proteins have conserved ATP-binding domains known as Walker boxes A and B. The role of these ATP-binding domains is unclear however, since substitution of highly conserved residues within Walker box A in XRCC2 has little effect on XRCC2 functions (O'Regan et al., 2001). Rad51D, a binding partner of XRCC2, is a DNA-stimulated ATPase (Braybrooke et al., 2000) and it may be that only one member of a complex is required to retain the ATP-binding requirement.

Correct control of replication fork progression following DNA damage is crucial for cell viability and genomic stability. *irs1SF* cells fail to slow replication fork progression after DNA damage, a response that is restored by complementation with XRCC3 (Henry-Mowatt et al., 2003). Similar results were obtained with mutant *xrcc2* DT40 cells suggesting that XRCC2 and XRCC3 are required for the modulation of

replication fork progression on damaged vertebrate chromosomes via their role in HR (Henry-Mowatt et al., 2003).

The *irs1* and *irs1SF* cells show a 100- and 25-fold decrease in frequency of DSB repair by HR respectively, that can be corrected by complementation with the wild type gene (Johnson et al., 1999, Pierce et al., 1999). XRCC2 deficiency results in an HR defect but does not affect NHEJ and XRCC3 deficiency leads to a specific defect in gene conversion in HR (Johnson et al., 1999, Pierce et al., 1999). The correlation between HR defects, decreased cell viability and chromosomal instability in XRCC2- and XRCC3-deficient cells implies that these genes are credible downstream targets in cancer development and has led to others in the field proposing that they are tumour suppressor genes (Thompson and Schild, 1999, Johnson and Jasin, 2001).

CHO cells lacking Xrcc2 or Xrcc3 show chromosome segregation defects (Griffin et al., 2000) increasing the likelihood that these genes are guardians of the genome. Therefore, loss of efficient XRCC2 or XRCC3 gene function may promote malignant development by increasing genetic instability in the cell.

Figure 1.4.2.1 Schematic representation of the XRCC2 or XRCC3 protein structure. XRCC2 is 280aa in length whereas XRCC3 is 346aa. The only known functional domains of these proteins are the Walker box A (putatively at residues 48-55 in XRCC2 and 127-134 in XRCC3) and Walker box B motifs (residues 145-150 in XRCC2 and 218-223 in XRCC3) [Cartwright et al., 1998, Rafii et al., 2003].

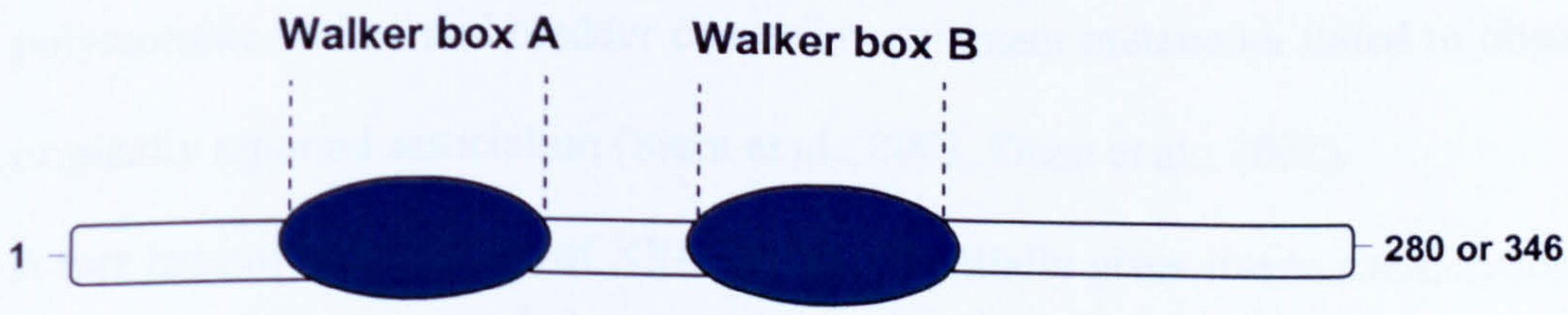

1.4.3 XRCC2, XRCC3 and Cancer

A polymorphism of XRCC2, that causes an R188H amino acid substitution, has a subtle effect on the cells ability to repair MMC-induced DNA damage and shows a small but consistent association with breast cancer risk (Rafii et al., 2002, Kuschel et al., 2002). However, the role of amino acid 188 in functioning of XRCC2 is not known as it does not appear to be necessary for XRCC2-Rad51D interaction (Rafii et al., 2002) and integrity of XRCC2 Walker box A is not essential for protein function (O'Regan et al., 2001) but amino acid 188 is a conserved residue between mouse and human (Cartwright et al., 1998).

A MMR-deficient uterine cancer cell line was also found to carry a heterozygous frameshift mutation of XRCC2 that is expected to disrupt the Walker box B (Mohindra et al., 2002). A screen of primary uterine sarcomas associated this polymorphism with hyperplastic tissue suggesting that it may play a role in a rare subset of uterine cancers (Mohindra et al., 2003).

A C/T polymorphism of XRCC3 is present in the healthy, cancer-free population (Shen et al., 2002). This polymorphism leads to a non-conservative amino acid substitution, T241M, the functional consequences of which are not known. The T241M variant was reported to be associated with an increased risk of malignant melanoma, bladder cancer and breast cancer (Winsey et al., 2000, Matullo et al., 2001, Kuschel et al., 2002). However, cells expressing the T241M variant show no defect in HR repair and are no more sensitive to MMC than wild type cells (Araujo et al., 2002). In addition, further studies to confirm the relationship between this polymorphic variant and bladder cancer or malignant melanoma failed to observe the originally reported association (Stern et al., 2002, Duan et al., 2002).

A rare heterozygote variant of XRCC3 that potentially gives rise to a non-synonymous D213N substitution in the conserved Walker box B was found to abrogate the function

of XRCC3 (Rafii et al., 2003). However, this heterozygote variant was not associated with breast cancer and was only observed in three non-cancer controls (Rafii et al., 2003) further suggesting that this gene is not a tumour suppressor.

Therefore, it remains to be determined whether there are mutations or polymorphisms of *XRCC2* and *XRCC3* that have subtle effects on DNA repair capacity and thereby increase the risk of colorectal cancer.

1.5 Mus81

A Holliday junction (HJ) is a symmetrical branched DNA structure that needs to be resolved to re-establish duplex DNA. Holliday junctions can occur during recombination when newly synthesised DNA becomes associated with the displaced strand. These are typically resolved by an enzyme that cuts either pair of similarly oriented strands (Chen et al., 2001).

Holliday junctions can also be created at stalled replication forks when the Y-branched stalled fork regresses by annealing two newly synthesised strands together to form an X-shaped HJ (Haber and Heyer, 2001, Osborn et al., 2002). This can be resolved by introducing nicks into non-complementary strands of the HJ to leave one intact duplex along with unprotected DNA ends that can invade the template to re-initiate replication (Osborn et al., 2002).

Mus81 is a putative component of the endonuclease that resolves Holliday junctions to linear duplex products (Chen et al., 2001, Boddy et al., 2000). Mus81 was initially identified in *S. pombe* through its ability to interact with the forkhead associated (FHA) domain of checkpoint kinase cds1 (human homologue is Chk2) (Boddy et al., 2000). The human Mus81 protein was subsequently isolated through its interaction with the FHA domain of hChk2 (Chen et al., 2001). Human Mus81 is located on chromosome 11q13 and codes for a 551 amino acid protein.

Mus81 is a member of the XPF family of endonucleases with a highly conserved $VERKX_3D$ motif that is proposed to form the catalytic site (Boddy et al., 2000). Other conserved motifs include a C-terminal helix-hairpin-helix signature that is found in other XPF proteins and proteins involved in DNA metabolism. A second helix-hairpin-helix motif is present in the N-terminus that is predicted to allow non-specific DNA binding via the phosphate backbone (Boddy et al., 2000). Mus81 possesses one of the defining features of a HJ resolvase in that it is able to introduce nicks into strands of like polarity across a 4-way helical branch point (Boddy et al., 2001).

Cells exposed to agents that damage DNA or block DNA replication have increased levels of hMus81 and hMus81 has an associated endonuclease activity against synthetic HJs (Chen et al., 2001). These observations led to the suggestion that Mus81 has a role in resolution of HJs that arise when DNA replication is blocked by damage or nucleotide depletion (Chen et al., 2001, Haber and Heyer, 2001).

Improper resolution of the HJ may lead to chromosome segregation defects and increased genomic instability, therefore it is possible that mutations in Mus81 promote malignant transformation.

Figure 1.5.1 Diagrammatic representation of the putative domains of Mus81 as predicted by protein alignments (Chen et al., 2001).

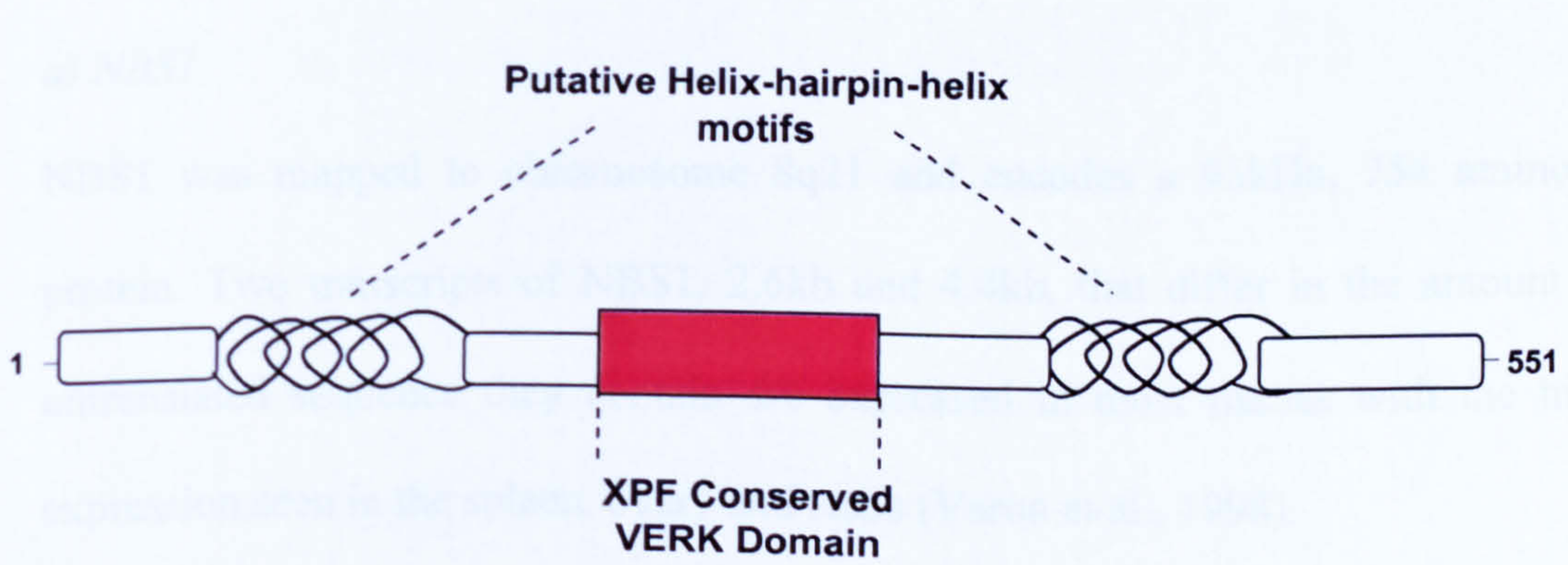

1.6 The MRE11 Complex

The MRE11 complex consists of MRE11, NBS1 and Rad50 and the MRE11-Rad50 proteins appear to form the core of the complex since these are well conserved from archaea to humans (Anderson et al., 2001). The Xrs2 protein of *Saccharomyces cerevisiae* shares little homology with the human NBS1 protein except in the N-terminus and there is no corresponding prokaryotic protein (Anderson et al., 2001). It appears as though the MRE11-Rad50 core proteins are ancient proteins that have acquired recent binding partners in evolutionary history (Petrini, 2000b).

The MRE11 complex is hypothesised to have several roles in the cell including DNA damage recognition (Petrini and Stracker, 2003), prevention of DSB formation during DNA replication (Costanzo et al., 2001), cell-cycle checkpoint activation (Grenon et al., 2001), participation in some aspects of NHEJ (Paull and Gellert, 2000) and telomere maintenance (Zhu et al., 2000). A number of these suggested roles for the complex come from studies of the conserved yeast MRE11 complex, as discussed later in this chapter. The biochemical or biological basis for many of these proposed functions of the MRE11 complex is unknown and remains an area of controversy. Moreover, investigations into the precise function of the MRE11 complex have been hampered by the fact that null mutations of these genes are lethal to vertebrate cells (Yamaguchi-Iwai et al., 1999, Luo et al., 1999, Zhu et al., 2001).

a) NBS1

NBS1 was mapped to chromosome 8q21 and encodes a 95kDa, 754 amino acid protein. Two transcripts of NBS1, 2.6kb and 4.4kb, that differ in the amount of 3′ untranslated sequence they contain are expressed in most tissues with the highest expression seen in the spleen, ovary and testis (Varon et al., 1998).

The NBS1 protein (also known as p95 and nibrin) contains a 150 amino acid FHA domain in its N-terminus that may be associated with phospho-specific protein-protein interactions (Zhao et al., 2002). Adjacent to the FHA domain is a 70-80 amino acid BRCA1 carboxy-terminal (BRCT) motif (D'Amours and Jackson, 2002). BRCT domains are generally required to mediate protein-protein interactions and are often found in DNA damage responsive cell-cycle checkpoint proteins (Zhao et al., 2002, Varon et al., 1998).

b) Rad50

Rad50 resides on chromosome 5q31 and codes for a 1312 amino acid protein that forms a stable complex with MRE11 (Dolganov et al., 1996). At least two transcripts of Rad50, 4.6kb and 5.9kb, are produced by alternative splicing of the gene (Kim et al., 1999).

Rad50 belongs to the structural maintenance of chromosomes (SMC) family of proteins whose features include a Walker box A at the N-terminus and a Walker box B at the C-terminus (Dolganov et al., 1996). These ATP-binding domains are separated by a coiled-coil motif that is interrupted by a putative globular domain (Dolganov et al., 1996). Examination of the *S. cerevisiae* Rad50 suggested that the protein forms an anti-parallel homodimer through a flexible hinge region to bring the catalytic domains together and create a functional ATP-binding domain (Anderson et al., 2001). This homodimer appears to bind ScMre11 at or close to the catalytic domains so that the ScMre11 nuclease activity is closely associated with ScRad50 ATPase activity (Anderson et al., 2001).

Human Rad50 recognises dsDNA and may have a role in tethering or bridging DNA ends to assist repair (Connelly and Leach, 2002, de Jager et al., 2001b).

c) MRE11

MRE11 lies on chromosome 11q21 and codes for a 708 amino acid protein (Petrini et al., 1995). Two MRE11 mRNA species, one of 2.4kb and a second of 6.6kb, exist in all tissues with the expression pattern of the smaller transcript directly correlating with the level of tissue proliferation and being most abundant in the testis (Petrini et al., 1995, Carney et al., 1998). MRE11 shares a promoter with the foetal globin-inducing factor gene and the two genes are transcribed divergently (Pitts et al., 2001). This type of promoter organisation is seen in other genes involved in the DNA damage response such as ATM and BRCA1.

It has been proposed that *S. cerevisiae* Mre11 forms a homodimer and that regions in both the N- and C-terminus of the protein are required for this self-interaction (Chamankhah and Xiao, 1999). It has further been suggested that NBS1 binding requires hMRE11 dimerisation (D'Amours and Jackson, 2002).

The N-terminal nuclease domain of hMRE11 consists of four phosphoesterase motifs, the first three of which are common to many phosphoesterases and the fourth has homology to nuclease motifs found in *E. coli* SbcD and bacteriophage T4 gp47 (D'Amours and Jackson, 2002). The C-terminus of MRE11 is more divergent and has charged clusters of amino acids required for DNA binding (D'Amours and Jackson, 2002). Rad50 binding to MRE11 requires several sites in the N-terminus of MRE11 and may stabilise the MRE11 protein and/or facilitate NBS1 binding (Desai-Mehta et al., 2001). MRE11-NBS1 binding requires the last 101 amino acids of NBS1 and amino acids 1-319 of MRE11 (Desai-Mehta et al., 2001).

Figure 1.6.1 Diagrammatic representation of the human NBS1, Rad50 and MRE11 protein structures.

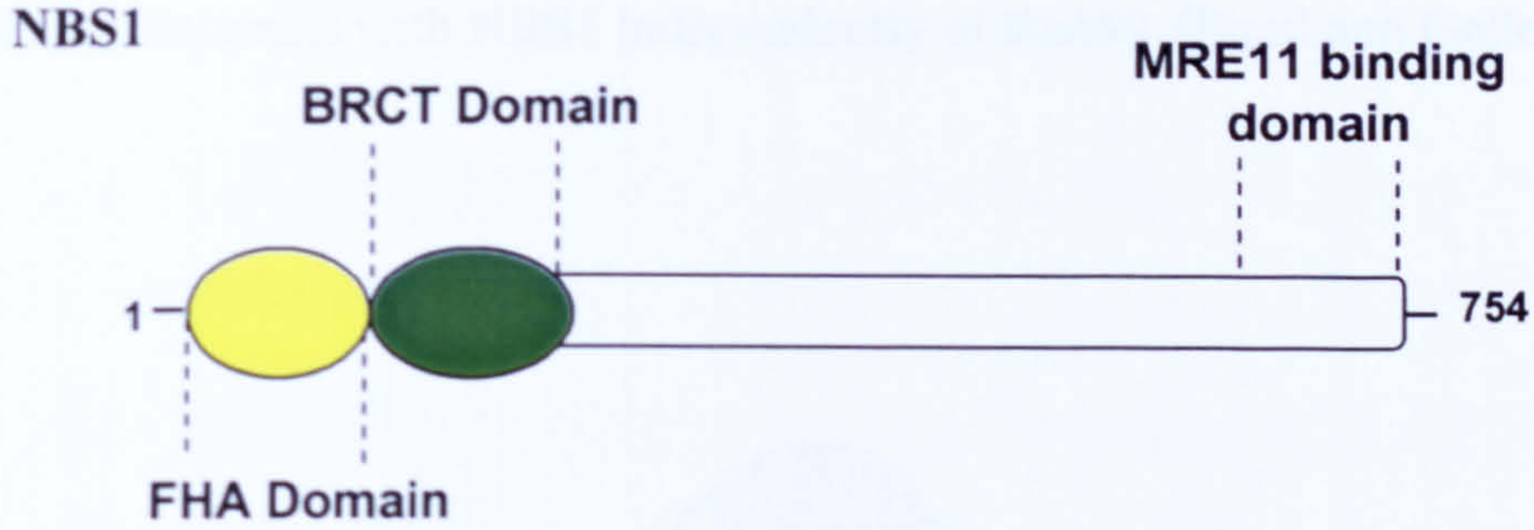

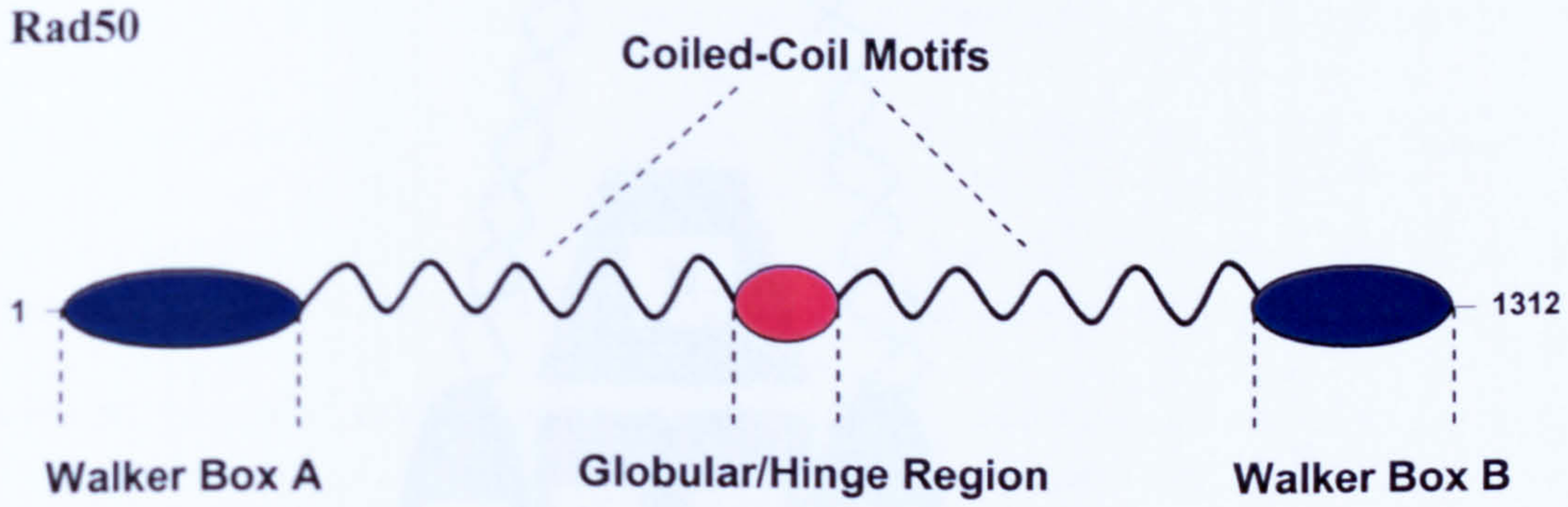

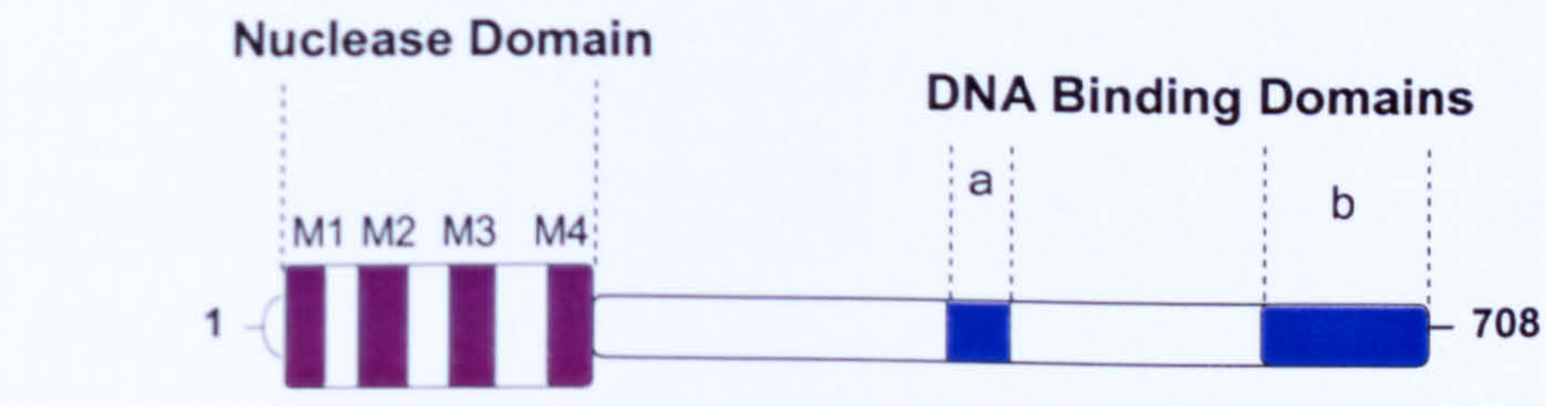

Figure 1.6.2 Model depicting the putative architecture of the MRE11 complex as proposed by D'Amours and Jackson, 2002 and supported by analysis of the yeast complex (Anderson et al., 2001). Rad50 is predicted to dimerise and adopt a flexible conformation. The MRE11 dimer binds close to the Rad50 ATPase domains and MRE11 interacts with NBS1 independently of Rad50 (Paull and Gellert, 1999).

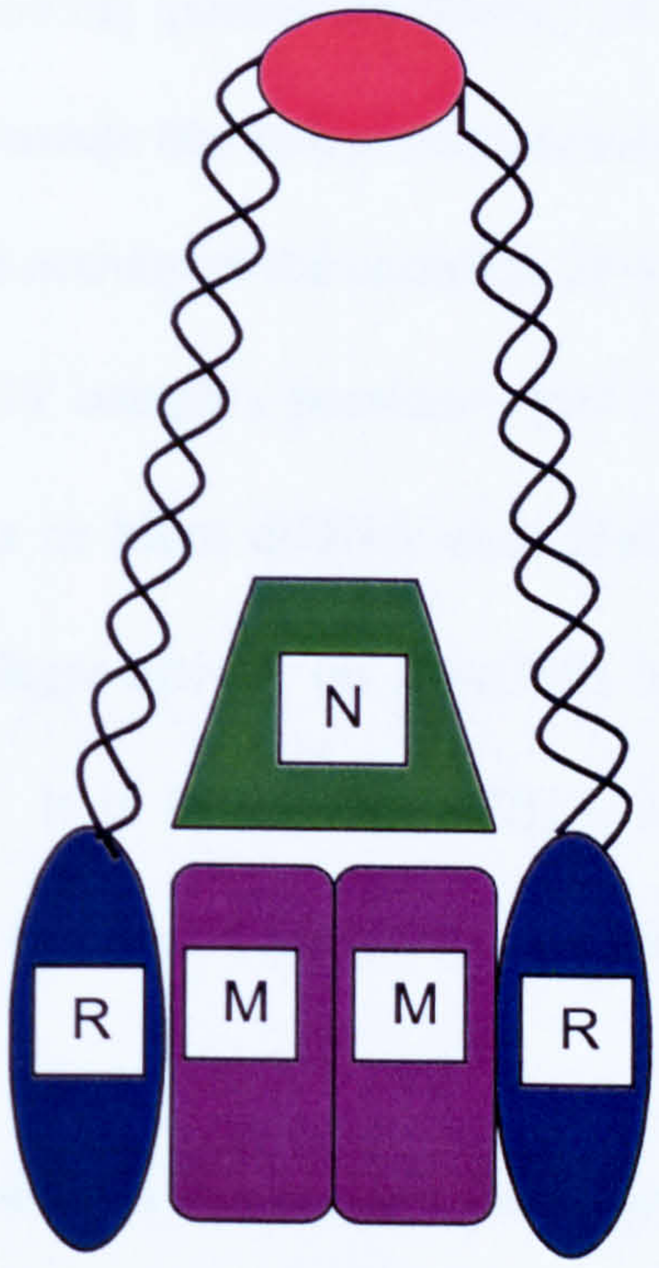

1.6.1 Catalytic Activities of the MRE11 Complex

MRE11 has single-strand annealing activities that may facilitate joining of non-homologous ends or might be important for the rescue of collapsed replication forks (Paull and Gellert, 1998, de Jager et al., 2001a). MRE11 by itself also has 3′-5′ dsDNA exonuclease activities and endonuclease activities that are enhanced 3-4 fold in the presence of Rad50 (Paull and Gellert, 1998). Binding of NBS1 can alter the specificity of the nuclease activities by stabilising MRE11-Rad50 protein-DNA complexes and allowing partial unwinding of DNA duplexes (Paull and Gellert, 1999). The DNA-damage dependent phosphorylation of NBS1 and MRE11 may also modify the nuclease activity of the complex (D'Amours and Jackson, 2002).

Together the MRE11 complex possesses Mn^{2+}-dependent 3′-5′ exonuclease activity on 3′ recessed ends or blunt dsDNA ends (Paull and Gellert, 1998, Trujillo et al., 1998) and endonuclease activity on 3′ ssDNA branches and hairpin structures (Paull and Gellert, 1999). It is likely that MRE11 is the only nuclease in the MRE11 complex and NBS1 and Rad50 modify and regulate its activities.

1.6.2 Links between DNA Repair and Cell-Cycle Checkpoint Functions

Mutations in the ATM gene lead to ataxia telangiectasia (A-T), an inherited disorder characterised by cerebellar ataxia, oculocutaneous telangiectasia and an increased incidence of cancer, especially lymphoid tumours (Kraakman-van der Zwet et al., 1999). Cells from A-T patients show increased sensitivity to IR, genomic instability and a failure to suppress replication fork firing after DNA damage, a phenomenon known as radio-resistant DNA synthesis (RDS) (Kraakman-van der Zwet et al., 1999). Nijmegen breakage syndrome (NBS), caused by mutations in NBS1, is characterised by microcephaly, developmental defects, immune deficiency and a high incidence of lymphoma. NBS cells display increased IR sensitivity, increased chromosomal

aberrations, decreased survival and RDS indicating a loss of S-phase checkpoint activation (Franchitto and Pichierri, 2002, Varon et al., 1998). The founder mutation 657del5 is seen in 90-95% of NBS patients and this mutation leads to premature truncation of NBS1 downstream of the FHA and BRCT domains (Desai-Mehta et al., 2001, Varon et al., 1998). The striking cellular and clinical similarities between A-T and NBS indicated that ATM and NBS1 function in the same checkpoint pathway. This idea was further supported by evidence that ATM phosphorylates NBS1 after IR and this event is required for S-phase checkpoint activation (Petrini, 2000a, Wu et al., 2000).

MRE11 and Rad50 accumulate in nuclear foci after IR-induced damage in a dose-dependent manner (Maser et al., 1997). These irradiation-induced foci (IRIF) are thought to represent sites of ongoing repair and therefore these proteins were predicted to have some role in DNA DSB repair (Carney et al., 1998). In NBS cells the MRE11-Rad50 interaction remains intact but these proteins are not restricted to the nucleus and do not form IRIF, suggesting that NSB1 is required for the nuclear localisation of MRE11-Rad50 (Desai-Mehta et al., 2001). This fact, together with the discovery that NBS1 was a member of the MRE11 complex, highlighted a link between proteins involved in DSB repair and those implicated in the checkpoint response.

Mutations in MRE11 cause A-TLD (A-T like disorder) whose phenotype is almost indistinguishable from A-T (Stewart et al., 1999). A-TLD cells share similar features with A-T and NBS cells, such as chromosomal instability, IR sensitivity and RDS (Stewart et al., 1999), thereby strengthening the connection between DSB repair by the MRE11 complex and cell-cycle checkpoint responses controlled by ATM.

The fact that A-TLD, NBS and A-T cells display RDS, together with the observation of impaired IRIF formation in these cells suggests that the MRE11 complex, together

with ATM, plays a significant role in both S-phase checkpoint activation and DNA damage recognition (Stewart et al., 1999, Carney et al., 1998).

1.6.3 Potential Functions of the MRE11 Complex

A role for the MRE11 complex in NHEJ is tentative. Some reports suggest that yeast *rad50*, *mre11* and *xrs2* mutants are deficient in both HR and NHEJ (Wilson, 2002) whereas others report that these mutants solely display decreased efficiency of some aspects of NHEJ (Moore and Haber, 1996). However, it is hypothesised that the single-strand annealing activities of human MRE11 could be important in certain elements of NHEJ (Paull and Gellert, 2000, Paull and Gellert, 1999).

Another putative function of the hMRE11 complex is in the maintenance of telomeres as a small fraction of the hMRE11 complex was found to be located at telomeres and associated with TRF2, a telomere repeat binding factor (Zhu et al., 2000). Experiments using a temperature sensitive mutant form of *ScMre11* that carried a Pro162Ser mutation showed defects in telomere maintenance even at permissive temperatures suggesting that the 162 residue is important for telomere function of the ScMre11 complex (Chamankhah et al., 2000). This residue may be important for secondary or tertiary structure of ScMre11 and was suggested to be important for interaction with other proteins (Chamankhah et al., 2000). Residues in the C-terminal region of ScMre11 also appear to be critical for telomere preservation (Chamankhah and Xiao, 1999). The nuclease activity of the MRE11 complex may not be required for its role at telomeres, however, as nuclease-deficient *mre11* yeast mutants have a normal telomere length (Moreau et al., 1999).

The MRE11 complex may also have roles in meiotic recombination events. Deletion of Mre11 in yeast leads to severe defects in processing and formation of DSB during meiosis (Usui et al., 1998). The ScMre11 DNA binding site B was shown to be required for formation of meiotic DSBs (Moreau et al., 1999) whereas both the nuclease activity and the DNA binding site A were found to be essential for meiotic DSB processing (Usui et al., 1998).

Although it is now thought unlikely that the hMRE11 complex is involved in DSB end-resection during mitotic recombination a role for the complex in HR has not been ruled out. A deficiency in *S. cerevisiae* Mre11 leads to a decrease in IR-induced sister chromatid recombination suggesting a primary role for the Mre11-Rad50-Xrs2 complex in DNA damage-induced HR (Bressan et al., 1999). Using chicken DT40 NBS1 knockout cells it was also shown that NBS1 was essential for HR in vertebrates (Tauchi et al., 2002) supporting the hypothesis that this complex functions in recombination repair. The exact nature of this role is still of some controversy however, especially since cells from A-TLD and NBS patients do not show gross DSB repair defects (Stewart et al., 1999, Varon et al., 1998). A likely role for the MRE11 complex is as a key organiser of DSB repair that determines the type of processing to be used depending on the nature of ends at the break (Paull and Gellert, 1999).

A role for the hMRE11 complex in replication is supported by the observation that the complex co-localises with PCNA throughout the S-phase and it has been proposed that the hMRE11 complex is loaded onto chromatin in a replication-dependent manner (Mirzoeva and Petrini, 2003). The N-terminal FHA and BRCT domains of NBS1 associate with the E2F1 transcription factor under normal unstressed conditions and this interaction may direct the MRE11 complex to origins of replication (Maser et al.,

2001). The failure of NBS and A-TLD cells to repress firing of DNA replication origins in response to IR also suggests the MRE11 complex is a negative regulator of DNA replication following DNA damage (Maser et al., 2001). Putative replication functions of the MRE11 complex are further supported by the fact that mammalian cells that lack a functional MRE11 show increased chromosomal breaks and accumulation of DSBs during DNA replication (Yamaguchi-Iwai, 1999, Costanzo, 2001). By analogy with the homologous *E.coli* SbcCD functions, the MRE11 complex may act at the replication fork by associating with or resolving unusual DNA structures that are formed during replication (Xiao and Weaver, 1997, Petrini, 2000b).

Checkpoint functions for the Mre11 complex were proposed as it was found that yeast lacking functional Xrs2 or Mre11 were defective in S-phase checkpoint activation (D'Amours and Jackson, 2001, Grenon et al., 2001, Myung and Kolodner, 2002). Cells from A-TLD and NBS patients also fail to activate the S-phase checkpoint following IR-induced damage (Stewart et al., 1999, Varon et al., 1998, Carney et al., 1998) further supporting a role for this complex in control of cell-cycle checkpoints.

Upon induction of a DSB, recruitment of the hMRE11 complex to sites of DNA damage occurs independently of ATM, suggesting that with respect to DNA damage recognition the complex is upstream of ATM (Mirzoeva and Petrini, 2003). However, activation of the S-phase checkpoint responses requires chromatin binding, NBS1 phosphorylation and possibly other interactions such as the E2F1 association (Mirzoeva and Petrini, 2001, Maser et al., 2001). The FHA and BRCT domains of NBS1 direct chromatin association and E2F binding in the nucleus and the ATM-dependent phosphorylation of NBS1 might only occur when the MRE11 complex is chromatin-bound (Zhao et al., 2002).

Recently it was suggested that changes in chromatin structure arising from DNA damage may well be the initiating event in the DNA damage response (Petrini and Stracker, 2003, Bakkenist and Kastan, 2003). One hypothesis proposed that these chromatin changes are recognised by a sensor that was chromatin-bound prior to the induction of the DSB and the sensor itself may then become a target for the transducing kinase (Petrini and Stracker, 2003). It is entirely possible that the MRE11 complex is a sensor of DNA damage as it is chromatin bound in an S-phase-specific manner and associates with DNA damage soon after its induction suggesting that the MRE11 complex functions at the earliest time points after DNA damage (Petrini, 2000b, Petrini and Stracker, 2003). It was further suggested that the DNA damage-dependent phosphorylation of NBS1 and MRE11 may then alter the activity of the complex from a sensor of DNA damage to a mediator of the checkpoint response (Petrini and Stracker, 2003). However, since MRE11 chromatin binding is cell-cycle specific the DNA damage response may vary according to cell-cycle phase and therefore the MRE11 complex may not be the sole sensor of DNA damage.

The MRE11 complex is undoubtedly important in maintaining genomic integrity. Inactivation of the *S. cerevisiae* Mre11, Rad50 or Xrs2 proteins increases the rate of gross chromosomal rearrangements by 500- to 600-fold in yeast cells (Chen and Kolodner, 1999). The human MRE11 complex is chromatin bound in a cell-cycle regulated, ATM-independent manner consistent with its role in surveillance of chromosome integrity (Zhao et al., 2002). In addition, an essential role for the MRE11 complex in maintaining chromosomal DNA during the normal cell-cycle is supported by the fact that null alleles of MRE11, Rad50 and NBS1 cause embryonic lethality in vertebrates (Yamaguchi-Iwai et al., 1999, Luo et al., 1999, Zhu et al., 2001). In contrast, chicken DT40 NBS1 knockouts display HR defects but not a lethal phenotype

(Tauchi et al., 2002) and NBS does not confer an extremely acute phenotype, probably due to the fact that truncated forms of NBS1 are expressed in these cells. Creation of a mouse model that reflected many of the characteristics of NBS suggested that NBS1 function retained by the truncated NBS1 protein (70kDa protein in human NBS) is sufficient to prevent embryonic lethality (Kang et al., 2002).

1.6.4 The MRE11 Complex and Cancer

The discovery that mutations of MRE11 and NBS1 cause syndromes that are associated with an increased cancer predisposition links alterations of the MRE11 complex genes with tumour development. Further mutations and polymorphisms of these genes are in fact seen in the cancer population.

A subset of breast and lymphoid primary tumours were found to have mutations of MRE11 at conserved positions (Fukuda et al., 2001) while polymorphisms and mutations of NBS1 are known to be present in some breast, ovarian and colon cancer cell lines (Tessitore et al., 2003) suggesting that alterations of MRE11 and NBS1 exist in at least a subset of cancers.

A mutation in a poly(T) tract in intron 4 of MRE11, leading to alternative splicing and generation of truncated MRE11 products, was found to be present in >90% of MSI^+ colorectal tumours (Giannini et al., 2002). This mutation was also seen in 12% of cases of MSI^+ therapy-related acute leukaemia (Casorelli et al., 2003). Heterozygous frameshift mutations of an A_9 tract in Rad50 were observed in 33% of MSI^+ CRCs and 28% of MSI^+ gastric cancers (Kim et al., 2001). This implies that MRE11 and Rad50 are major targets for inactivation in MMR-deficient cells.

1.7 Aims for this Study

Guarding the genome against unwanted genetic alterations is paramount in preventing malignant transformation. To protect genomic integrity a number of mechanisms have evolved to recognise and repair DNA damage. The supposition that loss of any of these pathways is sufficient to increase genetic instability and promote tumorigenesis is corroborated by evidence from HNPCC. These cancers develop through a multi-step process that is likely to involve a cascade of primary and secondary mutator genes that accelerate genomic instability (Kim et al., 2001). The primary mutator genes in this cascade are known to be the MMR genes that are inactivated in the majority of hereditary and sporadic MSI^+ colorectal tumours. It is now important to determine which genes are downstream mutational targets in these tumours. Likely candidates include genes involved in DNA repair and cell-cycle checkpoints, as mutations that compromise the functions of these genes would further increase genetic instability and might elevate the risk of malignant transformation.

This study aims to clarify whether the *XRCC2*, *XRCC3*, *Mus81* and *MRE11* complex genes are mutated in colorectal cancer or whether polymorphisms of these genes act as low-penetrance risk factors for cancer. This research will also investigate the phenotypic consequences of common mutations occurring in MSI^+ colorectal cancer cells.

CHAPTER 2

Materials and Methods

2.1 Materials

2.1.1 General Laboratory Equipment

2.1.2 Chemical, Biochemical and Molecular Biology Reagents

2.1.3 Preparation of Standard Solutions

2.1.4 Tissue Culture Materials

2.1.5 Western Blotting Materials

2.1.6 Microbiological Materials

2.1.7 Biological Materials

2.2 Methods

2.2.1 Tissue Sample Preparation and Microdissection

2.2.2 DNA Extraction

2.2.3 Microsatellite Analysis

2.2.4 PCR Amplification

2.2.5 Agarose Gel Electrophoresis

2.2.6 Clean-up of PCR Products

2.2.7 Single strand conformation polymorphism gels

2.2.8 Sequencing

2.2.9 RNA Extraction

2.2.10 RT-PCR

2.2.11 cDNA Synthesis from Total Cellular RNA

2.2.12 Tissue Culture

2.2.13 Microbiological Methods

2.2.14 Restriction Digestion

2.2.15 Stable Transfection of Adherent Cells

2.2.16 Growth Assay

2.2.17 Toxicity Assays

2.2.18 Recombination Assays

2.2.19 Western Blotting

2.2.20 Pulse-field Gel Electrophoresis

2.2.21 Apoptosis Measurements

2.2.22 Statistical Tests

2.1 Materials

2.1.1 General Laboratory Equipment

a) Laboratory equipment and instruments

Item	Supplier
Micro Centaur centrifuge	Sanyo Scientific
Eppendorf 5414D centrifuge	Eppendorf
Swing-out Bench Top Centra MP4 rotor	International Equipment Company
Heated Hybridisation Shaker	Stuart Scientific
Water-jacketed Incubator 3250 for Tissue culture	Thermo Forma Scientific
Class II A/B3 Biological Safety Cabinet	Thermo Forma Scientific
Water Bath	Sanyo Gallenkamp
Boekel BBA Heating block	Grant Instruments
Primus 96 Plus PCR Thermal Cycler	MWG Biotech AG
Eppendorf Mastercylcer Gradient	Eppendorf
AB104-S Balance	Mettler-Toledo
Scott II Ohaus Balance for >mg weights	Scaleman
Vortex Genie 2	Scientific Industries
12x15cm Agarose H5 Gel Electrophoresis System	Invitrogen
20x21cm Agarose Gel Electrophoresis Tank	Anachem
Polyacrylamide Gel Protean II xi cell	Bio-Rad
Kodak Analysis System 120 and 1D software	Scientific Imaging Systems
CHEF DR III Pulse-field Gel electrophoresis System	Bio-Rad
UV Transilluminator	UVP Incorporated
Light Box	Bennet Scientific
P2, P10, P20, P200 and P1000 Pipettes	Gilson Medical Electronics
1-10µl and 1-50µl Multi-channel Pipettes	Philip Harris Scientific
Electronic Pipette Aid	Hirshmann Laborgerate
12000-14000 Dalton Dialysis Membranes	MediCell
pH Meter	Denver Instrument Company
Standard Power-Pack	Biometra Savant
LI-COR Long Read Sequencer	MWG Biotech AG
Spectrophotometer	Eppendorf
Ice Machine	Scotsman Ice Systems Ltd
Semi-Dry Transfer Cell	Bio-Rad
Western Gel Mini Protean II Cell	Bio-Rad
Unitemp Microbiological Incubator	Harvard Apparatus
IBL 437 Cs-137 Irradiator	CIS Biointernational
Denley Anthos 2001 Plate Reader	Eppendorf
Sequencher Software	Gene Code
TE 200 Fluorescence Microscope	Nikon

b) Glassware, plastics and disposables

Item	Supplier
Pyrex Glassware	SLS or VWR
Pasteur Pipettes	Volac
250ml, 500ml, 1l glass bottles	SLS
Sterile Filter Gilson Pipette Tips	Continental Laboratory Products
Refill Tips for Gilson P10, P200 and P1000 Pipettes	Continental Laboratory Products
Plastic 15ml and 50ml polypropylene centrifuge tubes	Corning
35mm, 60mm, 100mm Tissue Culture Dishes	Sarstedt or Greiner
6-well Culture Plates	Greiner
Bacterial Culture Dishes	Bibby Sterilin
1.2ml Cryovial	Nalgene
5ml Bijoux	Sarstedt
150x25mm Tissue Culture Plates	Corning
0.5ml, 1.5ml and 2ml microcentrifuge Tubes	Sarstedt
50ml Plastipak Syringes	Becton Dickinson
8.5mm Cuvette 220-1600nm	Eppendorf
Universal Tubes	Bibby Sterilin
5ml and 10ml Stripettes	Bibby Sterilin
25ml and 50ml Stripettes	Continental Laboratory Products
0.2ml 96-well PCR Plates	ABgene
0.2ml Strips of 8 Tubes for PCR	SLS
6 x 26 x 1.0-1.2mm Microscope Slides	VWR
0.4cm Electrode Gap Gene Pulsar Cuvettes	Bio-Rad
96-well Lidded Plates	Corning
Cell Scraper	Sarstedt

c) Miscellaneous Disposable Laboratory Equipment

Item	Supplier
Swann Morton Disposable Sterile Scalpels	SLS
Aluchef Aluminium Foil	VWR
Bodyguards Low Protein Latex Examination Gloves	VWR
Autoclave Tape	VWR
Kimberley Clark Paper Tissue	SLS

d) Sterilisation

Plastic ware and glassware were washed in RBS detergents and rinsed several times in tap water followed by a final rinse in deionised water. Plastic and glassware was dried at 80°C in a hot air oven. Any items requiring sterilisation were autoclaved in a Rodwell MP24 autoclave, supplied by SLS, at 15p.s.i pressure, 120°C for 15 minutes. Filter sterilisation of solutions for tissue culture was carried out using sterile syringe filters.

e) Purified Water

Tap water was passed through a still to produce glass-distilled water. The water was sterilised by autoclaving for 15 minutes at 15 p.s.i. Ultra-pure deionised water was obtained from an installed Purite Prestige Labwater 250 purification system. A Purite Neptune Labwater system provided >18MΩ water for use in molecular biology experiments.

2.1.2 Chemicals, Biochemicals and Molecular Biology Reagents

a) Chemicals

Chemicals were always at least AnalR-grade or equivalent and were stored according to the supplier's instructions.

Unless otherwise stated all chemicals, acids, ethanol and methanol were supplied by VWR. Agarose was supplied by Cambrex Bioscience and pulse-field grade agarose was supplied by Bio-Rad. Thymidine, mitomycin C, hydroxyurea, camptothecin, puromycin and ampicillin were supplied by Sigma-Aldrich. Sigma-Aldrich also provided PMSF, leupeptin, pepstain, BSA and N-laurosarcosyl.

Coomasie brilliant blue, SDS and 30% acrylamide/bis acrylamide solution (37.5:1) were supplied by Bio-Rad. Microcystin phosphotase inhibitor was a kind gift from Professor Carl Smythe (Centre for Developmental Genetics). Hoechst 33342 stain was purchased from Sigma-Aldrich.

b) Biochemicals

Item	Supplier
LiofectAMINE	Invitrogen
T4 DNA Ligase	NEB
Proteinase K	Sigma-Aldrich
Hygromycin B	CalBiochem
Restriction Enzymes	Promega or NEB

c) RT-PCR/PCR Master Mix

2X PCR master mix, purchased from ABgene, was used for the majority of PCR reactions. This master mix contained 75mM Tris-HCl pH 8.8, 20mM $(NH_4)_2SO_4$, 1.5mM $MgCl_2$, 0.2mM of each dNTP, 0.01% Tween 20 and 1.25U *Taq* DNA polymerase.

The AccuPrime *Taq* DNA polymerase system, used for high fidelity amplifications, was purchased from Invitrogen. AccuPrime *Taq* DNA polymerase was provided in a storage buffer of 20mM Tris-HCl (pH 8.0), 0.1mM EDTA, 1mM DTT, stabilizers and 50% (v/v) glycerol. 10X AccuPrime PCR Buffer I and II contained 200mM Tris-HCl (pH 8.4), 500mM KCl, 15mM $MgCl_2$, 2mM dGTP, 2mM dATP, 2mM dTTP, 2mM dCTP, thermostable AccuPrime protein and 10% glycerol.

Native *Pfu* DNA polymerase, purchased from Stratagene, was supplied in 50mM Tris-HCl (pH 8.2), 1mM DTT, 0.1mM EDTA, 0.1% Tween 20, 0.1% Igepal CA-630 and 50% (v/v) glycerol.

One-step RT-PCR experiments were carried out using a *Reverse*-iT One Step RT-PCR kit purchased from ABgene. This kit included a 2X RT-PCR master mix and

50units/µl *Reverse*-iT RTase blend containing RNase inhibitor. The 2X RT-PCR mix contained optimised reaction buffer, 1.25U Thermoprime Plus DNA polymerase, 0.2mM each dNTP and 1.5mM $MgCl_2$. All master mixes and polymerases were stored at -20°C.

d) Molecular Biology Kits

QIAGEN supplied molecular biology kits for DNA extraction from human tissues (QIAamp DNA Mini Kit), RNA extraction from animal cells or tissues (RNeasy Mini Kit), RNA homogenisation (QIAshredder), extraction of DNA from bacterial cell cultures (QIAprep Miniprep Kit) and clean-up of PCR products (QIAquick Gel Extraction Kit or QIAquick PCR Purification Kit).

cDNA synthesis was carried out using the SuperScript II RNase H^- Reverse Transcriptase kit purchased from Invitrogen. This contained 200U/µl Superscript II, 5X first strand buffer and 0.1M DTT. SuperScript II was supplied in 20mM Tris-HCl (pH 7.5), 100mM NaCl, 0.1mM EDTA, 1mM DTT, 0.01% (v/v) NP-40, 50% (v/v) glycerol storage buffer. The 5X first strand buffer was supplied in 250mM Tris-HCl, 375mM KCl, 15mM $MgCl_2$. Oligo-$(dT)_{12-18}$ primer was supplied by Invitrogen.

In the main, sequencing reactions were carried out using a SequiTherm Excel II DNA Sequencing Kit-LC for 25-41cm gels. This kit, supplied by Epicentre Technologies, was designed specifically for use with a LI-COR automated DNA sequencer. Some sequencing reactions, especially those for sequencing mononucleotide runs, were carried out using the Thermo Sequenase Primer Cycle Sequencing Kit from Amersham Pharmacia Biotech. All reagents for the above kits were stored according to the manufacturer's instructions.

e) DNA molecular weight markers

A 100bp DNA ladder (0.5µg/µl), supplied by Invitrogen, was used to estimate size of PCR products on agarose gels. Hyperladder I supplied by Bioline was used for size estimation and quantification of PCR products on agarose gel.

f) Oligonucleotide primers

Unmodified oligonucleotide primers for PCR amplification were ordered from MWG Biotech AG or EurogenTech. Modified infrared dye (IRD) labelled oligonucleotides for sequencing were supplied by MWG Biotech AG.

2.1.3 Preparation of Standard Solutions

Solutions were prepared and stored at room temperature unless otherwise stated.

a) TBE buffer (10X, pH 8.0)

10X TBE was made up using 108g Tris-base, 55g boric acid, 40ml 0.5M EDTA and ddH_2O. The pH was adjusted to 8.0 such that the final volume was 1 litre.

b) TAE buffer (10X, pH 8.0)

10X TAE was made up using 48.4g Tris-base, 11ml acetic acid, 20ml 0.5M EDTA and ddH_2O. The pH was adjusted to 8.0 and the final volume was 1 litre.

c) TE buffer (10X, pH 7.4)

10X TE buffer was made up of 10mM Tris-Cl (pH 7.4) and 1mM EDTA (pH 8.0) and the final pH was adjusted to 7.4.

d) EDTA (0.5M, pH 8.0)

0.5M EDTA (ethylene diamine tetra-acetic acid) was made by dissolving 186.1g of disodium ethylene diamine tetra-acetate into 1 litre of water. The pH was adjusted to 8.0 with NaOH.

e) Phosphate Buffered Saline (PBS)

1X PBS was made with 10g/l NaCl, 0.25g/l KCl, 0.25g/l KH_2PO_4, 1.43g/l Na_2HPO_4 and distilled water. This solution was autoclaved for sterility.

f) Ethidium Bromide (5mg/ml)

One tablet of ethidium bromide, purchased from Sigma-Aldrich, was dissolved in 20ml of distilled water to prepare a 5mg/ml stock solution. Ethidium bromide was used at a working concentration of 0.5µg/ml. Ethidium bromide stocks were kept protected from light.

g) Bromophenol Blue Loading Buffer

0.5g of bromophenol blue was dissolved in 50ml ddH_2O. 50ml of glycerol was then added and this was mixed well. 20X Gibco blue (TBS), purchased from Invitrogen, was then added drop-wise until the colour stayed blue.

h) Formamide Loading Buffer

Loading buffer for single strand conformation polymorphism (SSCP) gels was made up of 0.1% xylene cyanol, 0.1% bromophenol blue, 2mM EDTA, 0.1M NaOH and 95% formamide. This was stored at -20°C.

i) SSCP Fixer

Fixer for SSCP gels was made up of 10% absolute ethanol, 0.5% acetic acid and ddH_2O.

j) SSCP Developer

Developer for SSCP gels was made up of 1.5% NaOH, 0.15% formaldehyde and ddH_2O.

k) Sodium Carbonate

0.75% Na_2CO_3 and ddH_2O were mixed to produce sodium carbonate solution used in SSCP gel developing.

l) Silver Nitrate (0.1%)

1g of silver nitrate was dissolved in 1 litre of water to make 0.1% silver nitrate solution that was kept protected from light.

m) DNA Lysis Buffer

DNA lysis buffer was made from 100mM Tris.HCl (pH 8.5), 5mM EDTA, 0.2% SDS, 200mM NaCl and 100µg/ml Proteinase K.

2.1.4 Tissue Culture Materials

a) Tissue Culture Medium

All tissue culture medium was stored at 4°C and sterility checked before use. Dulbeccos Modified Eagles Medium (DMEM) containing 4.5g/l glucose with L-glutamine was purchased from BioWhittaker or Invitrogen. 1X non-essential amino acids, supplied by BioWhittaker, were added to the medium before it was used for tissue culture. OptiMEM serum free medium was purchased from Invitrogen.

b) Foetal Calf Serum

Virus, endotoxin and mycoplasma screened foetal calf serum (FCS) was bought from Perbio. This was sterile filtered before use.

c) Antibiotics

Initial experiments were carried out with penicillin and streptomycin in tissue culture medium to inhibit the growth of bacterial species that may be harmful to cell yield. Penicillin was purchased from Britannia Pharmaceuticals and streptomycin supplied by Sigma-Aldrich. Penicillin was used at a final concentration of 100U/ml and streptomycin at 100µg/ml in culture medium. Stock solutions of antibiotics were stored at -20°C.

Fungizone, purchased Invitrogen, was used in tissue culture plates when needed to prevent the growth of fungus. This was used at a final concentration of 2µg/ml in growth medium. Fungizone was stored at 4°C.

d) Trypsin

Trypsin was purchased as a sterile 2.5% stock solution from Invitrogen. Trypsin was used at a concentration of 0.025% and stored at 4°C for up to a week.

e) Versene/EDTA

Versene/EDTA was purchased from VWR. 0.2g EDTA was dissolved in 1 litre of PBS (for use at 0.02%), distributed into 10ml aliquots and stored at 4°C until use.

f) Mycoplasma Testing

Mrs. Janet White (Institute for Cancer Studies) tested all cell lines for the presence of mycoplasma. A PCR-based mycoplasma ELSIA kit purchased from Roche was used for testing. All cells tested for this study were found to be free of contamination.

2.1.5 Western Blotting Materials

2.1.5.1 Preparation of Standard Western Blotting Solutions

a) 1.5M Tris (pH 8.8)

1.5M Tris was made by dissolving 187g of Tris-base into 1 litre of ddH_2O and the final pH was adjusted to 8.8 using HCl.

b) 1M Tris (pH 6.8)

Dissolving 121g of Tris-base into 1 litre of ddH2O made 1M Tris. The final pH was adjusted to 6.8 using HCl.

c) Lower Stacking Buffer

Lower buffer for 7.5% western gels was made by dissolving 187g of Tris-base (1.5M) and 4g SDS into 1 litre of water. The final pH was adjusted to 8.8 using HCl.

d) Upper Stacking Buffer

Upper buffer for 7.5% western gels was made by dissolving 60.5g of Tris-base (0.5M) and 4g SDS into 1 litre of water. The final pH was adjusted to 6.8 using HCl.

e) Protein Lysis Buffer

1X lysis buffer was made up of 20mM Tris/Acetate pH 7.5, 0.27M sucrose, 1mM EDTA, 1mM EGTA, 1mM sodium orthovanadate, 10mM sodium beta-glycerophosphate, 50mM NaF, 5mM sodium pyrophosphate and 1% (w/v) Triton X-100. Just before use the following components were added: 0.1% (v/v) beta-Mercaptoethanol, 1μM Microcystin, 0.2mM PMSF and 1X protease cocktail.

f) 100X Protease Cocktail

100X protease cocktail was made up of 5μg/μl leupeptin, 10μg/μl pepstain, 5mg/ml BSA and ddH_2O. This was stored at -20°C.

g) Phenylmethylsulphonyl Fluoride (PMSF)

A 10mg/ml solution was prepared by dissolving 100mg PMSF in 10ml isopropanol. Aliquots of PMSF were stored at -20°C.

h) Protein Loading Buffer

Protein loading buffer was made up using 2% SDS, 62.5mM Tris, 50% glycerol and 0.25mg/ml bromophenol blue. Aliquots of buffer were stored at room temperature and just prior to use 5% β-mercaptoethanol was added.

i) 10X TGS Running Buffer

10X TGS was made up of 30g Tris-base, 144g glycine, 10g SDS and the volume adjusted to 1 litre with ddH_20. This buffer was stored at room temperature.

j) 10X TBS and TBS-T

One litre of 10X TBS was prepared with 24.2g Tris-base, 80g NaCl and ddH_2O. The pH was adjusted to 7.6 with HCl. This buffer was then diluted to a 1X concentration and 0.1% Tween-20 added before using as a wash buffer.

k) Transfer Buffer

Transfer buffer was made of 3.03g Tris-base, 14.4g glycine, 200ml methanol and the volume adjusted to 1 litre with ddH_2O. This was stored at 4 °C.

l) Coomasie Blue Protein Stain and Destain

0.25% Coomasie brilliant blue was combined with 50% methanol, 10% acetic acid and ddH_2O for the protein stain. Destain was made from 10% methanol, 10% acetic acid and ddH_2O.

m) Isobutanol Saturated Water

50ml isobutanol was combined with 200ml distilled water and stored at room temperature.

2.1.5.2 Western Blotting Equipment

a) Coomasie Plus 200 Protein Assay Reagent

Coomasie Plus reagent for use in protein quantification assays was purchased from Perbio.

b) Protein Marker

Pre-stained precision plus protein marker was purchased from Bio-Rad. This marker was supplied in 30% (v/v) glycerol, 2% SDS, 62.5mM Tris, pH 6.8, 50mM DTT, 5mM EDTA, 0.02% NaN_3 and 0.01% bromophenol blue. Marker was stored at -20°C.

c) Nitrocellulose Membrane

Hybond ECL nitrocellulose membranes were purchased from Amersham Pharmacia Biotech. This is a 100% pure, unsupported nitrocellulose membrane.

d) Filter Paper

Extra think 7.5 x10cm filter paper for use in transfer was purchased from Bio-Rad.

e) ECL Detection Kit

ECL Western blotting detection reagents were purchased from Amersham Pharmacia Biotech. This system is a light emitting non-radioactive method for detection of immobilised specific antigens, conjugated with horseradish peroxidase-labelled antibodies.

f) Film, Developer and Fixer

13 x 18cm medical X-ray Fujifilm was supplied by GRI. Universal paper developer and fixer stocks, supplied by Ilford, were diluted 1 in 10 and 1 in 3, respectively, prior to use.

g) Antibodies

Primary Antibody	Supplied By	Dilution Factor for Primary	Mol. Weight (kDa)	Antibody Raised Against
hMRE11	Oncogene	1:800	86	Rabbit
hMRE11	Bethyl Labs Inc.	1:1000	86	Rabbit
NBS1	Oncogene	1:800	95	Rabbit
Phospho-NBS1 (Ser343)	Cell Signalling Technology	1:1000	95	Rabbit
Phospho-Chk2 (Thr68)	Cell Signalling Technology	1:800	62	Rabbit
Phospho-Chk1 (Ser345)	Cell Signalling Technology	1:1000	58	Rabbit
Actin	Sigma-Aldrich	1:2500	37	Rabbit

2.1.6 Microbiological Materials

a) LB Broth

LB broth was made up by suspending 25g LB broth in one litre of deionised water. This suspension was autoclaved as described. The LB broth has a pH of 7.0±0.2 at 25°C. Before use in cultures 100μg/ml of ampicillin was added to LB broth.

b) Agar Plates

For solid culture media that could be inoculated on the surface 12-15g of agar and 25g of LB broth were suspended in one litre of deionised water. The suspension was autoclaved as described.

c) Frozen Storage Buffer

Initially a solution of 10mM potassium acetate (pH 7.5) and 10% glycerol was made. To this solution was added 100mM KCl, 45mM $MnCl_2.4H_2O$, 10mM $CaCl_2.2H_2O$ and 3mM $HACoCl_3$. The pH was adjusted to 6.4 using HCl. This buffer was stored at 4°C.

d) SOB and SOC Medium

SOB medium was made up from 2% Bacto tryptone, 0.5% Bacto yeast extract, 10mM NaCl, 2.5mM KCl, 10mM $MgCl_2$ and 10mM $MgSO_4$. SOC medium is identical to SOB but contains 20mM glucose.

e) E.coli Strains

Strain of E.coli	Genotype	Supplier
DH5α	F⁻ ϕ 80 *lacZ*ΔM15 Δ(*lac*ZYA-argF) U169 *deo*R *rec*A1 *end*A1 *hsd*R17 (r_k^-, m_k^+) *pho*A *sup*E44 λ⁻ *thi*-1 *gyr*A96 *rel*A1	Invitrogen
TOP10	F⁻ *mcr*A Δ(*mrr-hsd*RMS-*mcr*BC) ϕ 80 *lacZ*ΔM15 Δ*lac*X74 *rec*A1 *deo*R *ara*D139 Δ(*ara-leu*)7697 *gal*U *gal*K *rps*L (Str^R) *end*A1 *nup*G	Invitrogen
EZ Competent Cells	[F'::Tn10(Tc') *pro*A^+B^+ *lacI*^{q}ZΔM15] *rec*A1 *end*A1 *hsd*R17 (r_{k12}^-, m_{k12}^+) *lac gln*V44 *thi*-1 *gyr*A96 *rel*A1	QIAGEN

f) Vectors

The expression vector pcDNA3.1/V5-His TOPO TA was supplied by Invitrogen. This vector was supplied as 10ng/μl plasmid DNA in 50% glycerol, 50mM Tris-HCl (pH 7.4 at 25°C), 1mM EDTA, 2mM DTT, 0.1% Triton X-100, 100μg/ml BSA and 30μM phenol red.

The pDrive cloning vector was supplied by QIAGEN, in a linear form ready for use in direct ligation of PCR products. This vector was supplied as 50ng/μl plasmid DNA.

ClonTech supplied the pIRES^{puro3} expression vector, a circular vector with ampicillin and puromycin selective markers. Maps of all the vectors used can be found in Appendix I.

2.1.7 Biological Materials

a) Human Colorectal Cancer Samples

Anonymous archival tissue samples from 106 patients with histologically confirmed sporadic colorectal cancer were obtained from the tumour bank at the Department of Pathology at Sheffield University Medical School. A further collection of 27 right-sided colorectal tumours was made from the same resource. For each tumour sample obtained the adjacent normal tissue was also provided. This was either normal colon tissue or lymph node material. Data provided with samples included a case number and information of either 'tumour' (T) or 'normal' (N), sex and age of the patient and staging information (Appendix VI). The samples were available as formalin-fixed paraffin-embedded blocks. Blood donor control DNA was acquired from a resource obtained by Saeed Rafii (Institute for Cancer Studies). Ethical approval for the use of these samples in this study was provided by the South Sheffield Research Ethics Committee.

b) Human Cell lines

All cell lines used were of human origin and were adherent cells. Details are provided below:

Cell Line	Supplied By	Tissue/Morphology	MMR Defect
HCT-116	ATCC	Colon, carcinoma	$hMLH1^{-/-}$, hPMS2 (reduced expression)
SK-UT-1	ATCC	Uterine, leiomyosarcoma	$hMSH2^{-/-}$
SW480	ATCC	Colon, adenocarcinoma	None
DLD-1	ATCC	Colon, adenocarcinoma	$hMSH6^{-/-}$
HEC-1-A	ATCC	Endometrial, adenocarcinoma	$hPMS2^{-/-}$, hMLH1 (reduced expression)
2774	ATCC	Ovarian, adenocarcinoma	$hMSH2^{+/-}$
SW48	ATCC	Colon, adenocarcinoma	$hMSH6^{-/-}$, hMLH-methylation silenced expression
MRC5VA	CRC Cell Repository	Lung, fibroblasts	None
LS174T	ATCC	Colon, adenocarcinoma	$hMSH6^{-/-}$

2.2 METHODS

2.2.1 Tissue Sample Preparation and microdissection

Microdissection was needed for tumour (and normal) tissue when less than 80% of the sample originated from the tumour (or normal) population. Sections of 5μm were provided on uncoated slides. The paraffin wax was removed from the slides in two washes of xylene. The sample was then re-hydrated using consecutive washes in 100% ethanol, 95% ethanol, 70% ethanol and distilled water. The required tissue was identified using an H&E stained slide and then microdissected out using a scalpel. The tissue was transferred to a 1.5ml microcentrifuge tube along with 25μl Tris-EDTA buffer. Before DNA extraction, these microdissected samples were centrifuged at full speed for 10 minutes to pellet the tissue and the Tris-EDTA buffer was removed. Those samples that did not undergo microdissection had to be xylene treated to remove the paraffin wax. Sections cut into microcentrifuge tubes were treated with 1200μl xylene and vortexed vigorously. The sample was centrifuged for five minutes on full speed at room temperature and the supernatant discarded. The pellet was washed with 1200μl 100% ethanol and vortexed. The sample was again centrifuged at room temperature at full speed for five minutes and supernatant discarded. The ethanol wash was repeated once and the pellet was then air-dried at 37°C for 10-15 minutes.

2.2.2 DNA Extraction

a) DNA Extraction from Human Tissue

DNA was extracted from tissue samples using a QIAamp DNA mini-kit. Following xylene treatment or microdissection the tissues were lysed in 360µl tissue lysis buffer and 400µg proteinase K and incubated at 56°C overnight in an orbital shaker. Following this, 400µl lysis buffer was added; samples were vortexed for 15 seconds and then incubated at 70°C for 10 minutes. The tubes were then briefly centrifuged and 400µl ethanol was added. Samples were again vortexed for 15 seconds and briefly centrifuged to remove drops from the lid of the tube. The samples were then applied to QIAamp spin columns and the DNA was adsorbed onto the silica-gel membrane during a centrifuge step of 8000rpm for one minute. After disposal of the filtrate the column was then washed with 500µl wash buffer to improve the purity of the eluted DNA and centrifuged at 8000rpm for one minute. The filtrate was again discarded, the column washed with 500µl of a second wash buffer to remove residual contaminants and then centrifuged at full speed for three minutes. The column was placed in a clean 1.5ml micro-centrifuge tube and 200µl elution buffer (10mM Tris-Cl, 0.5mM EDTA; pH 9.0) was added to the column. The column was incubated at room temperature for five minutes and then centrifuged at 8000rpm for one minute. This elution step was repeated twice to increase yield of the DNA so that DNA was eluted in a final volume of 600µl elution buffer.

b) DNA Extraction from Human Cell Lines

DNA was extracted from adherent cell lines after removing the medium and washing cells twice with PBS. To each 10cm tissue culture dish 800µl DNA lysis buffer was added, the plate was rocked and left for 2 minutes. A cell scraper was used to scrape off the cells, which were then collected with a pipette and placed in a 15ml centrifuge tube. 200µg proteinase K was added to the tube, mixed and tubes were incubated in a 37°C water bath overnight. An equal volume of isopropanol was then added to the tube and mixed by inverting. DNA was recovered by lifting the aggregated precipitate from the solution using a pipette. This was placed in a 1.5ml microcentrifuge tube and the DNA pellet was allowed to air-dry. The pellet was re-suspended in ddH_2O.

2.2.3 Microsatellite Analysis

Matched normal and tumour DNA were analysed with the Bethesda Consensus panel of microsatellites (Boland et al., 1998). These markers included three mononucleotide (BAT25, BAT26, BAT40), six $(CA)_n$ dinucleotide (MFD15, APC, D2S123, D18S69, D18S58 and D10S197) and one tetranucleotide (MYCL1) microsatellites.

Forward primers were labelled with infrared dye (IRD-700 or IRD-800). PCR amplification was performed with 40ng purified genomic DNA, 2X PCR master mix and 1-2pmoles of each primer. PCR reactions were carried out in a final volume of 10µl and subjected to 40 cycles of amplification in a Primus 96^+ thermocycler. PCR products were analysed on a LI-COR 4200 automated sequencer. PCR profiles and primer sequences for each microsatellite marker are summarised in Appendix II.

2.2.4 PCR Amplification

Normally PCR amplifications were carried out in a total volume of 20µl containing at least 40ng of extracted genomic DNA or 20ng cDNA, 10µl 2X PCR master mix and 6-10pmol of each primer. PCR reactions were subject to the following cycling programme: 1 cycle of 95°C, 3 minutes; 35-40 cycles of 94°C for 30 seconds, 25-40 seconds at the optimally determined annealing temperature for each primer pair (see Appendix II), 72°C for 1 minute per 600bp and 1 cycle of 72°C, 5 minutes. Reactions were maintained at 4°C after cycling and then stored at -20°C until use. Primer sequences and annealing temperatures used in PCR are reported in Appendix II.

For PCR reactions where a more accurate *Taq* polymerase was required the AccuPrime *Taq* DNA polymerase system was used. This system improves PCR specificity and improves the fidelity of *Taq* by 2-fold. PCR amplifications with this system were carried out in a total volume of 25µl containing at least 40ng of genomic DNA or 20ng cDNA, 2.5µl 10X AccuPrime buffer I (for small genomic DNA <200bp, plasmid or cDNA) or buffer II (for genomic DNA 200bp-4kb), 5pmol each primer and 0.5µl AccuPrime *Taq* DNA polymerase. PCR reactions were subject to the following cycling programme: 1 cycle 94°C, 2 minutes; 30-35 cycles of 94°C for 30 seconds, 30 seconds at 55-60°C, 68°C for 1 minute per kb. Reactions were maintained at 4°C after cycling and then stored at -20°C until use.

To create blunt-ended PCR products (i.e. with no A-overhang) 2.5U of *Pfu* was added to PCR products amplified as above. The PCR reaction was then run for 10 more cycles to fill in the DNA ends.

2.2.5 Agarose Gel Electrophoresis

Electrophoresis is the movement of charged molecules through a matrix by an electric field. The mobility of the molecule is dependent on the strength of the electric field, the size and shape of the molecule and the net charge of the molecule.

Agarose electrophoresis gels, stained with ethidium bromide, were used to separate and visualise DNA and RNA products. 0.8-2% agarose gels were used to analyse PCR or RT-PCR products.

For a 1% agarose gel 1g of agarose was weighed out and 100ml of 1X TAE was added. The solution was melted in a microwave in order to dissolve the agarose and the solution was then left to cool to ~60°C. At this point 0.5µg/ml ethidium bromide was added and the gel was poured into the gel tray. After the gel had solidified, 1X TAE running buffer was poured into the gel box, 0.5µg/ml ethidium bromide was added to the running buffer, and the comb was removed. Amplified products were mixed with bromophenol blue loading dye and then loaded, alongside a DNA size ladder, into the wells. Gels were run at 100V for 30-60 minutes, depending on separation needed. The gels were visualised on an UV transilluminator.

2.2.6 Clean-up of PCR Products

A QIAquick PCR purification kit was used for direct purification of PCR products from amplification reactions. A QIAquick gel extraction kit was used for extraction of DNA fragments from standard agarose gels.

In PCR purification, to allow efficient binding of PCR products to the column 5 volumes of binding buffer were added to one volume of PCR reaction. The sample was then applied to a silica-membrane spin column and centrifuged at full speed for one minute to allow adsorption of DNA to the membrane. The flow-through, containing contaminants such as unwanted primers, enzymes and unincorporated

nucleotides, was discarded and salts were removed from the column by adding 750µl wash buffer and centrifuging the column for one minute at full speed. The flow-through was discarded and residual ethanol was removed in an additional one minute centrifugation step. The column was then placed in a clean microcentrifuge tube and DNA was eluted with 50µl elution buffer (10mM Tris-Cl, pH 8.5) in a one minute centrifugation.

During gel extraction, the required DNA fragment was excised from the agarose gel with a clean, sharp scalpel. The gel slice was weighed and 3 volumes of solubilisation buffer were added to one volume of gel. The mixture was incubated at 50°C for 10 minutes to release the DNA from the agarose and one gel volume of isopropanol was added to the tube. The sample was then applied to a spin column and centrifuged at full speed for one minute to allow adsorption of the DNA to the membrane.

The column flow-through was discarded and a further 500µl solubilisation buffer was added to the column. The column was centrifuged at full speed for one minute to remove any traces of agarose. The column was washed with 750µl wash buffer in a one minute centrifugation step to remove contaminating salts. The flow-through was discarded and residual ethanol from the wash buffer was removed by placing the column in a clean microcentrifuge tube and centrifuging at full speed for a further minute. DNA was eluted from the column in 50µl elution buffer (10mM Tris-Cl, pH 8.5).

2.2.7 Single strand conformation polymorphism (SSCP) gels

The principle of the SSCP method is based on the fact that the electrophoretic mobility of nucleic acids in non-denaturing gels is sensitive to both size and shape. Unlike double-stranded DNA, single-stranded DNA is flexible and will adopt a conformation determined by intramolecular interactions and base stacking that is uniquely dependent on composition (Orita et al., 1989). This conformation can be affected when even a single base is changed. Conformational changes can be detected as alterations in the electrophoretic mobility of the single-stranded DNA on a non-denaturing polyacrylamide gel. SSCP is a simple and sensitive method but it does not reveal the nature or position of sequence changes.

a) Casting and Running of SSCP Gels

10% and 12% SSCP gels were made up according to Table 2.2.7.1 below. The gels were poured between vertical glass plates and left to set for ~1 hour. Prior to loading of samples, gels were placed at 4°C to cool for 15 minutes.

Table 2.2.7.1. Composition of SSCP gels

Component	10% SSCP gel	12%SSCP gel
30% Acrylogel	20ml	24ml
1X TBE	6ml	6ml
ddH_2O	34ml	30ml
25% APS	160µl	160µl
TEMED	12µl	12µl

1-2μl of amplified DNA was mixed with denaturing formamide loading dye to a final volume of 10μl. The samples were denatured to single-stranded DNA for 5 minutes at 95°C and then placed on ice for one minute before being loaded onto a 10-12% polyacrylamide gel. Samples were electrophoresed at 17°C in 1X TBE running buffer. Appendix III shows the SSCP running profiles for each of the exons analysed.

b) Silver Staining of SSCP Gels

After electrophoresis SSCP gels were placed in a plastic container for staining. Fixer solution was added and the gel shaken for 10 minutes. The fixer solution was then discarded and the gel was washed with ddH_2O. Gels were then covered with 0.1% silver nitrate and shaken for 20 minutes. Silver nitrate solution was then removed and the gel was washed twice with ddH_2O. SSCP gels were developed in 500ml fresh developer shaking for 25-30 minutes. Once clear bands were apparent on the gel the developer was discarded and 0.75% sodium carbonate solution was added to cover the gel. The gel was shaken for a further 2-3 minutes then the sodium carbonate solution was discarded. The gel was then sealed in a plastic bag and analysed on a light box.

2.2.8 Sequencing

Samples were usually subject to cycle sequencing using a SequiTherm EXCEL II DNA Sequencing Kit-LC for 25-41cm gels. All reagents were thawed on ice and vortexed before use to ensure uniform distribution of components. The following components were added to a microcentrifuge tube to make the premix: 7.2μl 3.5X sequencing buffer, 2pmoles each IRD-labelled primer, 2-3μl amplified DNA template, 5U DNA polymerase and deionised water to 17μl. Four lanes of a 96-well plate were labelled A, C, G and T and 2μl of the termination mixes for A, C, G or T containing

45μM each of dATP, dCTP, dTTP and 7-deaza-dGTP along with the specific ddNTP, were placed in the appropriate well. On ice, 4μl of the premix was added to each of the four wells of termination mix and mixed by pipetting. Each reaction was overlaid with wax and the reactions then underwent the following cycling: 1 cycle of 95°C, 5 minutes; 30-40 cycles of 95°C for 30 seconds, annealing temperature (see Appendix II) for 15 seconds, 70°C for 1 minute. Once cycling was complete, 3μl of formamide loading buffer (95% (v/v) formamide, 10mM EDTA, 0.1% basic fuchsin, 0.01% bromophenol blue, pH 9.0) was added to each reaction ready for gel electrophoresis.

A second technique for sequencing of difficult templates, especially long templates (>750bp) and templates with mononucleotide runs in them, was carried out using the Amersham Thermo Sequenase Primer Cycle Sequencing kit. For each template to be sequenced the following master mix was prepared: 2-3μl amplified template DNA, 2pmoles each IRD-labelled primer and distilled water to 13μl. The components of the master mix were mixed by gentle vortexing. Four wells of a 96-well plate were labelled A, C, G and T for each termination reagent. The A, C, G and T reagents contained 40mM Tris-HCl pH 9.5, 6mM $MgCl_2$, 0.04% Tween-20, 0.04% Triton X-100, 0.08mM 2-mercaptoethanol, 1.67 units/μl DNA polymerase with 0.00028 units/μl *Thermoplasma acidophilum* inorganic pyrophosphatase, 0.4mM dATP, 0.4mM dCTP, 0.4mM 7-deaza-dGTP, 0.4mM dTTP and 1.33μM of the specific dideoxynucleotide terminator. Into each A well 2μl of the A reagent was added and this was repeated for C, G and T. Into each of the four labelled wells 2μl of the master mix was added and mixed by pipetting. Each reaction was overlaid with wax and the reactions underwent the following cycling: 1 cycle of 95°C, 2 minutes; 30-35 cycles of 95°C 30 seconds, annealing temperature (see Appendix II) 30 seconds, 72°C for 1 minute. Once cycling was complete, 4μl of formamide loading buffer was added to

each reaction ready for gel electrophoresis.

Prior to loading samples onto the gel each sample was heated to 95°C for 3 minutes. Dr. Ian Brock (Institute for Cancer Studies) loaded 1µl of each sample into separate lanes of the sequencing gel and reactions were run in a LI-COR automated long-read sequencer. Sequence data was analysed using the Sequencher computer software.

2.2.9 RNA Extraction

RNA was extracted from cells using an RNeasy mini kit. Media was removed from the plates of cells and cells were washed with 10ml PBS. The PBS was discarded and samples were lysed in the presence of a highly denaturing guanidine isothiocyanate-containing buffer which inactivated RNases and ensured isolation of intact RNA. Using a cell scraper cells were gathered together and collected into a 1.5ml microcentrifuge tube. The lysate was vortexed until no clumps of cells were visible. The lysate was pipetted onto a QIAshredder column sitting in a 2ml collection tube, which was centrifuged at full speed for 2 minutes to homogenise the lysate. The flow-through was collected and one volume of 70% ethanol was added to this to provide the appropriate binding conditions for RNA.

Up to 700µl of the sample was then loaded onto the silica-gel membrane of a mini-spin column sitting in a 2ml collection tube. The column was centrifuged for 15 seconds at 10000rpm to allow binding of the RNA and flow-through was discarded. Successive aliquots of the sample were added to the column and centrifuged as above, until all sample had been through the column. Contaminants were removed from the column in three consecutive steps with wash buffers and centrifugation at 10000rpm for 15 seconds. To eliminate any wash buffer carryover the column was placed in a new collection tube and this was centrifuged at full speed for 2 minutes. The column was then placed in a new 1.5ml collection tube and 50µl RNase-free water was

pipetted directly onto the membrane. The column was centrifuged for one minute at 10000rpm to elute RNA. Samples were stored at -20°C.

2.2.10 RT-PCR

RNA is prone to degradation and so RNase-free plastics, RNase-free water and filter tips were used and gloves were worn at all times during RT-PCR set-up.

RT-PCR amplifications were carried out in a total volume of 25µl containing 500ng of extracted RNA, 0.5µl reverse transcriptase blend (includes RNase inhibitor), 12.5µl 2X RT-PCR master mix and 10pmol of each primer. RT-PCRs were carried out using the following profile: 1 cycle of 47°C for 30 minutes for first strand synthesis; 1 cycle of 94°C for 2 minutes for RTase inactivation and initial denaturation; 40 cycles of 94°C 20 seconds, 54-60°C 30 seconds, 72°C 1 minute. RT-PCRs finished with a final extension of 72°C for 5 minutes.

2.2.11 cDNA Synthesis from Total Cellular RNA

When cDNA copies of the total RNA were required Superscript RT was used to reverse transcribe the RNA. RNA was prepared at 2µg in ddH_2O to a total volume of 9.5µl in a reaction tube. In a second tube, a master mix was made up containing 1µl 0.5µg/µl oligo-$(dT)_{12\text{-}18}$ primer, 0.5µl RNA guard (31600 units/ml), 4µl 5X buffer containing 250mM Tris-HCl, 375mM KCl and 15mM $MgCl_2$, 2µl 0.1M DTT, 2µl dNTP mix (10mM each) and 1µl Superscript-RT (200U/µl). The master mix was vortexed and to this 10.5µl volume the 9.5µl RNA was added and mixed. The tube was incubated at room temperature for 10 minutes then at 44°C for 2 hours.

2.2.12 Tissue Culture

Tissue culture was carried out in sterile conditions in a containment 2 laboratory cabinet. All cell lines were sustained in a 37°C, 5% CO_2 humidified incubator.

2.2.12.1 Passage

Cells were passaged when 80-100% confluent. This was determined by visualising cells using a light microscope or indicated by a colour change of medium from red to yellow. This colour change was caused by a decrease in pH in the growth medium. Cells were washed once with PBS to remove proteins and divalent cations that may inhibit the action of the trypsin. Cells were harvested using trypsin/versene. Plates of cells were placed in an incubator for 5 minutes and then cells were dislodged by gently tapping the side of the plate. Cells were re-suspended in a small amount of medium by pipetting with a 5ml or 10ml pipette. Cells were split and re-seeded by adding the desired amount of re-suspended cells to fresh medium in a plate and returning the plate to a 37°C incubator.

2.2.12.2 Cryopreservation

Excess cell stocks could be frozen for storage. Medium was removed from plates that were 60-80% confluent and the cells were washed with PBS. Cells were harvested in medium following trypsin/versene treatment and centrifuged at 1300rpm for 3 minutes. A mixture of 10% DMSO in medium was prepared and the cell pellet was re-suspended in 2ml of this mixture. The cell suspension was aliquoted into 1.2ml cryovials and these were placed at -80°C for storage.

2.2.12.3 Thawing of Cells

Cryovials were removed from the -80°C freezer and placed in 37°C water to thaw the cells rapidly. Rapid thawing minimises the toxic effect of DMSO on cells.

2.2.12.4. Preparation of Dialysed Serum

Small molecules and ions present in foetal calf serum might interfere with dose response experiments and so they need to be removed. This can be done by placing foetal calf serum in dialysis membranes and surrounding the membranes with 1X PBS. The dialysis membranes are semi-permeable and allow molecules under 12-14000 Daltons to pass out into the surrounding buffer. This surrounding PBS buffer was changed five times to achieve a dilution factor of 10^5. The resulting dialysed foetal calf serum was filter sterilised before use.

2.2.13 Microbiological Methods

2.2.13.1 Preparation of Competent Cells

New stocks of competent *E.coli* could be prepared by streaking an agar plate with DH5α and leaving to grow in a 37°C incubator overnight. Twenty 2-3mm diameter colonies were picked from the agar plate and inoculated into a 2 litre flask containing 200ml SOB medium (1 colony per 10ml culture medium; culture volume to flask volume ratio of 1:10). The inoculated medium was incubated in a 37°C shaking incubator until the cell density was 6-9 x 10^7 viable cells/ml (~3-4 hours). The culture was aliquoted into 50ml centrifuge tubes and chilled on ice for 10-15 minutes. Cells were then pelleted by centrifugation at 2000-3000rpm for 15 minutes at 4°C. The cell pellet was thoroughly drained and cells were re-suspended in 66ml (1/3 of the culture volume) of frozen storage buffer (FSB) by gently vortexing. Cells were incubated on ice for 10-15 minutes and again pelleted by centrifugation at 2000-3000rpm for 15

minutes at 4°C. The cell pellet was drained and cells re-suspended in 16ml (1/12.5 of the culture volume) FSB. A 3.5% aliquot of DMSO was added to the centre of the cell suspension and tubes were swirled for 5-10 seconds. Tubes were incubated on ice for 5 minutes. A second 3.5% aliquot of DMSO was added as above and tubes were incubated on ice for 10-15 minutes. 210µl aliquots were placed in chilled 1.5ml microcentrifuge tubes and cells were flash frozen by placing the tubes in dry ice for several minutes. Competent cells were stored at -80°C.

2.2.13.2 Preparation of Agar Plates

Before pouring, solid agar stocks were melted in a microwave and 100µg/ml of ampicillin was added after cooling. About 10ml of agar was then poured onto bacterial culture dishes. The lids of the dishes were replaced while the agar set, then the lids were removed and plates were placed in a containment hood with airflow to allow the plates to dry.

2.2.13.3 Preparation of SOB and SOC Medium

During preparation of SOB or SOC, 2% Bacto-tryptone, 0.5% Bacto-yeast extract, 10mM NaCl and 2.5mM KCl were combined in 18MΩ water. This was autoclaved for 15 minutes at 121°C. Just prior to use 10mM $MgCl_2$, 10mM $MgSO_4$ and 20mM glucose (for SOC only) were filter sterilised through a 0.22µ membrane and combined with the medium. The final pH of the SOC medium was 6.8-7.0

2.2.13.4 PCR Cloning

The amount of PCR product used in the ligation reaction depends on the size of the PCR product and molar ratio of PCR product DNA to vector DNA. The amount required can be calculated using the following equation:

$$\text{ng PCR product required} = \frac{\text{ng of vector used} \times \text{PCR product size (bp)} \times \text{molar ratio}}{\text{Vector size (bp)}}$$

The QIAGEN and TOPO TA cloning kits take advantage of the 3′ A-overhang generated at the end of each PCR product by non-proof-reading *Taq* polymerase. The cloning vectors are supplied in linear form with a single 3′ T overhang so that they specifically and efficiently hybridise with the PCR inserts. The TOPO vector also has topoisomerase-I covalently bound to the vector to prevent recircularisation and to provide the enzymatic activity for ligation.

The pIRES^{puro3} vector was supplied in circular form and therefore had to be cut within the multiple cloning site with a suitable restriction enzyme, usually Eco*R V*, to create a site for insertion of PCR product. PCR products were ligated to the digested pIRES^{puro3} vector in a blunt-end ligation reaction containing PCR product, 5ng vector, 1 unit of T4 DNA ligase and 1X T4 DNA ligase buffer (50mM Tris-HCl, 10mM $MgCl_2$, 10mM DTT, 1mM ATP, 25µg/ml BSA pH 7.5). Ligation reactions were carried out at room temperature overnight. DH5α chemically competent cells then were transformed with 3-5µl of this ligation mixture.

PCR products to be cloned for sequencing were cloned using the QIAGEN PCR cloning kit. For each cloning reaction the subsequent components were combined in the following order in a 10µl reaction: 50ng pDrive cloning vector, 13-26ng PCR product, 5µl 2X ligation master mix containing all reagents and cofactors required for ligation and ddH_2O. The ligation reaction was briefly mixed and incubated for 1 hour

at 4°C. 3-5µl of the ligation mixture was taken for transforming into EZ or DH5α chemically competent cells.

The TOPO cloning kit was used to clone PCR products into the pcDNA3.1/V5-His-TOPO expression vector. The following components were combined in each 5µl cloning reaction: 1µl salt solution (200mM NaCl, 10mM $MgCl_2$), 5ng pcDNA3.1/V5-His-TOPO and 5-10ng PCR product. The reaction mixture was mixed gently and incubated for 5 minutes at room temperature. 3-5µl of the reaction mixture was taken for transformation of TOP10 or DH5α chemically competent cells.

2.2.13.5 Transforming Chemically Competent Cells

Chemically competent cells were removed from their -80°C store and thawed on ice. 3-5µl of the ligation-reaction mixture was added to a 50µl vial of cells and mixed by gently flicking the tube. The vials were incubated on ice for 15-30 minutes and cells were then heat-shocked in a 37°C (TOPO or EZ) or 42°C (DH5α) water bath for 90 seconds. Tubes were returned to ice for 2 minutes and 950µl SOC medium was added. Since SOC is such a rich medium this step of the protocol was carried out near a flame to minimise contamination. Vials were then incubated in a shaking incubator at 37°C, 225rpm for 30-60 minutes to allow expression of the ampicillin resistance marker.

100-150µl transformation mixture was spread onto LB-agar plates containing 100µg/ml ampicillin. These agar plates were incubated overnight in a 37°C incubator to allow colony formation.

2.2.13.6 Preparation of Overnight Cultures

Clones were picked from agar plates following overnight incubation. To reduce the risk of contamination this procedure was carried out near a flame. Aliquots of 5ml LB medium plus 100µg/ml ampicillin were placed in universal tubes. A pipette tip was used to pick a clone from the agar plate and the tip was dropped in the LB medium. The cap of the universal tube was replaced but left loose to ensure enough air was present for bacterial culture growth. Universal tubes were incubated overnight in a shaking incubator at 37°C, 225rpm.

2.2.13.7 Purification of Plasmid DNA

The QIAprep miniprep kit was used for purification of high-copy plasmid DNA from overnight cultures of *E. coli* in LB medium. The overnight culture was centrifuged at 3000rpm for 10 minutes to pellet the bacterial cells and the LB medium was removed. The pellet was re-suspended in 250µl a buffer containing RNase A and transferred to a 1.5ml microcentrifuge tube. To lyse the bacterial cell wall and release the plasmid DNA 250µl of an alkaline lysis buffer was added and samples were mixed by inverting the tube 4-6 times. To neutralise the lysate and adjust to high-salt binding conditions 350µl neutralisation buffer was added and mixed by immediately inverting the tube 4-6 times. The tubes were then centrifuged for 10 minutes at maximum speed to pellet the unwanted components of the reaction. The supernatant was applied to a QIAprep silica-membrane column by decanting and plasmid DNA was selectively adsorbed to the membrane in high-salt conditions by centrifuging for 1 minute at maximum speed. The flow-through, containing RNA, cellular proteins and metabolites, was then discarded.

When *endA*$^+$ strains of *E. coli* were being used the column was washed with 500µl of

a wash buffer that removed any trace nuclease activity that may degrade the plasmid. The flow-through was discarded and salts were removed from the column by washing with 750µl of a second wash buffer and centrifuging for 1 minute at maximum speed. The flow-through was again discarded and the columns were centrifuged for a further minute at maximum speed to remove any residual wash buffer. The QIAprep column was placed in a clean 1.5ml microcentrifuge tube and 50µl elution buffer (10mM Tris-Cl, pH 8.5) was added to the centre of the column. After standing at room temperature for 1 minute the column was centrifuged for 1 minute at full speed to elute the plasmid DNA in low salt. The DNA was stored at 4°C until use.

2.2.14 Restriction Digestion

Restriction digests were carried out by combining the following in a 0.5ml microcentrifuge tube: 1X restriction buffer specific for the enzyme, 1-2U restriction enzyme, 0.1µg/µl Bovine Serum Albumin (BSA) and 0.5-1.5µg DNA. The tubes were then placed at a temperature specific to the restriction enzyme (usually 37°C) for 1-2 hours. The restriction digestion products were analysed on an agarose electrophoresis gel.

2.2.15 Stable Transfection of Adherent Cells

Cultured eukaryotic cells were transfected with plasmid DNA containing the gene of interest for functional studies. Table 2.2.15.1 below shows new cell lines that were produced and the constructs that were transfected in. Further details of mutant MRE11 constructs are provided in Chapter 4 and details of the SCneo recombination reporter are shown in Appendix IV.

2.2.15.1 Transfection with Lipofectamine

The day before transfection, 10^5 cells were seeded in 6 well dishes with 2ml of complete growth medium (DMEM) with serum. The cells were incubated for 18-24 hours at 37°C in a CO_2 incubator to become 50-80% confluent. The transfection efficiency is sensitive to culture confluence therefore the seeding protocol was exactly the same from experiment to experiment.

For each well in the transfection 2µg DNA was diluted into 100µl of medium without serum (Opti-MEM). For each well of the transfection 5µg LipofectAMINE reagent was diluted into 100µl Opti-MEM medium. The diluted DNA and diluted LipofectAMINE reagent were combined, mixed gently and incubated at room temperature for 30-45 minutes to allow DNA-liposome complexes to form.

Cells were taken from the incubator, medium was removed, the cells were rinsed with PBS and 450µl Opti-MEM medium was added. For each transfection 150µl Opti-MEM was added to the tube containing the complexes. Tubes were mixed gently and the diluted complex solution was placed on cells so that the transfection volume was 800µl. The cells were incubated for 18-24 hours at 37°C in a CO_2 incubator.

Following incubation, 800µl of DMEM growth medium with 20% serum was added to cells without removing the transfection mixture. The cells were incubated at 37°C in a CO_2 incubator for a further 18-24 hours.

For continued cell growth following this incubation the medium was replaced with DMEM medium with 10% serum and cells were incubated at 37°C in a CO_2 incubator for 48 hours.

To select for stable expression of the transfected DNA, cells were plated in medium containing the selective agent expressed by the vector. Cells were then incubated at

37°C in a CO_2 incubator until colonies formed. Single colonies were isolated and grown out in selective agent on 10cm tissue culture dishes.

2.2.15.2 Electroporation

2-3x10^6 cells were plated on 10cm tissue culture plates and allowed to grow for 2-3 days. Cells were trypsinised, counted and 1.5x10^6 cells/ml were re-suspended in PBS. To 0.75ml of the cell suspension 15ng SCneo plasmid was added and this mixture was placed in a 0.4cm cuvette on ice for 10 minutes. Cell suspensions were electroporated at 1kV/cm, 960μF then placed on ice for 10 minutes before being plated out on several 10cm dishes in complete medium. To select for cells carrying the SCneo plasmid hygromycin was added to the medium after 48 hours, to a final concentration of 0.1mM. Hygromycin resistant (*hyg*^{R}) colonies were isolated and expanded from each cell line.

To identify strains containing a single copy of SCneo, Southern blotting was carried out on 10μg genomic DNA isolated from each clone. The 1.1kb *Xho*I-*Hind*III fragment radio-labelled with [α-^{32}P]dCTP was used as a probe, and detection was performed by autoradiography. Southern blotting work was carried out by Mr. A. Mohindra (Institute for Cancer Studies).

Table 2.2.15.1. Cell lines created by stable transfection of new constructs.

Cell Line Created	Recipient cell line	Constructs Transfected In	Vectors Used	Selective Agent
SW480/ SN3	SW480	SCneo[a]	SCneo Reporter	0.1mM Hygromycin
SM1[b]	SW480/ SN3	SCneo + MRE11 314del345[c]	SCneo Reporter + pIRES^{puro3}	0.1mM Hygromycin + 1μg/ml puromycin
HCT116/ HN5	HCT116	SCneo	SCneo Reporter	0.1mM Hygromycin

[a]Details of the SCneo construct are provided in Appendix IV.

[b]Two independent SM1 clones (SM1.3 and SM1.6) were created.

[c]For more information of mutant MRE11 constructs see Chapter 4.

2.2.16 Growth Assay

To estimate the growth rate of cell lines 10 plates of 5 x 10^4 cells were plated on 10cm dishes. One plate of cells was trypsinised and counted every 1-2 days and cell numbers were plotted against time.

2.2.17 Toxicity Assay

Cytotoxic responses to various agents were measured to determine differences between transfected and parental cell lines. Unless otherwise stated, toxicity assays were carried out in medium supplemented with dialysed serum (to remove exogenous sources of deoxynucleosides). The cytotoxic agents were prepared by dissolving them in dialysed medium. Plating efficiency of each cell line was calculated by dividing the number of colonies at dose zero by the number of cells plated. Table 2.2.17.1 shows the effect of each toxic agent on the cell.

Table 2.2.17.1. Mode of action of each cytotoxic agent used.

Agent	Action
Thymidine	Depletes dCTP slowing replication fork progression and cells accumulate in S-phase
MMC	Creates DNA interstrand cross links
Hydroxyurea	Inhibits ribonucleotide reductase resulting in replication fork stall and S-phase arrest
Camptothecin	Creates replication-specific double strand breaks
Ionising Radiation	Creates global single and double strand breaks

2.2.17.1 Thymidine Toxicity Assay

Duplicate plates of 500 cells were plated in 10cm tissue culture dishes and treated with varying concentrations of thymidine (0 - 4mM). Plates were incubated at 37°C, 5% CO_2 for 14 days to allow for colony formation. Cells were then stained with 0.4% methylene blue/50% methanol and colonies containing >50 cells were scored. The surviving fraction was determined by dividing the average number of colonies at each dose by the average number of colonies on the control plates (dose 0mM). This number was then divided by the plating efficiency to correct for inter-experiment differences.

2.2.17.2 Mitomycin C (MMC) Toxicity Assay

For doses of less than or equal to 30nM MMC, 200 cells were plated in duplicate in each well of 6-well dishes. For doses >30nM MMC, 200 and 2000 cells were plated in each well of 6-well dishes. Cells were treated with varying doses of MMC from 0 - 100nM and plates were incubated at 37°C, 5% CO_2 for 10-12 days to allow for colony formation. Cells were stained, scored and the surviving fraction calculated as described above.

2.2.17.3 Hydroxyurea (HU) Toxicity Assay

Duplicate plates of 500 cells were plated in 10cm tissue culture dishes and treated with varying concentrations of HU (0 - 500μM). Plates were incubated at 37°C, 5% CO_2 for 14 days to allow for colony formation. Cells were stained, scored and the surviving fraction calculated as described above.

2.2.17.4 Camptothecin (CPT) Toxicity Assay

For zero doses duplicate plates of 200 cells were plated on 6cm tissue culture dishes. For all other doses 200 and 2000 cells were plated on 6cm dishes. Cells were treated with varying doses of CPT from 0 - 40nM and plates were incubated at 37°C, 5% CO_2 for 12-14 days to allow for colony formation. Cells were stained, scored and the surviving fraction calculated as described above.

2.2.17.5 Ionising Radiation (IR) Toxicity Assay

Cells were grown up on 10cm tissue culture dishes before being trypsinised and re-suspended at 5×10^5 cells/ml. Seven 2ml aliquots of these cells were placed in 15ml tubes and put on ice. The seven aliquots represented seven doses: 0, 1, 2, 5, 6, 8 and 10 gray gamma radiation. Cells were irradiated on ice in suspension and then diluted so that 500 cells were plated out on 10cm dishes in medium supplemented with 10% (non-dialysed) foetal calf serum. Plates were incubated at 37°C, 5% CO_2 for 14 days to allow for colony formation. Cells were stained, scored and the surviving fraction calculated as described above.

2.2.18 Recombination Assays

The I-*Sce*I system was developed for estimating the frequency of homologous recombination repair events in cells (Johnson et al., 1999). The system utilises the SCneo recombination substrate (see Appendix IV) that contains two non-functional copies of the neomycin-phosphotransferase (*neo*) gene. One copy (3′ neo) is a 5′ truncation of the *neo* gene so that it lacks the 5′ region but retains the 3′ region. The second copy (S2neo) is the full *neo* gene, having promoter and full open reading-frame, disrupted by an 18bp I-*Sce*I endonuclease site. Both copies of the *neo* gene are on a construct that is stably integrated into the mammalian genome. The two *neo* genes are in direct orientation and separated by a functional hygromycin gene to allow for selection of cells containing the construct.

I-*Sce*I is a yeast mitochondrial intron-encoded endonuclease with an 18bp recognition sequence. pCMV3nls-I-*Sce*I is an expression vector that contains a triplicated nuclear localisation signal fused to I-*Sce*I (see Appendix IV). This expression vector is transiently transfected into cells to induce a double-strand break. Double-strand break repair can occur by non-homologous end-joining that utilises little or no homology and so does not result in a functional *neo* gene. Or repair can occur by homologous recombination, resulting in a functional neo^+ gene that can be scored by resistance of cells to G418. The SCneo recombination substrate and the pCMV3nls-I-*Sce*I expression vector used for these experiments were kind gifts from Dr Maria Jasin, Memorial Sloan Kettering Cancer Centre.

2.2.18.1 Double Strand Break Induced Recombination Assay

Cell lines were plated in selective medium containing hygromycin for 3-5 days prior to the recombination assays.

On day one, 3 x 10^6 cells for each cell line were plated in duplicate on 10cm tissue culture dishes. These plates were incubated overnight at 37°C, 5% CO_2.

On day 2, for each cell line 2μg of pCMV3nls-I-*Sce*I expression vector was diluted into 200μl Opti-MEM and 20μg LipofectAMINE reagent was diluted into 200μl Opti-MEM. The diluted DNA and diluted LipofectAMINE reagent were combined and mixed gently to form the test solution for each cell line. A control solution of 20μg LipofectAMINE in a final volume of 400μl Opti-MEM was also made for each cell line. The test and control solutions were incubated at room temperature for 30-45 minutes to allow DNA-liposome complexes to form. Following this, medium was removed from the cell lines, cells rinsed with PBS and serum-free medium and overlain with 1.6ml Opti-MEM. Control solution was added to one of the two plates for each cell line, and test solution was added to the second plate. The cells were incubated for 5 hours at 37°C in a CO_2 incubator. Transfection mixture was then removed and replaced with 10ml DMEM supplemented with 10% serum. Plates were incubated overnight at 37°C, 5% CO_2.

On day 3 of the recombination assay, cells were trypsinised and counted. For each 'test' 10 plates of 10^5 cells, 5 plates of 5 x 10^4 cells and 5 plates of 2 x 10^4 cells were plated on 10cm dishes. For each 'control' 20 plates of 2 x 10^5 cells were plated on 10cm dishes. 500 cells from each 'test' and 'control' were also plated to measure plating efficiency. Plates were incubated at 37°C, 5% CO_2 overnight to allow cells to attach.

Recombination frequencies were determined by selection in media containing 1mg/ml G418 on day 4. Plates of 500 cells for plating efficiency were not placed under any selection. Cells were incubated for 10-14 days before staining and scoring colonies (as for toxicity assays). All recombination assays were repeated independently three to four times.

2.2.18.2 Cytotoxic Agent Induced Recombination Assays

The SCneo system can also be used to score homologous recombination repair events induced by exposure to cytotoxic agents.

3 x 6-well dishes per cell line were inoculated with 1000 cells and these cells were left to grow out until all 18 wells were confluent. Cells were then trypsinised, plated on 10cm plates and left to grow for a further 3-4 days. Plating relatively small numbers of cells and growing them out to a large number in this way, eliminates pre-existing neo^+ cells. All 18 plates were trypsinised, counted and re-seeded at 10^6 cells per 10cm dish. Cells were left to attach for 5 hours prior to treatment. Three doses of toxic agent were used on cells and 6 plates were treated with each dose for 24 hours. Following the 24-hour treatment the agent was removed and cells were left to recover in complete medium for 2 days. For each of the 18 cell lines 15 plates of 2×10^5 cells were re-plated on 10cm dishes and 500 cells were also plated to estimate plating efficiency. Cells were left to attach overnight at 37°C, 5% CO_2 before adding 1mg/ml G418. Plates of 500 cells for plating efficiency were not placed under any selection. Cells were incubated for 10-14 days before staining and scoring colonies (as for toxicity assays). All recombination assays were repeated independently two to three times. Recombination frequency was calculated by dividing the average number of colonies on the test plates by the average number of colonies on the control plates (dose 0mM).

2.2.19 Western Blotting

Protein samples were separated on the basis of size using sodium dodecyl sulphate polyacrylamide gel electrophoresis (SDS-PAGE). A discontinuous system was used to allow fine resolution of the individual proteins. This type of discontinuous system uses different buffers in the gel and electrode solutions and uses a stacking gel on top of a resolving gel to compress the samples to a thin starting band allowing better resolution.

2.2.19.1 Protein Extraction

Cells were plated at a density of 2 x 10^6 on 10cm tissue culture dishes and left to grow for 24 hours. Some cells were treated with a cytotoxic agent prior to protein extraction so that signalling events caused by the treatment could later be assessed. 10mM thymidine and 2mM hydroxyurea treatments were added to cells and cells were left to grow for a further 24 hours. For cells to be treated with IR, all medium was removed, cells washed with PBS and the plate of cells exposed to 10 gray IR. Medium was then replaced and cells were incubated for a further 2 hours. Protein from untreated control cells and treated cells was extracted 48 hours after initial plating.

Medium was removed from cells, cells were washed four times with PBS to remove serum proteins and the plates were placed on ice to prevent denaturation of proteins. 300µl of protein lysis buffer was added to each plate and cells were removed using a cell scraper and pipetted into a 1.5ml microcentrifuge on ice.

Tubes were centrifuged at full speed for 5 minutes and the supernatant removed and aliquoted. Aliquots of protein were stored at –85°C.

2.2.19.2 Protein Quantification

PBS was used to make 1 in 50, 1 in 100 and 1 in 200 serial dilutions of protein samples. Equal volumes of the protein dilution and Coomasie Plus 200 Protein Assay Reagent were mixed together and 80µl of each dilution was loaded in triplicate to a lidded 96-well plate. Known concentrations of BSA (25µg/ml, 20µg/ml, 15µg/ml, 10µg/ml, 5µg/ml and 1µg/ml) were used as protein standards. Equal volumes of each BSA standard and Coomasie Plus 200 Protein Assay Reagent were mixed together and 80µl of each concentration loaded in triplicate to the 96-well plate. A plate reader then read the absorbance of each solution at 595nm wavelength. By plotting the BSA standard absorbance readings against its known concentration a linear graph could be produced and concentration of the protein samples then estimated from the graph. This method was a variation of the Bradford assay (Bradford, 1976).

2.2.19.3 Casting Discontinuous Polyacrylamide Gels

Western gels were prepared according to the tables below. A 7.5-12% resolving gel was poured between vertical glass plates and overlaid with isobutanol saturated water. The gel was left to set for 30-60 minutes at room temperature. The isobutanol-saturated water was removed and the top of the gel was rinsed with distilled water before the 5% stacking gel was poured on top around the gel comb. The stacking layer was left for 20-30 minutes to set before samples were loaded into the wells. The 7.5% resolving gels were used specifically for obtaining resolution of phosphorylation induced mobility shifts.

Table 2.2.19.3.1. Composition of 8-12% Western resolving gels and 5% stacking gels.

Component	Stacking Gel	Resolving Gel		
	5%	**8%**	**10%**	**12%**
Acrylamide/Bis 37.5:1	0.83ml	2.6ml	3.2ml	3.8ml
1M Tris pH 8.8	Nil	3.75ml	3.75ml	3.75ml
1M Tris pH 6.8	0.63ml	Nil	Nil	Nil
Distilled H_2O	3.45ml	3.45ml	2.85ml	2.25ml
10% SDS	50µl	100µl	100µl	100µl
10% APS	50µl	100µl	100µl	100µl
TEMED	10µl	10µl	10µl	10µl

Table 2.2.19.3.2. Composition of 7.5% Western gels and the corresponding stacking gel.

Component	Stacking Gel	Resolving Gel
Acrylamide/Bis 37.5:1	1ml	5ml
Lower Buffer	Nil	5ml
Upper Buffer	2.5ml	Nil
Distilled H_2O	6.5ml	10ml
10% APS	50µl	100µl
TEMED	10µl	10µl

2.2.19.4 SDS-PAGE and Western Blotting

50µg protein was added to 1X SDS sample buffer and boiled for 3 minutes at 100°C. Heating a protein sample in the presence of a thiol reagent in this way fully dissociates the protein to its subunits. SDS can then associate with the subunits giving them all the same net negative charge so that separation is achieved strictly according to size. Samples were loaded onto the gel alongside 15µl Precision Protein Standards Marker used to estimate molecular weights of protein samples. The protein samples were run at 20mA through the stacking gel and 40mA through the resolving gel until the desired resolution had been obtained. The gel was removed from the glass plates and a clean scalpel was used to remove the stacking gel layer and any dye front still left on the gel. Gels were placed in Towbin transfer buffer for 10 minutes along with one nitrocellulose membrane per gel. Protein bands were transferred from the gel to the membrane in a semi-dry transfer cell at 10V for 30-45 minutes. The membrane was then placed in 5% milk for 1 hour to block non-specific protein binding sites. The primary antibody was diluted into 5% milk according to the manufacturer's instructions (see materials) and poured over the membrane. Membranes were left shaking at 4°C overnight. Unreacted primary antibody was washed off the membrane with four 10-minute washes in 1X TBS-T. The membrane was incubated for 1 hour at room temperature with the secondary antibody diluted 1:1000 in 5% milk, and membranes were then washed 4-5 times for 10 minutes with 1X TBS-T. Detection of the secondary antibody was achieved using the ECL system. An equal volume of detection solution 1 was mixed with detection solution 2 to give a final volume of 0.125ml/cm^2 membrane. Excess buffer was drained from the membrane and membranes were placed on cling-film, protein side up. The ECL detection solutions were pipetted over membranes and incubated for 1 minute at room temperature. Excess detection reagent was drained off and blots were placed in plastic in a film

cassette. In the dark, autoradiography films were placed on top of the membrane and exposed for 30-120 minutes in the closed cassette. Films were developed in the dark by placing them in developing solution for 3 minutes, washing the film in water, then placing in fixing solution for 2 minutes. Films were finally washed in water and then dried.

2.2.19.5 Gel Preservation

Western gels could be preserved following transfer of proteins to the nitrocellulose membrane. The gel was stained in Coomasie Blue protein stain for 1 hour and destained in 3-4 10-minute washes. Gels were then enclosed in cellophane and dried in a gel drier for 2 hours.

2.2.20 Pulse-field gel electrophoresis

10cm tissue culture plates were inoculated with 2-3x10^6 cells 24 hours prior to treatment. Cells were left untreated or treated with 2mM HU, 1-2mM thymidine (TdR), 5-10mM TdR or 10nM CPT for 24 hours. Cells were then trypsinised from the plates and 1x10^6 cells were melted into 0.8% agarose inserts. For the IR treatment, 1x10^6 cells were melted into 0.8% agarose inserts and inserts were placed in tubes in 2ml medium. Tubes were then placed on ice and exposed to 10gy IR. All agarose inserts were then incubated at 50°C in 0.5M EDTA, 1% N-laurylsarcosyl and 1mg/ml proteinase K for 48 hours. Inserts were washed four times for 2 hours in 1X TE buffer before being loaded onto a 0.8% agarose gel (made with pulsed-field grade agarose and 0.5X TBE). Pulsed field gel electrophoresis was carried out at 120° angle, 60-240 seconds switch time at 4V/cm for 24 hours. Gels were subsequently stained in a solution of 0.5X TBE and 1mg/ml ethidium bromide for 12 hours before being visualised on a UV illuminator.

2.2.21 Apoptosis Measurements

Cells were co-transfected with a GFP-plasmid and a pIRES^{puro3} plasmid in a standard 5hr transfection with Lipofectamine (see above). For transient transfection, DMEM containing 20% serum was added to cells without removing the transfection mixture and 22 hours after the start of transfection cells were given fresh DMEM supplemented with 10% serum for 2 hours. 0.01mg/ml Hoechst 33342 stain was added to medium to assess apoptosis based on nuclear morphology. After 30 minutes, cells were observed by fluorescence microscopy and a minimum of 500 nuclei expressing GFP were counted. Cells were counted as apoptotic if their nuclei were obviously bright blue and condensed.

2.2.22 Statistical Tests

Chi-squared, Student t-test, regression analysis and p values were calculated using Microsoft Excel or by using the Stata statistics and data analysis package. Haplotype analysis was performed by Dr. Angie Cox (Institute for Cancer Studies) using the PMplus programme (Zhao et al., 2000).

CHAPTER 3

Analysis of Candidate Genes

3.1 Introduction

Homologous recombination (HR) repair is an important pathway because it mediates faithful repair of DNA damage and prevents increased levels of illegitimate repair that may contribute to genetic instability. In addition to the role in maintaining genomic integrity, other work in the laboratory indicated that the HR repair pathway is defective in some mismatch repair (MMR)-deficient tumour cells (Mohindra et al., 2002), suggesting that HR genes are mutational targets in tumour development. Therefore, this study examined whether genes involved in the HR pathway were altered in colorectal cancers.

The *XRCC2* and *XRCC3* genes, along with *Rad51B*, *Rad51C* and *Rad51D*, are *Rad51* paralogs that may assist *Rad51* during HR. Cells that lack *XRCC2* or *XRCC3* are highly sensitive to DNA cross-linking agents such as mitomycin C (MMC), show genetic instability and possess HR defects (Brenneman et al., 2000, Johnson et al., 1999, Pierce et al., 1999). Severe homozygous mutations of *XRCC2* and *XRCC3* are embryonic lethal (Liu et al., 1998). However, mutations or polymorphisms of these genes giving more subtle effects on DNA repair capacity may have implications for cancer susceptibility in the population.

Mus81 was recently identified as a putative Holliday junction resolvase with a potential role in cleavage of a class of DNA structures that form at stalled or collapsed replication forks (Boddy et al., 2000, Chen et al., 2001). Cells with a defective *Mus81* show a checkpoint-dependent delay in the cell-cycle and do not display timely completion of DNA replication (Boddy et al., 2001). Loss of *Mus81* function may lead to accumulation and persistence of anomalous DNA structures in the cell that, potentially, could contribute to a malignant phenotype.

3.2 Aims and Objectives

Given that the HR pathway is defective in certain MMR-deficient cells (Mohindra et al., 2002) the hypothesis for this study was that the HR repair pathway is modified as a downstream event in the development of colorectal cancers, especially in those colorectal tumours already deficient in MMR. The primary objective in investigating this hypothesis was to determine whether there were any mutations of the candidate HR repair genes, *XRCC2*, *XRCC3* and *Mus81*, in a random collection of colorectal cancer samples and in a set of right-sided MSI^+ colorectal tumours using SSCP-PCR and sequencing. Polymorphisms that were detected during this study would be analysed to establish whether they were in Hardy-Weinberg equilibrium and evaluated to determine whether they were significantly associated with colorectal cancer. Any alterations of the candidate genes that appeared to contribute to colorectal cancer development or progression would be further investigated.

3.3 Characterisation of Colorectal Tumours

Human colorectal tumours were collected in two separate series. The first consisted of 106 tumours with histologically confirmed sporadic colorectal cancer diagnosed between 1997 and 1998. This was a random collection to reduce bias and attempt to eliminate confounding variables. The second collection included twenty-seven right-sided tumours, which are known to be predominantly microsatellite unstable (Cotran et al., 1999), to try to enrich the sample for unstable tumours. Since no molecular data were available for these tumours they were classified according to their microsatellite instability (MSI) status.

Tumour and corresponding normal DNA pairs were tested using the Bethesda panel of microsatellite markers. MSI was defined by the presence of novel bands following PCR amplification of tumour DNA that were not present in PCR products of the corresponding normal DNA. For the first collection of 106 tumours five mono- and di-nucleotide runs (BAT25, BAT26, MFD15, D2S123 and APC) were tested initially and a further five markers (BAT40, D18S58, D18S69, D10S197 and MYCL1) were used to distinguish between microsatellite stable and low microsatellite unstable tumours. The MSI status of the right-sided tumour collection was determined by testing all ten markers in all 27 tumours.

Colorectal tumours were scored as MSI-H (high MSI) when $\geq$ 40% of the tested markers were unstable. A score of MSI-L (low MSI) was given when <40% of markers tested were unstable and samples were considered stable when none of the tested markers showed instability (Figure 3.3.1). Results of the MSI classification are shown in Table 3.3.1.

Table 3.3.1. MSI status of samples from the first collection which was randomly chosen, the second right-sided collection and the combined collection.

Colorectal Tumour Collection	Frequency of MSS (%)	Frequency of MSI-L (%)	Frequency of MSI-H (%)	Total (%)
Initial randomly chosen tumours	99 (93.4)	3 (2.8)	4 (3.8)	106 (100)
Right-sided tumours	14 (51.9)	3 (11.1)	10 (37.0)	27 (100)
Total collection	113 (85.0)	6 (4.5)	14 (10.5)	133 (100)

Figure 3.3.1. Examples of banding patterns seen for the Bethesda microsatellite markers. **(A)** Normal (N) and tumour (T) DNA samples from the same patient show different banding patterns in these markers indicating microsatellite instability. **(B)** Normal and tumour DNA from the same patient shows the same amplification products indicating these samples are microsatellite stable (MSS).

A

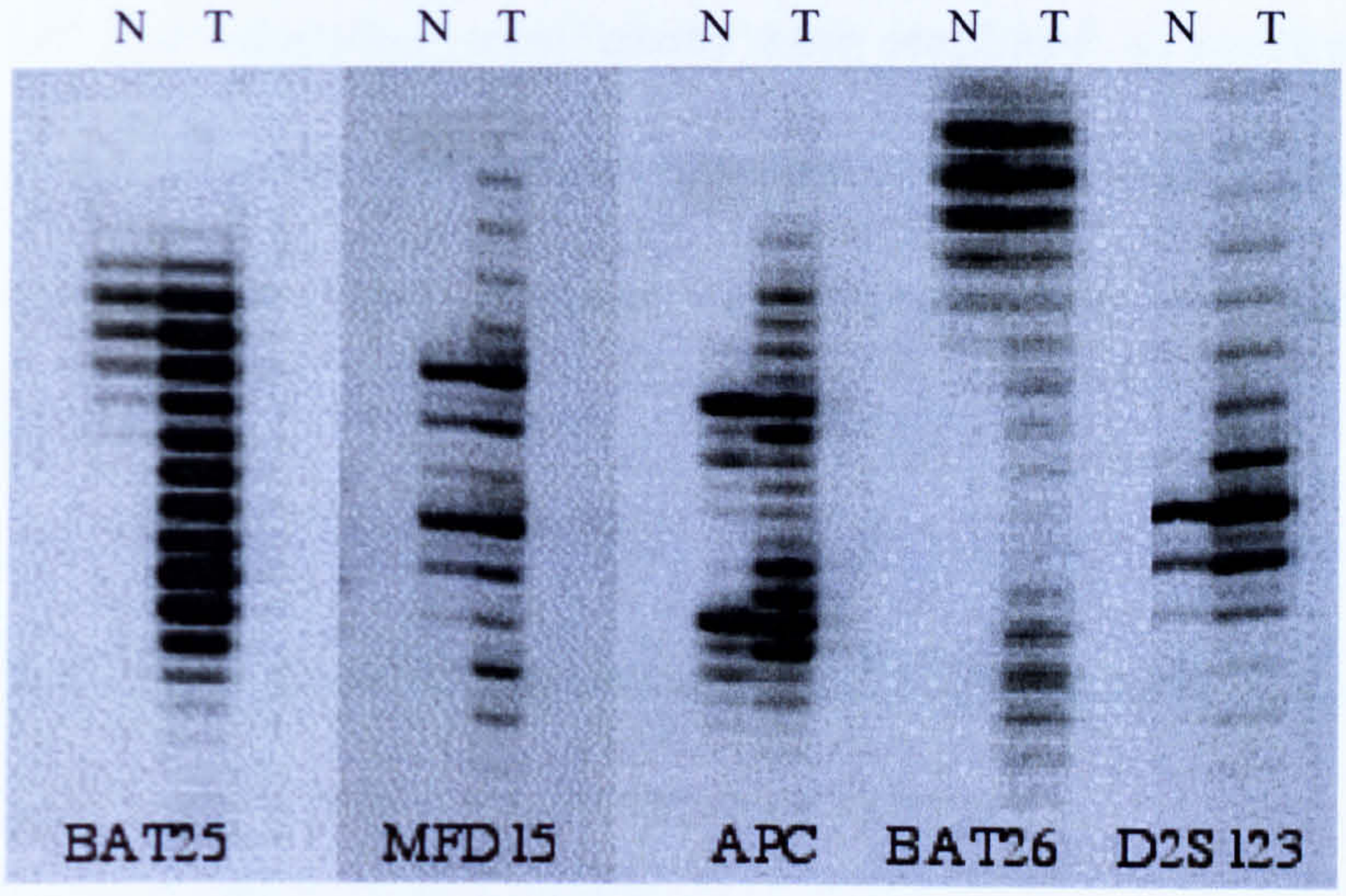

B

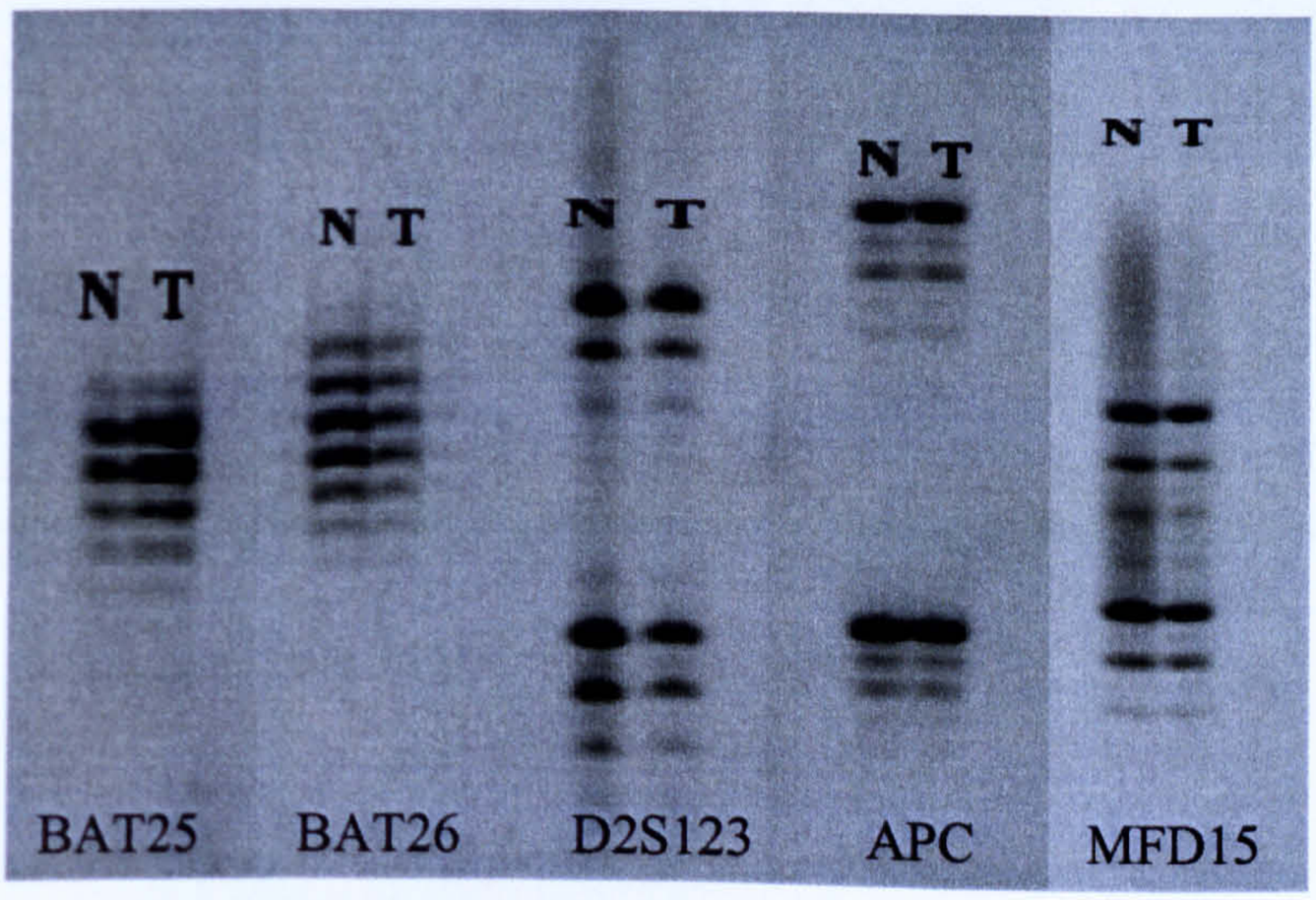

3.4 SSCP Analysis of Colorectal Tumours

The full coding sequence of each of the candidate genes was amplified by PCR in 106 colorectal tumours. PCR products were visualised on agarose gels and once it had been established that the correct fragment had been amplified, products were run on single-strand conformation polymorphism (SSCP) polyacrylamide gels to screen for base changes. A product size of 200-250bp is optimum for screening on SSCP (Orita et al., 1989) and therefore some exons were amplified as overlapping fragments to reduce the product size. Several samples showed altered banding patterns when run on SSCP gels but when these samples were sequenced no base change was apparent (Table 3.4.1).

Table 3.4.1. False positives can occur with SSCP. Samples that appear to have an altered SSCP pattern often have no sequence change.

Gene Amplified	No. of fragments amplified	No. of altered SSCP patterns	No. of altered sequences	No. of False Positives (%)
XRCC2	6	30	16	14 (46.7)
XRCC3	9	158	110	48 (30.4)
Mus81	16	235	194	41 (17.4)

3.5 *XRCC2* Mutation Screening

Sequencing of the *XRCC2* gene in tumour DNA from several individuals revealed a previously reported heterozygous G-A transition resulting in the alteration of amino acid arginine 188 to histidine (Figure 3.5.1). The functional consequences of this polymorphism are slight and previous investigations reported the allele frequency of the variant G allele of XRCC2 R188H in blood donor controls as 0.06 (Rafii et al., 2002). Using this published control allele frequency it was possible to compare unmatched controls with case data (Table 3.5.1). This comparison showed that there was no significant difference in genotype frequencies between cases and controls for XRCC2 R188H ($\chi^2 = 0.91$, $p = 0.6$).

It was observed in this study that the allele frequency of the G allele in colorectal cancer cases was 0.08. Using this information it could be shown that the genotype frequencies presented in colorectal cancer cases were consistent with those expected under Hardy-Weinberg equilibrium ($\chi^2 = 0.7$, $p = 0.7$) (Table 3.5.1).

3.6 *XRCC3* Mutation Screening

Screening of the *XRCC3* gene in tumour DNA revealed several previously reported polymorphisms. During screening of *XRCC3* exon 4 a C-T polymorphism in intron 4 at position 8995 was detected (Figure 3.6.1). PCR primers that had been designed to amplify the full coding sequence of *XRCC3* also included some overlapping intronic sequence which allowed this sequence variant to be seen.

SSCP analysis of exon 7 revealed six different patterns (Figure 3.6.2, A-F) and sequencing of these samples showed the presence of two polymorphisms. The first was a C-T polymorphism in exon 7 at 18067 resulting in an alteration of amino acid threonine 241 to methionine (T241M) and the second an A-G polymorphism in intron 6 at position 17893 (Figure 3.6.3).

The allele frequencies observed in the cancer population were used to test whether the genotype distributions for each polymorphism were in Hardy-Weinberg equilibrium (Table 3.6.1). The genotype frequencies in the tumour population for all polymorphisms were consistent with those expected under Hardy-Weinberg (intron 4 $\chi^2 = 0.0055$, $p = 0.97$, intron 6 $\chi^2 = 0.39$, $p = 0.82$ and exon 7 $\chi^2 = 1.95$, $p = 0.38$).

All three polymorphisms in *XRCC3* had been previously reported in healthy individuals (Shen et al., 1998). The reported control allele frequencies were used to estimate genotype distributions for a control population (Table 3.6.1). This analysis showed that none of the polymorphisms detected were significantly different between cases and controls (intron 4 $\chi^2 = 0.5$, $p = 0.78$, intron 6 $\chi^2 = 1.59$, $p = 0.45$ and exon 7 $\chi^2 = 2.4$, $p = 0.3$).

However, the control genotype distributions had been estimated using allele frequencies from an unmatched normal population. To attempt to match the case and control data more closely, *XRCC3* exon 7 genotype frequencies from the colorectal cancer population were compared to those obtained from a South Yorkshire collection of mammography screening controls (J. Shorto and S. Rafii, Institute for Cancer Studies) (Table 3.6.2). This showed that there was no statistically significant difference between cases and controls for T241M ($\chi^2 = 3.03$, $p = 0.22$).

Figure 3.6.1 **(A)** During SSCP screening of *XRCC3* exon 4 11/106 samples showed an extra band (shown by blue arrow) and were sequenced to check for base changes. **(B)** Sequencing revealed a C-T heterozygous polymorphism in the intronic region surrounding exon 4 at position 8995 that was indicated by the presence of a C and T peak at the same position. **(C)** Samples with the more common SSCP pattern were sequenced and found to have a wild type C/C homozygote genotype at position 8995. The rare T/T genotype was not seen.

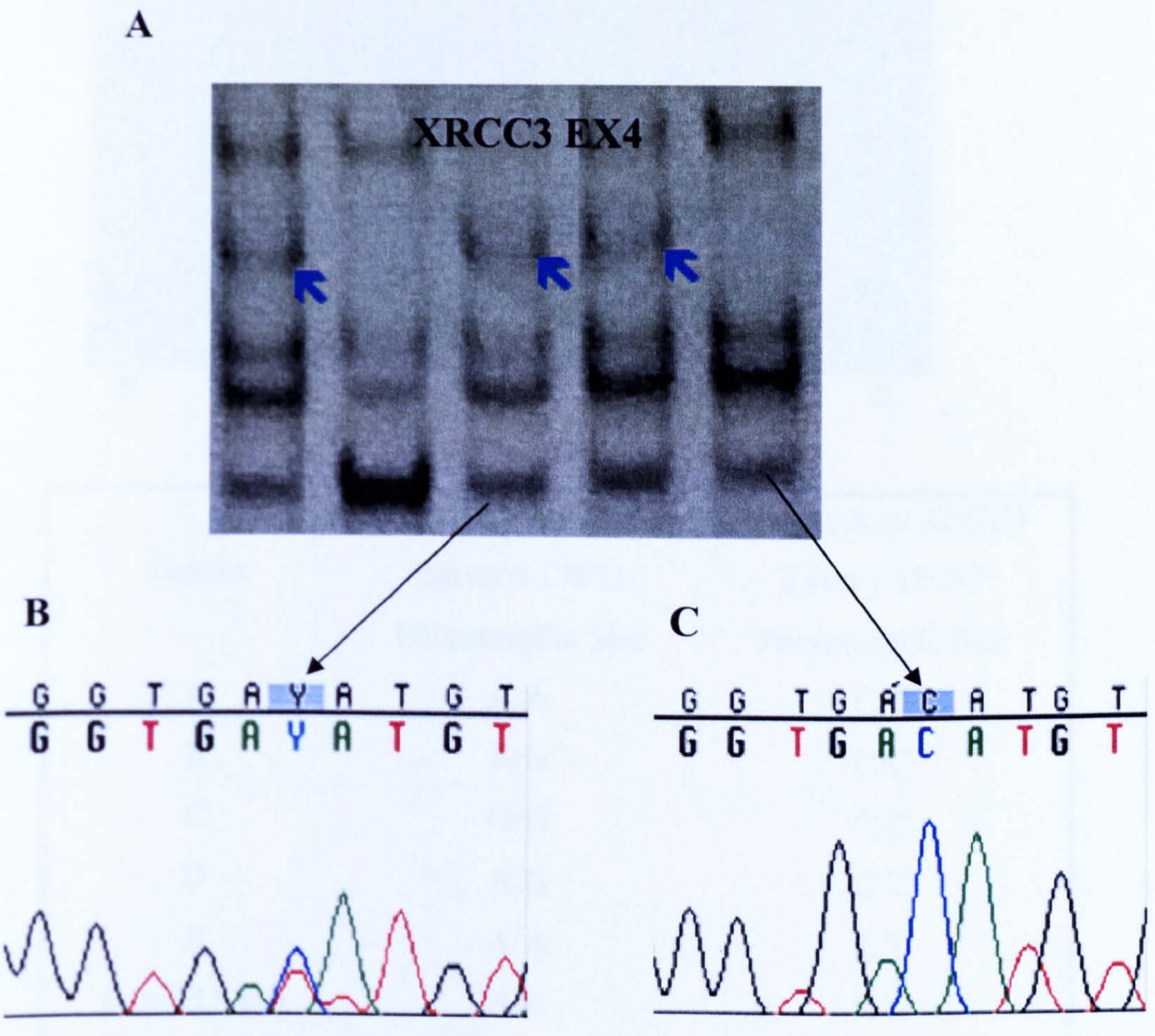

Figure 3.6.2. SSCP gel analysing *XRCC3* exon 7. Six different patterns (A-F) were seen suggesting that more than one polymorphism was being detected. Sequence analysis revealed two polymorphic loci, one in exon 7 and one in intron 6. The table shows which SSCP pattern corresponds to which genotype at each of the polymorphic loci.

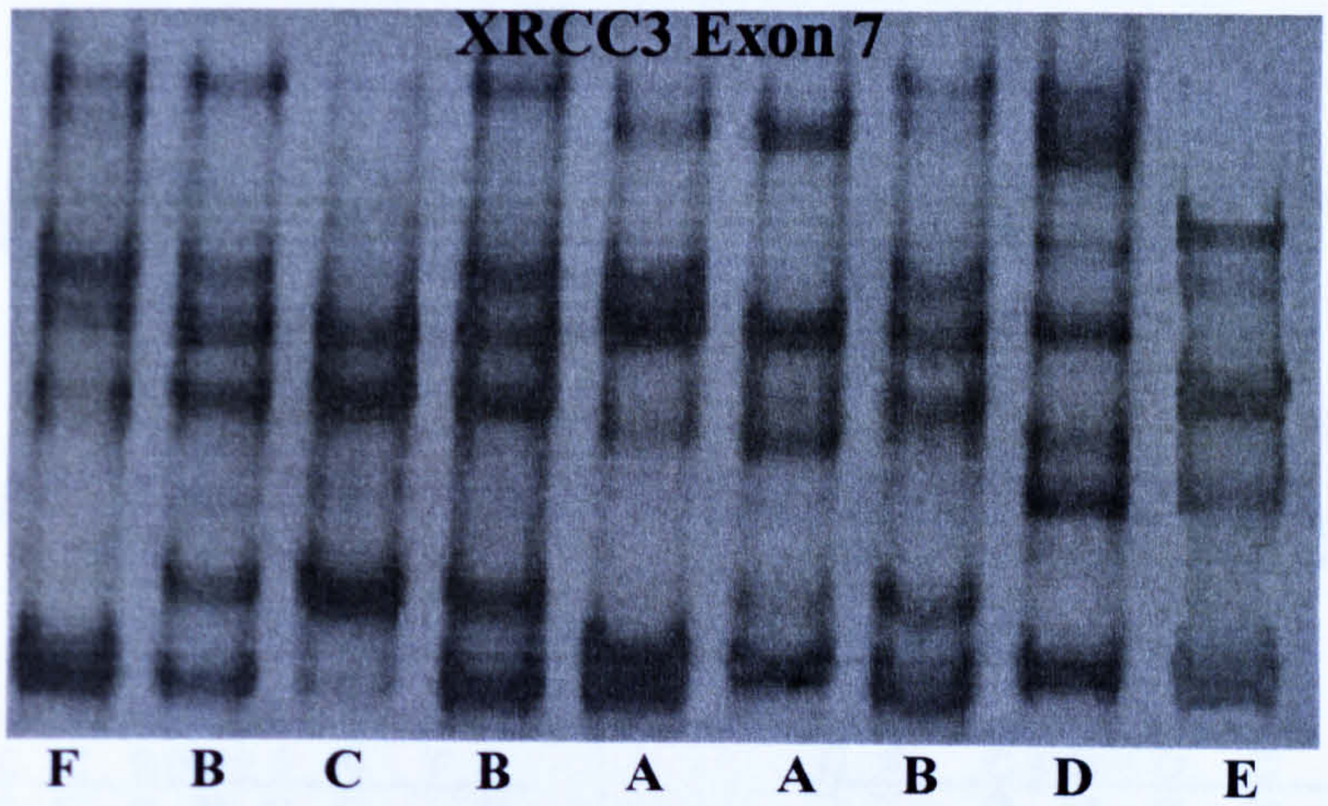

Pattern	Genotype at *XRCC3* Intron 6 17893 Polymorphic Site	Genotype at *XRCC3* Exon 7 18067 Polymorphic Site
A	A/A	C/T
B	A/G	C/C
C	G/G	C/C
D	A/G	C/T
E	A/A	T/T
F (wild type)	A/A	C/C

Figure 3.6.3. Sequence chromatograms for the polymorphisms in *XRCC3* intron 6 and exon 7. **(A)** Chromatograms show the C/C homozygous wild type, C/T heterozygote and the T/T homozygote genotypes for the exon 7 polymorphic site. **(B)** Sequence analysis showed examples of the A/A wild type homozygote, A/G heterozygote and the variant G/G homozygote genotypes for the intron 6 polymorphic site.

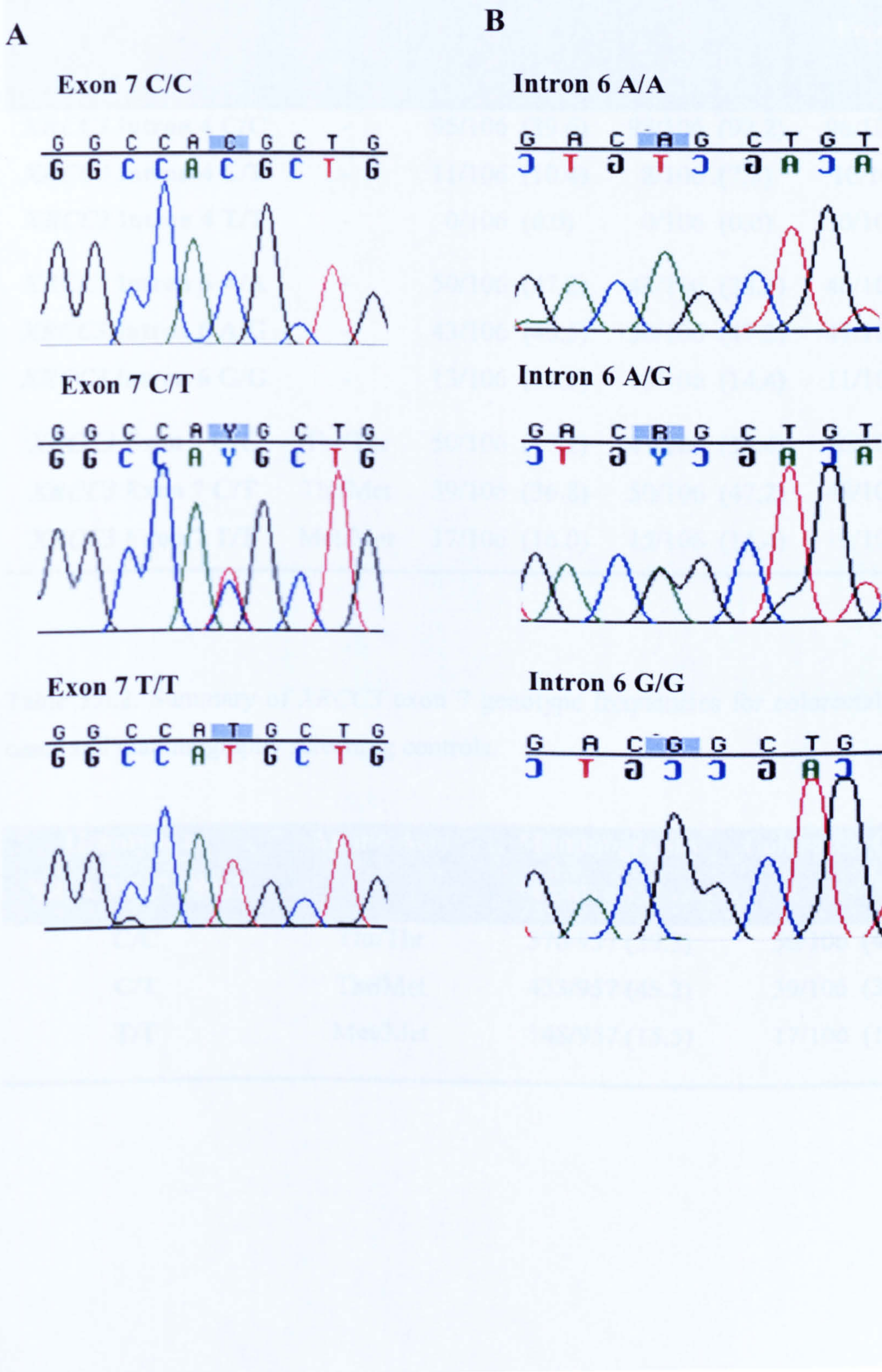

Table 3.6.1. Genotype frequency distributions of each polymorphism in a cancer and calculated control population.

[a]Reported control allele frequencies: intron 4 (T) = 0.04, intron 6 (G) = 0.38, exon 7 (T) = 0.38

[b]Allele frequencies in cases: intron 4 (T) = 0.05, intron 6 (G) = 0.33, exon 7 (T) = 0.34

Genotype	Amino Acid	Cases (%)	Controls [a] (%)	H-W Expected Frequency [b] (%)
XRCC3 Intron 4 C/C	-	95/106 (89.6)	98/106 (92.2)	96/106 (90.2)
XRCC3 Intron 4 C/T	-	11/106 (10.4)	8/106 (7.8)	10/106 (9.5)
XRCC3 Intron 4 T/T	-	0/106 (0.0)	0/106 (0.0)	0/106 (0.3)
XRCC3 Intron 6 A/A	-	50/106 (47.2)	41/106 (38.4)	48/106 (44.9)
XRCC3 Intron 6 A/G	-	43/106 (40.5)	50/106 (47.2)	47/106 (44.2)
XRCC3 Intron 6 G/G	-	13/106 (12.3)	15/106 (14.4)	11/106 (10.9)
XRCC3 Exon 7 C/C	Thr/Thr	50/106 (47.2)	41/106 (38.4)	46/106 (43.4)
XRCC3 Exon 7 C/T	Thr/Met	39/106 (36.8)	50/106 (47.2)	48/106 (45.3)
XRCC3 Exon 7 T/T	Met/Met	17/106 (16.0)	15/106 (14.4)	12/106 (11.3)

Table 3.6.2. Summary of *XRCC3* exon 7 genotype frequencies for colorectal cancer cases and mammography screening controls.

Genotype at XRCC3 Ex7 18067	Amino Acid	Mammography Controls (%)	Colorectal Cancer Cases (%)
C/C	Thr/Thr	376/957 (39.3)	50/106 (47.2)
C/T	Thr/Met	433/957 (45.2)	39/106 (36.8)
T/T	Met/Met	148/957 (15.5)	17/106 (16.0)

Linkage analysis of the exon 7 and intron 6 loci in 106 samples suggests that these two polymorphisms are strongly linked ($\chi^2 = 38.97$, $p = 7.07x10^{-8}$) (Table 3.6.3). Haplotype analysis of all three polymorphisms of *XRCC3* showed that the intron 4 8995, intron 6 17893 and exon 7 18067 sites are in linkage disequilibrium ($\chi^2 = 55.36$, $p = 2.7x10^{-11}$) and there are four common haplotypes (Table 3.6.4). The 17893 and 18067 polymorphisms were considered alone and haplotype frequencies compared to previously reported data that suggested an association between these two polymorphic sites (Kuschel et al., 2002). This analysis showed that the haplotype frequencies obtained in this study were consistent with those previously reported ($\chi^2 = 0.006$, $p = 0.97$) (Table 3.6.5).

Table 3.6.3. The polymorphisms at exon 7 and intron 6 of *XRCC3* are in linkage disequilibrium.

Genotype at XRCC3 Exon 7 18067 locus	Genotype at XRCC3 Intron 6 17893 locus		
	A/A	A/G	G/G
C/C	12/106 (11.3)	25/106 (23.6)	13/106 (12.3)
C/T	21/106 (19.8)	18/106 (17.0)	0/106 (0.0)
T/T	17/106 (16.0)	0/106 (0.0)	0/106 (0.0)

Table 3.6.4. Haplotype analysis for *XRCC3* polymorphisms.

Allele at Intron 4	Allele at Intron 6	Allele at Exon 7	Haplotype Independent	Frequency w/Association
C	A	C	0.417228	0.282185
C	A	T	0.219120	0.344247
C	G	C	0.201320	0.316965
C	G	T	0.105729	0.000000
T	A	C	0.025034	0.048004
T	A	T	0.013147	0.000093
T	G	C	0.012079	0.008507
T	G	T	0.006344	0.000000

Table 3.6.5. Comparison of haplotype frequencies observed for *XRCC3* intron 6 and exon 7 polymorphisms in colorectal cases and previously reported breast cancer cases (Kuschel et al., 2002).

XRCC3 Haplotype[a]	Observed Haplotype Frequency	Reported Haplotype Frequency
AC	0.3302	0.3056
AT	0.3443	0.3869
GC	0.3250	0.3023
GT	0.0000	0.0053

[a]Polymorphic bases listed in 5′ to 3′ order

3.7 *Mus81* Mutation Screening

SSCP screening of the *Mus81* gene in DNA from colorectal cancer patients detected altered banding patterns in exon 6, exon 9, exon 11 and exon 12. Subsequent sequencing revealed six previously unreported and two reported polymorphisms (Figures 3.7.1-3.7.5). To determine whether the polymorphisms were tumour specific and whether there was any loss of heterozygosity (LOH) in the tumour samples, normal and corresponding tumour DNA was analysed side-by-side on SSCP to detect differences (Figure 3.7.6).

Six of the detected polymorphisms did not give rise to amino acid changes but two, C314G in exon 6 and C617T in exon 9, led to non-synonymous amino acid changes (Table 3.7.1). These polymorphisms were further analysed in a population of 85 normal blood donor controls to determine the frequency of each genotype in a normal population. These genotype frequencies were compared to those observed in the tumour collection to determine whether there was any difference between the cases and controls and therefore whether the polymorphisms were tumour-associated (Table 3.7.2). Statistical analysis showed that the genotype frequencies for exon 6 C314G did not differ significantly between cases and controls ($\chi^2 = 3.18$, $p = 0.204$). Similarly, the genotype frequency distributions for exon 9 C617T were not statistically significantly different between colorectal cancer cases and blood donor controls ($\chi^2 = 0.18$, $p = 0.91$).

The frequency of the variant alleles in the tumour population was used to estimate genotype frequency distributions as predicted by Hardy-Weinberg (Table 3.7.2). This analysis showed that both C314G and C617T non-synonymous polymorphisms were in Hardy-Weinberg equilibrium in the colorectal cancer cases ($\chi^2 = 0.01$, $p = 0.99$ and $\chi^2 = 0.0$, $p = 1$, respectively).

Frequencies of the variant alleles observed in the colorectal cancer population were also used to estimate the Hardy-Weinberg genotype distributions for each of the synonymous polymorphisms (Table 3.7.3). This analysis showed that genotype distributions for all polymorphisms, except A840G, were consistent with those expected under Hardy-Weinberg equilibrium. To determine if this A840G difference was due to an association between loci, haplotype analysis was carried out on all the polymorphisms detected in *Mus81*. This analysis showed that there were three common haplotypes that occurred in >5% of cases, three haplotypes that were seen in 1-5% of cases and seven haplotypes seen in <1% of cases (Table 3.7.4). The other 243 possible haplotypes were not seen in any of the cases and the 8 loci examined were strongly associated ($\chi^2 = 423.29$, $p = 2x10^{-11}$).

Table 3.7.1. Synonymous and non-synonymous amino acid changes seen in *Mus81* during analysis of colorectal cancer samples.

Locus	Base Change	Amino acid number	Amino acid	Previously Reported
***Mus81* Exon 6**	C312T	104	Ala	Yes
***Mus81* Exon 6**	C314G	105	Pro-Arg	Yes
***Mus81* Exon 9**	C671T	224	Thr-Met	No
***Mus81* Exon 9**	T711C	237	Ala	No
***Mus81* Intron 9**	G-A	-	-	No
***Mus81* Exon 11**	A840G	280	Arg	No
***Mus81* Exon 11**	T852C	284	Cys	No
***Mus81* Exon 12**	T1023G	341	Thr	No

Figure 3.7.1. SSCP and sequencing analysis of *Mus81* exon 6 detected two polymorphic sites; C312T (blue boxes) and C314G (pink boxes). **(A)** Analysis of exon 6 revealed three different SSCP patterns. **(B)** Sequencing chromatogram showing the variant 312 T/T and 314 G/G homozygous genotype. **(C)** Chromatogram showing sample with a wild type sequence. **(D)** Sequence data showing double heterozygote C/T and C/G for *Mus81* exon 6.

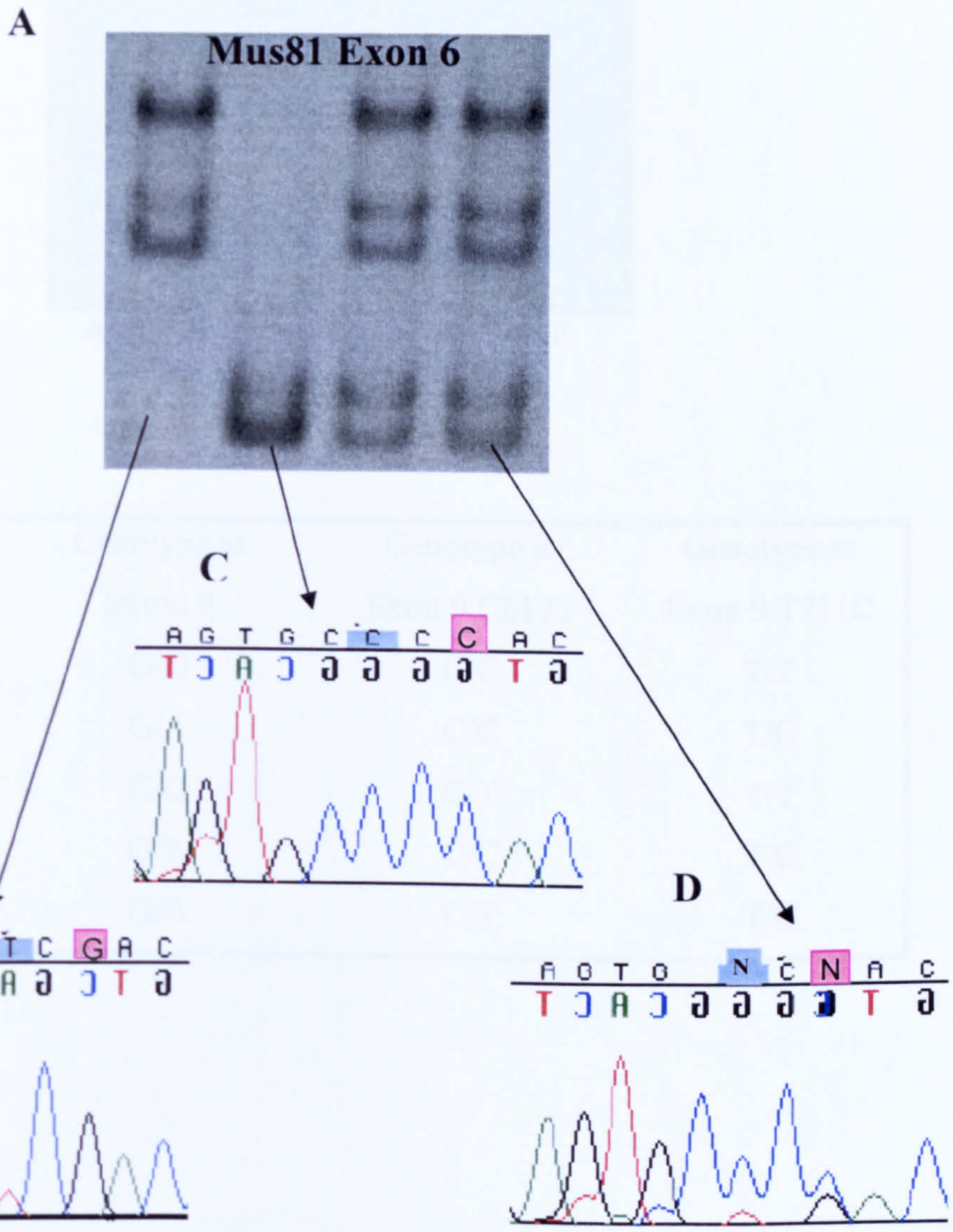

Figure 3.7.2. SSCP analysis of *Mus81* exon 9 showed several different banding patterns suggesting the presence of several polymorphisms. Sequencing revealed two polymorphic sites in exon 9 (positions 617 and 711) and one in intron 9. The genotype corresponding to each SSCP pattern is shown in the table below.

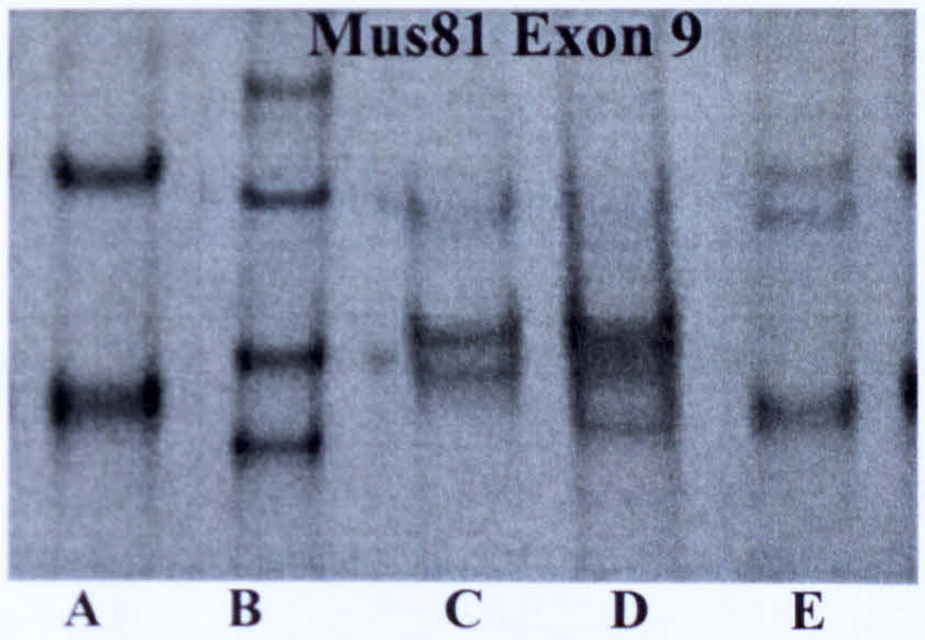

Pattern	Genotype at Intron 9	Genotype at Exon 9 C617T	Genotype at Exon 9 T711C
A	G/G	C/C	T/T
B	G/A	C/C	T/C
C	G/G	C/T	T/T
D	G/A	C/C	T/C
E	G/A	C/T	T/C

Figure 3.7.3. Sequence chromatograms showing the three polymorphisms in *Mus81* exon 9. **(A)** Chromatograms showing the detected G/G and G/A genotype for the intron 9 polymorphic site. The rare A/A genotype was not seen for this locus. **(B)** Sequence analysis showing the C/C and C/T genotypes for the C617T exon 9 polymorphic site. The rare T/T genotype was not seen. **(C)** Chromatograms showing the T/T and T/C genotypes for the T711C exon 9 polymorphic site. No samples were observed that were C/C homozygote at this locus.

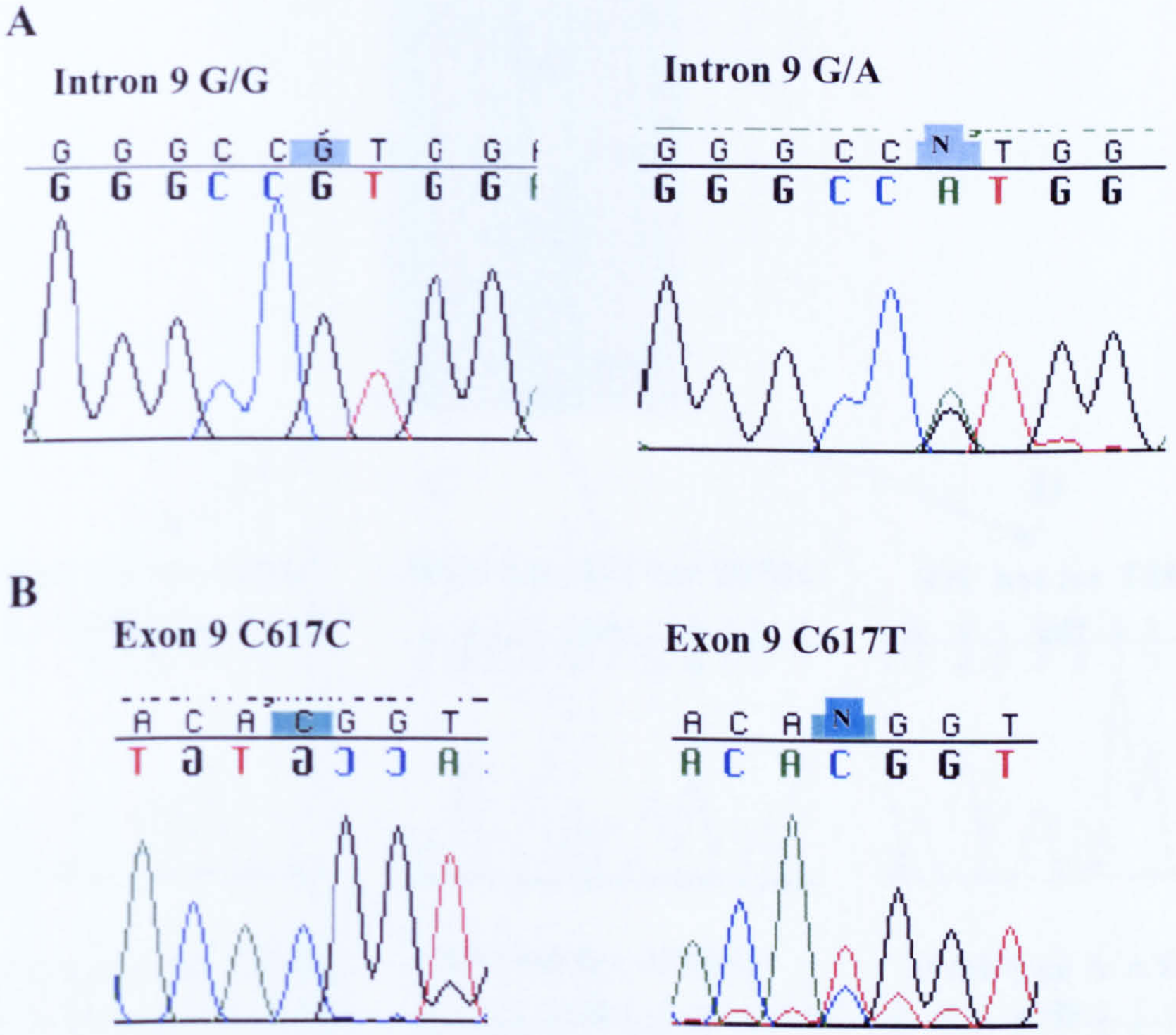

Figure 3.7.4. Two polymorphisms were detected in *Mus81* Ex11. **(A)** Analysis of *Mus81* exon 11 on SSCP revealed extra bands (blue arrows) in some samples. **(B)** Sequencing of samples with the most common SSCP pattern showed wild type sequence at both sites. **(C)** Some samples were A/G heterozygous at polymorphic site A840G but remained wild type for T852. **(D)** Chromatograms showing a sample heterozygous at the T852C polymorphic site and wild type for A840.

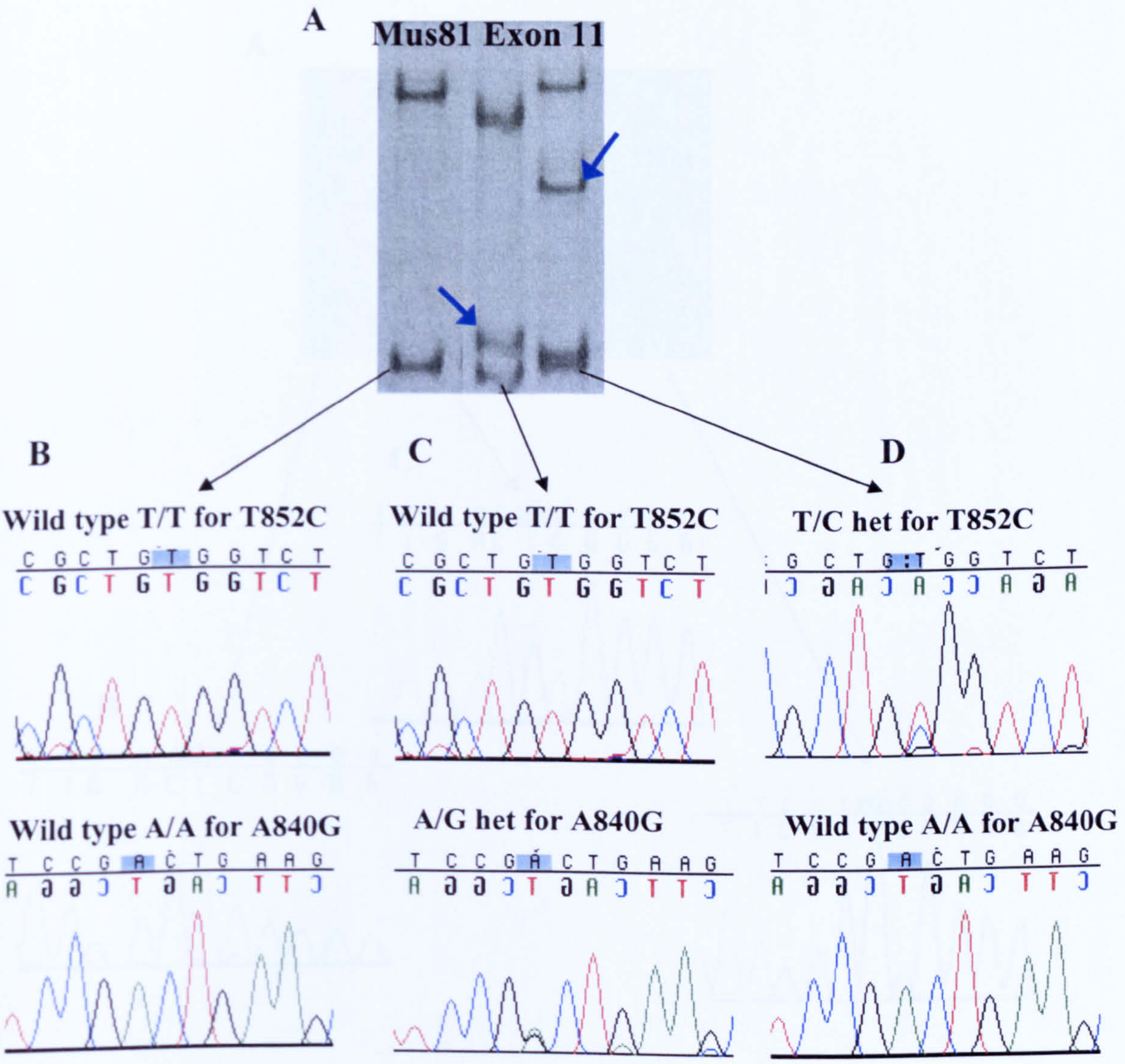

Figure 3.7.5. Analysis of *Mus81* exon 12 revealed a synonymous T1023G polymorphism. **(A)** SSCP analysis shows three different banding patterns on the gel. **(B)** Sequence analysis shows the T/T homozygote. **(C)** Chromatogram showing a T/G heterozygous sample. A G and T peak can be seen in the same position at 1023. **(D)** Sequence chromatogram showing the G/G rare homozygote for the *Mus81* exon 12 polymorphic site.

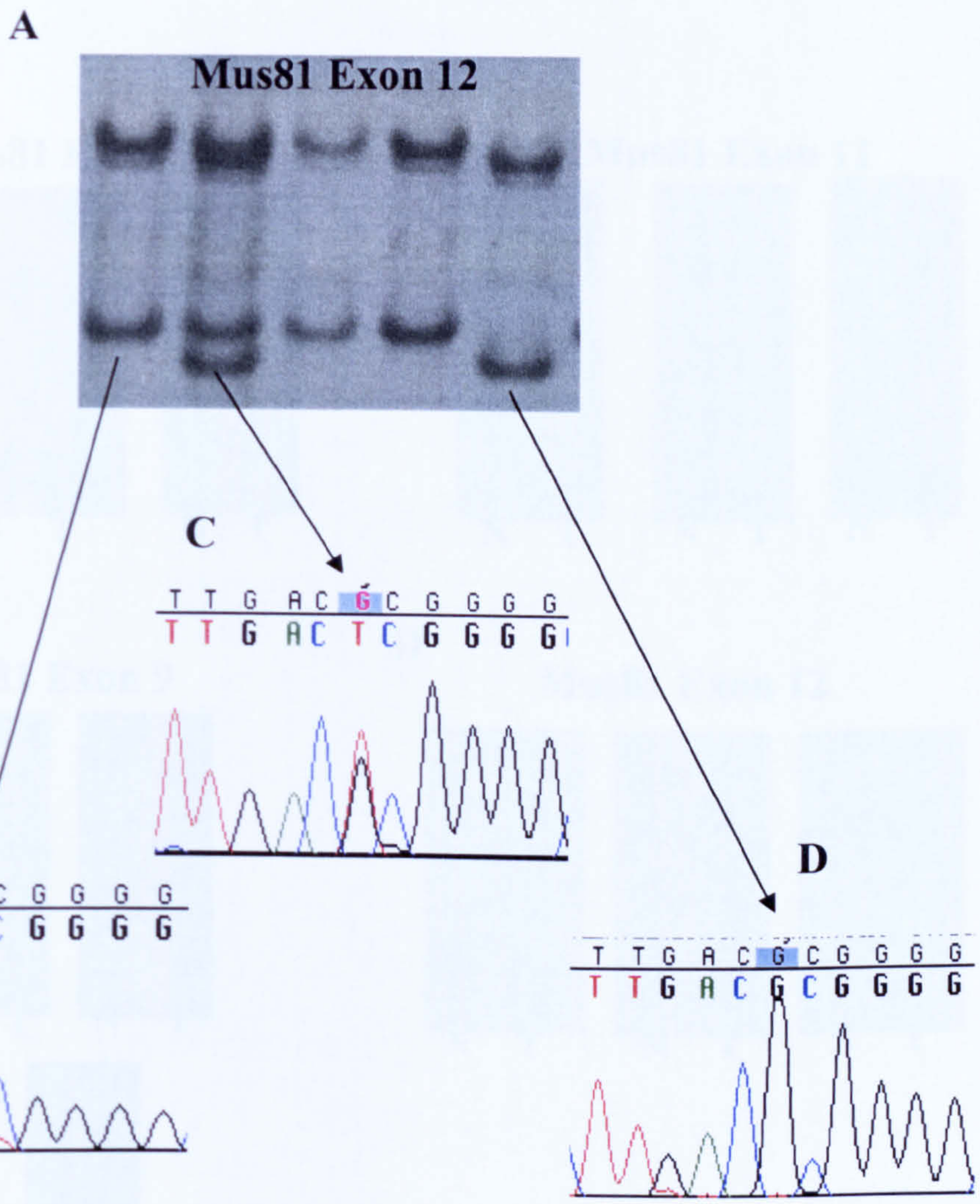

Figure 3.7.6. SSCP gel analysis of normal (N) and corresponding tumour (T) DNA suggests that the *Mus81* polymorphisms are not tumour specific and provides no evidence for LOH. **(A)** Samples showing variation in *Mus81* exon 6 have the same banding pattern in normal and tumour DNA. **(B)** Comparison of normal and tumour DNA for *Mus81* exon 9. **(C)** Tumour DNA shows variation in *Mus81* exon 11 on SSCP but corresponding normal DNA has same variant pattern. **(D)** Normal and tumour DNA from same patient showed the same SSCP pattern for *Mus81* exon 12.

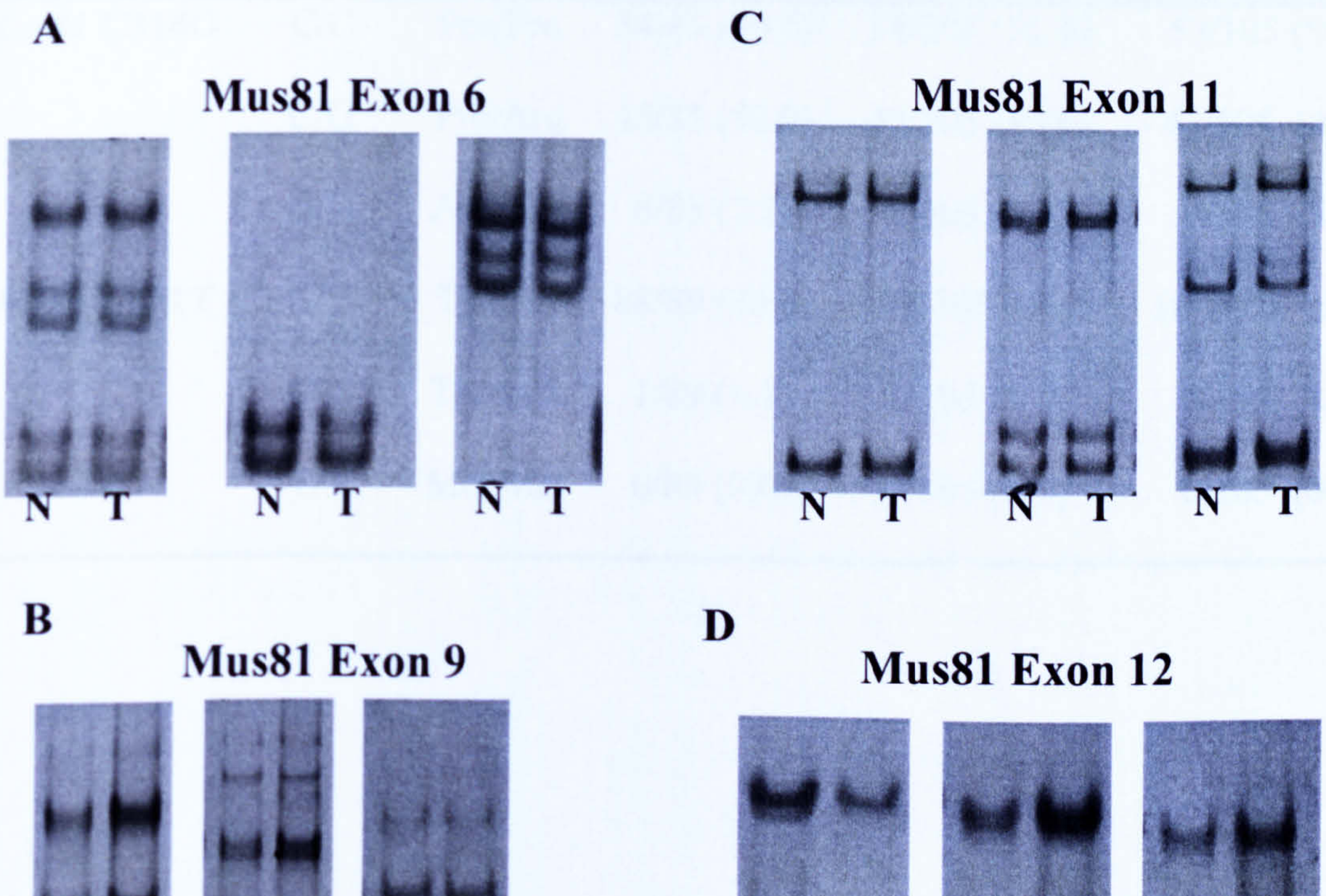

Table 3.7.2. Genotype frequencies of non-synonymous *Mus81* polymorphisms in a colorectal cancer and a normal blood donor control (BDC) population. Genotype frequencies expected by Hardy-Weinberg (H-W) are also shown.

[a]Allele frequencies in cancer cases: G = 0.29, T =0.01

Locus	Geno-type	Amino Acid	Frequency in Normal BDC (%)	Frequency in Tumours (%)	Frequency Expected by H-W[a] (%)
***Mus81* C314G**	C/C	Pro/Pro	34/85 (40.0)	54/105 (51.4)	53/105 (50.4)
	C/G	Pro/Arg	45/85 (52.9)	42/105 (40.0)	43/105 (41.2)
	G/G	Arg/Arg	6/85 (7.1)	9/105 (8.6)	9/105 (8.4)
***Mus81* C671T**	C/C	Thr/Thr	88/89 (98.9)	103/105 (98.0)	103/105 (98.0)
	C/T	Thr/Met	1/89 (1.1)	2/105 (2.0)	2/105 (2.0)
	T/T	Met/Met	0/89 (0.0)	0/105 (0.0)	0/105 (0.0)

Table 3.7.3. Comparison of the frequency of synonymous *Mus81* polymorphisms in the colorectal tumour population with the frequency expected by Hardy-Weinberg.

[a]Allele frequencies in cancer cases: T=0.29, C=0.02, A=0.01, G=0.22, C=0.01, G=0.28

Locus	Genotype	Frequency in Tumour Population (%)	Frequency Expected by H-W[a] (%)	Significance of Difference
***Mus81* C312T**	C/C	54/105 (51.4)	53/105 (50.4)	
	C/T	42/105 (40.0)	43/105 (41.2)	χ^2= 0.03
	T/T	9/105 (8.6)	9/105 (8.4)	p = 0.99
***Mus81* T711C**	T/T	102/106 (96.2)	102/106 (96.0)	
	T/C	4/106 (3.8)	4/106 (4.0)	χ^2= 0.0
	T/T	0/106 (0.0)	0/106 (0.0)	p =1
***Mus81* G-A Intron 9**	G/G	103/106 (97.1)	104/106 (98.0)	
	G/A	3/106 (2.9)	2/106 (2.0)	χ^2= 0.2
	A/A	0/106 (0.0)	0/106 (0.0)	p = 0.90
***Mus81* A840G**	A/A	60/106 (56.6)	65/106 (60.8)	
	A/G	46/106 (43.4)	36/106 (34.4)	χ^2= 6.3
	G/G	0/106 (0.0)	5/106 (4.8)	p = 0.04
***Mus81* T852C**	T/T	104/106 (98.1)	104/106 (98.0)	
	T/C	2/106 (1.9)	2/106 (2.0)	χ^2= 0.0
	C/C	0/106 (0.0)	0/106 (0.0)	p = 1
***Mus81* T1023G**	T/T	53/106 (50.0)	55/106 (51.9)	
	G/T	47/106 (44.3)	43/106 (40.3)	χ^2= 0.49
	G/G	6/106 (5.7)	8/106 (7.8)	p = 0.78

Table 3.7.4. Haplotype analysis of the 8 *Mus81* polymorphic loci detected in colorectal cancers showed 13 common haplotypes. The most common haplotypes (>5%) are listed first.

(HF = Haplotype Frequency, Indep = Frequency if loci are independent, Assn = Frequency with association)

			Allele	At				HF	HF
C312	C314	C671	T711	Int 9	A840	T852	T1023		
T	T	T	C	G-A	G	C	G	Indep	Assn
C	C	C	T	G	A	T	T	0.2701	0.6625
T	T	C	T	G	G	T	G	0.0049	0.1675
T	T	C	T	G	A	T	G	0.0169	0.0799
C	C	C	T	G	G	T	T	0.0779	0.0278
T	T	C	T	G	A	T	T	0.0432	0.0142
C	C	C	T	G	A	T	G	0.1055	0.0101
T	T	C	C	A	G	T	G	0.0000	0.0095
T	T	C	T	G	G	T	T	0.0125	0.0050
C	C	C	T	G	A	C	T	0.0026	0.0048
C	C	T	T	G	A	C	T	0.0000	0.0048
T	T	C	C	G	G	T	G	0.0000	0.0048
T	T	T	C	A	G	T	G	0.0000	0.0044
C	C	C	T	G	G	T	G	0.0304	0.0044

3.8 Analysis of XRCC2 Mononucleotide Runs

A frameshift mutation of a coding T_8 run of *XRCC2* was detected in a MMR-deficient uterine cell line (Mohindra et al., 2002) and therefore it was proposed that mutations of the coding mononucleotide runs of the candidate genes may be more common in MSI^+ tumours. No mutations of *XRCC2* were detected in 106 colorectal tumours during this study and SSCP screening did not reveal the frameshift mutation in *XRCC2* T_8, therefore 20 MSI^+ and 4 MSS colorectal tumours were analysed by sequencing. The T_8 run of *XRCC2* exon 3 along with the A_7 and T_7 mononucleotide runs of *XRCC2* exon 3 were examined (Figure 3.8.1). No coding mononucleotide tracts longer than six nucleotides were present in the other candidate genes. Samples were amplified and PCR products were subject to direct sequencing to determine the frequency of mutation in these runs in colorectal cancer samples. All colorectal samples analysed had wild type sequence in the *XRCC2* mononucleotide runs after direct sequencing (Figures 3.8.2-3.8.3).

Heterozygous mutations of mononucleotide runs are difficult to detect and the mutation in the T_8 run had been seen previously in the heterozygous form (Mohindra et al., 2002). Therefore the T_8 run was amplified in a selection of MSI^+ samples using the more accurate AccuPrime *Taq* system and PCR products were cloned into the pDrive cloning vector. Six independent clones per sample were chosen for sequencing using the Thermo-sequenase system. Samples where ≥ 50% (but <100%) of clones carried a mutant allele were classified as heterozygous and samples where no clones carried a mutant allele were classified as wild type. This extensive cloning analysis confirmed that none of the MSI^+ samples had a mutation in *XRCC2* T_8 (Figure 3.8.4).

Figure 3.8.1. Diagram showing relative position of the T_8, A_7 and T_7 mononucleotide runs in *XRCC2*.

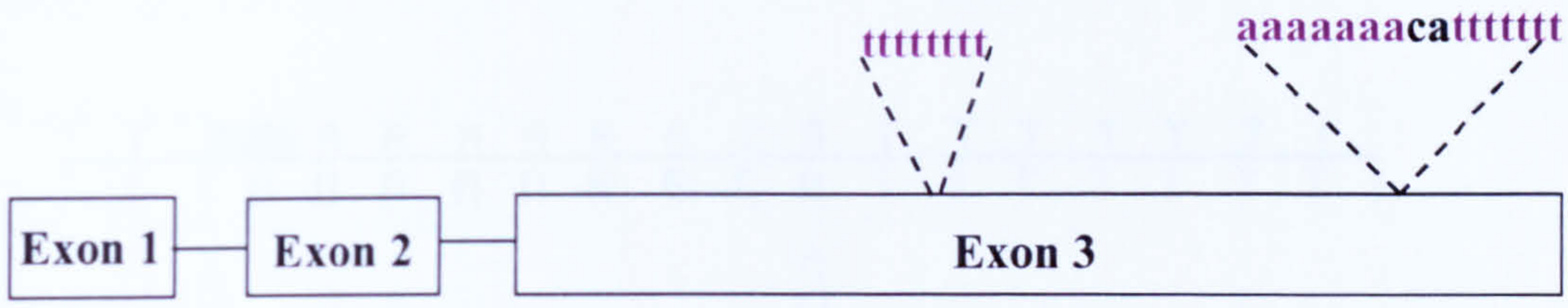

Figure 3.8.2. Sequencing of *XRCC2* T_8 in colorectal cancer samples reveals no mutations. **(A)** Sequencing gel for three different MSI^+ samples shows each have wild type T_8 runs. **(B)** Sequencing chromatogram showing the 8 thymines.

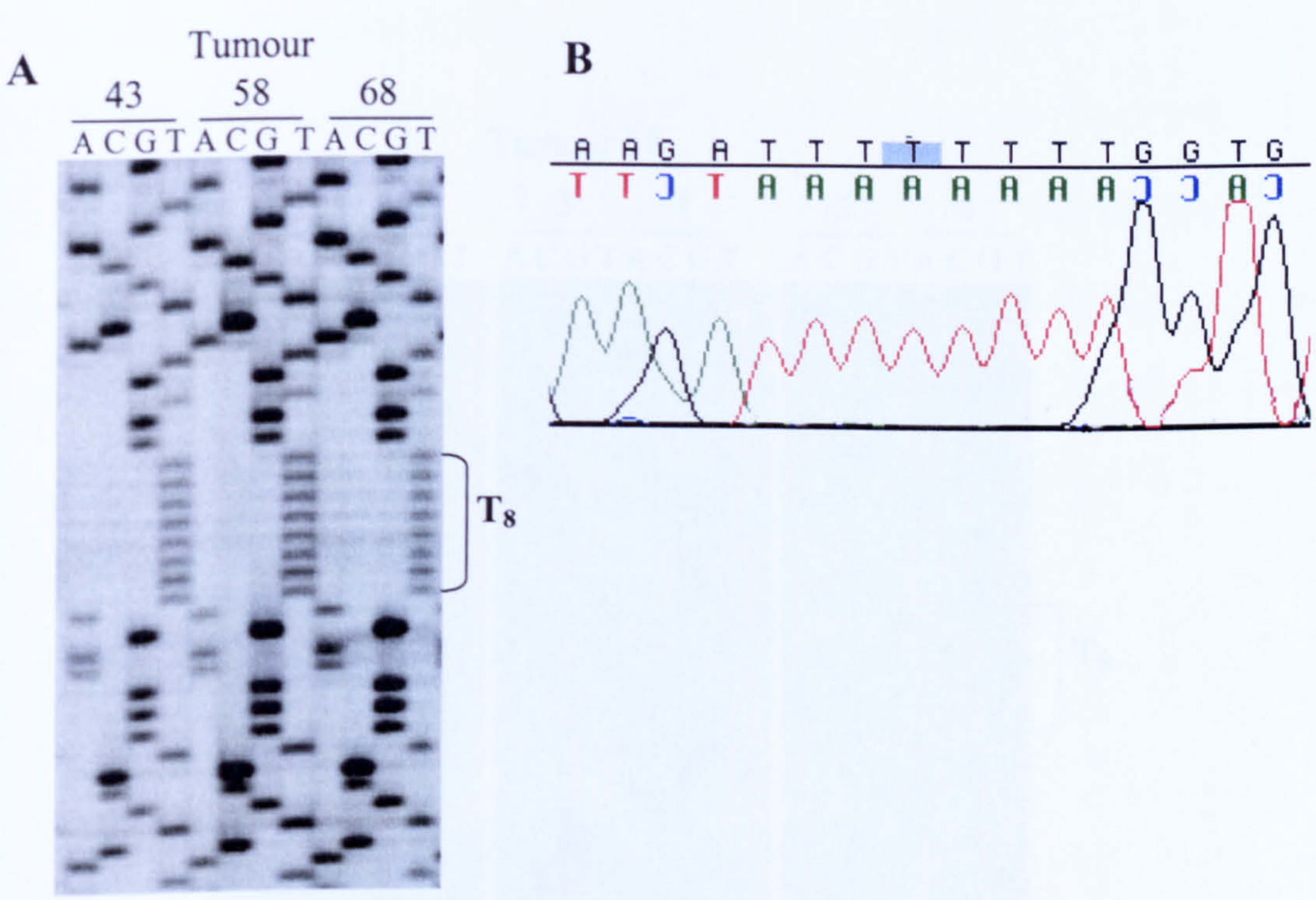

Figure 3.8.3. Sequencing chromatograms showing the wild type A_7 and T_7 mononucleotide runs in *XRCC2* exon 3 as seen for all MSI^+ CRC samples.

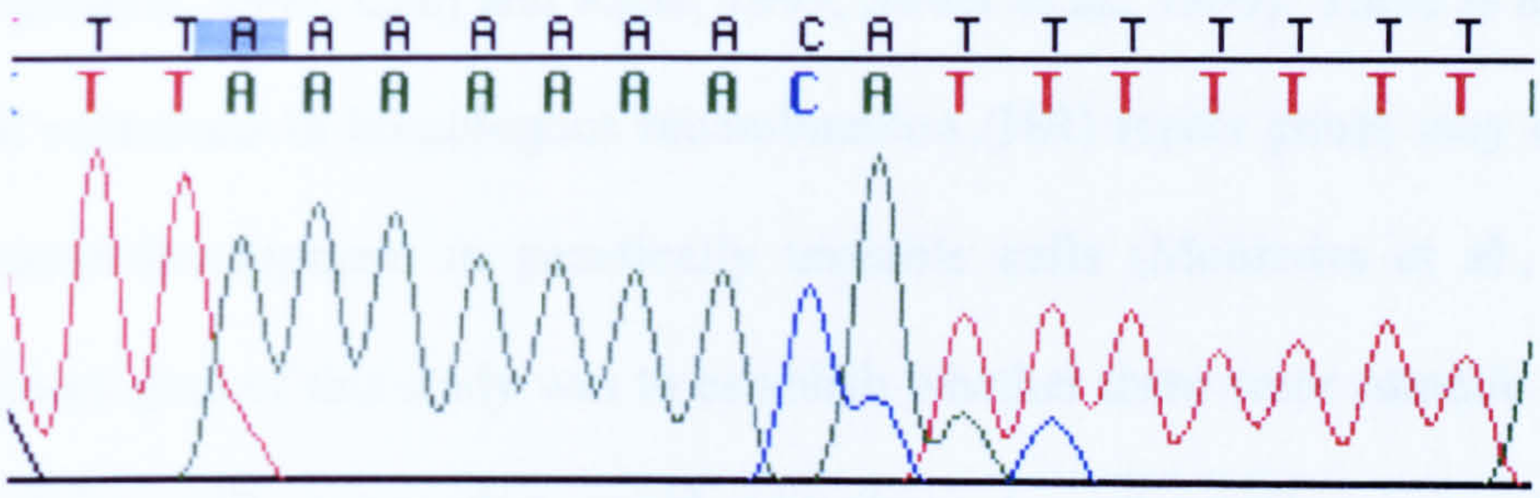

Figure 3.8.4. Six independent clones for an MSI^+ sample all carry a wild type T_8 allele suggesting this sample is truly wild type for *XRCC2* T_8.

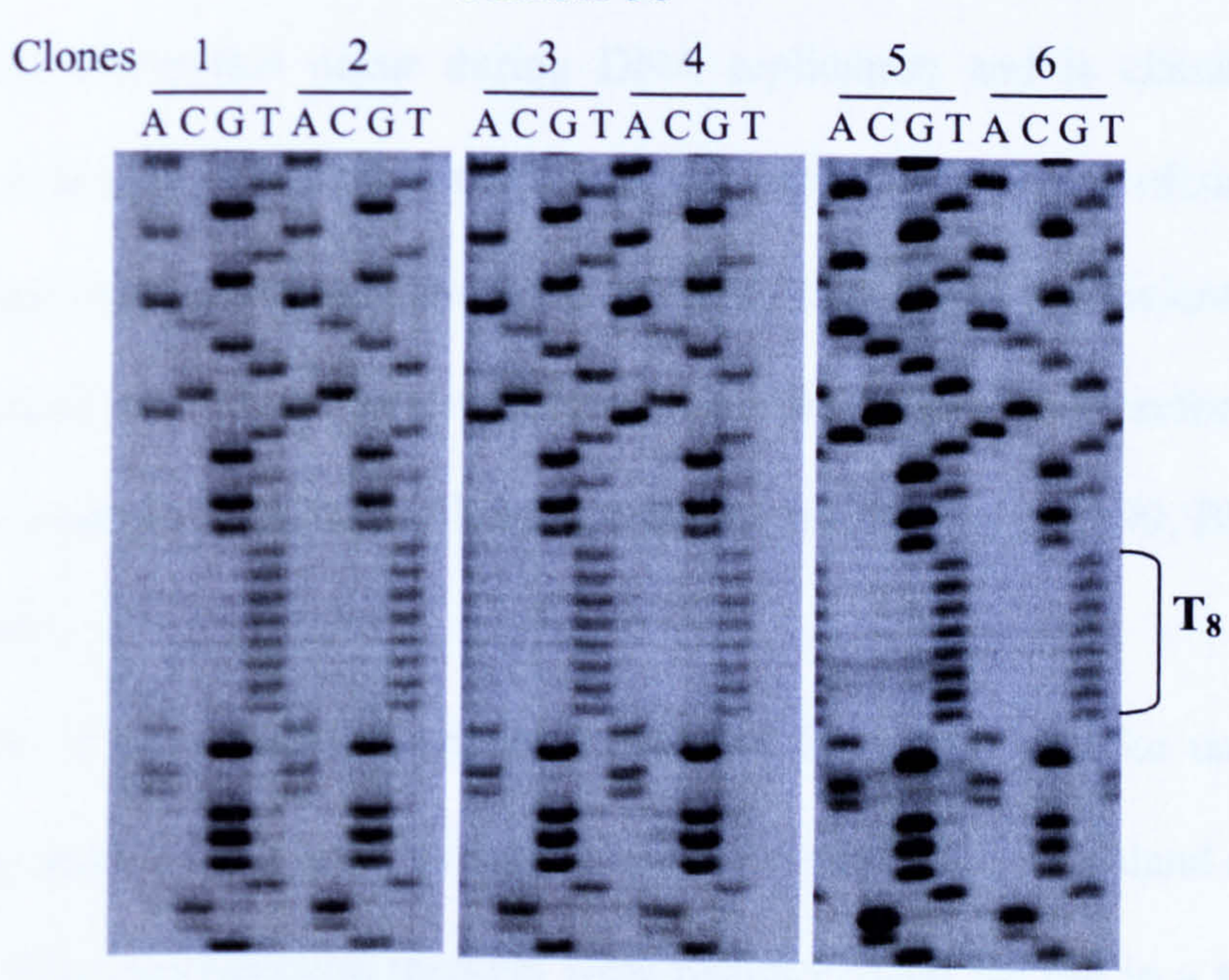

3.9 Discussion

There is now a large body of evidence suggesting that acquisition of genomic instability may represent an early step in malignant development (Kinzler and Vogelstein, 1997, Claij and Riele, 1999, Stoler et al., 1999). There is also evidence that mutations in homologous recombination (HR) repair genes may contribute to tumour development in genetically unstable cells (Mohindra et al., 2002). The primary goal of this study was to establish whether there were somatic mutations in candidate HR genes that could contribute to colorectal cancer development. Although no such mutations were detected, this analysis revealed several polymorphisms in the candidate HR genes and so it was determined whether these polymorphisms were likely to contribute to tumorigenesis.

The form of genomic instability associated with MMR-deficiency is known as microsatellite instability (MSI) and therefore this collection of tumours was classified according to MSI status. MSI is caused by a failure of the MMR system to repair errors that occur during DNA replication and is characterised by an increase in single nucleotide mutations and variation in length of simple repetitive sequences that occur throughout the genome. Cells with a deficient MMR system accumulate mutations more rapidly than normal cells and therefore mutations in critical genes become more likely (Coleman and Tsongalis, 1999, Bhattacharyya et al., 1994).

A panel of five markers to detect MSI have been validated for use in colorectal cancers and are recognised as the Bethesda reference panel (Boland et al., 1998). A further five microsatellite markers were recommended for use in a second panel to distinguish between low MSI (MSI-L) and microsatellite stable (MSS) samples (Dietmaier et al., 1997). Using these markers the level of MSI in sporadic colorectal tumours has previously been estimated to be 10-15% (Kim et al., 1994, Wheeler et

al., 2000). The frequency of MSI in the initial collection of sporadic colorectal tumours obtained for this study was 6.6%. This collection of tumours alone was used to determine the frequency of mutations in the candidate HR genes. It is therefore possible that the low level of MSI in this original tumour population limited our ability to detect DNA repair gene alterations that might be more common in tumours already deficient in MMR.

A second right-sided tumour collection was obtained to increase the number of MSI^+ tumours as it has been reported that tumours in the proximal colon are more likely to be MSI^+ (Chung, 2000, Burt, 2000). The level of MSI in the right-sided tumours was found to be 48.1% and so by combining the two collections the MSI frequency rose to 15%, which was closer to previously reported values. The MSI^+ tumours were later screened specifically for mutations in coding mononucleotide runs of candidate HR genes.

The methods chosen for screening the candidate genes were SSCP-PCR and sequencing. The results presented here show that, although SSCP is accurate and sensitive, it can introduce false positive data into the study. However, sequencing easily eliminates these false positives and all samples were sequenced in the forward and the reverse directions to confirm the results. When amplified products of 200-250bp are being screened SSCP can expect to detect 70-90% of all single base substitutions (Humphries et al., 1997).

The candidate genes chosen for SSCP-PCR analysis have a role in HR repair. These genes are potential targets for mutation since loss of any repair pathway destabilises the genome, making malignancy more likely and it has also been shown that certain MSI^+ tumour cell lines have HR repair defects (Mohindra et al., 2002, Mohindra et al., 2003).

XRCC2 is highly conserved in mammalian species and is essential for efficient repair of DNA double-strand breaks by HR between two sister chromatids (Deans et al., 2000). It interacts with Rad51D and has two potential Walker box ATP-binding domains. Analysis of *XRCC2* in the DNA of several colorectal cancer patients revealed a G-A polymorphism that led to an alteration of arginine 188 to histidine (R188H). This polymorphism has been reported to be associated with breast cancer (Rafii et al., 2002) but the results obtained here indicate that it may not be similarly associated with colorectal cancer. Analysis of genotype frequencies for the R188H polymorphism in the cancer and control populations showed no statistically significant difference between the two, suggesting that this polymorphism is not associated with colorectal cancer. However, the control values were estimated using allele frequencies from a previously reported unmatched blood donor control population. The blood donor control and colorectal cancer populations were both collected from the South Yorkshire area, but they are not sex-matched and are unlikely to be age-matched. To fully confirm that this polymorphism is not associated with colorectal cancer, screening data from a larger population of cancer patients would need to be compared to data from a matched normal population.

Although alignments of human, mouse and hamster *XRCC2* proteins show that arginine 188 is an invariant residue (Rafii et al., 2002, Cartwright et al., 1998) the R188H polymorphism seems to have a subtle effect on protein function. Expression of the R188H variant has a slight effect on the cells ability to repair MMC-induced

damage (Rafii et al., 2002). The 188 site does not overlap with the region that is required for XRCC2 interaction with Rad51D (Rafii et al., 2002) and the integrity of the ATP-binding domain is not necessary for XRCC2 function (O'Regan et al., 2001). XRCC2 R188H is a conservative amino acid change that does not appear to lie in a functional domain and it seems unlikely that this polymorphism has a role in colorectal cancer development or progression. No other polymorphisms or mutations of *XRCC2* were seen in the SSCP-PCR screening of colorectal cancer samples.

XRCC3 is required for correct chromosome segregation and for the efficient repair of DNA damage by the HR repair pathway making it a potential tumour suppressor gene (Griffin et al., 2000). Little is known, at present, about the specific functional domains of XRCC3. The protein has two putative ATP-binding domains, Walker boxes A and B, and interacts with Rad51C during HR (Masson et al., 2001a), although the residues critical for this interaction are unknown. Screening of *XRCC3* in a collection of colorectal cancer samples revealed several polymorphic sites within the gene and it is known that variants of *XRCC3* are common within the healthy population (Shen et al., 1998).

A C-T polymorphism in *XRCC3* intron 4 at position 8995 was detected in DNA from colorectal cancer patients. The genotype frequencies for this polymorphism were in Hardy-Weinberg equilibrium and did not differ from control data that had been estimated using allele frequencies reported for healthy individuals (Shen et al., 1998). This polymorphism is intronic and does not affect any of the important signal sequences directing intron removal and so is unlikely to affect *XRCC3* function. However, haplotype analysis suggested that this locus is linked to other

polymorphic loci in *XRCC3* and it may be that there is a linked dysfunctional variant that affects cancer susceptibility.

SSCP screening and sequencing of *XRCC3* exon 7 revealed that two polymorphisms had been detected, one A-G polymorphism in intron 6 at position 17893 and one C-T polymorphism in exon 7 at position 18067. The exon 7 change led to alteration of amino acid threonine 241 to methionine (T241M).

The presence of the T allele at position 18067 has been found to be significantly associated with increased risk of malignant melanoma development, bladder cancer and breast cancer (Winsey et al., 2000, Matullo et al., 2001, Kuschel et al., 2002) and has been associated with a non-statistically significant increased risk of squamous cell carcinoma of the head and neck (Shen et al., 2002). However, other studies have found no association between the T241M variant and lung cancer or non-small cell lung cancer (David-Beabes et al., 2001, Butkiewicz et al., 2001).

The A-G intronic polymorphism was also found to be associated with breast cancer cases and it seems that 17893G may have a dominant protective effect as the presence of the rare G allele was associated with a decreased risk of developing breast cancer (Kuschel et al., 2002).

Analysis using allele frequencies reported for healthy individuals (Shen et al., 1998) revealed that the intron 6 and exon 7 polymorphisms were not statistically significantly associated with colorectal cancer. Once again, however, there was no matching between normal and tumour populations and the allele frequency of 18067T in a normal population had been taken to be 0.38 whereas others have reported the allele frequency in healthy individuals to be 0.3-0.38 (Winsey et al., 2000, David-Beabes et al., 2001, Shen et al., 1998). The T241M polymorphic data was further investigated by comparing the genotype frequencies in colorectal cancer cases to those obtained from a large mammography screening control population.

These controls were more closely matched to the cases as they had a median age range of 50-65 years, and had all been collected from the South Yorkshire area. However, they were not sex matched as all the controls were female. This analysis further suggested that there was no significant association between colorectal cancer and the T241M polymorphism. A larger colorectal cancer sample and matched normal controls would need to be studied to establish whether there truly is an association between colorectal cancer and T241M. Indeed, attempts to verify the association of 18067 T with malignant melanoma and bladder cancer in other populations have been unsuccessful in confirming the original result (Duan et al., 2002, Stern et al., 2002).

The A-G intron polymorphism is non-coding and therefore unlikely to affect XRCC3 function. There is also little evidence that the T241M polymorphism affects the XRCC3 protein as the amino acid change does not alter either of the two ATP-binding domains, which are the only functional domains identified to date.

The T241M polymorphism changes a neutral hydrophilic amino acid with a hydroxyl group to a hydrophobic one with a methyl sulphur group. This may result in a change in protein structure or function (Kuschel et al., 2002) that may alter its ability to interact with Rad51C. However, the T241M variant is still capable of promoting homology directed repair of chromosomal double-strand breaks and cells expressing the variant protein are no more sensitive to MMC than those expressing wild type protein (Araujo et al., 2002).

The fact that the T241M variant appears to have no detrimental effect on XRCC3 function could be explained by evidence suggesting that T241M itself is not disease causing but is in linkage disequilibrium with a closely linked dysfunctional variant (Rafii et al., 2003). In fact, a rare haplotype containing T241M was more strongly associated with breast cancer than T241M itself (Kuschel et al., 2002). A haplotype

containing 17893G and 18067C was associated with a decreased risk of breast cancer whereas a haplotype containing 17893A and 18067T was associated with a significantly increased risk of breast cancer (Kuschel et al., 2002).

Haplotype analysis of the three *XRCC3* polymorphisms studied here (intron 4, intron 6 and exon 7) showed four frequent haplotypes and all other haplotypes were seen in less than 1% of cases. Haplotype analysis of the 17893 and 18067 polymorphisms alone provided haplotype frequencies that were in close agreement with previously reported data (Kuschel et al., 2002) and the analysis also showed a strong association between the intron 6 and exon 7 loci.

Some evidence indicates that the 17893G allele is protective whereas the 18067T allele increases risk of breast cancer (Kuschel et al., 2002) and indeed these two alleles did not appear together in a haplotype in any of the colorectal cancer cases. It seems that neither variant has an extensive effect on protein function lending support to the theory that the T241M allele is in linkage disequilibrium with another dysfunctional variant.

Mus81 is an endonuclease with a potential role in resolving Holliday junctions. The protein has a VERK motif that is conserved in the XPF family of nucleases and has helix-hairpin-helix DNA binding domains at the N- and C-termini that are also thought to be conserved (Chen et al., 2001). Mus81 interacts with the fork-head associated (FHA) domain of Chk2 and this interaction may require phosphorylation of Mus81 (Chen et al., 2001). These sites of interaction and potential phosphorylation are not yet determined for Mus81.

Several polymorphic sites of *Mus81* were identified in colorectal tumours but the majority of these did not lead to amino acid substitutions in the protein.

The majority of the detected polymorphisms were in Hardy-Weinberg equilibrium

within the tumour population. However, the genotype distributions for the A840G polymorphic site were statistically significantly different from those expected under Hardy-Weinberg equilibrium. This difference could be due to the strong association between this and the other 7 loci studied as the linkage disequilibrium may cause some bias and result in a deviation from Hardy-Weinberg at certain loci.

The frequency of the synonymous polymorphisms in a normal population was not determined since they were unlikely to affect protein function and therefore unlikely to be associated with colorectal cancer.

Two non-synonymous polymorphisms were identified in sequencing of *Mus81*. The first of these was a C-G polymorphism in exon 6 of the gene that led to substitution of proline 105 for arginine (P105R). The second was a C-T polymorphic site in exon 9 that led to alteration of threonine 224 to methionine (T224M). Comparison of genotype frequency distributions between a normal blood donor control and a colorectal cancer population showed no statistically significant differences between the two, suggesting the non-synonymous polymorphisms were not associated with colorectal cancer. However, the colorectal cancer population had again been compared to an unmatched blood donor control sample. Both the cancer and control populations had been collected from the South Yorkshire area but they were not sex-matched and the control population was likely to have a younger average age than the cancer population.

Therefore, to further study whether the polymorphisms observed were tumour-specific, corresponding normal and tumour DNA from the same patient was amplified for SSCP-PCR analysis of each of the polymorphisms detected in *Mus81*. This investigation showed that the normal and tumour DNA gave rise to the same pattern on SSCP further suggesting that the sequence changes are not tumour-specific.

The two non-synonymous polymorphisms of *Mus81* could have some effect on protein function as substitution of the small proline residue for a hydrophilic, positively charged arginine may have a significant effect on protein structure or function, as may replacing a hydrophilic threonine with the hydrophobic, sulphur-containing amino acid methionine. Furthermore, threonine 224 could potentially be a phosphorylation site in the Mus81 protein. However, this is unlikely since, similar to proline 105, the Thr224 residue is not absolutely conserved through eukaryotic species (Chen et al., 2001). Additionally, neither the Thr224 nor the Pro105 residues lie in the conserved VERK or helix-hairpin-helix domains (Chen et al., 2001) suggesting that these variants do not directly alter the functional domains of the protein. Therefore, it is perhaps unsurprising that these polymorphisms are not associated with colorectal cancer. This investigation has shown that, although variants of *Mus81* exist in the population, these variants do not appear to be associated with an increased risk of colorectal cancer development.

MMR-deficient tumours are more likely to accumulate mutations in critical genes that have repetitive sequences. This is seen for MMR-deficient sporadic colorectal tumours that acquire mutations in the repetitive elements of genes such as TGFβRII and BAX (Chung, 2000).

Since the original mutation screen of the candidate genes in this study did not reveal any tumour specific changes it was hypothesised that mutations in these genes might be more common in MMR-deficient tumours. Sequence alterations may be seen more frequently in the mononucleotide runs of these genes and notably a frameshift mutation of an *XRCC2* T_8 run was found to be associated with MMR-deficient uterine cancer cells (Mohindra et al., 2002, Mohindra et al., 2003). This heterozygous frameshift mutation leads to the introduction of a premature stop

codon and generates a truncated protein. Cells expressing this variant protein become more sensitive to thymidine- and MMC-induced DNA damage than cells expressing the wild type protein (Mohindra et al., 2002). However, a screen for this mutation in MSI^+ colorectal cancer samples did not provide any evidence for its association with MMR-deficient colorectal tumours. Analysis of the A_7 and T_7 tracts of *XRCC2* also failed to reveal any tumour-specific frameshift mutations of these runs. Therefore, although the *XRCC2* T_8 run might be important in development of a rare subset of MMR-deficient uterine tumours, results obtained here suggest that mutations in the mononucleotide runs of *XRCC2* do not play a role in MMR-deficient colorectal tumour development.

CHAPTER 4

Analysis of the MRE11 Complex

4.1 Introduction

The central hypothesis for this research was that the homologous recombination (HR) repair pathway is defective specifically in MMR-deficient tumour cells. Previous studies revealed that MMR-deficient cells display thymidine sensitivity and an HR repair deficiency (Mohindra et al., 2002). Thymidine treatment slows DNA synthesis and may create substrates at the replication fork that must be resolved by recombination and indeed it was shown that the HR pathway alone was required for cell survival following thymidine treatment (Lundin et al., 2002). Increasing evidence suggests that HR is involved in repair of collapsed or impaired DNA replication forks (Henry-Mowatt et al., 2003, Flores-Rozas and Kolodner, 2000) similar to those that might be created by thymidine treatment.

Together, these data suggest that loss of HR repair and thymidine sensitivity are a result of events downstream of MMR loss. Initial analysis of three candidate HR genes, *XRCC2*, *XRCC3* and *Mus81*, in a collection of primary colorectal tumours failed to reveal any tumour-specific mutations. Therefore, further candidate genes involved in recombination repair and maintenance of replication fork integrity were identified for screening.

The MRE11 complex consists of MRE11, NBS1 and Rad50 and this complex is a potential key organiser of double-strand break (DSB) repair (Paull and Gellert, 1999). It has been proposed that the MRE11 complex might be a sensor of S-phase DNA damage or an effector of the DNA damage-dependent S-phase checkpoint, or may fulfil both these roles (Petrini and Stracker, 2003).

The MRE11 complex has been shown to be associated with several other proteins with roles in recognition of abnormal DNA structures or damaged DNA in the BRCA1-associated genome surveillance complex (BASC) (Wang, 2000). It has

further been suggested that interference with the functions of BASC may be a central event in tumorigenesis (Wang, 2000).

The MRE11 complex is known to be active during S-phase in unstressed cells and the complex associates with chromatin in a replication-dependent manner (Mirzoeva and Petrini, 2003). Depletion of MRE11 from *Xenopus* extracts leads to the accumulation of DSBs during genomic DNA replication (Costanzo, 2001). Therefore, an additional potential role for the MRE11 complex is in surveillance of the genome during the normal cell cycle to preserve genomic integrity.

The components of the MRE11 complex are obviously important and as such, mutations in these genes might increase genetic instability and predispose to malignancy. Loss of MMR increases the chance of further mutations in genes involved in fundamental cellular processes and therefore mutations of the MRE11 complex are more likely in MMR-deficient cells.

4.2 Aims and Objectives

Acquired mutations in *MRE11*, *NBS1* or *Rad50* may affect MRE11 complex formation or function and therefore lead to a decreased repair capacity or surveillance ability and an increased chance of malignancy. The aim of this study was to screen several MMR-deficient tumour cell lines and MSI^+ primary colorectal cancers for mutations of the MRE11 complex. Mutations that were found to be significantly associated with colorectal cancer would be further investigated to determine the phenotypic effects of the mutation.

4.3 Analysis of *MRE11*, *NBS1* and *Rad50* in Cell Lines

RNA extracted from one MMR-proficient and five MMR-deficient cell lines was analysed for mutations in the *MRE11*, *NBS1* and *Rad50* genes.

The full-length cDNA of each gene was amplified in overlapping fragments (*MRE11* fragments 1-3, *NBS1* fragments 1-4, *Rad50* fragments 1-6) and these cDNA sequences were analysed for base changes. None of the cell lines tested; the MMR-deficient colon cancer cell lines HCT116 and DLD-1, MMR-deficient endometrial cancer lines SK-UT-1, 2774 and HEC-1-A, and the MMR-proficient colon cancer cell line SW480, showed any mutation in the coding sequence of any of the tested genes.

4.4 Analysis of *MRE11*, *NBS1* and *Rad50* in MSI$^+$ Colorectal Tumours

It is well established that the mononucleotide runs of genes, especially runs with 6 or more nucleotides, are targets for mutation in MSI$^+$ tumours (Toft and Arends, 1998, Chung, 2000, Bhattacharyya et al., 1994). All mononucleotide runs (N>6) of *MRE11*, *NBS1* and *Rad50* were amplified from 20 MSI$^+$ colorectal tumours and amplification products were subject to direct sequencing (Table 4.4.1). Sequence analysis suggested that some cancer samples had heterozygous mutations in the coding A_8 and A_9 runs of *Rad50* and in an exonic A_7 and an intronic A_7 run of *MRE11* (Figure 4.4.1).

Table 4.4.1. Summary of mutation screening using direct sequencing of mononucleotide runs of the MRE11 complex genes in MSI-L and MSI-H colorectal cancer samples.

Mononucleotide Run	Nucleotide Position	Frequency of MSI-L Samples Mutated (%)	Frequency of MSI-H Samples Mutated (%)
Rad50 T_6	536-541	0/5 (0.0)	0/13 (0.0)
Rad50 A_6	1717-1722	0/6 (0.0)	0/14 (0.0)
Rad50 A_9	2157-2165	1/6 (16.7)	4/13 (30.7)
Rad50 A_8	2794-2801	0/6 (0.0)	1/14 (7.1)
NBS1 A_6	242-247	0/6 (0.0)	0/14 (0.0)
NBS1 A_7	1390-1396	0/5 (0.0)	0/13 (0.0)
NBS1 A_7	1645-1651	0/6 (0.0)	0/14 (0.0)
NBS1 A_6	1953-1958	0/5 (0.0)	0/13 (0.0)
MRE11 A_6	596-601	0/5 (0.0)	0/14 (0.0)
MRE11 T_6	1209-1214	0/6 (0.0)	0/13 (0.0)
MRE11 A_6	1235-1240	0/6 (0.0)	0/13 (0.0)
MRE11 $A_{7(intronic)}$	Intron 11	0/6 (0.0)	2/13 (15.4)
MRE11 A_6	1458-1463	0/5 (0.0)	0/13 (0.0)
MRE11 $A_{7(coding)}$	1550-1556	0/5 (0.0)	1/13 (7.7)

Figure 4.4.1. Direct sequencing of mononucleotide runs in *MRE11* and *Rad50* reveals possible heterozygous mutations (shown by blue arrows). The stutter bands on the gel are characteristic of frameshift mutations. **(A)** Several samples have potential mutations in *Rad50* A_9. **(B)** One sample appears to have a frameshift mutation in *Rad50* A_8. **(C)** One sample shows a potential heterozygous mutation in an intronic A_7 run of *MRE11*. **(D)** One MSI^+ colorectal cancer sample may have a mutation in the coding *MRE11* A_7 run.

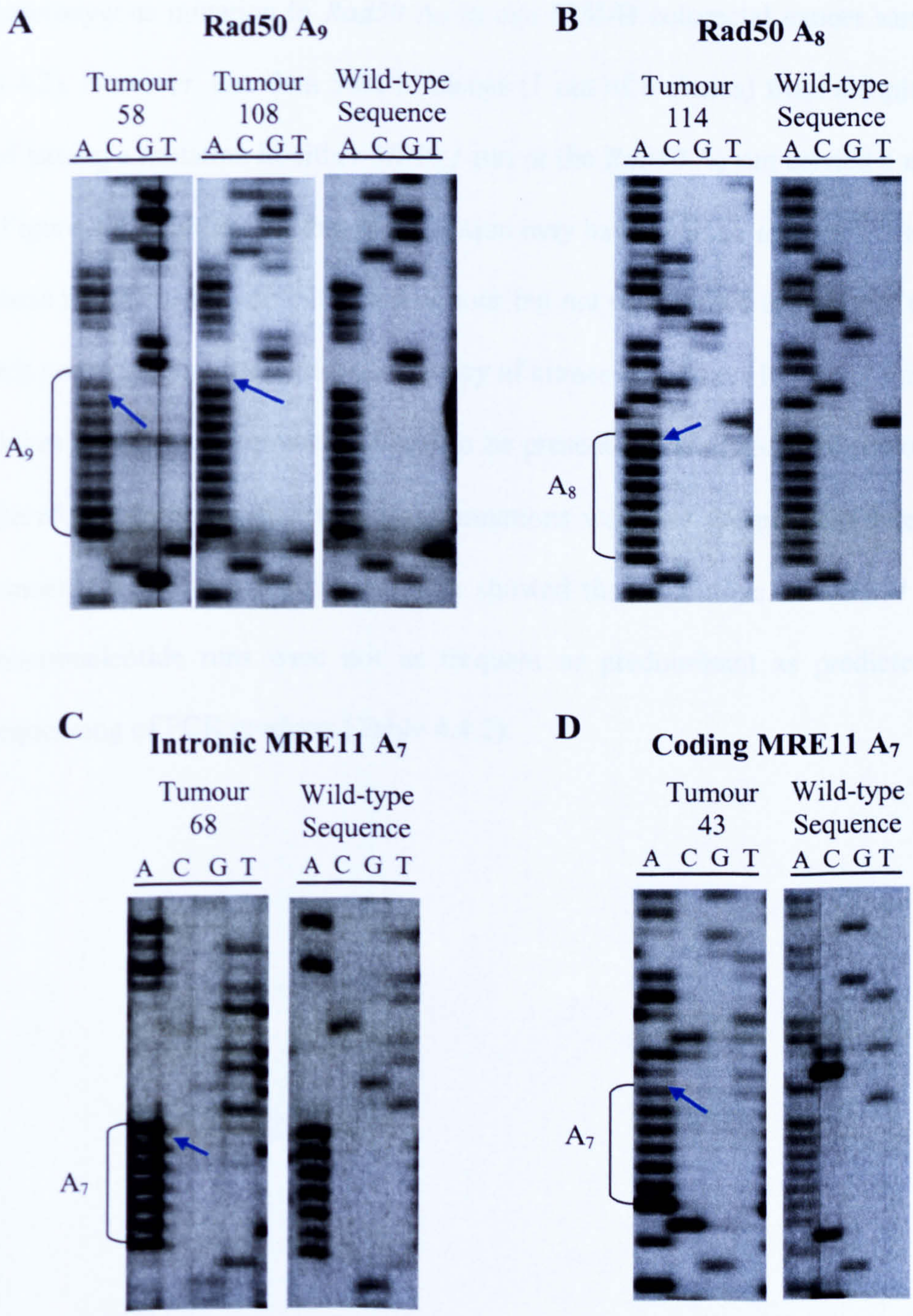

There is, however, a possibility that heterozygous mutations introduced to repetitive elements are an artefact of PCR and sequencing procedures. Therefore, samples that appeared to have mutations from direct sequencing were re-analysed. The run was amplified with the more accurate AccuPrime *Taq* polymerase and PCR products were cloned into a pDrive vector. Six clones were chosen for sequencing and where ≥ 50% (but <100%) of the clones had taken up a mutant allele the sample was classified as having a heterozygous mutation. Cloning analysis confirmed the presence of a heterozygous mutation in *Rad50* A_9 in one MSI-H colorectal cancer sample (Figure 4.4.2). However, less than 50% of clones (1 out of 6 clones) from samples suspected of having a mutation in either *MRE11* run or the *Rad50* A_8 run carried a mutant allele (Figure 4.4.2) indicating that the mutation may have been an artefact. Alternatively, if these mutations are present in the tumour but not represented in 100% of tumour cells this could account for the low frequency of clones observed. However, a mutation that drives tumour development is likely to be present in the majority of tumour cells and therefore it was assumed that these mutations were not the primary determinants of cancer. Overall, this cloning analysis showed that mutations in *MRE11* and *Rad50* mononucleotide runs were not as frequent or predominant as predicted by direct sequencing of PCR products (Table 4.4.2).

Table 4.4.2. Summary of mutations seen in MSI-L and MSI-H colorectal cancer samples in mononucleotide runs of the MRE11 complex after cloning of PCR products.

Mononucleotide Run	Frequency of MSI-L Samples Mutated (%)	Frequency of MSI-H Samples Mutated (%)
Rad50 A_9	0/6 (0.0)	1/13 (7.7)
Rad50 A_8	0/6 (0.0)	0/14 (0.0)
MRE11 $A_{7(intronic)}$	0/6 (0.0)	0/13 (0.0)
MRE11 $A_{7(coding)}$	0/5 (0.0)	0/13 (0.0)

Figure 4.4.2. Sequencing of cloned samples. **(A)** Over 50% of clones from one sample show a mutation in *Rad50* A_9 confirming the presence of a heterozygous mutation in this sample. **(B)** Less than 50% of clones from one sample show a mutation in *Rad50* A_8. **(C)** The majority of clones have taken up a wild-type allele for the coding *MRE11* A_7. **(D)** Only one clone out of 6 carries a mutant allele for the intronic *MRE11* A_7.

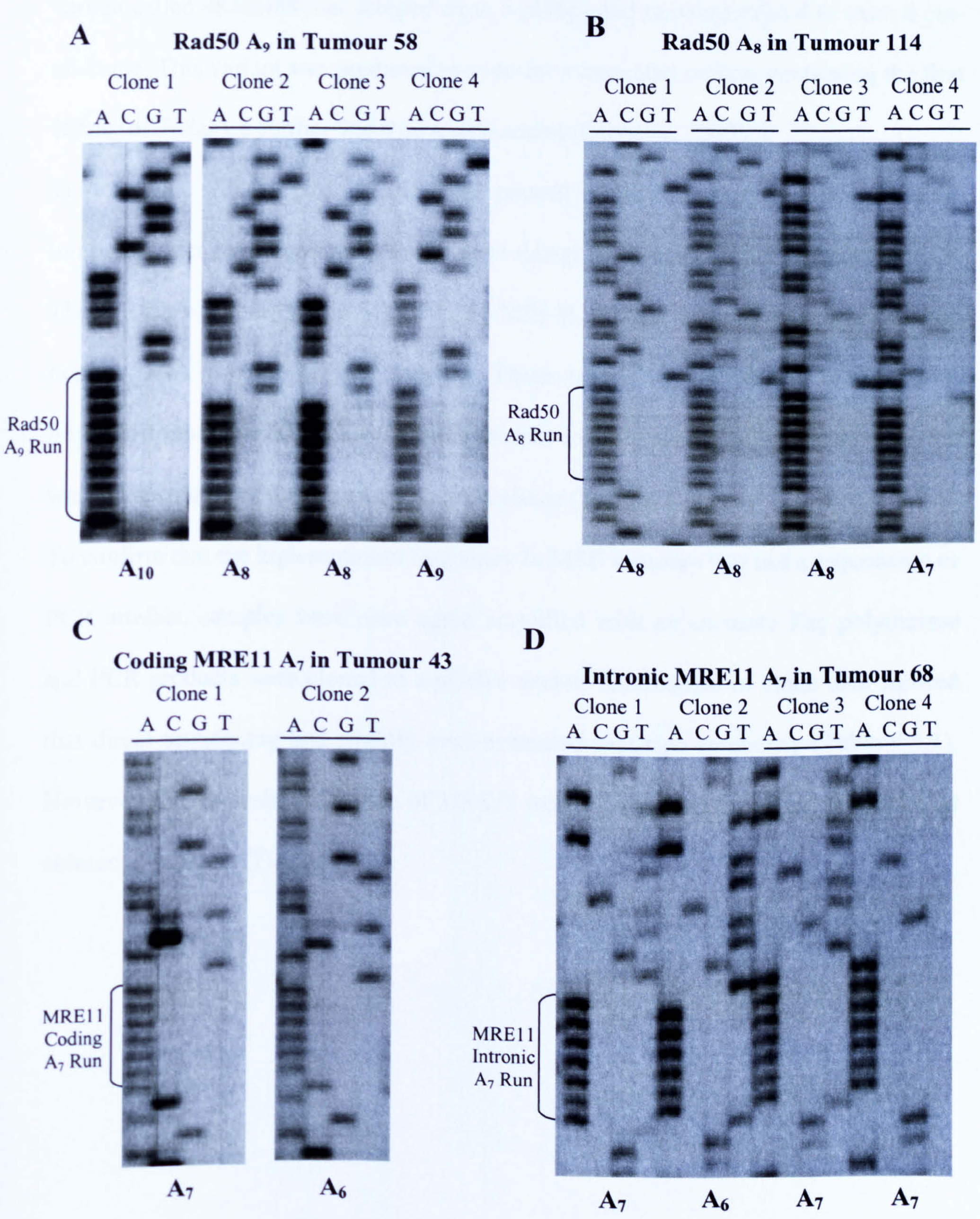

4.5 Analysis of the Intron 4 T_{11} Tract of *MRE11* in MSI^+ Colorectal Tumours

A mutation of the *MRE11* gene was recently reported in MSI^+ colon cancer cell lines (Giannini, 2002). This mutation is a -1 or -2 frameshift in a run of 11 thymine residues in intron 4 of *MRE11* and results in altered splicing and generation of truncated MRE11 products (Giannini, 2002). The alternative splicing was reported to create a variant called 484del88 that skipped exon 5 (88bp) and rejoined exon 4 to exon 6 out-of-frame. This variant was predicted to code for a truncated protein containing the first 105aa (of 708aa), a further 9aa then a stop codon (Giannini, 2002).

To determine whether this mutation was present in the collection of MSI^+ colorectal tumours under investigation, primers were designed to amplify the tract in intron 4. The T_{11} run was analysed in 6 MSI-L, 14 MSI-H, 4 MSS tumours and corresponding normal DNA from 4 MSI-H tumours. These results showed that a heterozygous frameshift mutation in *MRE11* T_{11} was present in the majority of MSI^+ tumours, but was not seen in MSS tumours or in normal tissue (Table 4.5.1).

To confirm that the high mutation frequency in MSI^+ tumours was not a sequencing or PCR artefact, samples were once again amplified with an accurate *Taq* polymerase and PCR products were cloned to a pDrive vector. Assessment of clone data showed that direct sequencing had slightly over-estimated mutation frequency (Table 4.5.1). However, the frameshift mutation of *MRE11* intron 4 T_{11} was present in >85% MSI-H colorectal tumours (Figure 4.5.1).

Table 4.5.1. Comparison of *MRE11* T_{11} mutation frequency seen after direct sequencing of PCR products and sequencing of cloned PCR products.

Method of Detection	No. of MSI-L samples mutated (%)	No. of MSI-H samples mutated (%)	No. of MSS samples mutated (%)	No. of normal samples mutated (%)
Direct Sequencing of PCR products	1/6 (16.7)	14/14 (100)	0/4 (0.0)	0/4 (0.0)
Sequencing of cloned products	0/6 (0.0)	12/14 (85.7)	0/2 (0.0)	0/2 (0.0)

Figure 4.5.1. Sequencing of *MRE11* T_{11} intronic mononucleotide run in colorectal cancer samples. **(A)** Direct sequencing suggests that heterozygous mutations are present at a high frequency in MSI^+ samples. **(B)** Sequencing of clones from one sample shows 50% of clones carry a mutant allele confirming this sample has a heterozygous frameshift mutation.

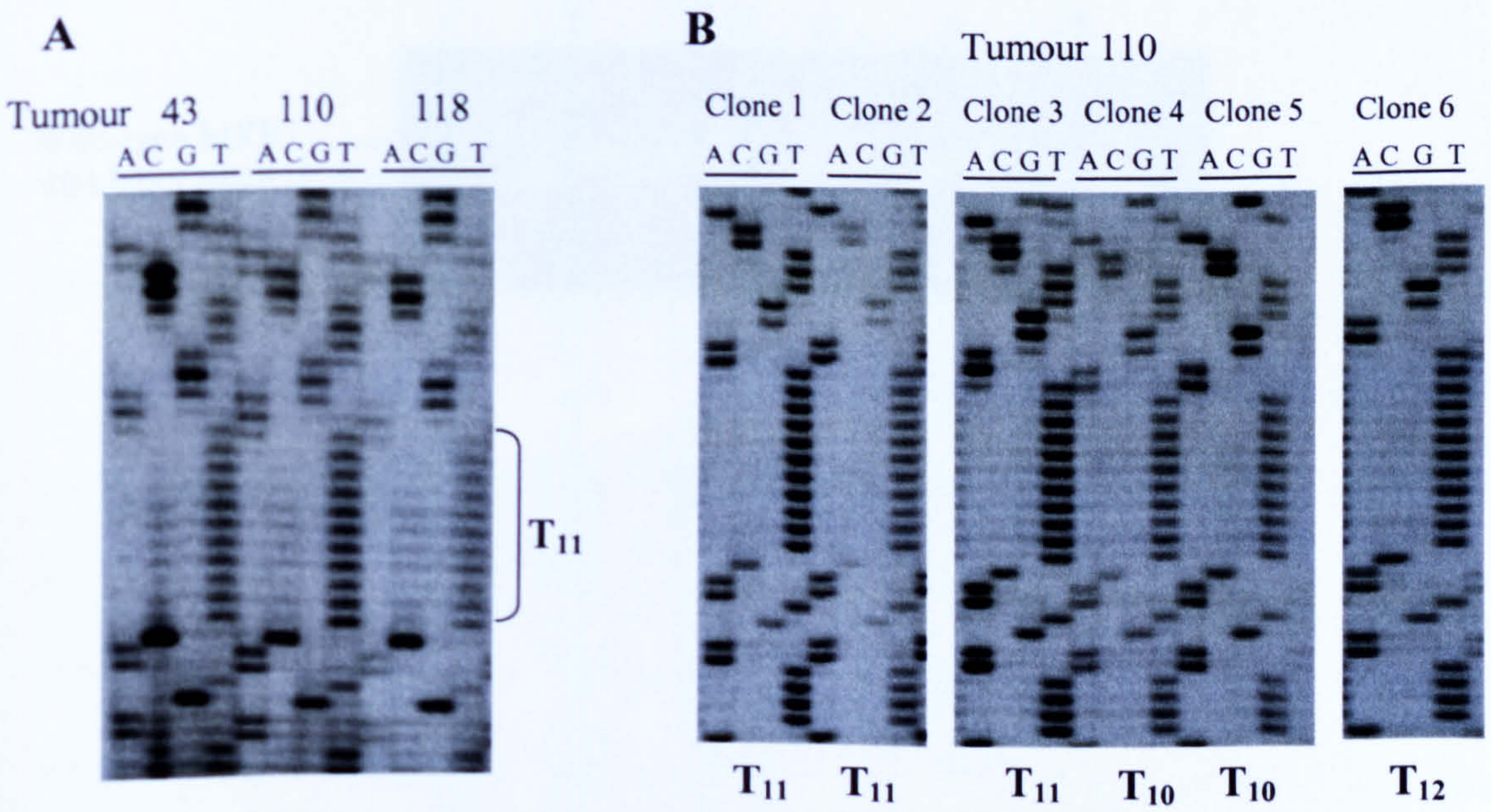

4.6 Creating Mutant MRE11 Expression Constructs

a) Amplification of MRE11 from Cell Lines

A 5′ fragment of *MRE11* was amplified from total cDNA of one MMR-proficient and 4 MMR-deficient cell lines and amplification products were run on an agarose gel (Figure 4.6.1). This suggested that two MMR-deficient cells lines, HCT116 and SW48, carried an MRE11 mutant product that was approximately 88bp smaller than the wild type. In both cell lines, the mutant cDNA appeared to be present at a lower level compared to the wild-type MRE11. This was consistent with the results from the original report identifying this mutation where the smaller PCR product had been named 484del88 (Giannini, 2002). Sequencing confirmed that these two cell lines contained a frameshift mutation in the intronic T_{11} tract of *MRE11*.

Figure 4.6.1. Amplification of *MRE11* fragment-1 in cell lines HCT116 (**1**), SW480 (**2**), SW48 (**3**), HEC-1-A (**4**) and DLD-1 (**5**). HCT116 and SW48 show a smaller amplification product along with the wild type suggesting the presence of a mutation in *MRE11*.

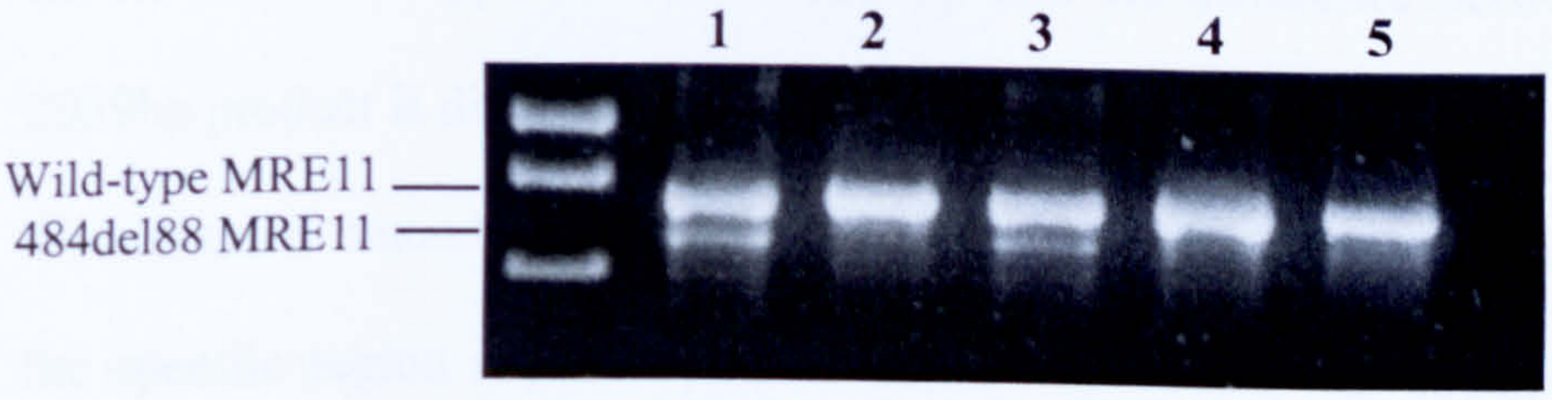

b) Isolation of Reported Mutant MRE11 Variant

A construct expressing MRE11 484del88 was required to assess the phenotypic consequences of this mutation. Attempts were made to isolate this variant from HCT116 and SW48. Although RT-PCR results suggested that a mutant MRE11 product was being produced in both cell lines, at least at the RNA level, a corresponding cDNA could not be directly isolated. A 5′ RT-PCR product of *MRE11* from HCT116 was run on a high percentage agarose gel to give better separation of products and clearly showed the presence of a variant that corresponds to 484del88 (Figure 4.6.2A). A further variant that was 300-350bp smaller than the wild-type MRE11 also appeared to be amplified in the RT-PCR reaction at lower levels (Figure 4.6.2A).

It was noted that when full length *MRE11* was amplified from HCT116 several smaller atypical *MRE11* products were also detected, and these were not seen when *MRE11* was amplified from SW480 (Figure 4.6.2B). These smaller products might represent other alternative splice variants arising due to the mutation of *MRE11* T_{11} in HCT116. The mutant 484del88 product could not be detected on this agarose gel because the wild-type product is 2127bp and the difference between a 2127bp and 2039bp product is difficult to see on a standard agarose gel.

The reported mutant 484del88 *MRE11* allele was re-created by designing primers to the specific region required (ex2-4) and a stop codon was added to the end of the primer. Amplification of HCT116 cDNA using these primers provided the desired mutant *MRE11* product, which was named 314del88. This name reflected the fact that the sequence runs from the ATG through to the end of exon 4 (314bp) and misses the 88bp of exon 5. MRE11 314del88 was cloned into the pIRES^{puro3} expression vector by blunt-end ligation and clones carrying the correct product in the correct orientation were isolated (Figure 4.6.3).

Figure 4.6.2. **(A)** *MRE11* products amplified from HCT116. The two main products are the wild type (WT) *MRE11* and the reported 484del88 mutant *MRE11*. When excess PCR product is loaded onto the gel, a further band is apparent. **(B)** Smaller anomalous PCR products are apparent when full length *MRE11* is amplified from HCT116 but not from SW480.

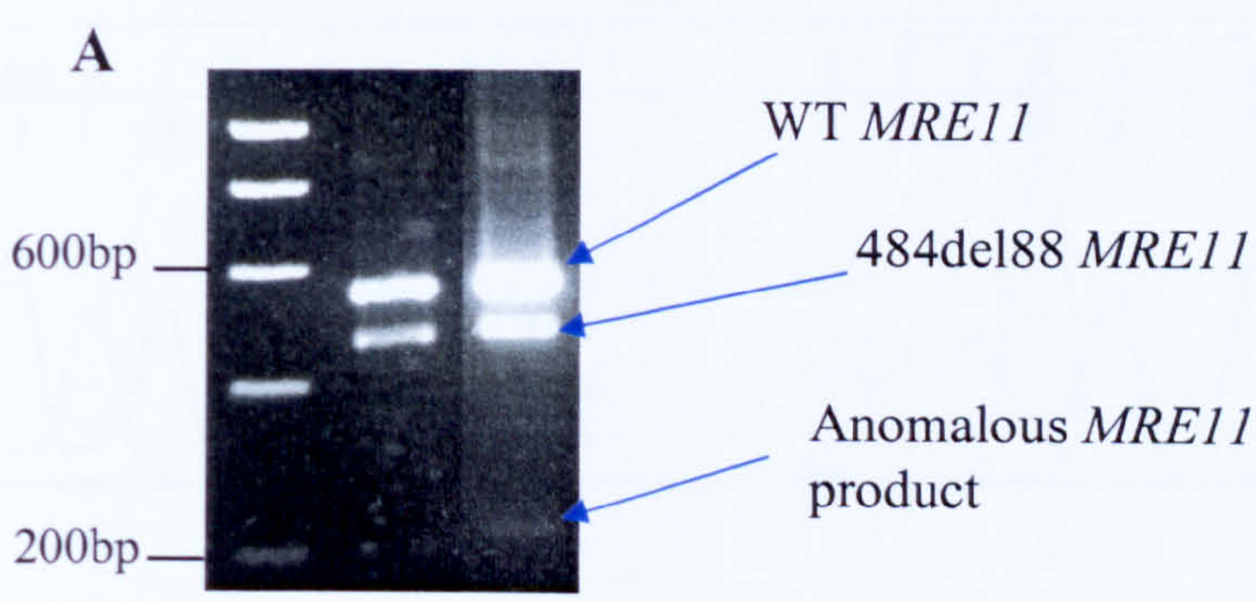

Figure 4.6.3. PCR-engineered *MRE11* 314del88. Primers were designed to amplify from the ATG start codon in exon 2, through exon 4 and to a stop codon added to the end of the primer.

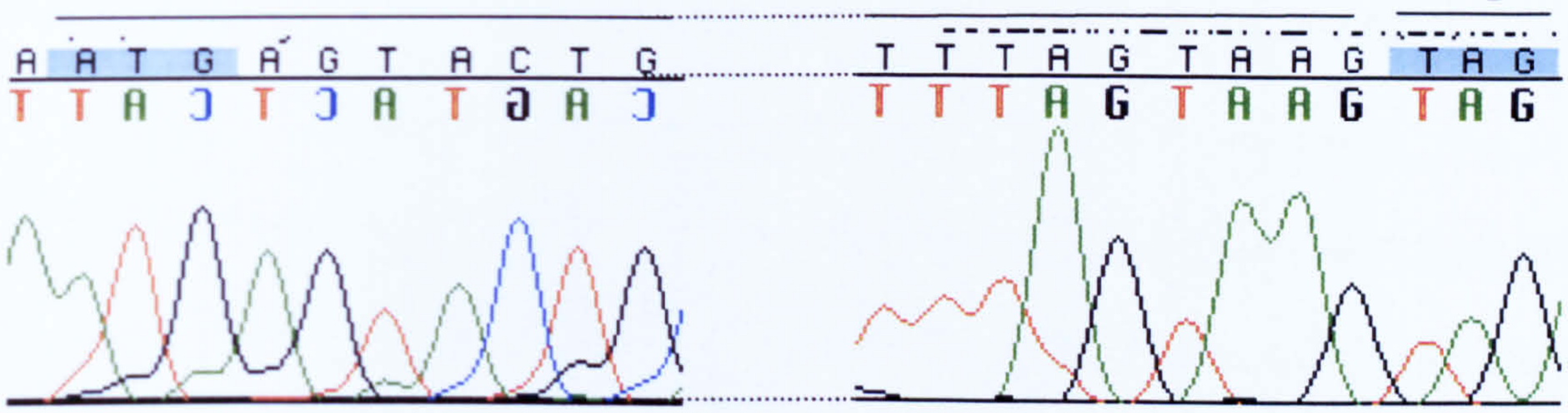

c) Isolation of Other MRE11 Splice Variants

Whilst attempting to isolate MRE11 484del88 cDNA several other interesting splice variants were obtained from HCT116.

One of these splice variants, named 314del92, lost exon 5 and the last 4 bases of exon 4 (92nt) and also lacked exons 7-10. Exon 4 re-joined out-of-frame to exon 6 creating a premature stop codon and this variant was predicted to code for a truncated protein containing the first 103aa (of 708aa) of the wild-type protein, then 10aa, then a stop codon. This truncated protein of 113aa was almost identical to the 114aa protein coded for by 314del88 (Figure 4.6.4). *MRE11* 314del92 and the engineered 314del88 code for similar proteins that lack the last two of four conserved motifs in the nuclease domain of MRE11 and miss the C-terminal DNA binding domains (Figure 4.6.5). These variants were chosen for further study because of their similarity to the reported MRE11 mutant 484del88.

A second interesting *MRE11* splice variant, named 314del345 was revealed during the cloning process. This variant skipped exons 5-7 (345nt) so that exons 4 and 8 re-joined in-frame and was predicted to code for a 593aa (out of 708aa) protein (Figure 4.6.4). This mutation eliminates the third of four conserved phosphoesterase motifs from the protein that are necessary for nuclease activity of MRE11 and some of the surrounding amino acids (Figure 4.6.5 and Appendix V). MRE11 314del345 was chosen for further study because it codes for a protein that is similar in size to the wild-type protein but specifically lacks one functional motif.

The mutant *MRE11* alleles were blunt-end ligated into the pIRES^{puro3} vector and clones carrying the correct sequences in the correct orientation were obtained (Figure 4.6.6).

Figure 4.6.4. Alternatively spliced alleles of *MRE11*. **(A)** The wild-type splicing pattern gives rise to a 708aa protein. **(B)** Loss of 1-2 thymines from the intronic T_{11} tract can promote skipping of exon 5 and generation of a truncated protein as reported by Giannini et al. **(C)** Splicing pattern seen in 314del345 allele isolated from HCT116. **(D)** Splicing pattern seen in 314del92 isolated from HCT116, similar to reported mutant it codes for a truncated protein.

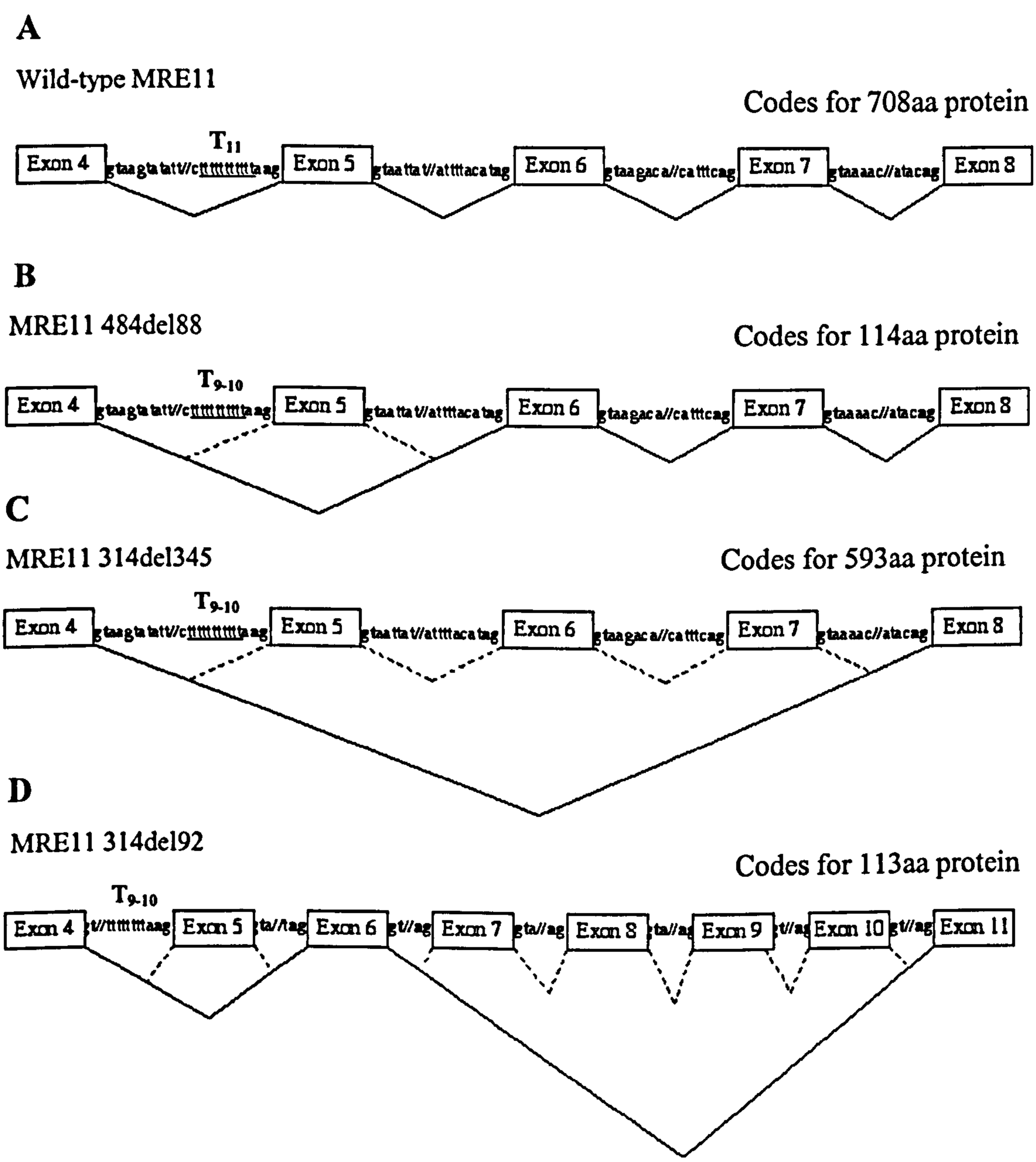

Figure 4.6.5. The protein product of MRE11 has four motifs (M1-M4) in a conserved nuclease domain. The first three are common to many phosphoesterases and the fourth is common to some nucleases. **(A)** *MRE11* 314del345 codes for a protein that lacks the third phosphoesterase motif and some surrounding amino acids. **(B)** *MRE11* 314del88 and 314del92 code for similar truncated proteins that lack two motifs of the nuclease domain and all of the C-terminus of the protein.

A

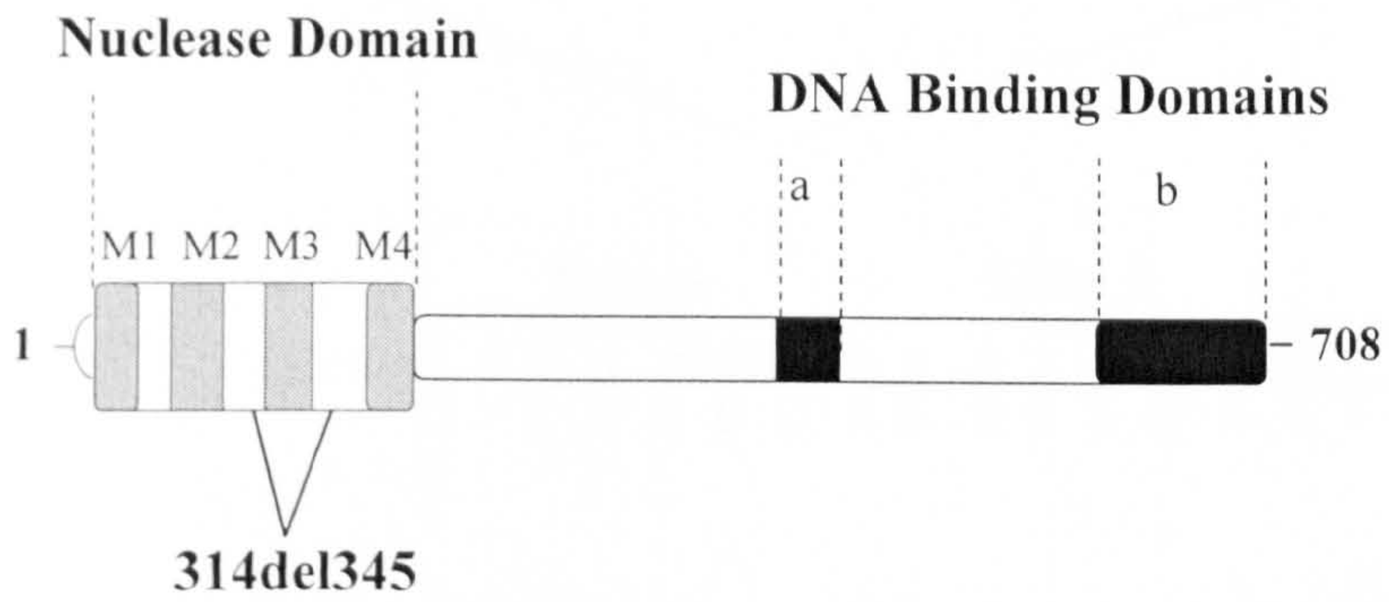

B

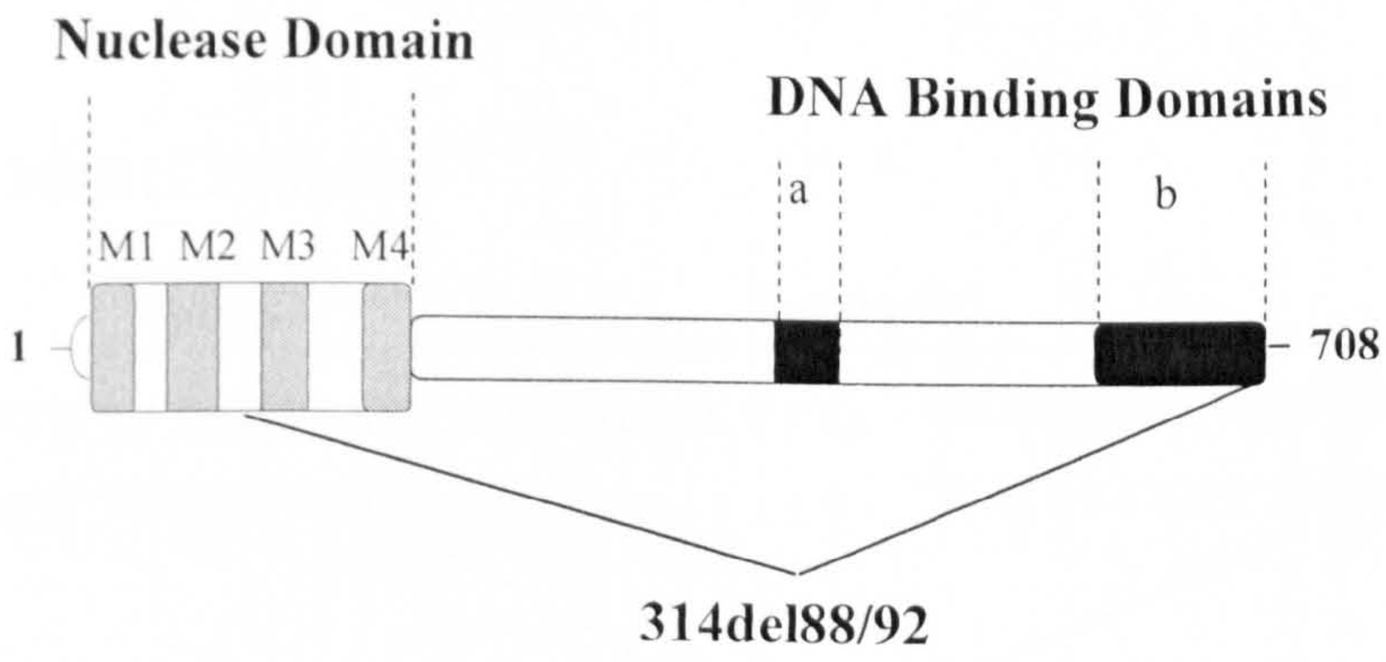

Figure 4.6.6. Sequence analysis of 314del345 and 314del92. **(A)** 314del92 skips the last 4 bases of exon 4, all exon 5 and rejoins to exon 6. **(B)** 314del345 skips exons 5-7 and re-joins exon 4 to exon 8.

A

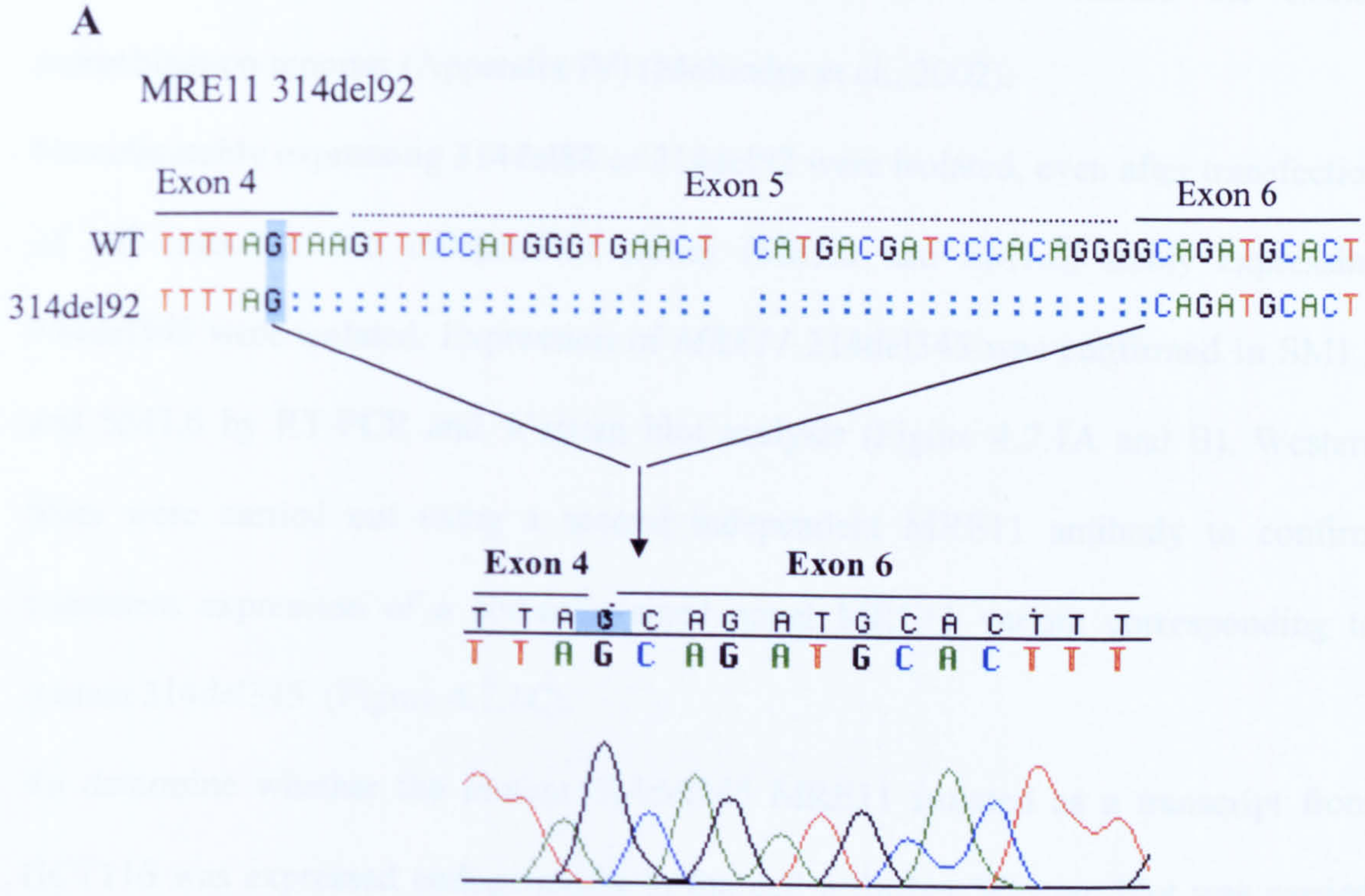

B

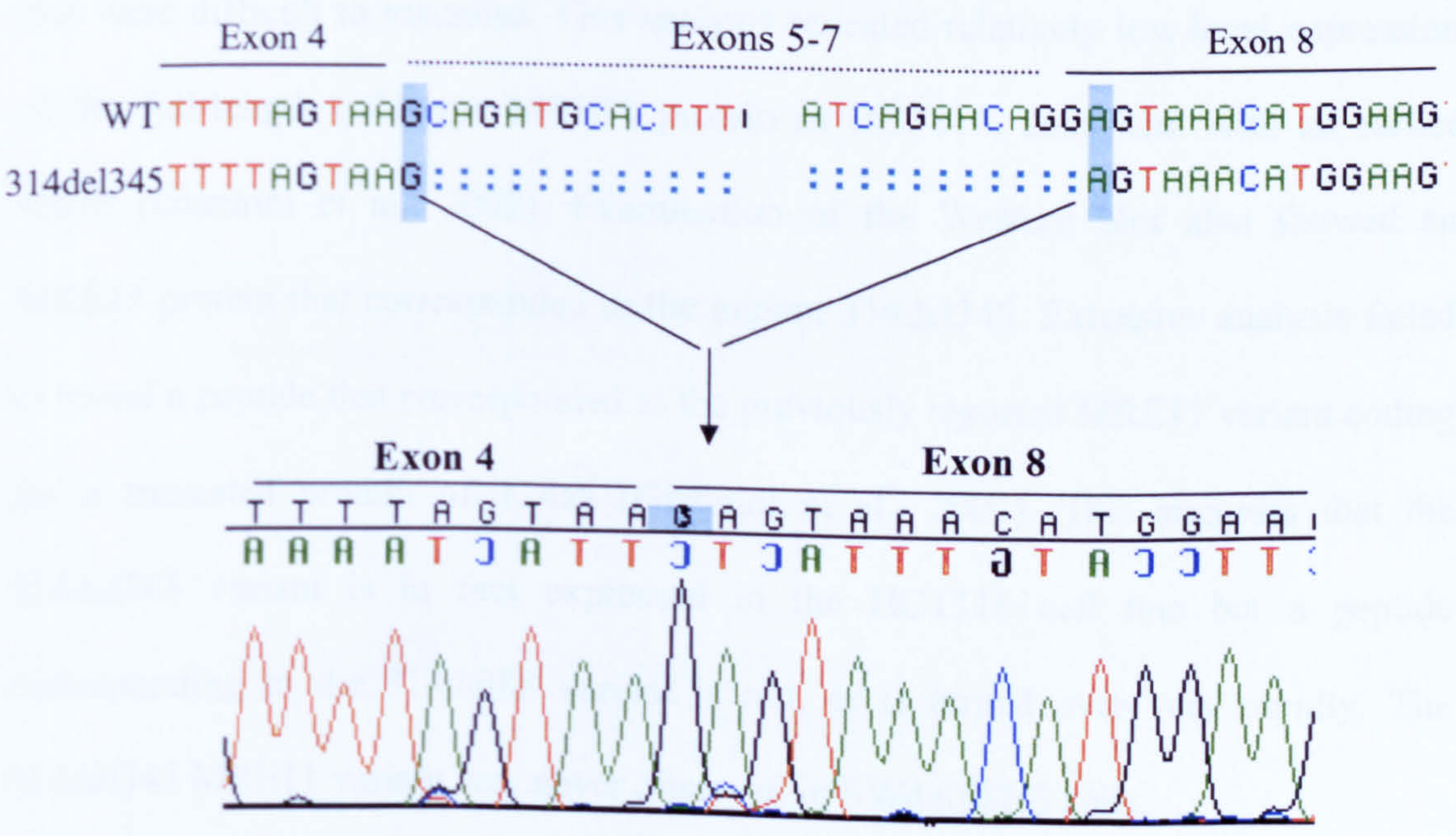

4.7 Mutant MRE11 Expression in MMR-proficient Cells

For expression of the MRE11 variants in cultured cells, 314del88, 314del92 and 314del345 were transfected to SW480/SN3 using lipofectamine treatment. SW480/SN3 is a MMR-proficient tumour cell line that carries the SCneo recombination reporter (Appendix IV) (Mohindra et al., 2002).

No cells stably expressing 314del88 or 314del92 were isolated, even after transfection of 10^6 cells but two independent clones (SM1.3 and SM1.6) stably expressing 314del345 were isolated. Expression of *MRE11* 314del345 was confirmed in SM1.3 and SM1.6 by RT-PCR and Western blot analysis (Figure 4.7.1A and B). Western blots were carried out using a second independent MRE11 antibody to confirm consistent expression of a correctly sized novel MRE11 variant corresponding to mutant 314del345 (Figure 4.7.1C).

To determine whether the mutant 314del345 MRE11 isolated as a transcript from HCT116 was expressed endogenously in the cell a further Western blot was carried out to probe HCT116 cell lysate with MRE11 antibody (Figure 4.7.1D). This blot had to be over-exposed to detect not only the wild-type MRE11 but also minor products that were difficult to visualise. This analysis revealed relatively low-level expression of the full-length wild-type MRE11 protein in HCT116, consistent with an earlier report (Giannini et al., 2002). Examination of the Western blot also showed an MRE11 protein that corresponded to the mutant 314del345. Extensive analysis failed to reveal a peptide that corresponded to the previously reported MRE11 variant coding for a truncated protein of 114aa (Giannini et al., 2002). This suggests that the 314del345 variant is in fact expressed in the HCT116 cell line but a peptide corresponding to the 314del88 variant is not, or is turned over very rapidly. The 314del345 MRE11 variant was never observed in SW480/SN3 cells.

Figure 4.7.1. Expression of MRE11 314del345 in the transfected colon cancer cell line SW480/SN3 and endogenous expression in HCT116. **(A)** RT-PCR showing expression of the mutant *MRE11* allele in transfected cells. Reactions were carried out with (+) and without (-) RT to control for contaminating genomic DNA. **(B)** and **(C)** Western blot analysis with independent MRE11 antibodies showing consistent expression of 314del345 in transfected cells. **(D)** Western blot analysis showing endogenous expression of MRE11 314del345 from HCT116. This blot was over-exposed to detect variant MRE11 products that were difficult to visualise.

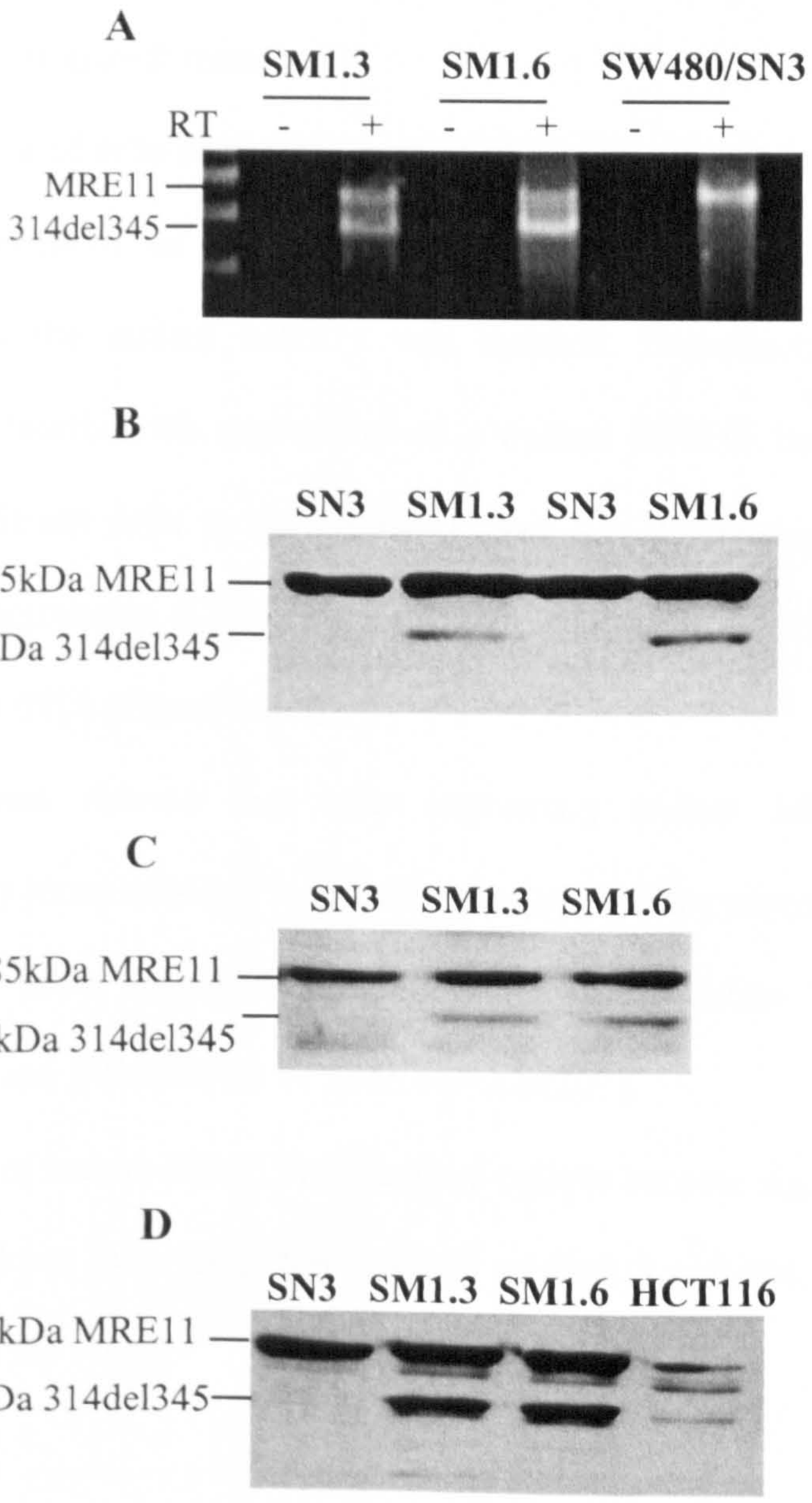

4.8 Phenotypic Consequences of *MRE11* Mutation

To determine the phenotypic effects of mutant MRE11 expression several functional studies were carried out on two independent isolates carrying 314del345, SM1.3 and SM1.6.

To establish whether the expression of mutant MRE11 or presence of puromycin (the selective agent for pIRES^{puro3} expression vector) affected cell growth a growth assay was carried out (Figure 4.8.1). This showed that the transfected lines did grow slightly slower than the SW480/SN3 parental cell line, although the presence of puromycin did not seem to exacerbate this. Therefore, expression of a mutant MRE11 appears to affect cellular growth rates.

The response of cells expressing mutant MRE11 to various toxic agents was compared to the response of the parental SW480/SN3 cells and to HCT116, the cell line from which that the mutant MRE11 was isolated. Experiments were carried out to determine whether the expression of a mutant MRE11 could affect sensitivity of MMR-proficient cells to thymidine (Figure 4.8.2), ionising radiation (IR) (Figure 4.8.3), camptothecin (CPT) (Figure 4.8.4), mitomycin C (MMC) (Figure 4.8.5) and hyroxyurea (HU) (Figure 4.8.6).

This analysis showed that cells expressing mutant MRE11 314del345 were dramatically more sensitive to thymidine relative to the parental SW480/SN3, even at the lowest doses (Students t-test at 0.25mM thymidine SW480/SN3 vs SM1.3 $p=2.5x10^{-3}$ and SW480/SN3 vs SM1.6 $p=3.6x10^{-7}$).

Expression of mutant MRE11 also caused cells to become significantly more sensitive to CPT at doses over 5nM (SW480/SN3 vs SM1.3 p=0.004, SW480/SN3 vs SM1.6 p=0.001, by the t-test).

The effect of mutant MRE11 expression on IR sensitivity was more complex. The SM1.3 and SM1.6 cells showed a significant increase in IR sensitivity relative to parental cells only at higher doses ($p=0.042$ at 8Gy by the t-test).

Both control cell lines (SW480/SN3 and HCT116) showed a similar response to MMC exposure, and cells expressing 314del345 were only significantly more sensitive than parental cells to MMC at 60nM MMC (SW480/SN3 vs SM1.3 $p=6x10^{-5}$ and SW480/SN3 vs SM.16 $p=8.4x10^{-5}$, by the t-test).

HCT116 cells were more resistant to HU treatment relative to parental SW480/SN3 cells. Introduction of a mutant MRE11 into the parental SW480/SN3 cell line caused a slight but significant increase in HU sensitivity (SW480/SN3 vs SM1.3 $p=0.018$ and SW480/SN3 vs SM.16 $p=0.03$ at 50μM HU, by the t-test).

Figure 4.8.1. Growth assay comparing the growth rate of the parental SW480/SN3 with the transfected cell lines, in the presence or absence of puromycin.

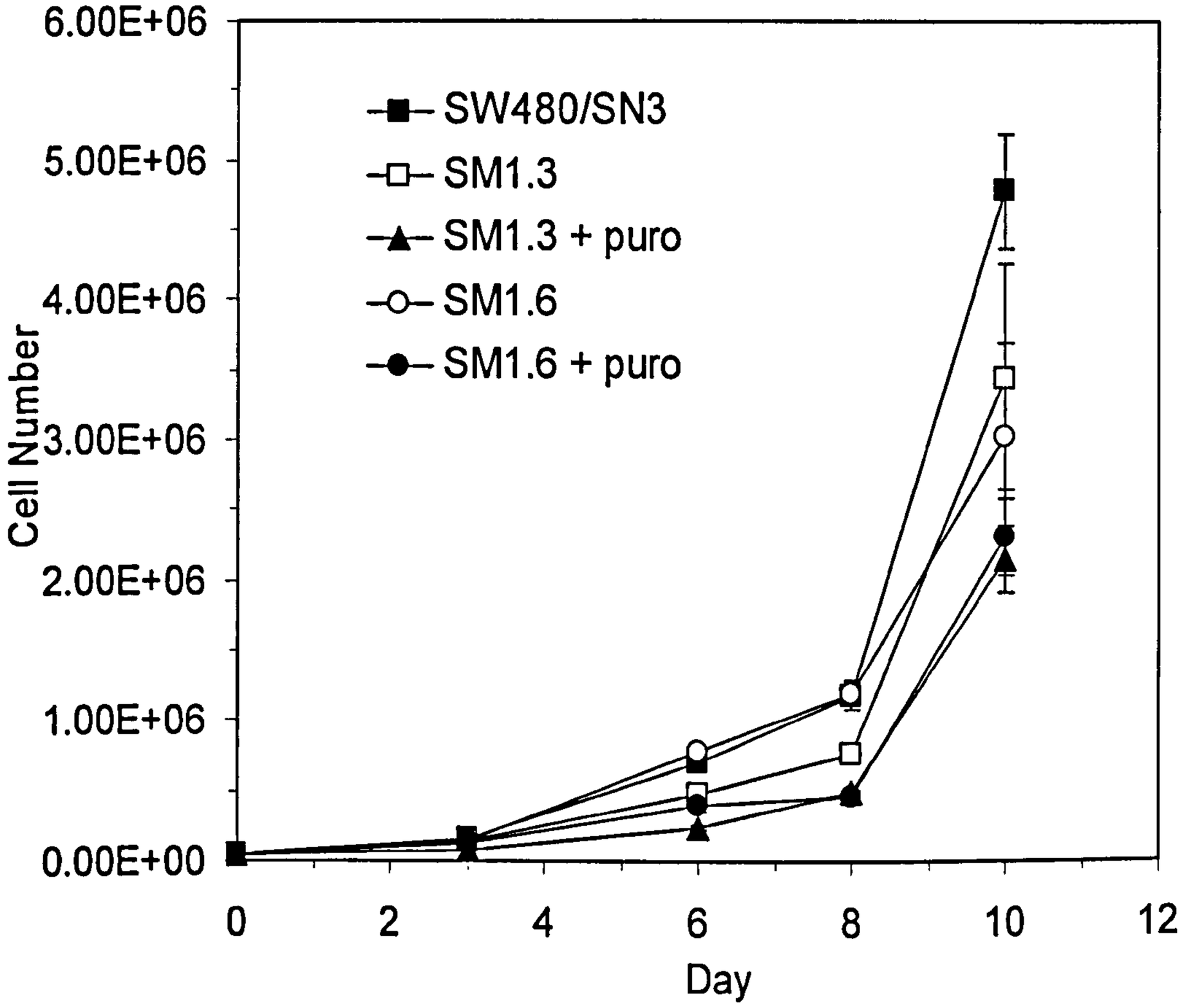

Figure 4.8.2. Expression of hMRE11 314del345 in the colon cancer cell line SW480/SN3 sensitises cells to thymidine. Lines show an average of three independent colony-forming assays, error bars represent standard deviations.

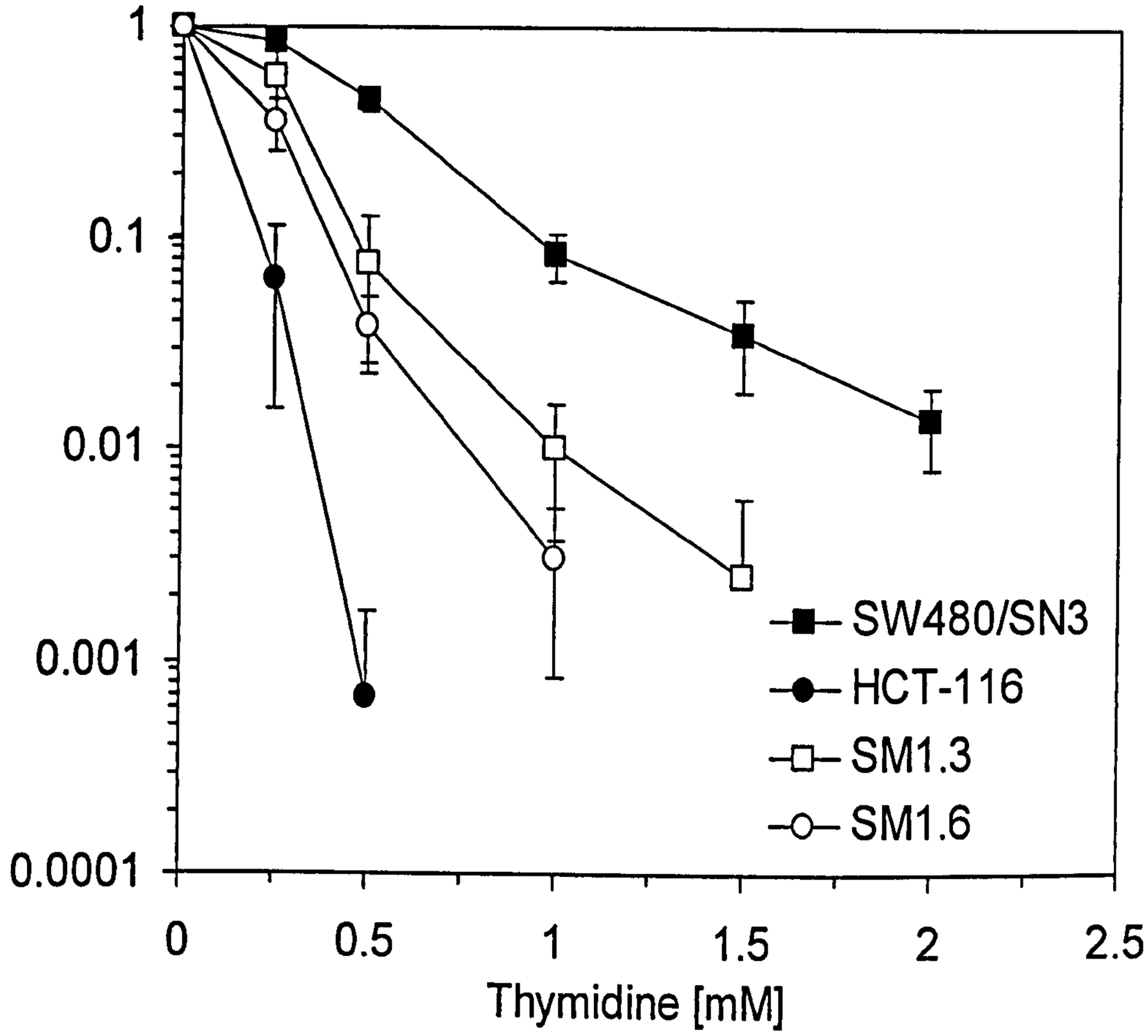

Figure 4.8.3. Cells expressing MRE11 314del3454 are sensitive to ionising radiation (IR) only at higher doses. Shown is an average of three independent colony-forming assays, error bars represent standard deviations.

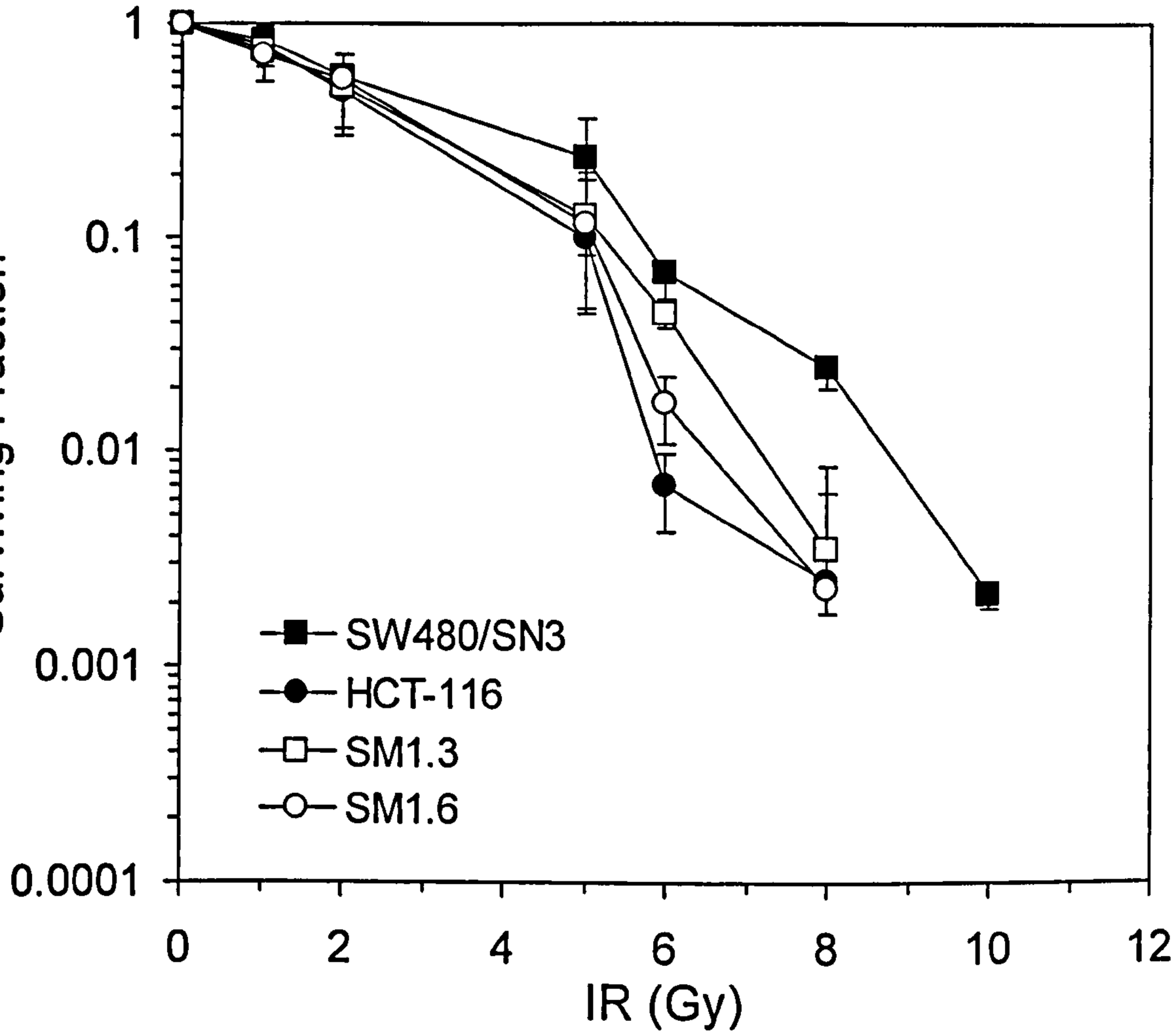

Figure 4.8.4. Sensitivity of SM1.3 and SM1.6 cells, expressing MRE11 314del345, to camptothecin (CPT). Colony forming assays were performed independently three times. Error bars represent standard deviations.

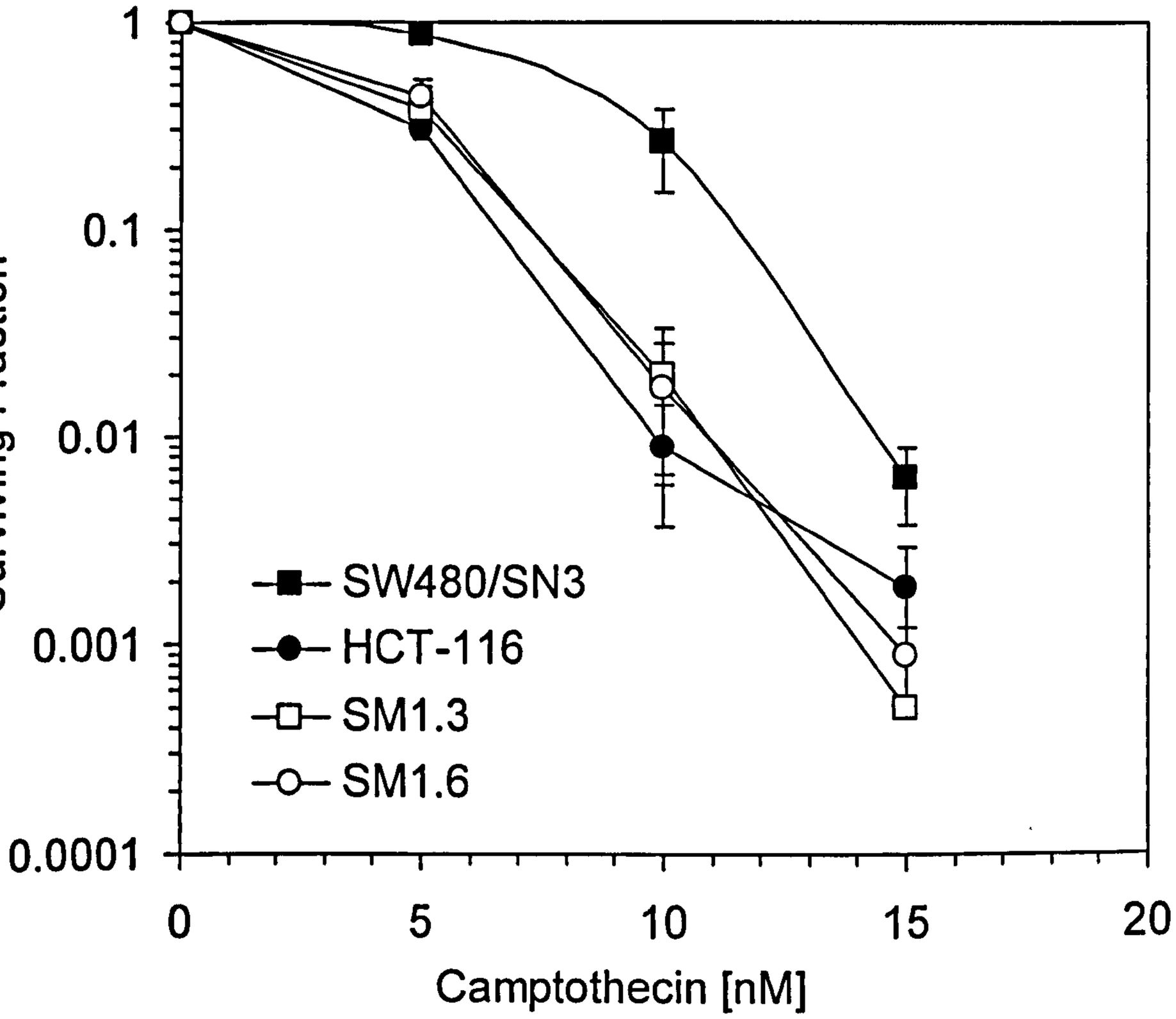

Figure 4.8.5. Introduction of mutant MRE11 314del345 to SW480/SN3 does not significantly alter response to mitomycin C (MMC), except at 60nM MMC. Shown is an average of three independent assays, error bars represent standard deviations.

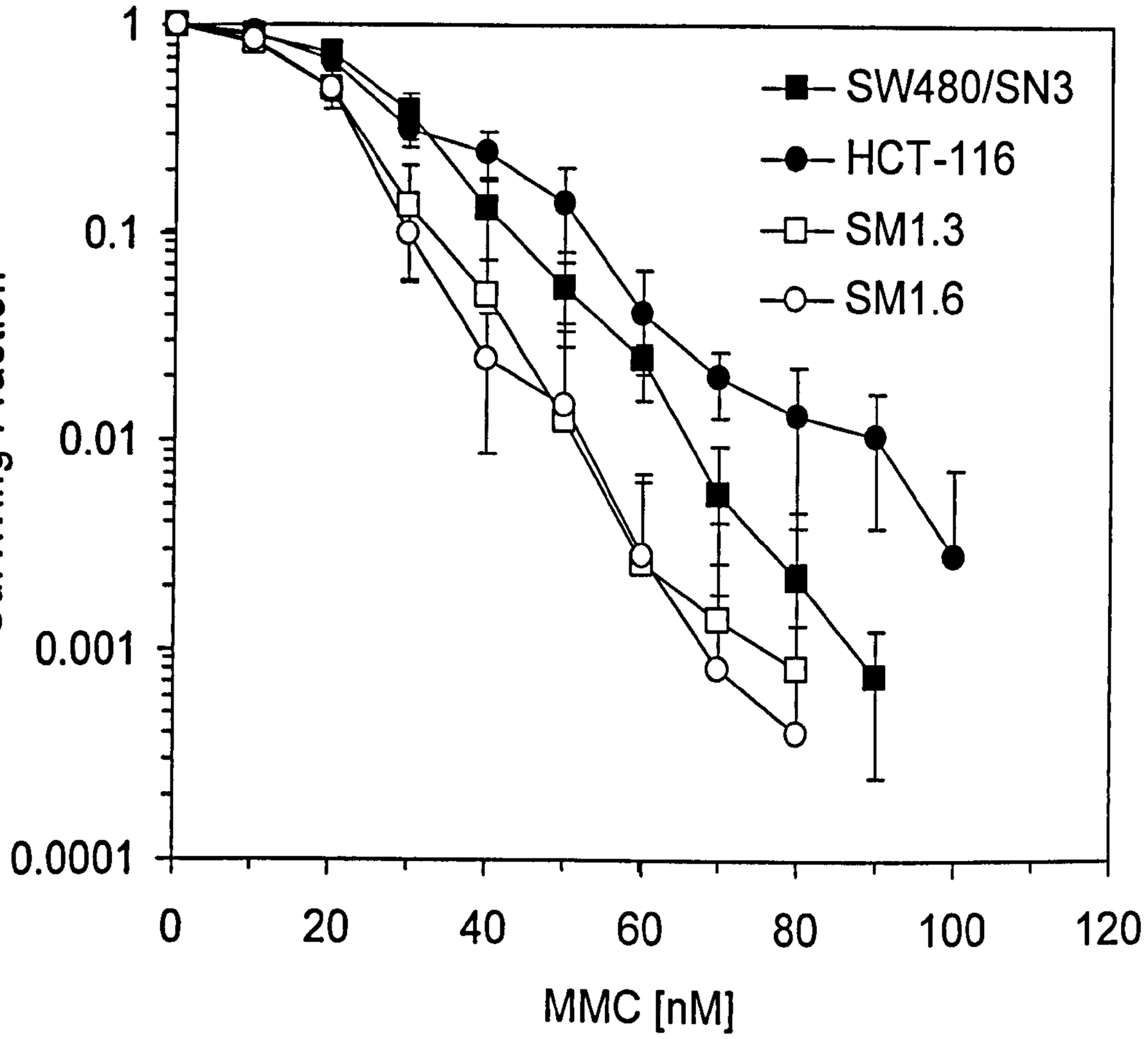

Figure 4.8.6. Mutant MRE11 expression slightly increases sensitivity to HU, relative to the parental cell line. Shown is an average of three independent colony-forming assays, error bars represent standard deviations.

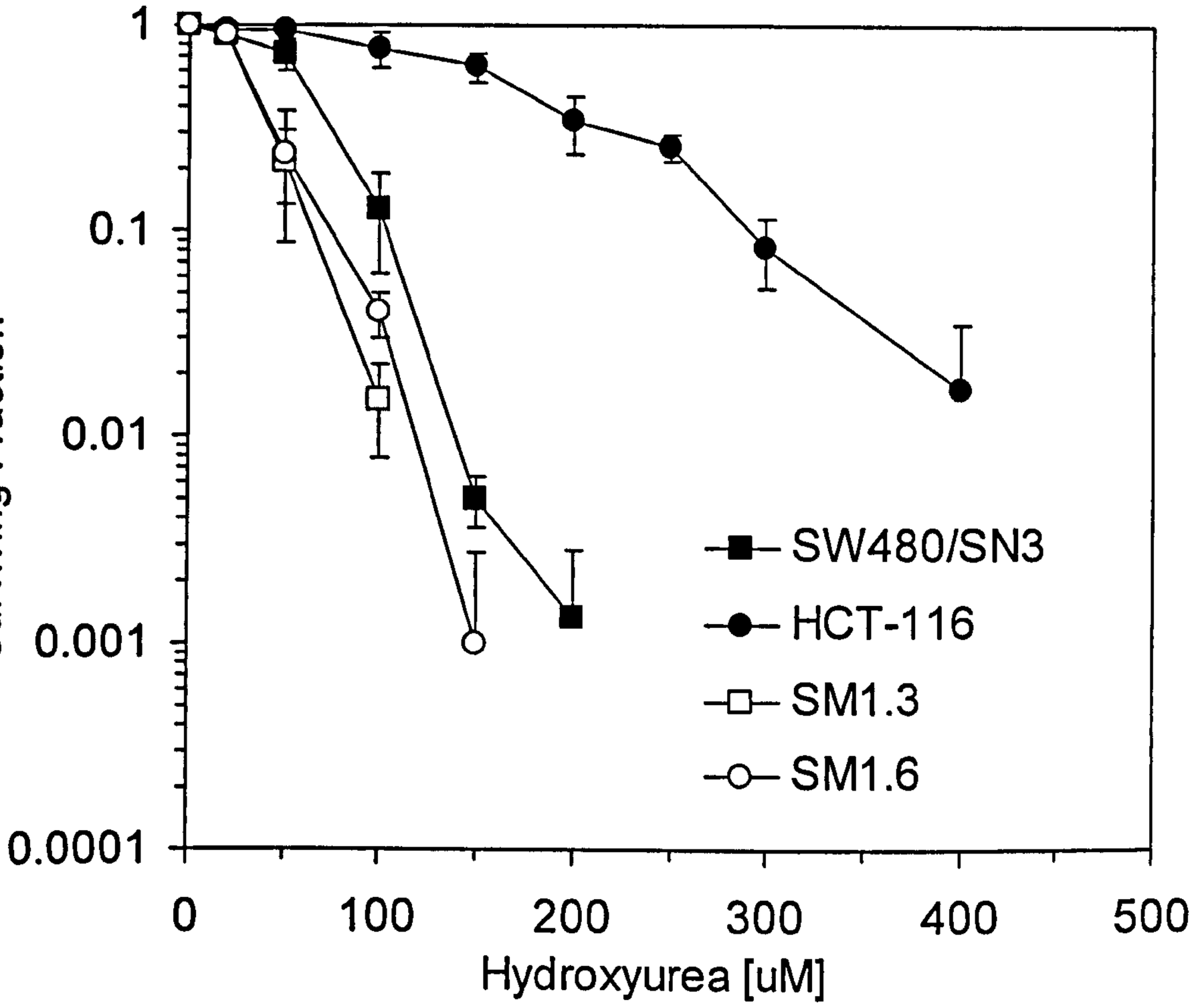

4.9 Activation and Expression of MRE11 and NBS1

It had previously been determined that HCT116 was defective in the phosphorylation of MRE11 following treatment with either thymidine or IR (E. Bolderson, personal communication). To establish whether this response was due to expression of a mutant MRE11 Western blots were carried out. Cell free extracts were prepared from SW480/SN3, SM1.3, SM1.6 and HCT116 cells treated with thymidine, IR and HU and analysed by Western blotting using antibodies against MRE11, NBS1 and the ATM-phosphorylated form of NBS1 (Phospho-Ser343 NBS1). Thymidine treatment of the parental SW480/SN3 cell line induced a shift in the electrophoretic mobility of the full length MRE11, similar to the phosphorylation dependent band shift found following treatment with IR or HU (Figure 4.9.1 and (Dong, 1999). In contrast, SM1.3, SM1.6 and HCT116 did not show such activated forms of MRE11. Phosphorylation of NBS1 could be detected in all the cells tested following treatment with thymidine, HU or IR.

Figure 4.9.1. Cells expressing 314del345 activate NBS1 but not MRE11 following treatment with 10mM thymidine (TdR), 2mM HU or 10Gy IR. The mobility shifts characteristic of MRE11 phosphorylation (*) are evident in treated SW480/SN3 but not SM1.3, SM1.6 or HCT116 cells. Actin loading controls are also presented.

(P-S323-NBS1 = Phospho-Ser343 NBS1)

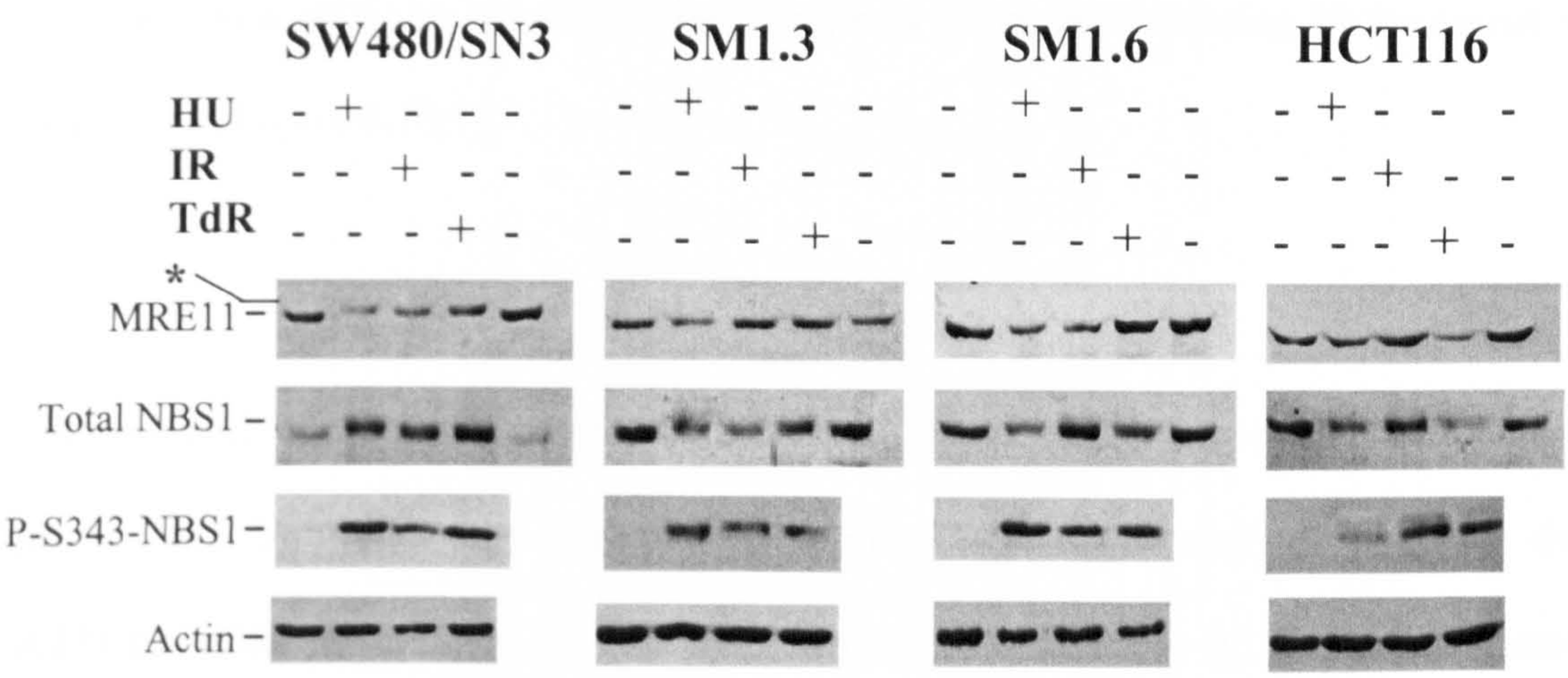

4.10 Activation and Expression of Chk1 and Chk2

To discover whether cells expressing a mutant MRE11 were capable of activating Chk2 and Chk1 following DNA damage Western blots were carried out using antibodies against the ATM-phosphorylated form of Chk2 and the ATR-phosphorylated form of Chk1. The parental cell line and cells expressing MRE11 314del345 did phosphorylate Chk1 and Chk2 as a consequence of DNA damage (Figure 4.10.1). Chk1 phosphorylation was apparent after DNA damage in lysates prepared from HCT116 but Chk2 signalling was strongest following IR treatment in these cells (Figure 4.10.1).

Figure 4.10.1. Cells were treated with 2mM HU, 10mM thymidine or 10Gy IR before protein was harvested and analysed by Western blot using antibodies against the ATM-phosphorylated form of Chk2 (P-Thr68-Chk2) and the ATR-phosphorylated form of Chk1 (P-Ser345-Chk1).

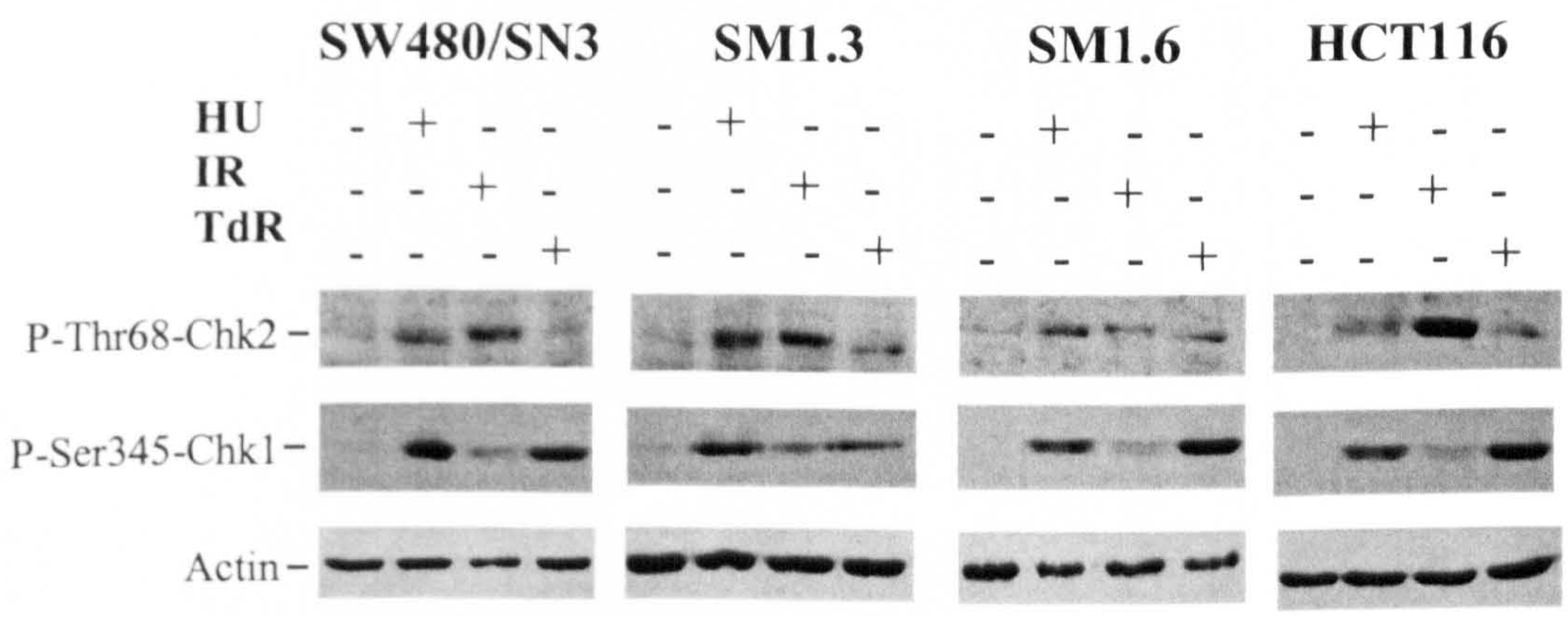

4.11 Double-Strand Break Induced Recombination

It has previously been shown that MMR-deficient cell lines are defective in homologous recombination repair following a single site-specific double-strand break (Mohindra et al., 2002). To determine whether a mutant MRE11 could contribute to this phenotype a recombination assay was carried out. Recombination was measured using the SCneo recombination reporter which measures homology-based recombination events between two defective neomycin resistance genes (Appendix IV and (Johnson et al., 1999). A site-specific DSB was introduced by transient transfection of an I-*Sce*I expression construct into cells carrying a single copy of SCneo and cells were plated on G418 to select for neo^+ recombinants.

The frequency of neo^+ recombinants in the parental SW480/SN3 and the SM1.3 and SM1.6 cells increased 87- to 110-fold whereas HCT116 cells showed no significant increase in neo^+ recombinants following a site-specific DSB (Figure 4.11.1).

Figure 4.11.1. Parental SW480/SN3 cells and cell expressing MRE11 314del345 induce homology-directed repair following a site-specific DSB. MMR-deficient HCT116 cells fail to induce HR following a site-specific DSB.

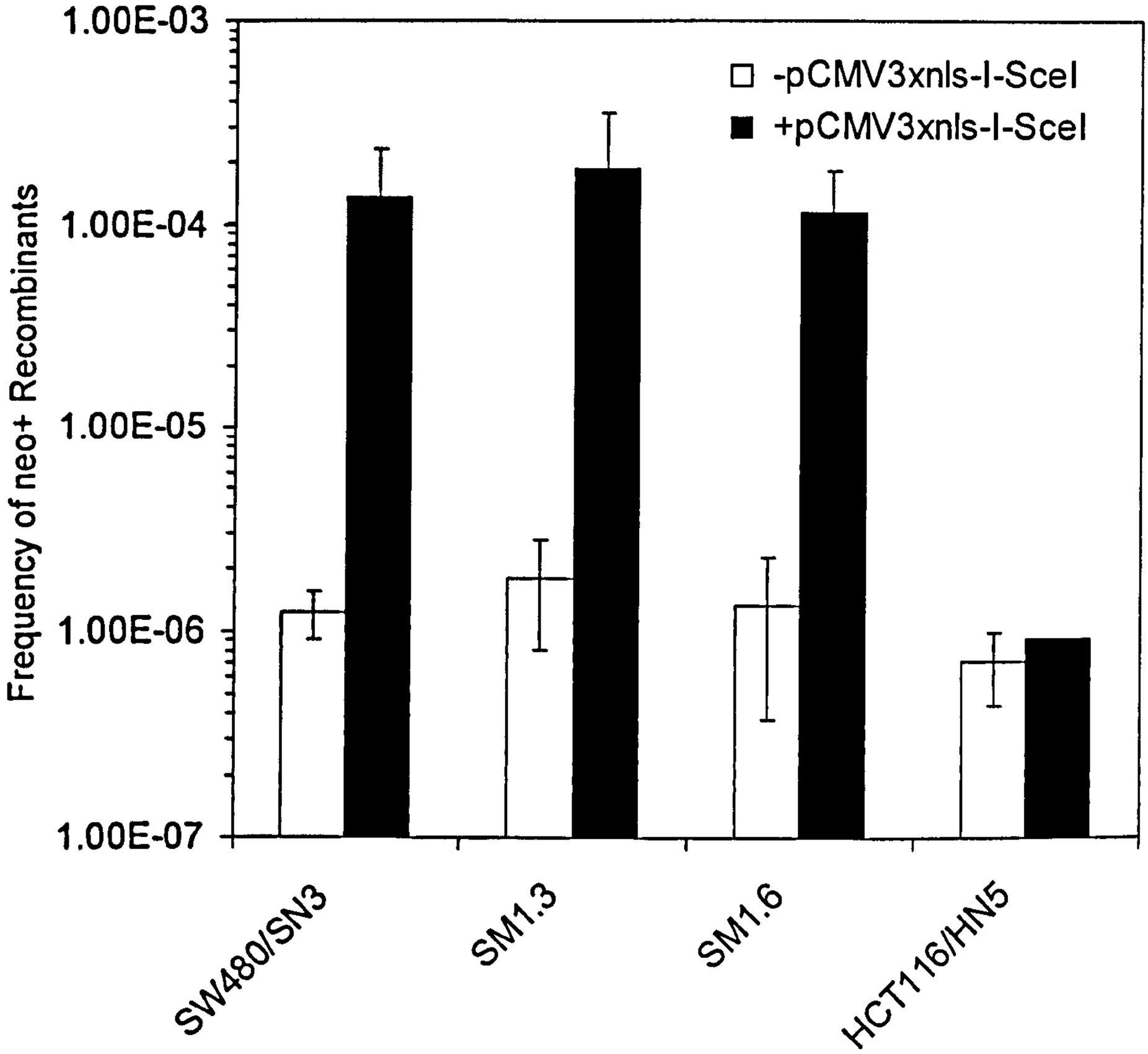

4.12 Thymidine-Induced Recombination

Previous work has shown that cells defective in HR repair become sensitive to thymidine and that thymidine is a potent inducer of HR (Lundin et al., 2002). These observations indicate that thymidine induces the accumulation of DNA lesions and that cell survival depends on the resolution of these lesions by HR. Given the increased thymidine sensitivity of cells expressing mutant MRE11 314del345 it was important to establish whether this response was caused by an inability to repair thymidine-induced DNA damage.

Replica cultures of 1000 cells were plated for SW480/SN3, SM1.3, SM1.6 and HCT116. These cultures were allowed to grow out to $1x10^6$ cells before being treated for 24 hours with increasing concentrations of thymidine. Treated cultures were left for two days to allow recovery before plating on G418 to select for neo^+ recombinants.

This analysis showed that thymidine treatment increased the frequency of neo^+ recombinants up to 12-fold in SW480/SN3 cells in a dose-dependent manner (Figure 4.12.1). SM1.3 and SM1.6 cells expressing a mutant MRE11, and the MMR-deficient HCT116 cells, showed no increase in the frequency of neo^+ recombinants after thymidine treatment (Figure 4.12.1). Comparison of the responses using regression analysis showed that the SW480/SN3 cell line had a significantly increased recombination frequency in response to thymidine compared to the SM1.3 and SM1.6 cell lines (likelihood ratio test $p=0.0025$).

Figure 4.12.1. Thymidine induces recombination in SW480/SN3 but fails to significantly induce recombination in SM1.3, SM1.6 or HCT116 cells.

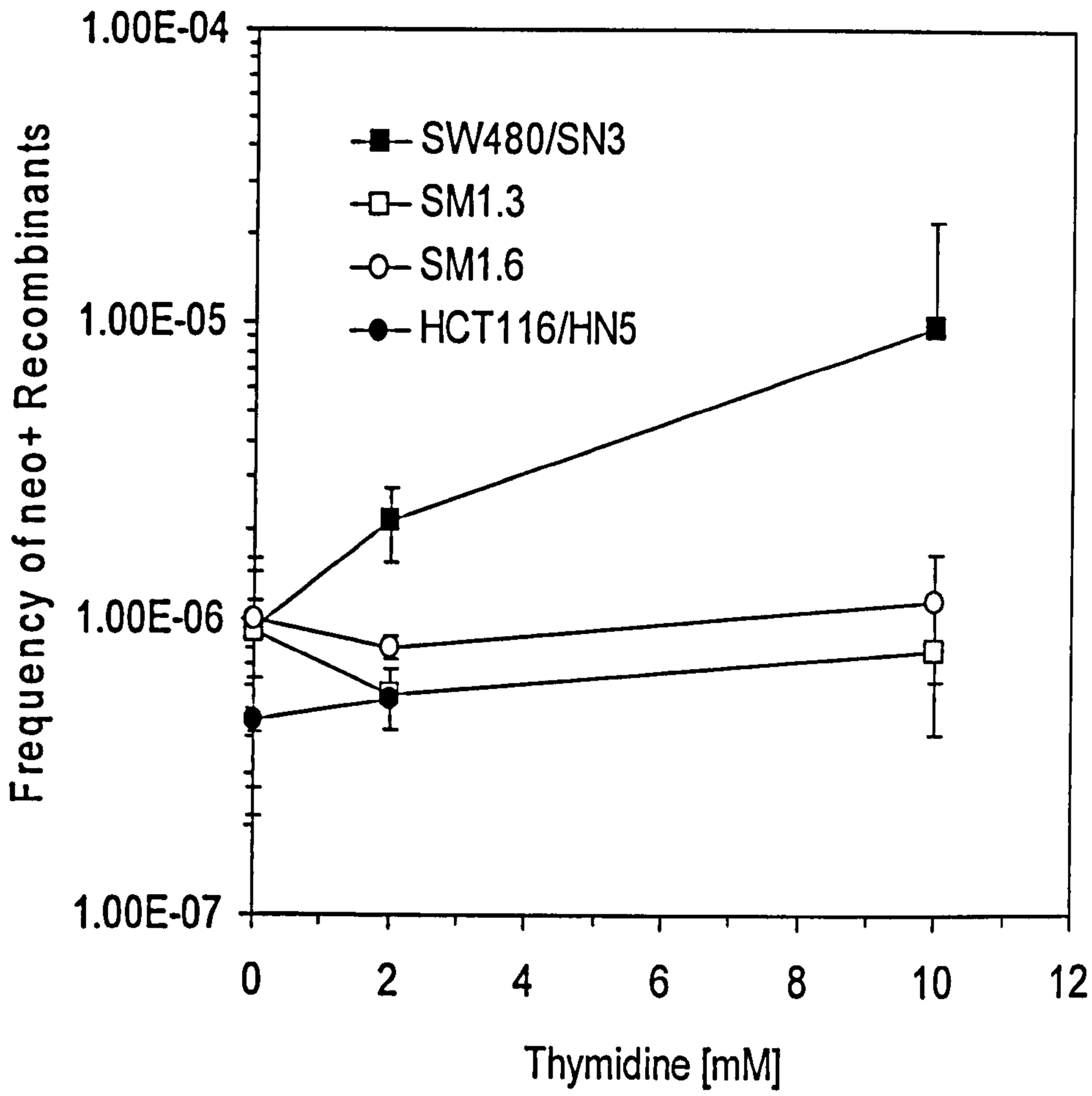

4.13 Camptothecin-Induced Recombination

Cells expressing a mutant MRE11 may not be able to tolerate the level of damage induced by thymidine treatment. Alternatively, it is possible that thymidine treatment creates a specific recombinogenic lesion that requires MRE11 to resolve it. To distinguish between these possibilities HR events following CPT treatment were measured. This analysis showed that cells expressing MRE11 314del345 remained proficient in homology-directed repair following CPT treatment (Figure 4.13.1). A similar stimulation of HR following CPT treatment was seen in the parental SW480/SN3 cells (A. Mohindra, personal communication).

These results were very interesting in that a considerable induction (100-fold) in HR was seen in SM1.3 and SM1.6 cells after treatment with 7.5nM CPT. Such a large induction following treatment with relatively low doses suggests altered kinetics in HR activation following CPT treatment. The nature of this phenomenon is beyond the scope of this thesis but certainly merits further investigation in the future.

Figure 4.13.1. Camptothecin treatment induces recombination in cells expressing mutant MRE11 314del345.

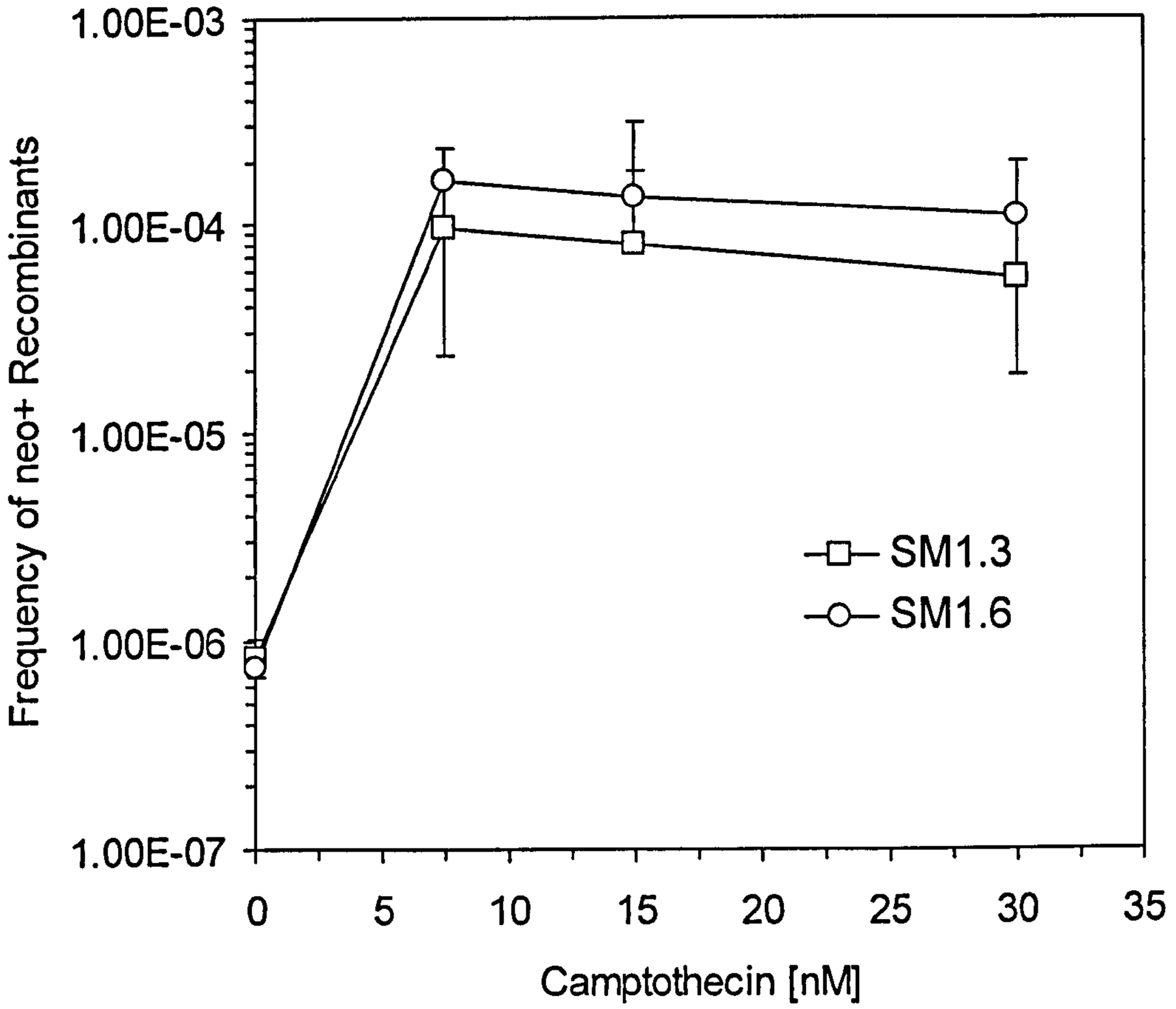

4.14 Pulsed-Field Gel Electrophoresis

Pulse-field gel electrophoresis (PFGE) was used to determine whether thymidine treatment induced DNA DSBs in SW480/SN3, SM1.3, SM1.6 and HCT116 cells. Cultures of each cell line were treated with HU, CPT, thymidine, and IR and harvested for analysis (Figure 4.14.1).

PFGE showed that thymidine did not induce detectable DSBs in any of the cell types. DSBs were evident in all cell types following treatment with CPT and IR, although CPT treatment did appear to induce less DSBs in HCT116 cells. Some lower molecular weight DNA, which may represent cells undergoing apoptosis, was observed following HU and thymidine treatment in most cell types.

This investigation confirmed that thymidine treatment does not generate the same level of DNA double-strand breaks as CPT or IR treatment.

Figure 4.14.1. Pulse-field gel electrophoresis shows damaged DNA in all cells following treatment with CPT or IR. Thymidine and HU do not introduce the same level of double-strand breaks.

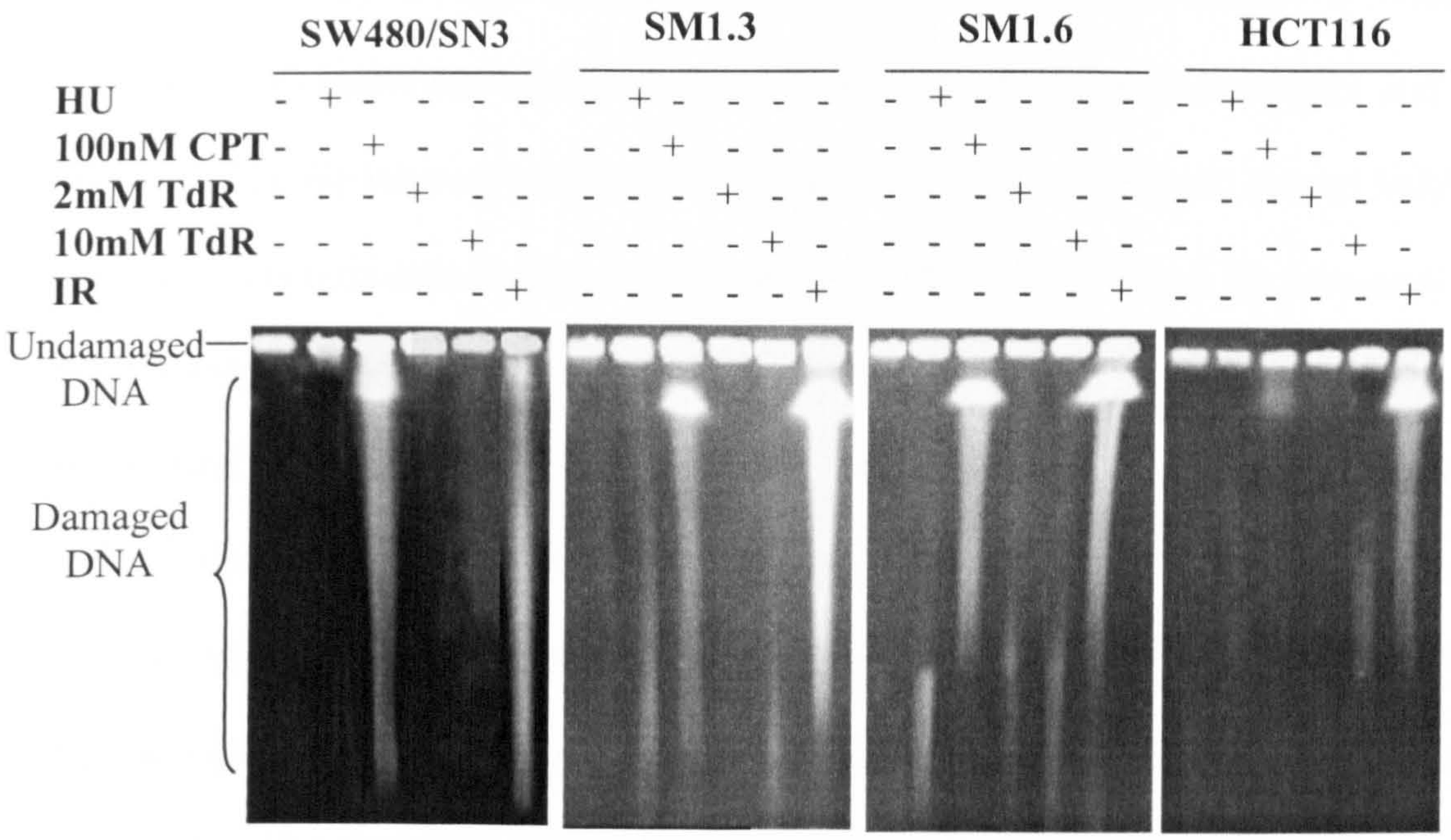

4.15 Transfection of MRE11 314del345 to MRC5VA

The cellular background of the parental SW480/SN3 tumour cell line may have contributed to the phenotypic response of SM1.3 and SM1.6 cells in this investigation. The effects observed thus far have been attributed to the presence of MRE11 314del345. To determine whether they were solely due to the mutant MRE11 and not intensified by the inherent nature of the SW480/SN3 tumour cells the mutant MRE11 construct was introduced into a second cell line, MRC5VA. This is an immortalised normal lung fibroblast cell line.

Expression of 314del345 in two transfected MRC5VA clones (MM1.2 and MM1.3) was confirmed by RT-PCR and Western blot (Figure 4.15.1). This analysis showed that the MRC5VA and SW480/SN3 clones did not express comparable levels of the mutant MRE11 protein, with expression of the 314del345 variant being much reduced in transfected MRC5VA cells. Time limitations of this project meant it was not possible to screen further transfectants to establish clones expressing comparable levels of mutant MRE11. However, this is a priority for future experiments.

The thymidine sensitivity of MM1.2 and MM1.3 was compared to the thymidine sensitivity of the MRC5VA parental cell line (Figure 4.15.2). MRC5VA cells expressing mutant MRE11 were slightly but not significantly more sensitive to thymidine than the parental cell line (MRC5VA vs MM1.2 $p=0.49$, MRC5VA vs MM1.3 $p=0.27$ at 2mM thymidine with the Students t-test).

Figure 4.15.1. Expression of MRE11 314del345 in the immortalised normal lung fibroblast cell line MRC5VA. **(A)** RT-PCR showing expression of the mutant *MRE11* allele in two transfected clones. RT-PCR analysis reactions were run with (+) and without (-) RT to ensure that the truncated product was not caused by genomic DNA contamination. **(B)** Western blot analysis showing expression of *MRE11* from SW480/SN3 **(1)**, SM1.3 **(2)**, SM1.6 **(3)**, MM1.2 **(4)**, MM1.3 **(5)** and MRC5VA **(6)**.

A

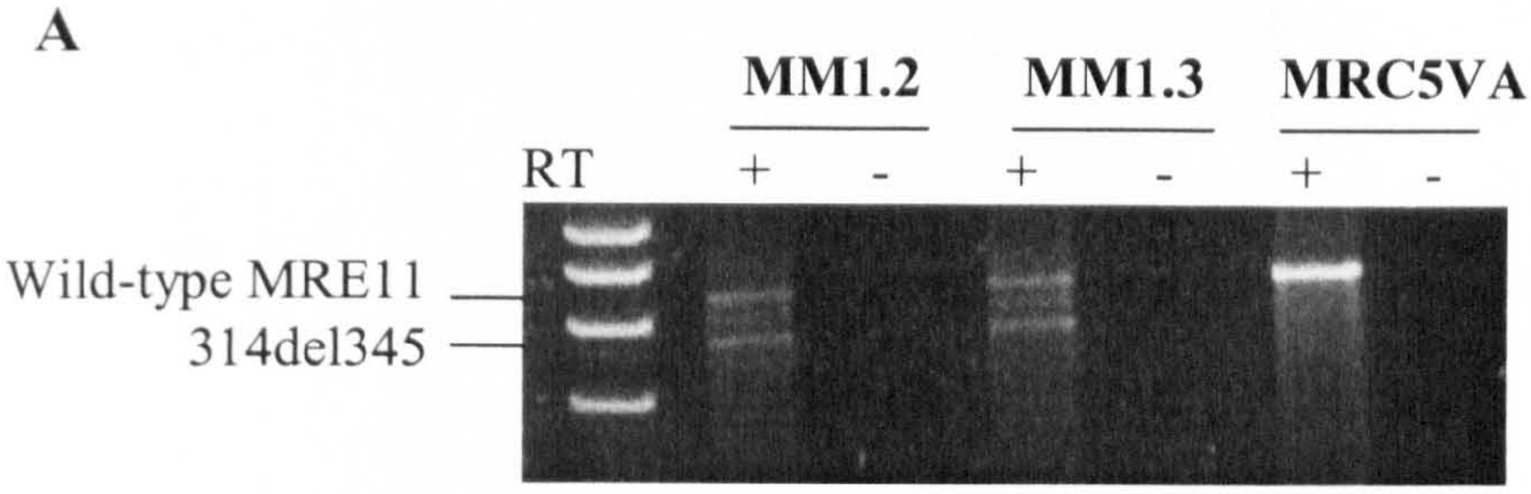

B

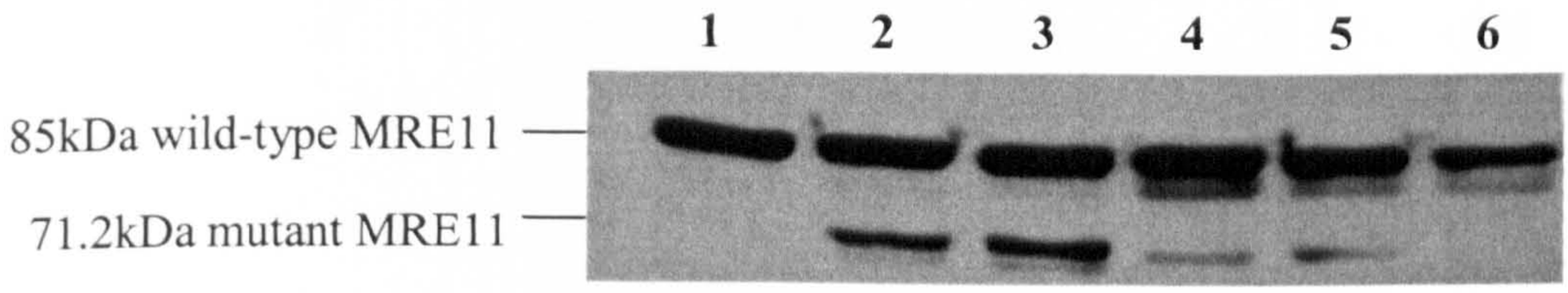

Figure 4.15.2. Thymidine sensitivity of the MRC5VA parental cell line does not differ significantly from sensitivity of MRC5VA cells transfected with mutant 314del345 MRE11 (MM1.2 and MM1.3).

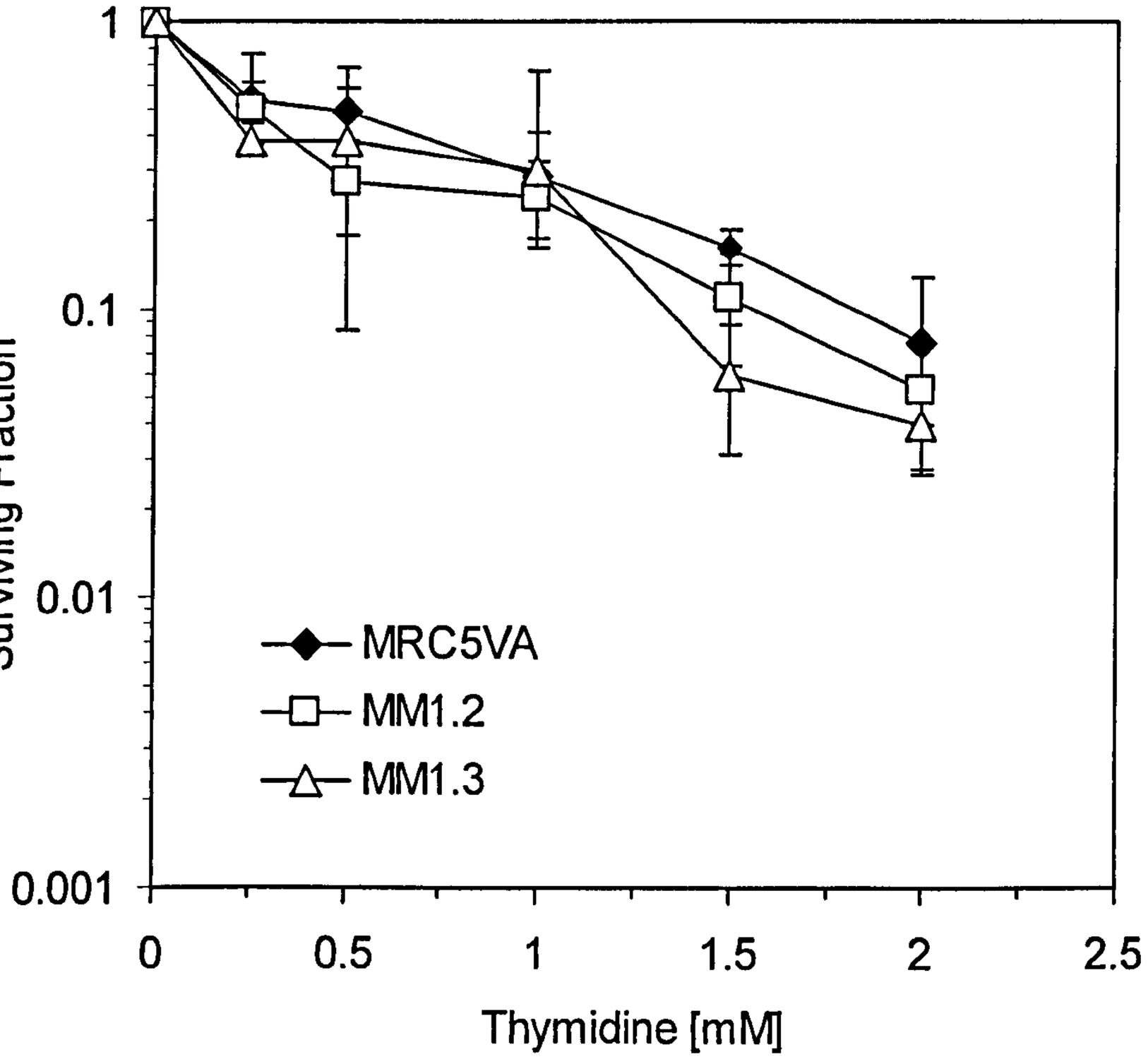

4.16 Transient expression of 314del88 and 314del345

Cells that stably express mutant MRE11 314del88 could not be established. One potential reason for this is that 314del88 codes for a severely truncated protein that causes cell death. To test this possibility cells were transiently co-transfected with a GFP-tagged vector and MRE11 314del88, MRE11 314del345 or empty pIRES^{puro3} vector. Cells that expressed GFP were presumed to also be expressing the second construct. Apoptosis events following the transfection were measured using Hoechst 33342 staining. The level of apoptosis in cells expressing empty pIRES^{puro3} vector was taken as the background apoptotic level following transfection and apoptosis induced by the introduction of a mutant MRE11 was compared to this (Figure 4.16.1).

Figure 4.16.1. Hoechst 33342 staining of cells 24 hours after transfection with a mutant MRE11 allele or empty pIRES^{puro3} vector. Data shows percentages of apoptotic cells exhibiting condensed nuclear morphology. Averages (columns) and standard deviations (bars) of 2 trials are shown.

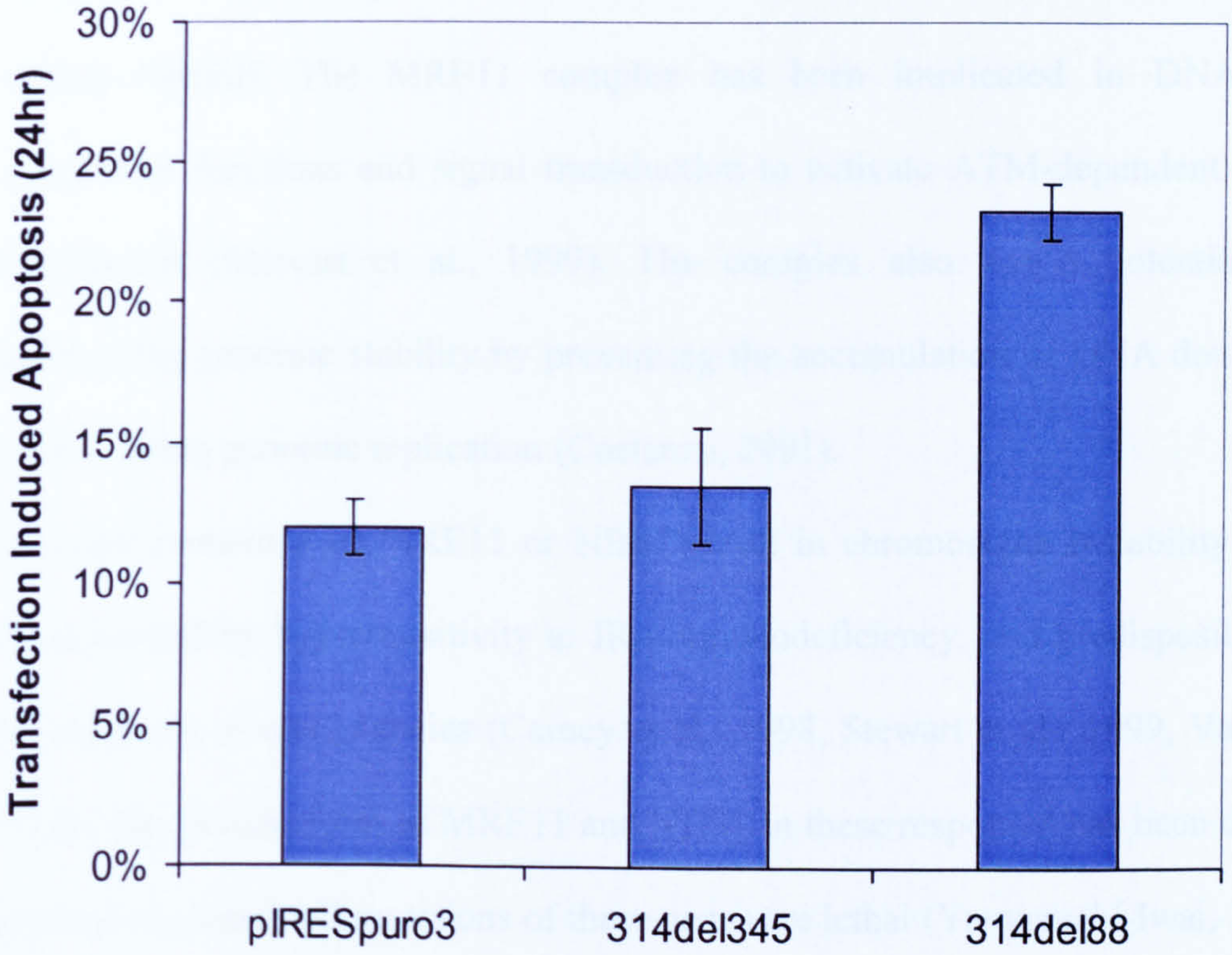

4.17 Discussion

The MRE11 complex (composed of MRE11, NBS1 and Rad50) plays a key role in DNA replication and the cellular response to DNA damage (D'Amours, 2002, Mirzoeva and Petrini, 2003). The complex has potential roles in homologous recombination (HR) repair of DNA double-strand breaks and non-homologous end-joining (NHEJ). The MRE11 complex has been implicated in DNA damage recognition functions and signal transduction to activate ATM-dependent cell-cycle checkpoints (Stewart et al., 1999). The complex also has a potential role in maintaining genomic stability by preventing the accumulation of DNA double-strand breaks during genomic replication (Costanzo, 2001).

Inherited mutations of MRE11 or NBS1 result in chromosome instability disorders characterized by hypersensitivity to IR, immunodeficiency, and predisposition to the development of malignancies (Carney et al., 1998, Stewart et al., 1999, Varon et al., 1998). The precise roles of MRE11 and NBS1 in these responses has been difficult to establish because null mutations of these genes are lethal (Yamaguchi-Iwai, 1999, Zhu et al., 2001).

Since the MRE11 complex has important roles in maintaining genomic integrity it was hypothesised that the *MRE11*, *NBS1* and *Rad50* genes were potential targets for mutation in the development of cancer. Given that loss of MMR increases overall genomic instability and promotes further mutations in other key repair proteins, mutations in *MRE11*, *NBS1* and *Rad50* became even more probable in MMR-deficient tumour cells.

a) Mutation of the MRE11 Complex is Frequent in MSI$^+$ Cancers

Previously, mutations and polymorphisms in the coding sequence of *MRE11* and *NBS1* have been observed in primary tumours and cell lines (Fukuda, 2001, Tessitore et al., 2003). However, analysis of the colon and endometrial cancer cell lines available for this study revealed no mutations in the coding sequence of any of the candidate genes.

A further investigation of primary colorectal tumours revealed heterozygous frameshift mutations in mononucleotide runs of the *Rad50* and *MRE11* genes.

Analysis showed that the *Rad50* A_9 coding mononucleotide run was mutated in 7.7% of MSI$^+$ CRC samples whereas previous studies have reported the mutation frequency of *Rad50* A_9 in MSI$^+$ colorectal tumours to be 28-33% (Kim et al., 2001, Duval and Hamelin, 2002). Although the observed incidence of *Rad50* A_9 mutations is much lower than previous reports the extensive cloning analysis in this study suggests that the mutation frequency obtained for this population is accurate. The inter-experimental variation could be due to population differences, such as age, ethnicity or sex. An alternative explanation for the difference is that not all tumour cells examined in this study express the mutant allele. If this were the case then this frameshift mutation would not be expected to play a primary role in tumour development since mutations that predispose to malignancy are likely to be present in the majority of tumour cells.

However, a frameshift in the A_9 tract of *Rad50* would truncate the protein from 1312aa to 734aa. The functional consequences of this truncated Rad50 have yet to be established. Future studies to examine the phenotypic consequences of this mutation will be important in determining the impact of Rad50 alteration on cancer development.

A recent study reported a -1/-2 frameshift mutation in the T_{11} polypyrimidine tract in *MRE11* intron 4 (Giannini, 2002). T_9 and/or T_{10} alleles were seen in 93% of MMR-deficient primary colorectal cancers and all MMR-deficient cancer cell lines studied but were not detected in MMR-proficient cancer cell lines or primary tumours (Giannini, 2002). This mutation has also been observed in 12% of MMR-defective acute leukaemia (Casorelli et al., 2003).

Extensive cloning and sequencing analysis of 20 MSI^+ colorectal tumours estimated that this mutation occurred in >85% of MSI-H colorectal tumours. The frameshift mutation was not seen in non-cancer (normal) tissue surrounding the MSI^+ cancers or in MSS tumours suggesting that the MRE11 mutation is associated with a MMR-deficiency. Interestingly, the mutation was not seen in any MSI-L tumours and this is consistent with other studies that have reported that MSI-H tumours have distinct clinicopathological and molecular characteristics from MSI-L and MSS tumours (Duval and Hamelin, 2002, Halford et al., 2002).

Polypyrimidine tracts are important *cis*-acting signal sequences directing intron removal. Tracts with 11 continuous uridines are the strongest tracts and decreasing numbers of uridines in the tract can alter 3′ splice site selection and reduce efficiency of splicing (Coolidge et al., 1997). The mutation in the T_{11} run of *MRE11* intron 4 shortens the polypyrimidine tract, reduces its strength as a signal sequence and so reduces but not abolish the correct splicing process. Cells with the *MRE11* T_{11} frameshift mutation produce a mixture of wild type and mutant MRE11 products.

It was reported that in >50% of MMR-deficient colorectal cancer samples with the mutation in MRE11 T_{11} the wild-type allele was under-represented compared with the mutant alleles, suggesting a homozygous change (Giannini, 2002). However, the homozygous nature of the mutation was not confirmed and no homozygous mutations

were seen in this current study. However, since the MRE11 mutation reduces but does not completely abolish the correct splicing process a combination of wild-type and variant transcription products are generated both when the mutation is heterozygous and homozygous.

To investigate the phenotypic consequences of the mutation in MRE11 a cDNA copy of the principal reported mutant product, 484del88 was required. Expression of the 484del88 cDNA could be confirmed in HCT116 and SW48 but a cDNA copy of the MRE11 variant could not be isolated directly from these cell lines. The 484del88 MRE11 variant cDNA or peptide was not isolated in the study that originally identified this variant either (Giannini et al., 2002). It is possible that the transcript does not exist in the cell for an extensive enough time to allow isolation and it was noted that nonsense mediated decay was taking place to degrade the aberrant 484del88 transcript (Giannini et al., 2002). MRE11 Western blots on protein extracts from HCT116 showed no peptide corresponding to 484del88, suggesting that translation of the aberrant transcript does not take place in this cell line or that turnover of this small product is rapid. If this mutant MRE11 protein is not stably produced then the significance of the 484del88 variant in the cell is questionable.

During analysis of cloned MRE11 products from HCT116, several other alternative mutant MRE11 alleles were detected. It was hypothesised that these variants were created by alternative splicing promoted by the mutation in the T_{11} tract of *MRE11*. Cells that stably expressed the isolated MRE11 truncating variants 314del88 and 314del92 could not be obtained. Analysis revealed that transfection of 314del88 to cultured cells caused twice as much apoptosis as uptake of either empty vector or MRE11 314del345. This result is consistent with the idea that severely truncated

mutant MRE11 transcripts cause cell death upon their expression in the cell and it is known that null mutants of MRE11 are lethal (Yamaguchi-Iwai, 1999). This also raises the possibility that shorter aberrant transcripts that might be present in HCT116 are transient, as is the case for 484del88 (Giannini, 2002), to prevent induction of apoptosis.

b) MRE11 314del345 Affects Response to DNA-damaging Agents

Functional studies to investigate the phenotypic effects of a mutant lacking the third phosphoesterase motif, 314del345, provided insights into the consequences of compromising wild-type functioning of MRE11.

One proposed role for the MRE11 complex is to prevent the accumulation of DNA DSBs at replication forks (Costanzo, 2001, Mirzoeva and Petrini, 2003). Treatment of cells with camptothecin induces replication fork-associated DNA DSBs in the S-phase of the cell cycle (Arnaudeau et al., 2001, Furuta et al., 2003). Since only S-phase cells are susceptible to CPT-induced DNA damage and in wild-type S-phase cells MRE11 is associated with the replication fork (Maser, 2001) accumulation of DSBs in these cells could be prevented. In contrast, expression of a mutant MRE11 conferred CPT sensitivity, possibly by reducing surveillance ability or efficiency at the replication fork thereby allowing accumulation of CPT-induced DSBs and causing cell death.

Cells from A-TLD patients expressing a severely truncated form of MRE11 show extreme sensitivity to IR, whereas cells from patients with a point mutation close to the third phosphoesterase motif do not show acute IR sensitivity (Stewart et al., 1999). Similarly, yeast mutants carrying a point mutation in motif III of the ScMre11 nuclease domain do not show a dramatically increased sensitivity to IR (Bressan et al., 1998). These results suggest that MRE11 mutations that decrease the efficiency of but do not abolish MRE11 function might not lead to severe IR sensitivity. The IR

sensitivity of cells expressing MRE11 314del345 was only significantly increased relative to parental cells at doses greater than 8Gy IR. This may reflect an inability to cope with increasing levels of IR-induced damage due to reduced MRE11 nuclease activity.

Expression of MRE11 314del345 led to a slightly but significantly increased sensitivity to HU relative to the parental cell line. HU inhibits the ribonucleotide reductase enzyme and depletes cells of all dNTPs required for DNA synthesis. This suspends DNA replication by limiting the dNTP pools and leads to stalling of the replication fork (Lopes 01). HU is known to trigger phosphorylation of NBS1 in an ATM-independent manner (Wu et al., 2000) but the role of MRE11 in this response is unknown. Potentially, MRE11 314del345 could impair MRE11 complex formation or de-regulate NBS1 phosphorylation so that the response to HU is altered. Alternatively, the presence of a mutant MRE11 may force the cell to use a second, less efficient pathway to process the HU-induced damage and this might be reflected as an increase in sensitivity to HU.

Sensitivity to MMC was not dramatically affected by expression of 314del345, suggesting that the mutant MRE11 does not significantly impair the response to MMC-induced damage. MMC-induced interstrand cross-links are usually resolved by sister chromatid exchanges mediated by HR (Hoeijmakers, 2001, Sonoda et al., 2001) and MMC sensitivity is more frequently associated with defects in HR genes that have a direct role in the resolution of cross-links, such as the Rad51 paralogs (Takata et al., 2001). It is possible that the endogenous wild-type MRE11 in the transfected cells has sufficient activity to process the damage caused MMC.

Together, these results support a role for MRE11 in the DNA damage response triggered by impaired DNA replication forks or DSBs in the cell.

c) MRE11 314del345 Affects Phosphorylation Events Following DNA Damage

The MRE11 314del345 variant appears to block phosphorylation of the wild-type protein upon DNA damage to prevent MRE11 activation. The phosphorylation of MRE11 is likely to increase its nuclease activity (Costanzo et al., 2001) and therefore loss of this post-translational modification may compromise repair functions of the MRE11 complex. Phosphorylation of MRE11 in response to DNA damage precedes foci formation (Dong et al., 1999) and therefore may play a role in targeting the MRE11 complex to sites of repair. However, the exact role of MRE11 modification has yet to be established and further studies are required to determine the biochemical consequences of defective MRE11 phosphorylation. Whether MRE11 phosphorylation is required for all downstream functions of the MRE11 complex also merits investigation.

Examination of cell-free extracts from HCT116 suggested that this cell line expressed MRE11 314del345 endogenously. This result indicates that the 314del345 variant may exist in cells carrying a frameshift mutation in the intronic T_{11} tract of MRE11 and may well be exerting an effect *in vivo*.

Further analysis showed that all cell lines remained proficient in ATM-dependent NBS1 phosphorylation induced by DNA-damage, showing that the mutant MRE11 did not interfere with NBS1 signalling.

Cells expressing mutant 314del345 remained proficient in DNA damage-induced phosphorylation of the Chk2 and Chk1 kinases. Furthermore, phosphorylation events in cells expressing 314del345 did not appear to be up-regulated compared to those in SW480/SN3 cells suggesting that there was no attempt to compensate for a defective MRE11 pathway by up-regulating other branches of the DNA damage-dependent S-phase checkpoint response. Defects in the ATM-Chk2-Cdc25A branch of the pathway

do not affect the ATM-NBS1-MRE11 branch (Falck, 2002), and the results obtained here show that the reverse is also true.

One observation made during analysis of Chk2 phosphorylation conflicted with a previous report. It was suggested that the MMR-deficient cell line HCT116 fails to undergo ATM-mediated Chk2 phosphorylation following IR and that Chk2 phosphorylation depends on MMR (Brown et al., 2003). This does not agree with data obtained here where Chk2 phosphorylation was seen following IR treatment in HCT116 cells. There are several possible explanations as to why there are differences between the two studies. Firstly, this study uses 10Gy IR to induce damage whereas Brown et al use 5Gy. It is possible that there is a threshold switch within the cell to activate certain response pathways above specific levels of damage. Secondly, the stage of the cell-cycle at which IR-induced damage occurs may affect the checkpoint pathway that is activated (Xu et al., 2002). Lastly, these cells are in dynamic cultures where various events take place over time that may affect cellular outcomes.

It was noted however, that two other impartial researchers, one in the same laboratory, the second in an independent laboratory obtained equivalent data showing phosphorylation of Chk2 from HCT116 after IR-induced damage (E. Bolderson and J. Dziegielewski, personal communication).

d) MRE11 is Essential for HR Repair of Thymidine-impaired Replication Forks

Depletion of dCTP pools through the allosteric regulation of ribonucleotide reductase following thymidine treatment slows but does not arrest DNA replication fork progression and cells accumulate in S-phase (Bjursell and Reichard, 1973). The disruption of DNA replication caused by the dCTP depletion appears to generate substrates for recombination that must be resolved by HR for cell survival (Lundin et al., 2002). Expression of MRE11 314del345 dramatically increased cellular sensitivity

to thymidine, possibly by disrupting the HR repair response to thymidine-induced damage. In support of this hypothesis, cells expressing the variant MRE11 were proficient in HR following a site-specific DSB but failed to induce HR following thymidine treatment. Thymidine has previously been shown to be a potent inducer of HR in hamster cells (Lundin et al., 2002) and results obtained from the SW480/SN3 parental cell line indicate that it also induces HR in human cells. It was initially proposed that thymidine did not activate HR in transfected cell lines because cells with a mutant MRE11 would be overwhelmed by the level of damage. However, further experiments revealed that cells expressing 314del345 could activate HR following CPT treatment. This suggested that it was not that cells with a mutant MRE11 failed to cope with the level of damage as both CPT and thymidine have the potential to act at every replication fork in the cell.

This raised the interesting possibility that a specific lesion is created at the replication fork by thymidine treatment. Results from PFGE experiments imply that thymidine does create a different lesion to CPT as CPT treatment creates detectable levels of DSBs, whereas treatment with thymidine does not. This research shows for the first time that HR-mediated rescue of thymidine-impaired replication forks requires a functional MRE11 and supports increasing evidence for a role of MRE11 in maintaining the integrity of DNA replication forks (Yamaguchi-Iwai et al., 1999, Costanzo et al., 2001, Mirzoeva and Petrini, 2003).

e) Putative Requirement for Threshold Levels of Mutant MRE11

Expression of MRE11 314del345 in MRC5VA cells did not give as dramatic phenotypic consequences as when expressed in SW480/SN3 cells.

If the mutant MRE11 is interfering with wild-type MRE11 activation, as was suggested by the lack of phosphorylation of wild-type MRE11 protein following DNA damage in SW480/SN3 transfected cells, then it would make sense that a threshold level of mutant protein would be necessary to alter MRE11 responses. It follows then, that the mutant 314del345 MRE11 transfected to MRC5VA cells fails to introduce a significant detrimental phenotype because there is insufficient mutant MRE11 expression. A normal cell line expressing comparable levels of mutant MRE11 to the SW480/SN3 transfectants needs to be created for future studies to establish the impact of cellular background on mutant MRE11 phenotype.

CHAPTER 5

Discussion

5.1 Discussion

The primary focus of this research was to undertake a systematic study of mutations and polymorphisms in candidate genes with roles in homologous recombination (HR) repair and cell-cycle checkpoints. The frequency of such mutations and polymorphisms has been determined in MMR-deficient cancer cell lines and primary colorectal tumours and the validity of these mutation frequencies confirmed by extensive cloning analysis. The phenotypic consequences of a common MRE11 mutation have been comprehensively investigated and a role for MRE11 in repair of impaired DNA replication forks has been proposed.

5.2 Alteration of HR Genes in Colorectal Cancer

This investigation found little evidence to support the hypothesis that mutations in *XRCC2*, *XRCC3* or *Mus81* are associated with colorectal cancer. Mutations of these genes are likely to have severe consequences for the cell and therefore may not be tolerated. Some polymorphisms of these genes are present in the cancer population, although results from this study suggest that they are not associated with a significantly increased risk of colorectal cancer development. A mutation of *XRCC2* has been found in rare cases of uterine cancers (Mohindra et al., 2003) and a subtle acting polymorphism of *XRCC2* has been shown to be associated with a subset of breast cancers (Rafii et al., 2002). A common polymorphic variant of *XRCC3*, T241M has been reported to be associated with increased risk of malignant melanoma, bladder cancer and breast cancer (Winsey et al., 2000, Matullo et al., 2001, Rafii et al., 2003). However, there is conflicting evidence regarding the *XRCC3* findings and the originally observed association was not detected in other bladder cancer or malignant melanoma populations (Duan et al., 2002, Stern et al., 2002).

Whereas the majority of previous studies have associated the 241Met *XRCC3* variant with increased cancer risk, a recent study found a weak association between the 241Thr variant and colorectal cancer (Mort et al., 2003). Therefore, there is still debate as to whether this polymorphism of *XRCC3* increases cancer risk and no conclusive evidence has been gathered to show that *XRCC2*, *XRCC3* and *Mus81* are involved in colorectal cancer development. Studies designed to detect associations between DNA repair gene polymorphisms and cancer susceptibility may have differing results because of insufficient sample sizes or population differences.

While this study does not exclude the possibility that HR gene polymorphisms may make minor contributions to colorectal cancer predisposition an exhaustive study would be required to examine the relationship of polymorphisms in these genes with colorectal cancer. Extensive genotyping followed by comparison of genotype distributions of a larger colorectal cancer population and a large matched normal population would provide a more accurate insight into the role of *XRCC2*, *XRCC3* and *Mus81* gene polymorphisms in colorectal cancer. Such analysis was beyond the scope of this research since the primary focus was to determine whether somatic mutations of candidate HR genes are present in colorectal cancers and to establish the phenotypic consequences of such mutations.

5.3 Essential Cellular Roles of MRE11

This research revealed that a high proportion of MSI-H colorectal tumours have a mutation in the intronic T_{11} run of *MRE11* that leads to the creation of several *MRE11* splice variants. Comprehensive investigation of the phenotypic consequences one of these variants, 314del345, suggested an essential role for MRE11 in the HR repair-mediated rescue of DNA replication forks arrested by thymidine.

The exact nature of this role is not yet clear as the lesion created by thymidine treatment is not known. It has been proposed that impairment of replication fork progression by thymidine treatment causes the replication fork to regress leading to a four-way junction known as a 'chicken foot' (Lundin et al., 2002). These structures can be resolved into Holliday junctions that then act as substrates for recombination. A role for MRE11 in maintaining DNA replication fork integrity has previously been suggested. Chicken DT40 cells depleted of MRE11 die with chromosomal breaks (Yamaguchi-Iwai et al., 1999) and MRE11 is required to prevent the accumulation of DSBs at DNA-replication forks in cell-free extracts prepared from *Xenopus* eggs (Costanzo et al., 2001). The MRE11 complex is known to be associated with PCNA at replication forks throughout S-phase (Mirzoeva and Petrini, 2003) and a proposed function for the MRE11 complex is in resolution of damaged or stalled replication forks (Maser et al., 2001). Therefore, it has been hypothesised that the MRE11 complex may associate with and resolve unusual structures formed during DNA replication (Xiao and Weaver, 1997).

This research supports a model in which the MRE11 branch of the ATM-mediated S-phase response is required for thymidine-induced HR. The MRE11 mutant studied here blocks activation of wild type MRE11 and prevents thymidine-induced HR. These data, together with the fact that A-TLD cells show radio-resistant DNA synthesis (Stewart et al., 1999), suggests that a fully activated MRE11 is critical for both damage-dependent activation of the S-phase checkpoint and HR-mediated rescue of DNA replication forks impaired by thymidine (Figure 5.3.1).

Figure 5.3.1 Model predicting an essential role for the MRE11 complex in activating the S-phase checkpoint response and homologous recombination (HR) following exposure to thymidine.

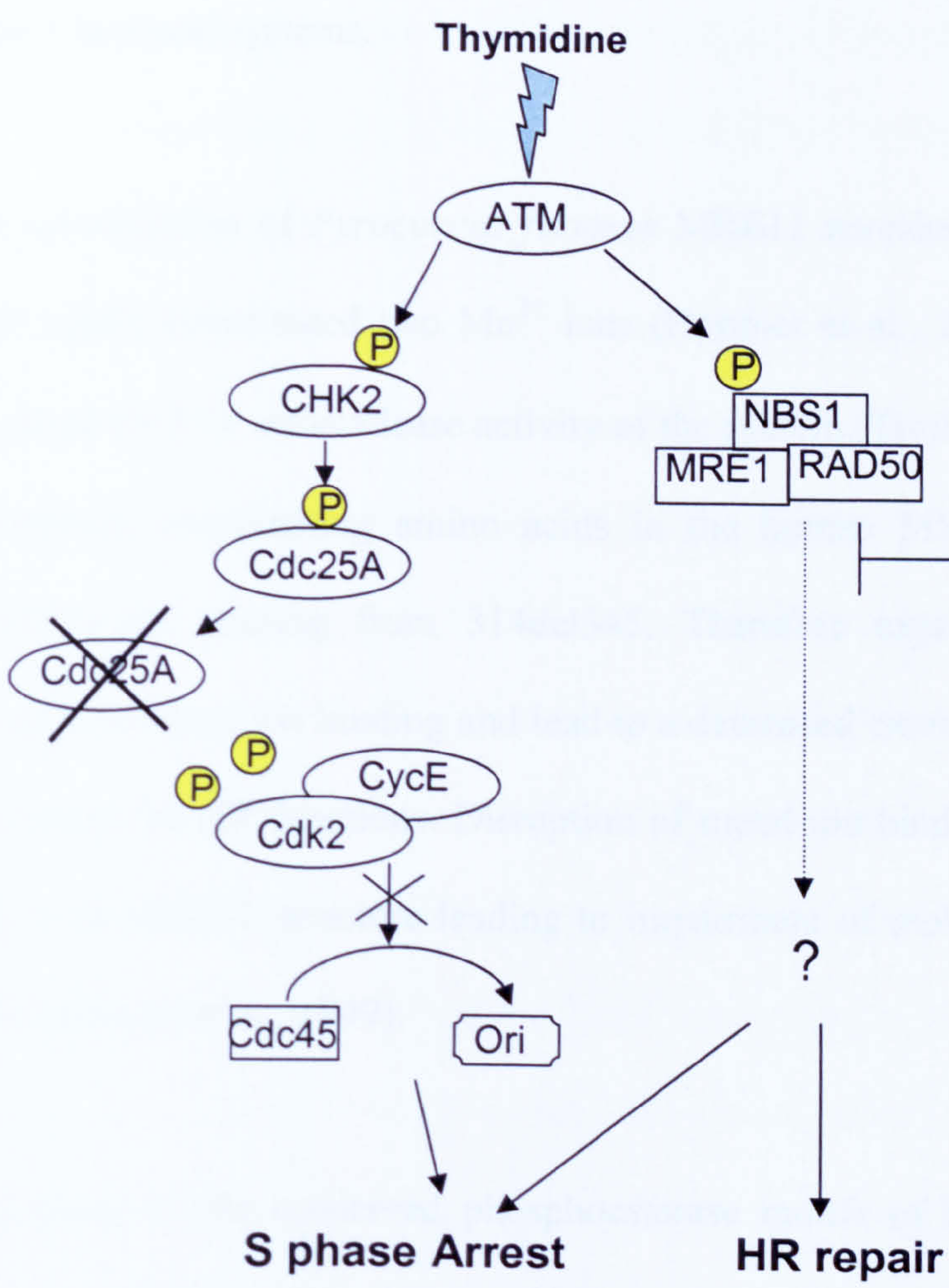

5.4 Disruption of MRE11 Motif III

Although, MRE11 314del345 appears to function in a dominant-negative manner the mechanism by which it exerts its effect is still unclear. The protein encoded by MRE11 314del345 has amino acids 106-219, including the third phosphoesterase motif, deleted. The function of this region of the protein has been investigated to some extent in model systems.

An investigation of *Pyrococcus furiosus* MRE11 revealed seven conserved residues that tightly coordinated two Mn^{2+} ions (Hopfner et al., 2001). The Mn^{2+} binding is required for 3′-5′ exonuclease activity of the protein (Trujillo et al., 1998). Two of the conserved, coordinating amino acids in the human MRE11 protein (Asn128 and His217) are missing from 314del345. Therefore expression of 314del345 may destabilise metal ion binding and lead to a decreased exonuclease activity that may be necessary for HR functions. Disruption of metal ion binding may also have a global effect on MRE11 structure leading to impairment of molecular interactions at distal sites (Stewart et al., 1999).

Mutations of the conserved phosphoesterase motifs of MRE11 were created in *S. cerevisia* (Bressan et al., 1998). Ablation of one of the critical residues of motif III did not affect spontaneous mitotic HR, IR-directed DSB repair or the MRE11-Rad50 interaction in yeast cells (Bressan et al., 1998) suggesting that motif III is not crucial for these functions. However, the study in yeast mutated only one residue whereas 314del345 has a complete deletion of motif III and therefore expression of this mutant may have a more detrimental effect on the cell.

A potential Chk2 phosphorylation site on MRE11 was identified between amino acids 152-163 (Seo et al., 2003). This region is deleted in 314del345 but the significance of this is unknown as the phosphorylation of MRE11 by Chk2 has not been proven *in vivo*.

One A-TLD family carries an MRE11 mutation in close proximity to motif III leading to N117S (Stewart et al., 1999). This mutation weakens or alters NBS1 binding such that MRE11 does not undergo nuclear localisation (Stewart et al., 1999). MRE11 amino acids 1-319 are required for interaction with NBS1 (Desai-Mehta et al., 2001) and since 314del345 misses amino acids 106-219 it is likely that NBS1 binding is disrupted in cells expressing this mutant. Indeed, further biochemical analysis is needed to assess whether 314del345 affects MRE11 complex formation. It will also be important to determine whether expression of 314del345 impairs nuclear foci formation or the hypothesised DNA damage sensor function of the MRE11 complex.

It has been proposed that association of the MRE11 complex with chromatin during S-phase may allow the complex to function as a sensor of DNA damage that detects chromatin changes induced by a DSB (Petrini and Stracker, 2003). Chromatin association of the MRE11 complex requires sequences in the N-terminus of NBS1 (Zhao et al., 2002) and therefore MRE11 must maintain the interaction with NBS1 to become chromatin bound. If the mutant 314del345 disrupts NBS1 binding, as suggested above, MRE11 may not become targeted to chromatin. However, biochemical evidence to support the proposed sensor function of the MRE11 complex has yet to be established and the requirement for MRE11 and its nuclease activity in this suggested role needs to be examined.

Future studies should also include investigation into whether this variant affects cell-cycle checkpoint functions as well as repair. The loss of S-phase checkpoint activation in HCT116 was presumed not to stem from abrogation of the ATM-NBS1 pathway but to be a consequence of MMR-deficiency in these cells (Brown et al., 2003). However, if MRE11 314del345 is expressed in HCT116, as is suggested by this research, then the ATM/NBS1 pathway is defective and this could potentially be the source of the S-phase checkpoint defects seen in HCT116.

Nevertheless, if the 314del345 mutant affected all roles of MRE11, a more severe or lethal phenotype might be expected. The variant MRE11 may actually decrease the efficiency of MRE11 functioning by interfering with the endogenous wild type protein.

5.5 The MRE11 Complex in MSI$^+$ Cancer

This investigation also revealed a frameshift mutation of an A_9 run of *Rad50* in a subset of MSI$^+$ colorectal tumours. This mutation has previously been detected in other MSI$^+$ colorectal tumours and in MMR-deficient gastric cancers (Kim et al., 2001, Duval and Hamelin, 2002). This frameshift mutation is predicted to truncate the Rad50 protein and, although the phenotypic consequences of such a truncation are not yet known, this is an interesting result supporting the hypothesis that all components of the MRE11 complex are downstream mutational targets in MSI$^+$ cells.

5.6 Conclusions

Derivation of hypomorphic alleles, as used in this study, may help address functional issues such as whether the MRE11 complex is the primary sensor of DNA damage.

It will be interesting in the future to examine the biochemical effects of this mutation to give additional insight into the role of MRE11. Further elucidation of MRE11 complex functions promotes understanding of the DNA damage response and the coordination of the checkpoint responses and DNA repair. As the functions of the MRE11 complex become more apparent it might be possible to predict the response of tumours that carry mutations in MRE11, NBS1 or Rad50. The DNA damage response pathway that includes the MRE11 complex appears to be disrupted in >85% of MSI^+ colorectal tumours. Since disruption of this pathway increases sensitivity to certain therapeutic agents these finding have important implications for novel treatment strategies directed specifically against this subset of tumours.

REFERENCES

Aaltonen, L. A., Salovaara, R., Kristo, P., Camzian, F., Hemminki, A., Peltomaki, P., Chadwick, R. B., Kaariaimen, H., Eskelinen, M., Jarvinen, H., Mecklin, J. P. and de la Chapelle, A. (1998). Incidence of hereditary nonpolyposis colorectal cancer and molecular screening for the disease. *New England journal of medicine,* **338:** 1481-1487.

Acharya, S., Wilson, T., Gradia, S., Kane, M. F., Guerrette, S., Marsischky, G. T., Kolodner, R. and Fishel, R. (1996). hMSH2 forms specific mispair-binding complexes with hMSH3 and hMSH6. *PNAS,* **93:** 13629-13634.

Anderson, D. E., Trujillo, K. M., Sung, P. and Erickson, H. P. (2001). Structure of the Rad50-Mre11 DNA Repair Complex from Saccharomyces cerevisiae by Electron Microscopy. *J. Biol. Chem.,* **276:** 37027-37033.

Araujo, F. D., Pierce, A. J., Stark, J. M. and Jasin, M. (2002). Variant XRCC3 implicated in cancer is functional in homology-directed repair of double-strand breaks. *Oncogene,* **21:** 4176-4180.

Arnaudeau, C., Lundin, C. and Helleday, T. (2001). DNA Double-Strand Breaks Associated with Replication Forks are Predominantly Repaired by Homologous Recombination Involving an Exchange Mechanism in Mammalian Cells. *Journal of Molecular Biology,* **307:** 1235-1245.

Bakkenist, C. J. and Kastan, M. B. (2003). DNA damage activates ATM through intermolecular autophosphorylation and dimer dissociation. *Nature,* **421:** 499-506.

Baross-Francis, A., Andrew, S. E., Penney, J. E. and Jirik, F. R. (1998). Tumors of DNA mismatch repair-deficient hosts exhibit dramatic increases in genomic instability. *PNAS,* **95:** 8739-8743.

Bhattacharyya, N., Skandalis, A., Ganesh, A., Groden, J. and Meuth, M. (1994). Mutator Phenotypes in Human Colorectal Carcinoma Cell Lines. *PNAS,* **91:** 6319-6323.

Bishop, D. K., Ear, U., Bhattacharyya, A., Calderone, C., Beckett, M., R.R., W. and Shinohara, A. (1998). Xrcc3 is required for assembly of Rad51 complexes in vivo. *The Journal of Biological Chemistry,* **273:** 21482-21488.

Bjursell, G. and Reichard, P. (1973). Effects of thymidine on deoxyribonucleoside triphosphate pools and deoxyribonucleic acid synthesis in Chinese hamster ovary cells. *J. Biol. Chem.*, **248:** 3904-9.

Boddy, M. N., Gaillard, P. H., McDonald, W. H., Shanahan, P., Yates, J. R. and Russel, P. (2001). Mus81-Eme1 are essential components of a Holliday junction resolvase. *Cell,* **107:** 537-548.

Boddy, M. N., Lopez-Girona, A., Shanahan, P., Interthal, H., Heyer, W. and Russel, P. (2000). Damage tolerance protein Mus81 associates with FHA1 domain of checkpoint kinase Cds1. *Mol. Cell Biol.,* **20:** 8758-8766.

Boland, C. R., Thibodeau, S. N., Hamilton, S. R., Sidransky, D., Eshelman, J. R., Burt, R. W., Meltzer, S. J., Rodriguez-Bigas, M. A., Fodde, R., Ranzani, N. R. and S., S. (1998). A national cancer institute workshop on microsatellite instability for cancer detection and familial predisposition: development of international criteria for the determination of microsatellite instability in colorectal cancer. *Cancer Research,* **58:** 5248-5257.

Bradford, M. (1976). A rapid and sensitive method for the quantification of microgram quantities of protein utilizing the principle of protein dye binding. *Anal. Biochem,* **72:** 248-254.

Braybrooke, J. P., Spink, K. G., Thacker, J. and Hickson, I. D. (2000). The RAD51 family member, RAD51L3, is a DNA-stimulated ATPase that forms a complex with XRCC2. *The Journal of Biological Chemistry,* **275:** 29100-29106.

Brenneman, M. A., Weiss, A. E., Nickoloff, J. A. and Chen, D. J. (2000). XRCC3 is required for efficient repair of chromosome breaks by homologous recombination. *Mutation Research,* **459:** 89-97.

Bressan, D. A., Olivares, H. A., Nelms, B. E. and Petrini, J. H. (1998). Alteration of N-terminal phosphoesterase signature motifs inactivates Saccharomyces cerevisiae Mre11. *Genetics.,* **150:** 591-600.

Brown, K. D., Rtahi, A., Kamath, R., Beardsley, D. I., Zhan, Q., Mannino, J. and Baskaran, R. (2003). The mismatch repair system is required for S-phase checkpoint activation. *Nature genetics,* **33:** 80-84.

Burt, R. W. (2000). Colon Cancer Screening. *Gastroenterology,* **119:** 837-853.

Butkiewicz, D., Rusin, M., Enewold, L., Shields, P. G., Chorazy, M. and Curtis, C. H. (2001). Genetic polymorphisms in DNA repair genes and risk of lung cancer. *Carcinogenesis,* **22:** 593-597.

Carney, J. P., Maser, R. S., Olivares, H., Davis, E. M., Le Beau, M., Yates, J. R. r., Hays, L., Morgan, W. F. and Petrini, J. H. (1998). The hMre11/hRad50 protein comples and Nijmegen breakage syndrome: linkage of double-strand break repair to the cellular DNA damage response. *Cell,* **93:** 477-486.

Cartwright, R., Tambini, C. E., Simpson, P. J. and Thacker, J. (1998). The XRCC2 DNA repair gene from human and mouse encodes a novel member of the recA/RAD51 family. *Nucleic Acids Research,* **26:** 3084-3089.

Casorelli, I., Offman, J., Mele, L., Pagano, L., Sica, S., Mariarosaria, D., Giannini, G., Leone, G., Bignami, M. and Karran, P. (2003). Drug treatment in the development of mismatch repair defective acute leukemia and myelodysplastic syndrome. *DNA Repair,* **2:** 547-559.

Claij, N. and Riele, H. (1999). Microsatellite instability in human cancer: a prognostic marker for chemotherapy? *Experimental cell research,* **246:** 1-10.

Chamankhah, M., Fontanie, T. and Xiao, W. (2000). The Saccharomyces cerevisiae mre11(ts) Allele Confers a Separation of DNA Repair and Telomere Maintenance Functions. *Genetics,* **155:** 569-576.

Chamankhah, M. and Xiao, W. (1999). Formation of the yeast Mre11-Rad50-Xrs2 complex is correlated with DNA repair and telomere maintenance. *Nucleic Acids Research.,* **27:** 2072-9.

Chen, C. and Kolodner, R. (1999). Gross chromosomal rearrangements in Saccharomyces cerevisiae replication and recombination defective mutants. *Nature genetics,* **23:** 81-85.

Chen, X. B., Melchionna, R., Denis, C. M., Gaillard, P. H., Blasina, A., Van de Weyer, I., Boddy, M. N., Russell, P., Vialard, J. and McGowan, C. H. (2001). Human Mus81-associated endonuclease cleaves Holliday junctions in vitro. *Molecular Cell,* **8:** 1117-1127.

Chung, D. C. (2000). The genetic basis of colorectal cancer: Insights into critical pathways of tumorigenesis. *Gastroenterology,* **119:** 854-865.

Chung, D. C. and Rustgi, A. K. (2003). The Hereditary Nonpolyposis Colorectal Cancer Syndrome: Genetics and Clinical Implications. *Annals of Internal Medicine,* **138:** 560-570.

Coleman, W. B. and Tsongalis, G. J. (1999). The role of genomic instability in human carcinogenesis. *Anticancer Research,* **19:** 4645-4664.

Connelly, J. C. and Leach, D. R. F. (2002). Tethering on the brink: the evolutionarily conserved Mre11-Rad50 complex. *Trends in Biochemical Sciences,* **27:** 410-418.

Coolidge, C. J., Seely, R. J. and Patton, J. G. (1997). Functional analysis of the polypyrimidine tract in pre-mRNA splicing. *Nucleic Acids Research,* **25:** 888-896.

Costanzo, V., Robertson, K., Bibikova, M., Kim, E., Grieco, D., Gottesman, M., Carroll, D. and Gautier, J. (2001). Mre11 protein complex prevents double-strand break accumulation during chromosomal DNA replication. *Molecular Cell,* **8:** 137-147.

Cotran, R. S., Kumar, V. and Collins, T. (1999) *Robbins Pathological Basis of Disease.,* WB Saunders Company.

D'Amours, D. and Jackson, S. P. (2001). The yeast Xrs2 complex functions in S phase checkpoint regulation. *Genes Dev.,* **15:** 2238-2249.

D'Amours, D. and Jackson, S. P. (2002). The Mre11 complex: at the crossroads of dna repair and checkpoint signalling. *Nature Reviews Molecular Cell Biology.,* **3:** 317-27.

David-Beabes, G. L., Lunn, R. M. and London, S. J. (2001). No association between the XPD (Lys751Gln) polymorphism or the XRCC3 (Thr241Met) polymorphism and lung cancer risk. *Cancer Epidemiol Biomarkers Prev,* **10:** 911-912.

de Jager, M., Dronkert, M. L., Modesti, M., Beerens, C. E., Kanaar, R. and van Gent, D. C. (2001a). DNA-binding and strand-annealing activities of human Mre11: implications for its roles in DNA double-strand break repair pathways. *Nucleic Acids Research.,* **29:** 1317-25.

de Jager, M., van Noort, J., van Gent, D. C., Dekker, C., Kanaar, R. and Wyman, C. (2001b). Human Rad50/Mre11 is a flexible complex that can tether DNA ends. *Molecular Cell.,* **8:** 1129-35.

Deans, B., Griffin, C. S., Maconochie, M. and Thacker, J. (2000). Xrcc2 is required for genetic stability, embryonic neourogenesis and viability in mice. *The EMBO Journal,* **19:** 6675-6685.

Desai-Mehta, A., Cerosaletti, K. M. and Concannon, P. (2001). Distinct functional domains of nibrin mediate Mre11 binding, focus formation, and nuclear localization. *Molecular & Cellular Biology.*, **21:** 2184-91.

Dietmaier, W., Wallinger, S., Bocker, T., Kullman, F., Fishel, R. and Ruschoff (1997). Diagnostic Microsatellite instability: Definition and Correlation with Mismatch Repair Protein Expression. *Cancer Research,* **57:** 4749-1756.

Dolganov, G. M., Maser, R. S., Novikov, A., Tosto, L., Chong, S., Bressan, D. A. and Petrini, J. H. (1996). Human Rad50 is physically associated with human Mre11: identification of a conserved multiprotein complex implicated in recombinational DNA repair. *Molecular & Cellular Biology.*, **16:** 4832-41.

Dong, Z., Zhong, Q. and Chen, P.L. (1999). The Nijmegen breakage syndrome protein is essential for Mre11 phosphorylation upon DNA damage. *Journal of Biological Chemistry,* **274:** 19513-19516.

Duan, Z., Shen, H., Lee, J. E., Gershenwald, J. E., Ross, M. I., Mansfield, P. F., Duvic, M., Strom, S. S., Spitz, M. R. and Wei, Q. (2002). DNA repair gene XRCC3 241Met variant is not associated with risk of cutaneous melanoma. *Cancer Epidemiol Biomarkers Prev,* **11:** 1142-1143.

Duval, A. and Hamelin, R. (2002). Mutations at Coding Repeat Sequences in Mismatch Repair-deficient Human Cancers: Toward a New Concept of Target Genes for Instability. *Cancer Research,* **62:** 2447-2454.

Edmonston, T., Cuesta, K., Burkholder, S., Barusevicius, A., Rose, D., Kovatich, A., Boman, B., Fry, R., Fishel, R. and Palazzo, J. (2000). Colorectal Carcinoma with high microsatellite instability: defining a distinct immunologic and molecular entity with respect to prognostic markers. *Human Pathology,* **31:** 1506-1514.

Falck, J., Petrini, J. H., Williams, B. R., Lukas, J. and Bartek, J. (2002). The DNA damage-dependent intra-S phase checkpoint is regulated by parallel pathways. *Nature Genetics.*, **30:** 290-4.

Fishel, R. and Kolodner, R. (1995). Identification of mismatch repair genes and their role in the development of cancer. *Current Opinion in Genetics & Development,* **5:** 382-395.

Fleisher, A. S., Esteller, M., Wang, S., Tamura, G., Suzuki, H., Yin, J., Zou, T.-T., Abraham, J. M., Kong, D., Smolinski, K. N., Shi, Y.-Q., Rhyu, M.-G., Powell, S. M., James, S. P., Wilson, K. T., Herman, J. G. and Meltzer, S. J. (1999). Hypermethylation of the hMLH1 Gene Promoter in Human Gastric Cancers with Microsatellite Instability. *Cancer Res,* **59:** 1090-1095.

Flores-Rozas, H. and Kolodner, R. (2000). Links between replication, recombination and genomic instability in eukaryotes. *Trends in Biochemical Sciences,* **25:** 196-200.

Fornasarig, M., Viel, A., Valentini, M., Capozzi, E., Sigon, R., de Paoli, A., Puppa, L. D. and Boiocchi, M. (2000). Microsatellite instability and MLH1 and MSH2 germline defects are related to clinicopathological features in sporadic colorectal cancer. *Oncology reports,* **7:** 39-43.

Franchitto, A. and Pichierri, P. (2002). Protecting genomic integrity during DNA replication: correlation between Werner's and Bloom's syndrome gene products and the MRE11 complex. *Human Molecular Genetics.,* **11:** 2447-53.

Fukuda, T., Sumiyoshi, T., Takahasht, M., Kataoka, T., Asahara, T., Inui, H., Watatani, M., Yasutomi, M., Kamada, N. and Miyagawa, K. (2001). Alterations of Double-Strand Break Repair Gene *MRE11* in cancer. *Cancer Research,* **61:** 23-26.

Furuta, T., Takemura, H., Liao, Z.-Y., Aune, G. A., Redon, C., Sedelnikova, O. A., Pilch, D. R., Rogakou, E. P., Celeste, A., Chen, H. T., Nussenzweig, A., Aladjem, M. I., Bonner, W. M. and Pommier, Y. (2003). Phosphorylation of Histone H2AX and Activation of Mre11, Rad50 and Nbs1 in Response to Replication-dependent DNA Double-strand Breaks Induced by Mammalian DNA Topoisomerase I Cleavage Complexes. *Journal of Biological Chemistry,* **278:** 20303-20312.

Giannini, G., Ristori, E., Cerignoli, F., Rinaldi, C., Zani, M., Viel, A., Ottini, L., Crescenzi, M., Martinotti, S., Bignami, M., Frati, L., Screpanti, I. and Gulino, A. (2002). Human MRE11 is inactivated in mismatch repair-deficient cancers. *EMBO Reports.,* **3:** 248-54.

Grenon, M., Gilbert, C. and Lowndes, N. F. (2001). Checkpoint activation in response to double-strand breaks requires the Mre11/Rad50/Xrs2 complex. *Nature Cell Biology.,* **3:** 844-7.

Griffin, C. S., Simpson, P., Wilson, C. R. and Thacker, J. (2000). Mammalian recombination-repair genes XRCC2 and XRCC3 promote correct chromsome segregation. *Nature Cell Biology,* **2:** 757-761.

Haber, J. E. and Heyer, W. (2001). The Fuss about Mus81. *Cell,* **107:** 551-554.

Halford, S., Sasieni, P., Rowan, A., Wasan, H., Bodmer, W., Talbot, I., Hawkins, N., Ward, R. and Tomlinson, I. (2002). Low-Level Microsatellite Instability Occurs in Most Colorectal Cancers and Is a Nonrandomly Distributed Quantitative Trait. *Cancer Research,* **62:** 53-57.

Harfe, B. D. and Jinks-Robertson, S. (2000). DNA mismatch repair and genetic instability. *Annual Review of Genetics,* **34:** 359-399.

Henry-Mowatt, J., Jackson, D., Masson, J., Johnson, P. A., Clements, P. M., Benson, F. E., Thompson, L. H., Takeda, S., West, S. C. and Caldecott, K. W. (2003). XRCC3 and Rad51 Modulate Replication Fork Progression on Damaged Vertebrate Chromosomes. *Molecular Cell,* **11:** 1109-1117.

Hoeijmakers, J. H. J. (2001). Genome maintenance mechanisms for preventing cancer. *Nature,* **411:** 366-374.

Hopfner, K. P., Karcher, A., Craig, L., Woo, T. T., Carney, J. P. and Tainer, J. A. (2001). Structural biochemistry and interaction architecture of the DNA double-strand break repair Mre11 nuclease and Rad50-ATPase. *Cell.,* **105:** 473-85.

Humphries, S. E., Gudnason, V., Whittall, R. and Day, I. N. M. (1997). Single-strand conformation polymorphism analysis with high throughout modifications, and its use in mutation detection in familial hypercholesterolemia. *Clinical Chemistry,* **43:** 427-435.

Ivanov, E. l., Sugawara, N., White, C. I., Fabre, F. and Haber, J. E. (1994). Mutations In Xrs2 And Rad50 Delay But Do Not Prevent Mating-Type Switching In Saccharomyces-Cerevisiae. *Mol. Cell Biol.,* **14:** 3414-3425.

Jackson, S. P. (2002). Sensing and Repairing DNA double-strand breaks. *Carcinogenesis,* **23:** 687-696.

Jeggo, P. A. (1998). Identification of genes involved in repair of DNA double-strand breaks in mammalian cells. *Radiation Research.,* **150:** S80-91.

Jiricny, J. (1996). Mismatch Repair and Cancer. *Cancer Surveys,* **28:** 47-66.

Johnson, R. D. and Jasin, M. (2001). Double-strand-break-induced homologous recombination in mammalian cells. *Biochemical Society Transactions,* **29:** 196-201.

Johnson, R. D., Liu, N. and Jasin, M. (1999). Mammalian XRCC2 promotes the repair of DNA double-strand breaks by homologous recombination. *Nature,* **401:** 397-399.

Kane, M. F., Loda, M., Gaida, G. M., Lipman, J., Mishra, R., Goldman, H., Jessup, J. M. and Kolodner, R. (1997). Methylation of the hMLH1 promoter correlates with lack of expression of hMLH1 in sporadic colon tumours and mismatch repair-defective human tumour cell lines. *Cancer Research,* **57:** 808-811.

Kang, J., Bronson, R. T. and Xu, Y. (2002). Targeted disruption of NBS1 reveals its roles in mouse development and DNA repair. *EMBO Journal.,* **21:** 1447-55.

Katabuchi, H., van Rees, B., Lambers, A., Ronnett, B., Blazes, M., Leach, F., Cho, K. and Hedrick, L. (1995). Mutations in DNA mismatch repair genes are not responsible for microsatellite instability in most sporadic endometrial carcinomas. *Cancer Res,* **55:** 5556-5560.

Khanna, K. K. and Jackson, S. P. (2001). DNA double strand breaks: signalling, repair and the cancer connection. *Nature genetics,* **27:** 247-254.

Kim, H., Jen, J., Vogelstein, B. and Hamilton, S. R. (1994). Clinical and pathological characteristics of sporadic colorectal carcinomas with DNA replication errors in microsatellite sequences. *American Journal of Pathology,* **145:** 148-156.

Kim, K. K., Shin, B. A., Seo, K. H., Kim, P. N., Koh, J. T., Kim, J. H. and Park, B. R. (1999). Molecular cloning and characterization of splice variants of human RAD50 gene. *Gene.,* **235:** 59-67.

Kim, N.-G., Choi, Y. R., Baek, M. J., Kim, Y. H., Kang, H., Kim, N. K., Min, J. S. and Kim, H. (2001). Frameshift Mutations at Coding Mononucleotide Repeats of the hRAD50 Gene in Gastrointestinal Carcinomas with Microsatellite Instability. *Cancer Research,* **61:** 36-38.

Kinzler, K. W. and Vogelstein, B. (1996). Lessons from hereditary colorectal cancer. *Cell,* **87:** 159-170.

Kinzler, K. W. and Vogelstein, B. (1997). Gatekeepers and caretakers. *Nature,* **386:** 761-763.

Kolodner, R. (1995). Mismatch repair: mechanisms and relationship to cancer susceptibility. *Trends in Biochemical Sciences,* **20:** 397-401.

Kraakman-van der Zwet, M., Overkamp, W. J. I., Friedl, A. A., Klein, B., Verhaegh, G. W., Jaspers, N. G., Midro, A. T., Eckardt-Schupp, F., Lohman, P. H. M. and Zdzienicka, M. Z. (1999). Immortalisation and characterisation of Nijmegen Breakage Syndrome fibroblasts. *Mutation Research,* **434:** 17-27.

Kurumizaka, H., Ikawa, S., Nakada, M., Enomoto, R., Kagawa, W., Kinebuchi, T., Yamazoe, M., Yokoyama, S. and Shibata, T. (2002). Homologous pairing and ring filament structure formation activities of the human Xrcc2.Rad51D complex. *The Journal of Biological Chemistry,* **277:** 14315-14320.

Kuschel, B., Auranen, A., McBride, S., Novik, K. L., Antoniou, A., Lipscombe, J. M., Day, N. E., Easten, D. F., Ponder, B., P., P. and Dunning, A. (2002). Variants in DNA double-strand break repair genes and breast cancer susceptibility. *Human Molecular Genetics,* **11:** 1399-1407.

Lee, S. E., Bressan, D. A., Petrini, J. H. and Haber, J. (2002). Complementation between N-terminal Saccharomyces cerevisiae mre11 alleles in DNA repair and telomere length maintenance. *DNA Repair,* **1:** 27-40.

Lengauer, C., Kinzler, K. W. and Vogelstein, B. (1998). Genetic instabilities in human cancers. *Nature,* **396:** 643-649.

Leung, S. Y., Yuen, S. T., Chung, L. P., Chu, K. M., Chan, A. S. Y. and Ho, J. C. I. (1999). hMLH1 Promoter Methylation and Lack of hMLH1 Expression in Sporadic Gastric Carcinomas with High-Frequency Microsatellite Instability. *Cancer Res,* **59:** 159-164.

Liu, B., Nicolaides, N. C., Markowitz, S., Willson, J. K. V., Parsons, R., Jen, J., Papadopolous, N., Peltomaki, P., de la Chapelle, A., Hamilton, S. R., Kinzler, K. W. and Vogelstein, B. (1995). Mismatch repair gene defects in sporadic colorectal cancers with microsatellite instability. *Nature genetics,* **9:** 48-55.

Liu, N., Lamerdin, J., Tebbs, R., Schild, D., Tucker, J., Shen, M., Brookman, K., Siciliano, M., Walter, C., Fan, W., Narayana, L., Zhou, Z., Adamson, A., Sorenson, K., Chen, D., Jones, N. and Thompson, L. H. (1998). XRCC2 and XRCC3, new human Rad51-family members, promote chromosome stability and protect against DNA cross-links and other damages. *Molecular Cell,* **1:** 783-793.

Liu, N., Schild, D., Thelen, M. P. and Thompson, L. H. (2002). Involvement of Rad51C in two distinct protein complexes of Rad51 paralogs in human cells. *Nucleic Acids Research,* **30:** 1009-1015.

Loeb, L. (1991). Mutator phenotype may be required for multistage carcinogenesis. *Cancer Research,* **51:** 3075-3079.

Lukas, C., Falck, J., Bartkova, J., Bartek, J. and Lukas, J. (2003). Distinct spatiotemporal dynamics of mammalian checkpoint regulators induced by DNA damage. *Nature Cell Biology,* **5:** 255-260.

Lundin, C., Erixon, K., Arnaudeau, C., Schultz, N., Jenssen, D., Meuth, M. and Helleday, T. (2002). Different Roles for Nonhomologous End Joining and Homologous Recombination following Replication Arrest in Mammalian Cells. *Mol. Cell Biol.,* **22:** 5869-5878.

Luo, G., Yao, M. S., Bender, C. F., Mills, M., Bladl, A. R., Bradley, A. and Petrini, J. H. (1999). Disruption of mRad50 causes embryonic stem cell lethality, abnormal embryonic development, and sensitivity to ionizing radiation. *Proceedings of the National Academy of Sciences of the United States of America.,* **96:** 7376-81.

Lynch, H. T. and de la Chapelle, A. (2003). Genomic Medicine: Hereditary Colorectal Cancer. *The New England Journal of Medicine,* **348:** 919-932.

Markowitz, S. D., Dawson, D. M., Willis, J. and Willson, J. K. V. (2002). Focus on colon cancer. *Cancer Cell,* **1:** 233-236.

Markowitz, S. D., Wang, J., Myeroff, L., Parsons, R., Sun, L., Lutterbaugh, J., Fan, R. S., Zborowska, E., Kinzler, K. W., Vogelstein, B., Brattain, M. and Willson, J. K. V. (1995). Inactivation of the Type II TGF-b Receptor in Colon Cancer Cells with Microsatellite Instability. *Science,* **268:** 1336-1338.

Maser, R. S., Mirzoeva, O. K., Wells, J., Olivares, H., Williams, B. R., Zinkel, R. A., Farnham, P. J. and Petrini, J. H. (2001). Mre11 complex and DNA replication: linkage to E2F and sites of DNA synthesis. *Molecular & Cellular Biology.,* **21:** 6006-16.

Maser, R. S., Monsen, K. J., Nelms, B. E. and Petrini, J. H. (1997). hMre11 and hRad50 Nuclear Foci are Induced during the Normal Cellular Response to DNA Double-Strand Breaks. *Mol. Cell Biol.,* **17:** 6087-6096.

Masson, J., A.Z., S., Stasiak, A., F.E., B. and S.C., W. (2001a). Complex formation by the human RAD51C and XRCC3 recombination repair proteins. *Proc. Natl. Acad. Sci. USA,* **98:** 8440-8446.

Masson, J., Tarsounas, M. C., A.Z., S., Stasiak, A., Shah, R., McIlwraith, M. J., F.E., B. and S.C., W. (2001b). Identification and purification of two distinct complexes containing the five RAD51 paralogs. *Genes and Development,* **15:** 3296-3307.

Matullo, G., S., G., Carturan, S., Peluso, M., Malaveille, C., Davico, L., Piazza, A. and Vineis, P. (2001). DNA repair gene polymorphisms, bulky DNA adducts in white blood cells and bladder cancer in a case-control study. *Int. J. Cancer,* **92:** 562-567.

McCormick, D., Kibbe, P. J. and Morgan, S. W. (2002). Colon Cancer: Prevention, Diagnosis, Treatment. *Gastroenterology Nursing,* **25:** 204-211.

McGowan, C. H. (2002). Checking in on Cds1 (Chk2): a checkpoint kinase and tumor suppressor. *BioEssays,* **24:** 502-511.

Miller, J. H. (1998). Mutators in Escherichia coli. *Mutation research,* **409:** 99-106.

Miller, K. A., Yoshikawa, D., McConnell, I. R., Clark, R., Schild, D. and Albala, J. S. (2002). RAD51C Interacts with RAD51B and Is Central to a Larger Protein Complex *in Vivo* Exclusive of RAD51. *The Journal of Biological Chemistry,* **277:** 8406-8411.

Mirzoeva, O. K. and Petrini, J. H. (2001). DNA damage-dependent nuclear dynamics of the Mre11 complex.[erratum appears in Mol Cell Biol 2001 Mar;21(5):1898]. *Molecular & Cellular Biology.,* **21:** 281-8.

Mirzoeva, O. K. and Petrini, J. H. (2003). DNA Replication-Dependent Nuclear Dynamics of the Mre11 Complex. *Molecular Cancer Research,* **1:** 207-218.

Mohindra, A., Bolderson, E., Stone, J., Wells, M., Helleday, T. and Meuth, M. (2003). A Tumour Derived Mutant Allele of XRCC2 Preferentially Suppresses Homologous Recombination at DNA Replication Forks. *Submitted for Publication.*

Mohindra, A., Hays, L., Phillips, E. N., Preston, B. D., Helleday, T. and Meuth, M. (2002). Defects in homologous recombination repair in mismatch-repair-deficient tumour cell lines. *Human Molecular Genetics,* **11:** 2189-2200.

Moore, J. and Haber, J. (1996). Cell cycle and genetic requirements of two pathways of nonhomologous end-joining repair of double-strand breaks in Saccharomyces cerevisiae. *Mol. Cell. Biol.,* **16:** 2164-2173.

Moreau, S., Ferguson, J. R. and Symington, L. S. (1999). The nuclease activity of Mre11 is required for meiosis but not for mating type switching, end joining, or telomere maintenance. *Molecular & Cellular Biology.*, **19:** 556-66.

Mort, R., Mo, L., McEwan, C. and Melton, D. W. (2003). Lack of involvement of nucleotide excision repair gene polymorphisms in colorectal cancer. *British Journal of Cancer,* **89:** 333-337.

Myung , K. and Kolodner, R. (2002). Suppression of genomic instability by redundant S-phase checkpoint pathways in *Saccharomyces cerevisiae. Proc. Natl. Acad. Sci. USA,* **99:** 4500-4507.

Nelson, H. H., Kelsey, K. T., Mott, L. A. and Karagas, M. R. (2002). The XRCC1 Arg399Gln polymorphism, sunburn and non-melanoma skin cancer: evidence of gene-environment interaction. *Cancer Research,* **62:** 152-5.

O'Regan, P., Wilson, C., Townsend, S. and Thacker, J. (2001). XRCC2 is a nuclear RAD51-like protein, required for damage-dependent RAD51 focus formation without the need for ATP binding. *Journal of Biological Chemistry,* **276:** 22148-22153.

Orita, M., Iwahana, H., Kanazawa, H., Hayashi, K. and Sekiya, T. (1989). Detection of polymorphisms of human DNA by gel electrophoresis as single strand conformation polymorphisms. *Proc. Natl. Acad. Sci. USA,* **86:** 2766-2770.

Osborn, A. J., Elledge, S. J. and Zou, L. (2002). Checking on the fork: the DNA-replication stress-response pathway. *Trends in Cell Biology,* **12:** 509-516.

Pastink, A. and Lohman, P. H. M. (1999). Repair and consequences of double-strand breaks in DNA. *Mutation Research,* **428:** 141-156.

Paull, T. T. and Gellert, M. (1998). The 3' to 5' exonuclease activity of Mre11 facilitates repair of DNA double-strand breaks. *Molecular Cell.,* **1:** 969-79.

Paull, T. T. and Gellert, M. (1999). Nbs1 potentiates ATP-driven DNA unwinding and endonuclease cleavage by the Mre11/Rad50 complex. *Genes & Development.,* **13:** 1276-88.

Paull, T. T. and Gellert, M. (2000). A mechanistic basis for Mre11-directed DNA joining at microhomologies. *Proceedings of the National Academy of Sciences of the United States of America.,* **97:** 6409-14.

Petrini, J. H. (2000a). The Mre11 complex and ATM: collaborating to navigate S phase. *Current Opinion in Cell Biology,* **12:** 293-296.

Petrini, J. H. (2000b). S-phase functions of the Mre11 complex. *Cold Spring Harbor Symposia on Quantitative Biology.*, **65:** 405-11.

Petrini, J. H. and Stracker, T. H. (2003). The cellular response to DNA double-strand breaks: defining the sensors and the mediators. *Trends in Cell Biology,* **13:** 458-462.

Petrini, J. H., Walsh, M. E., DiMare, C., Chen, X.-N., Korenberg, J. R. and Weaver, D. T. (1995). Isolation and Characterization of the Human MRE11 Homologue. *Genomics,* **29:** 80-86.

Pierce, A. J., Johnson, R. D., Thompson, L. H. and Jasin, M. (1999). XRCC3 promotes homology-directed repair of DNA damage in mammalian cells. *Genes and Development,* **13:** 2633-2638.

Pitts, S. A., Kullar, H. S., Stankovic, T., Stewart, G. S., Last, J. I., Bedenham, T., Armstrong, S. J., Piane, M., Chessa, L., Taylor, A. M. and Byrd, P. J. (2001). hMRE11: genomic structure and a null mutation identified in a transcript protected from nonsense-mediated mRNA decay. *Human Molecular Genetics.*, **10:** 1155-62.

Price, A. S. (2002). Primary and Secondary Prevention of Colorectal Cancer. *Gastroenterology Nursing,* **26:** 73-81.

Rafii, S., Lindbliom, A., Reed, M., Meuth, M. and Cox, A. (2003). A naturally occuring mutation in an ATP-binding domain of the recombination repair gene XRCC3 ablates function without causing cancer susceptibility. *Human Molecular Genetics,* **12:** 915-923.

Rafii, S., O'Regan, P., Xinarianos, G., Azmy, I., Stephenson, T., Reed, M., Meuth, M., Thacker, J. and Cox, A. (2002). A potential role for the XRCC2 R188H polymorphic site in DNA-damage repair and breast cancer. *Human Molecular Genetics,* **11:** 1433-1438.

Raschle, M., Marra, G., Nystrom-Lahti, M., Schar, P. and Jiricny, J. (1999). Identification of hMutLbeta , a Heterodimer of hMLH1 and hPMS1. *J. Biol. Chem.*, **274:** 32368-32375.

Rouse, J. and Jackson, S. P. (2002). Interfaces Between the Detection, Signalling and Repair of DNA Damage. *Science,* **297:** 547-551.

Schild, D., Lio, Y., Collins, D. W., Tsomondo, T. and D.J., C. (2000). Evidence for simultaneous protein interactions between human Rad51 paralogs. *The Journal of Biological Chemistry,* **275:** 16443-16449.

Seo, G. J., Kim, S. E., Lee, Y. M., Lee, J. W., Lee, J. R., Hahn, M. J. and Kim, S. T. (2003). Determination of substrate specificity and putative substrates of Chk2 kinase. *Biochemical & Biophysical Research Communications.*, **304:** 339-43.

Shen, H., Sturgis, E. M., Dahlstrom, K. R., Zheng, Y., Spitz, M. R. and Wei, Q. (2002). A variant of the DNA repair gene XRCC3 and risk of squamous cell carcinoma of the head and neck: a case-control analysis. *Int. J. Cancer,* **99:** 869-872.

Shen, M. R., Jones, I. M. and Mohrenweiser, H. (1998). Nonconservative amino acid substitution variants exist at polymorphic frequency in DNA repair genes in healthy individuals. *Cancer Research,* **58:** 604-608.

Shiloh, Y. (2001). ATM and ATR: networking cellular responses to DNA damage. *Current Opinion in Genetics & Development,* **11:** 71-77.

Shiloh, Y. (2003). ATM and Related Protein Kinases: Safeguarding Genome Integrity. *Nature Reviews Cancer,* **3:** 155-68.

Sonoda, E., Takata, M., Yamashita, Y. M., Morrison, C. and Takeda, S. (2001). Homologous DNA recombination in vertebrate cells. *Proc. Natl. Acad. Sci. USA,* **98:** 8388-8394.

Stern, M. C., Umbach, D. M., Lunn, R. M. and Taylor, J. A. (2002). DNA repair gene XRCC3 codon 241 polymorphism, its interaction with smoking and XRCC1 polymorphisms, and bladder cancer risk. *Cancer Epidemiol Biomarkers Prev,* **11:** 939-943.

Stewart, G. S., Maser, R. S., Stankovic, T., D.A., B., Kaplan, M. I., Jaspers, N. G., Raams, A., Byrd, P. J., Petrini, J. H. and Taylor, M. R. (1999). The DNA double-strand break repair gene hMRE11 is mutated in individuals with an ataxia-telangiectasia-like disorder. *Cell,* **99:** 577-587.

Symington, L. S. (2002). Role of RAD52 Epistasis Group Genes in Homologous Recombination and Double-Strand Break Repair. *Microbiology and Molecular Biology Reviews,* **66:** 630-670.

Takata, M., Sasaki, M. S., Tachiiri, S., Fukushima, T., Sonoda, E., Schild, D., Thompson, L. H. and Takeda, S. (2001). Chromosome instability and defective recombinational repair in knockout mutants of the five Rad51 paralogs. *Molecular and Cellular Biology,* **21:** 2858-2866.

Tambini, C. E., George, A. M., Rommens, J. M., Tsui, L., Scherer, S. W. and Thacker, J. (1997). The XRCC2 DNA repair gene: identification of a positional candidate. *Genomics,* **41:** 84-92.

Tauchi, H., Kobayashi, J., Morishima, K., van Gent, D. C., Shiraishi, T., Verkaik, N. S., vanHeems, D., Ito, E., Nakamura, A., Sonoda, E., Takata, M., Takeda, S., Matsuura, S. and Komatsu, K. (2002). Nbs1 is essential for DNA repair by homologous recombination in higher vertebrate cells. *Nature.,* **420:** 93-8.

Tebbs, R. S., Zhoa, Y., Tucker, J. D., Scheerer, J. B., Sicilliano, M. J., Hwang, M., Liu, N., Legerski, R. J. and Thompson, L. H. (1995). Correction of chromosomal instability and sensitivity to diverse mutagens by a cloned cDNA of the XRCC3 DNA repair gene. *Proc. Natl. Acad. Sci. USA,* **92:** 6354-6358.

Tessitore, A., Biordi, L., Flati, V., Toniato, E., Marchetti, P., Ricevuto, E., Ficorella, C., Scotto, L., Giannini, G., Frati, L., Masciocchi, C., Tombolini, V., A., G. and Martinotti, S. (2003). New mutations and protein variants of NBS1 are identified in cancer cell lines. *Genes and Development,* **36:** 198-204.

Thompson, L. H. and Schild, D. (1999). The contribution of homologous recombination in preserving genome integrity in mammalian cells. *Biochimie,* **81:** 87-105.

Thompson, L. H. and Schild, D. (2001). Homologous recombination repair of DNA ensures mammalian chromosome stability. *Mutation Research,* **477:** 131-153.

Toft, N. J. and Arends, M. J. (1998). DNA mismatch repair and colorectal cancer. *Journal of Pathology,* **185:** 123-129.

Trujillo, K. M., Yuan, S. S., Lee, E. Y. and Sung, P. (1998). Nuclease activities in a complex of human recombination and DNA repair factors Rad50, Mre11, and p95. *Journal of Biological Chemistry.,* **273:** 21447-50.

Tsubouchi, H. and Ogawa, H. (1998). A novel mre11 mutation impairs processing of double-strand breaks of DNA during both mitosis and meiosis. *Molecular & Cellular Biology.,* **18:** 260-8.

Umar, A., Boyer, J., Thomas, D., Nguyen, D., Risinger, J., Boyd, J., Ionov, Y., Perucho, M. and Kunkel, T. (1994). Defective mismatch repair in extracts of colorectal and endometrial cancer cell lines exhibiting microsatellite instability. *J. Biol. Chem.,* **269:** 14367-14370.

Usui, T., Ohta, T., Oshiumi, H., Tomizawa, J., Ogawa, H. and Ogawa, T. (1998). Complex formation and functional versatility of Mre11 of budding yeast in recombination. *Cell,* **95:** 705-716.

Varon, R., Vissinga, C., Platzer, M., Cerosaletti, K. M., Chrzanowska, K. H., Saar, K., Beckmann, G., Seemanova, E., Cooper, P. R., Nowak, N. J., Stumm, M., Weemaes, C., Digweed, M., Rosenthal, A., Sperling, K., Concannon, P. and Reis, A. (1998). Nibrin, a novel DNA double-strand break repair protein, is mutated in Nijmegen Breakage syndrome. *Cell,* **93:** 467-476.

Vassileva, V., Millar, A., Briollais, L., Chapman, W. and Bapat, B. (2002). Genes Involved in DNA Repair Are Mutational Targets in Endometrial Cancers with Microsatellite Instability. *Cancer Research,* **62:** 4095-4099.

Veigl, M. L., Kasturi, L., Olechnowicz, J., Ma, A., Lutterbaugh, J. D., Periyasamy, S., Li, G.-M., Drummond, J., Modrich, P. L., Sedwick, W. D. and Markowitz, S. D. (1998). Biallelic inactivation of hMLH1 by epigenetic gene silencing, a novel mechanism causing human MSI cancers. *PNAS,* **95:** 8698-8702.

Vermeulen, K., Van Bockstaele, D. R. and Berneman, Z. N. (2003). The cell cycle: a review of regulation, deregulation and therapeutic targets in cancer. *Cell Proliferation,* **36:** 131-149.

Vogelstein, B. and Kinzler, K. W. (1993). The multistep nature of cancer. *Trends in Genetics,* **9:** 138-41.

Wang, Y., Cortez, D., Yazdi, P., Neff, N., Elledge, S.J. and Qin, J. (2000). BASC, a super complex of BRCA1-associated proteins involved in the recognition and repair of aberrant DNA structures. *Genes and Development,* **14:** 927-939.

Wheeler, J. M. D. and Bodmer, W. F. (2000). DNA mismatch repair genes and colorectal cancer. *Gut,* **47:** 148-153.

Wheeler, J. M. D., Loukola, A., Aaltonen, L. A., Mortensen, N. J. and Bodmer, W. F. (2000). The role of hypermethylation of the hMLH1 promoter region in HNPCC versus MSI+ sporadic colorectal cancers. *Journal of medical genetics,* **37:** 588-592.

Wiese, C., Collins, D. W., Albala, J. S., Thompson, L. H., Kronenberg, A. and Schild, D. (2002). Interactions involving the Rad51 paralogs Rad51C and XRCC3 in human cells. *Nucleic Acids Research,* **30:** 1001-1008.

Wilson, T. E. (2002). A Genomics-Based Screen for Yeast Mutants With an Altered Recombination/End-Joining Repair Ratio. *Genetics,* **162:** 677-688.

Winsey, S. L., Haldar, N. A., Marsh, H. P., M., B., Marshall, S. E., A.L., H., Wojnarowska, F. and Welsh, K. (2000). A variant within the DNA repair gene XRCC3 is associated with the development of melanoma skin cancer. *Cancer Research,* **60:** 5612-5616.

Wu, X., Ranganathan, V., Weisman, D. S., Heine, W. F., D.N., C., O'Neill, T. B., Crick, K. E., Pierce, K. A., Lane, W. S., Rathbun, G., Livingston, D. M. and Weaver, D. T. (2000). ATM phosphorylation of Nijmegen breakage syndrome protein is required in a DNA damage response. *Nature,* **405:** 477-482.

Xiao, Y. and Weaver, D. T. (1997). Conditional gene targeted deletion by Cre recombinase demonstrates the requirement for the double-strand break repair Mre11 protein in murine embryonic stem cells. *Nucleic Acids Research.,* **25:** 2985-91.

Xu, B., O'Donnell, A. H., Kim, S.-T. and Kastan, M. B. (2002). Phosphorylation of Serine 1387 in Brca1 Is Specifically Required for the Atm-mediated S-phase Checkpoint after Ionizing Radiation. *Cancer Research,* **62:** 4588-4591.

Yamaguchi-Iwai, Y., Sonoda, E., Sasaki, M. S., Morrison, C., Haraguchi, T., Hiraoka, Y., Yamashita, Y. M., Yagi, T., Takata, M., Price, C., Kakazu, N. and Takeda, S. (1999). Mre11 is essential for the maintenance of chromosomal DNA in vertebrate cells. *EMBO Journal.,* **18:** 6619-29.

Zhao, S., Renthal, W. and Lee, E. Y. (2002). Functional analysis of FHA and BRCT domains of NBS1 in chromatin association and DNA damage responses. *Nucleic Acids Research.,* **30:** 4815-22.

Zhao, J. H., Curtis, D. and Sham, P. C. (2000). Model free analysis and permutation test for allelic associations. *Human Hereditary,* **50:** 138-139.

Zhu, J., Peterson, S., Tessarollo, L. and Nussenzweig, A. (2001). Targeted disruption of the Nijmegen breakage syndrome gene NBS1 leads to early embryonic lethality in mice. *Current Biology,* **11:** 105-109.

Zhu, X.-D., Kuster, B., Mann, M., Petrini, J. H. and de Lange, T. (2000). Cell-cycle-regulated association of RAD50/MRE11/NBS1 with TRF2 and human telomeres. *Nature genetics,* **25:** 347-352.

Appendix I

Maps of Cloning Vectors

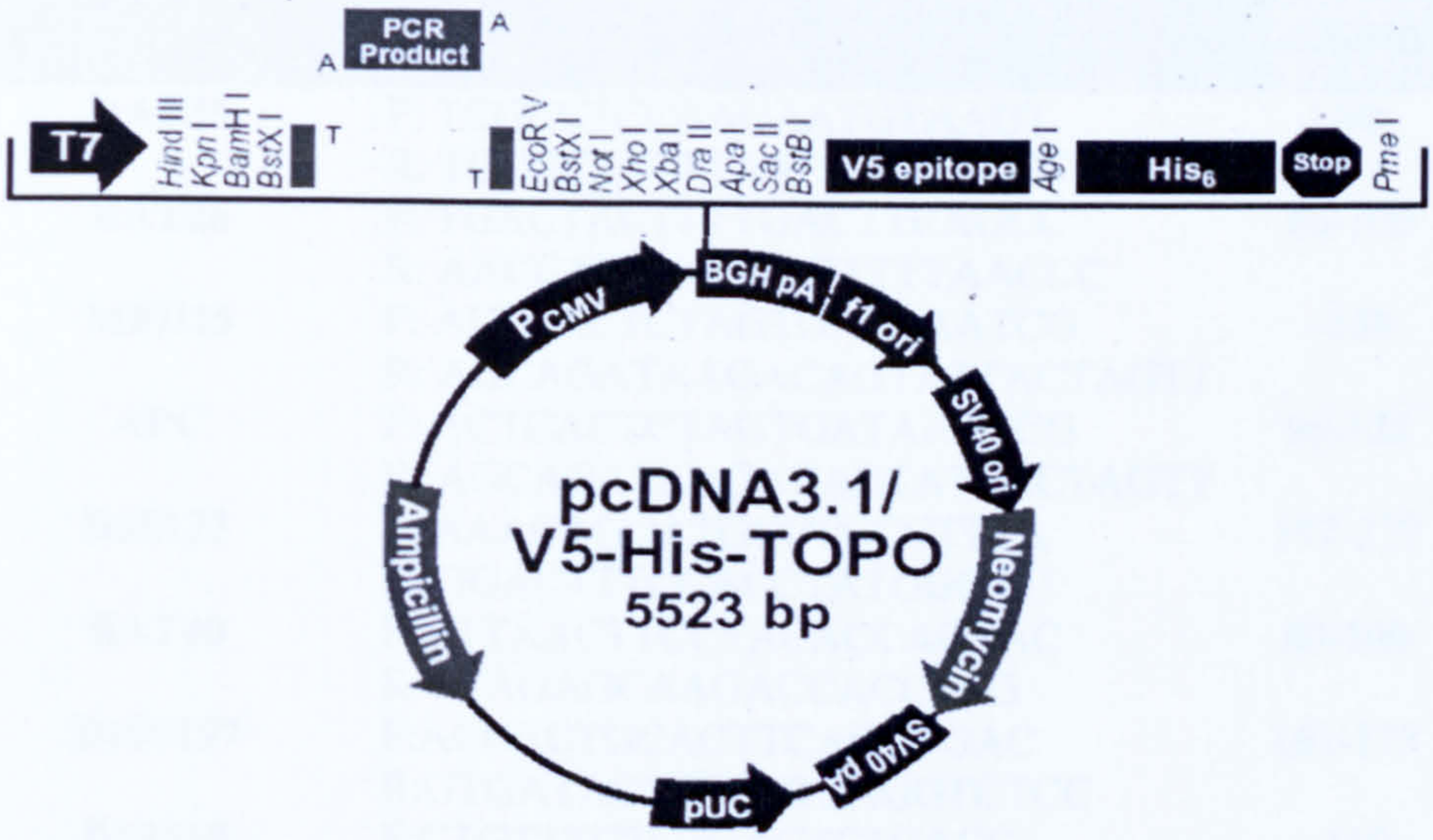

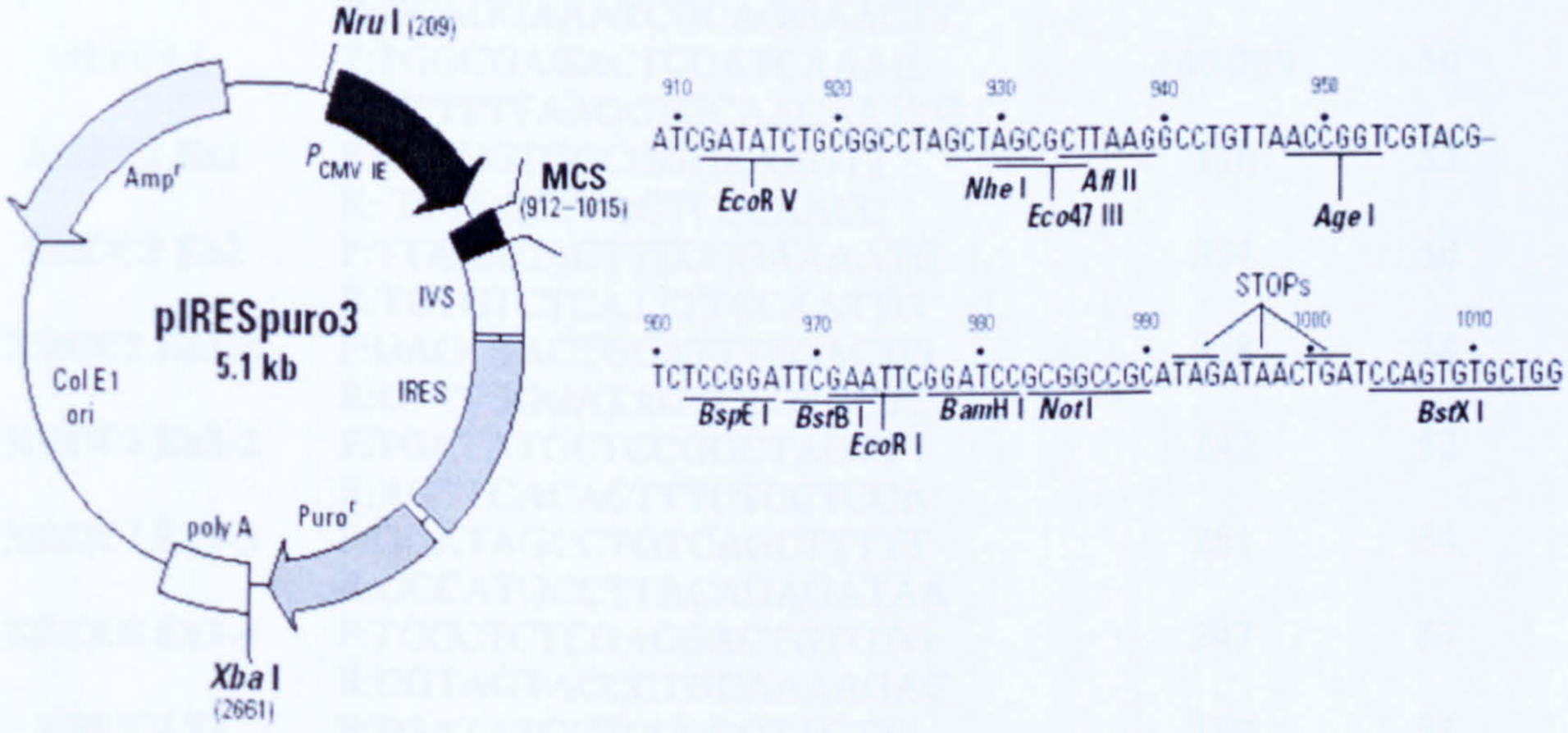

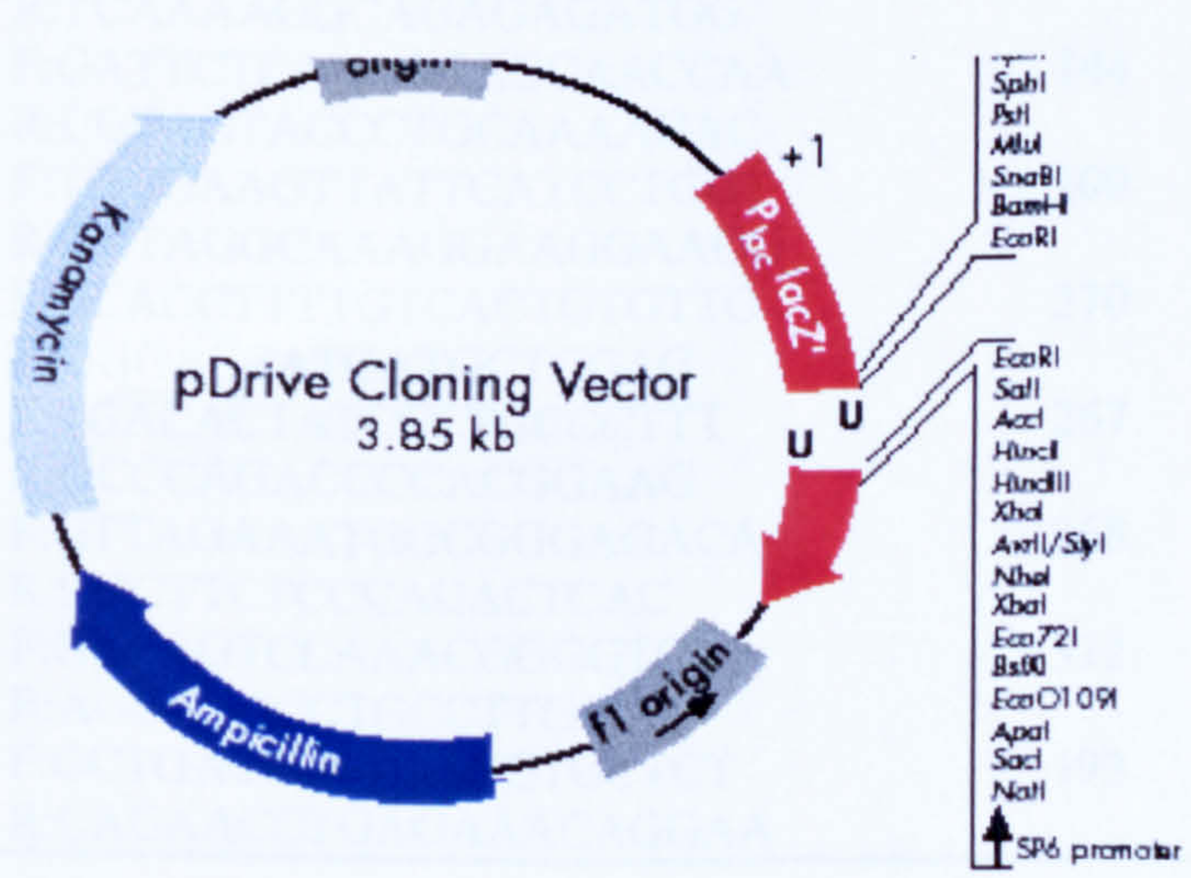

Appendix II

PCR Primers and PCR Conditions

Locus	Primer Sequence (5'-3')	PCR product size (bp)	Annealing (°C)
BAT25	F: TCGCCTCCAAGAATGTAAGT R: TCTGCATTTTAACTATGGCTC	~90	54
BAT26	F: TGACTACTTTTGACTTCAGCC R: AACCATTCAACATTTTTAACCC	80-100	51
MFD15	F: ACTCACTCTAGTGATAAATCG R: AGCAGATAAGACAGTATTACTAGTT	~150	52
APC	F: ACTCACTCTAGTGATAAATCG R: AGCAGATAAGACAGTATTACTAGTT	96-122	54
D2S123	F: AAACAGGATGCCTGCCTTTA R: GGACTTTCCACCTATGGGAC	197-227	59
BAT40	F:ATTAACTTCCTACACCACAAC R:GTAGAGCAAGACCACCTTG	80-100	58
D10S197	F:ACCACTGCACTTCAGGTGAC R:GTGATACTGTCCTCAGGTCTCC	161-173	62
D18S69	F:CTGTTTCTCTGACTCTGACC R:GACTTTCTAAGTTCTTGCCAG	~110	57
D18S58	F:GCTCCCGGCTGGTTTT R:GCAGGAAATCGCAGGAACTT	144-160	52
MYCL1	F:TGGCGAGACTCCATCAAAG R:CTTTTTAAGCTGCAACAATTC	140-209	50
XRCC2 Ex1	F:GTTGGTGGCGGGAAAGTT R: TCTCCCTCACTCCCAACC	118	53
XRCC2 Ex2	F:TTACAGACTTTCGGAAAATG R:TGTGTCTCATTTTCCAATTG	304	50
XRCC2 Ex3-1	F:GAGCTACTGCATTTTGACTG R:CTTTGGGATAGTCTGTGCTC	228	54
XRCC2 Ex3-2	F:TGATATGCTCCGGCTAGTT R:AGTTCACACTTTCTCCTCCA	242	52
XRCC2 Ex3-3	F:GGATAGCCTGTCAGCTTTTT R:GCCATGCCTTACAGAGATAA	251	54
XRCC2 Ex3-4	F:TGCCTCTCGACGACTGTGTG R:CGTAGTACCCTGCAAAAGAC	247	57
XRCC2 T_8	F:TGATATGCTCCGGCTAGTT R:TCAAAAGGCAGAGAGATGG	179	53
XRCC2 A_7/T_7	F:GATTCTCAAAGCAGCAACCAA R:CGTAGTACCCTGCAAAAGAC	144	57
XRCC3 Ex3	F:TGGGAAGTTATTCATCCTGGT R:GGTAGGCAAAGGAAGGAAGG	200	56
XRCC3 Ex4	F:GCACCTTTTGTCACTGTGTTG R:GGGACCATGATGCTGGAG	270	54
XRCC3 Ex5	F:TGACACTATCCCTGCCCTTT R:GCCCAGACCCCACGGAAG	267	54
XRCC3 Ex6	F:GTTAGAAATGGCGGGAGACA R:GGCTTCTCCCACACTCAC	268	54
XRCC3 Ex7	F:GACAGTCCAAACGGGGTCT R:AGCAACCCTGCCTTGGTG	312	54
XRCC3 Ex8	F:GCTGACCTGGACTGTGCTCT R:CAGAACCTGAGAAACAGGAA	193	58

Locus	Primer Sequence (5'-3')	PCR product size (bp)	Annealing (°C)
XRCC3 Ex9	F:TGCCTGCTTCCTGTTTCTC R:TCTCAGGCAGGGCTGTTGT	275	52
Mus81 Ex1	F:TCGAATCCCGACTCCAGAAC R:CCAGCAGCTTTTCCCATC	247	54
Mus81 Ex2	F:AAGCTGCTGGCCAGGTCAG R:AGGAGAGTACGGAGGCTCC	252	57
Mus81 Ex3	F:GGTTGCATCCCAGATCCT R:CATACTCCCGCACTCCCA	206	53
Mus81 Ex4	F:GGACTTATTCAAAGATGACTG R:CAGGTGGCTGGGATAATCTT	263	55
Mus81 Ex5	F:AAGATTATCCCAGCCACCTG R:GTACCACCACAAGTCCATG	277	54
Mus81 Ex6	F:CATGGACTTGTGGTGGTAC R:TGGGTGACTCTAAGGCCCT	209	54
Mus81 Ex7	F:GCCTGCCAGGAATGAGTGA R:GCTTTGGCCTCATTTCCCA	259	54
Mus81 Ex8	F:CGGGTGGCATGGGTGTGG R:CCTAGATCAGAGCAGGGCA	243	58
Mus81 Ex9	F:AGATGATCAGAGGAGGCTGG R:CGTTAGCTTGCGATCCCCT	259	56
Mus81 Ex10	F:AGGTGAAGGGCCGTGGAC R:CCCTGGATTGCTCTGGGC	254	56
Mus81 Ex11	F:TTGAGTGTGACATCATGGAT R:TAGACCATGAACCATGGAC	260	52
Mus81 Ex12	F:GGTCCATGGTTCATGGTCTA R:GCCCAGGCAAGGTGAATTC	220	54
Mus81 Ex13	F:TTCGAGCTCCAGCCTGGC R:TTCTCGCACCGACTGGGC	260	55
Mus81 Ex14	F:CTGTCTCTGCCTAGCTTCT R:CCTCCACGAAGCATGGATT	257	53
Mus81 Ex15	F:CCACTCTTCCATCCCATGCT R:CCTCCAGGTTCCGTCTCTTG	212	57
Mus81 Ex16	F:GGAACCTGGAGGGAGTGG R:GGCTGGCTAGCCTGGGTT	203	55
MRE11 $A_{6(nt596)}$	F:CCATTCCAGATGAAAGGCTCT R:CCTCAGCACTTGGCTCAAAC	153	57
MRE11$A_{6(nt1235)}$/ $T_{6(nt1209)}$/$A_{7(intron)}$	F:CAGTGTTCTTCGCTTTAGCC R:AAGAGAATTATTCCCACTGTCA	244	57
MRE11 $A_{6(nt1458)}$	F:GGAGAAAGATGCCATTGAGG R:CTCATCGATTTTGTCTTCGAG	103	56
MRE11 $A_{7(coding)}$	F:GGAATAGGCAACATGTTTGTGA R:TCCCCTAGACCTCTGGACTG	205	58
NBS1 $A_{6(nt242)}$	F:TCAAACAGATGAAATCCCTGTA R:GTAATACCATCCCCCGACTT	120	54
NBS1 $A_{7(nt1390)}$	F:CCCAAACTATCAGCTTTCACC R:CTGCAGCAGCAGAAGCATAC	236	58
NBS1 $A_{7(nt1645)}$	F:CTGCCAGTAAATCTCATGCTG R:AACTCTGGTTTTGTGTCCTTG	118	57
NBS1 $A_{6(nt1953)}$	F:CCTATCCATCTTAACCCCATTT R:TTTCAAACACTGACCTCTTGTG	222	57
Rad50 $T_{6(nt536)}$	F: CAGTTCTCTTGGGGTTTCCA R: TCCAAATTGCAAACACAGTTC	192	55

Locus	Primer Sequence (5'-3')	PCR product size (bp)	Annealing (°C)
Rad50 $A_{6\ (nt1717)}$	F:AGGCACAGTGATGAATTAACCT R:TACTTCAATTTGGCAAGTCTGT	125	57
Rad50 $A_{9(nt2157)}$	F:CTGCGACTTGCTCCAGATAA R:ACAGGGCATACCAGCTCAGA	210	58
Rad50 $A_{8(nt2794)}$	F:AGAGCAGGTAAGCCCTTTGG R:AGTGTCCGACGTGGTGCTAT	177	57
MRE11 Frag1	F:CCCAGAGGAGCTTGACTGACC R:TGTTCATGGCCCCAGATAAC	768	57
MRE11 Frag2	F:TTCCAGAACAATTTTTGGATGA R:TTCGAGGGCATCAATATGAC	797	53
MRE11 Frag3	F:GGAGAAAGATGCCATTGAGG R:ATTTTCCTGTATCTTGCATGT	780	55
NBS1 Frag1	F:GTCTAGCAGCCCCGGTTAC R:GTTTTCTTTCCTGCCGTCCT	768	56
NBS1 Frag2	F:TACCCACCTCTTGATGAACC R:CTGCTGAGAAGCCCTATCT	763	58
NBS1 Frag3	F:CCCAAACTATCAGCTTTCACC R:GCTGACCATAGTGAGTCTTCC	624	58
NBS1 Frag4	F:CAAGAAAATGAAATTGGGAAGA R: TGTTGGCCTGAAGTAGATGC	482	55
Rad50 Frag1	F:CCTTGCTTCGGCCTCAGTTA R:CGAATCTCACAAGCTTTTTCC	740	55
Rad50 Frag2	F:CGTCAGACACAAGGTCAGAAA R:CTCAATTCTTCTTCCCAGTCCA	747	57
Rad50 Frag3	F:GAATGACTTTGCAGAAAAAGAG R:CTGGGAGTAAACTGCTGTGG	760	57
Rad50 Frag4	F:GCCAGGATTTTGAAAGTGATT R:CTCCTCCAGTTGCTGACGAC	763	54
Rad50 Frag5	F:CCAGCAGGAACAGATTCAAC R:CTCAGCATCCCGAAATTGTG	739	55
Rad50 Frag6	F:GCGACAGAAAGGTTATGAAGA R:GAGGACCTACATTTCTATGGC	739	55
MRE11 T_{11}	F:AATATTTTGGAGGAGAATCT R:AATTGAAATGTTGAGGTT	122	51
MRE11 314del88	F:CCCAGAGGAGCTTGACTGACC R:CTACTTACTAAAACCAAAGTT	345	54

Appendix III

SSCP Conditions

Exon	Percentage of SSCP gel used in analysis	Running speed (Volt Hours, VH)
XRCC2 Ex1	12	2500
XRCC2 Ex2	12	4000
XRCC2 Ex3-1	10	3500
XRCC2 Ex3-2	10	3500
XRCC2 Ex3-3	10	4000
XRCC2 Ex3-4	10	3500
XRCC3 Ex3	12	3000
XRCC3 Ex4	12	4500
XRCC3 Ex5	12	3500
XRCC3 Ex6	12	5000
XRCC3 Ex7	12	6000
XRCC3 Ex8	10	3500
XRCC3 Ex9	10	4500
Mus81 Ex1	12	4500
Mus81 Ex2	12	4000
Mus81 Ex3	10	3500
Mus81 Ex4	10	4000
Mus81 Ex5	12	3500
Mus81 Ex6	10	3000
Mus81 Ex7	12	4000
Mus81 Ex8	12	4000
Mus81 Ex9	12	4500
Mus81 Ex10	12	4500
Mus81 Ex11	12	4000
Mus81 Ex12	10	3500
Mus81 Ex13	10	3500
Mus81 Ex14	10	3500
Mus81 Ex15	10	3000
Mus81 Ex16	12	3000

Appendix IV

Recombination Reporter Constructs

SCneo Recombination Reporter

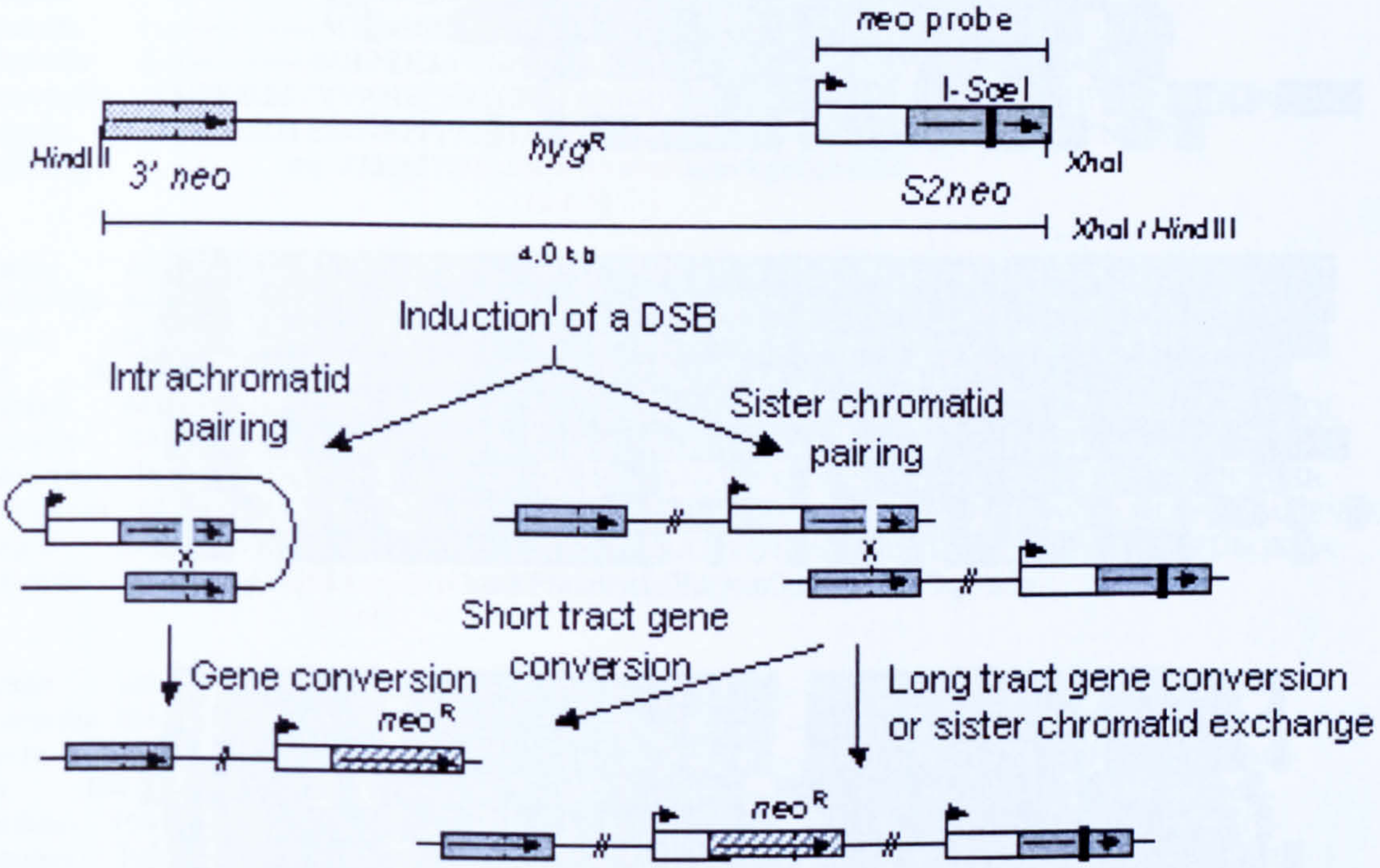

pCMV3xnls-I-SceI

HA = epitope tag

NLS = nuclear localisation signal

I-SceI = endonuclease

poly-A = human growth hormone polyadenylation site

SV40ori = SV40 origin for replication of plasmid COS1 cells

CMV = human cytomegalovirus promoter/enhancer

Appendix V

MRE11 Protein Alignments

The amino acids lost in 314del345 MRE11 are shown in blue, highly conserved motifs of the nuclease domain of the protein are shown in red.

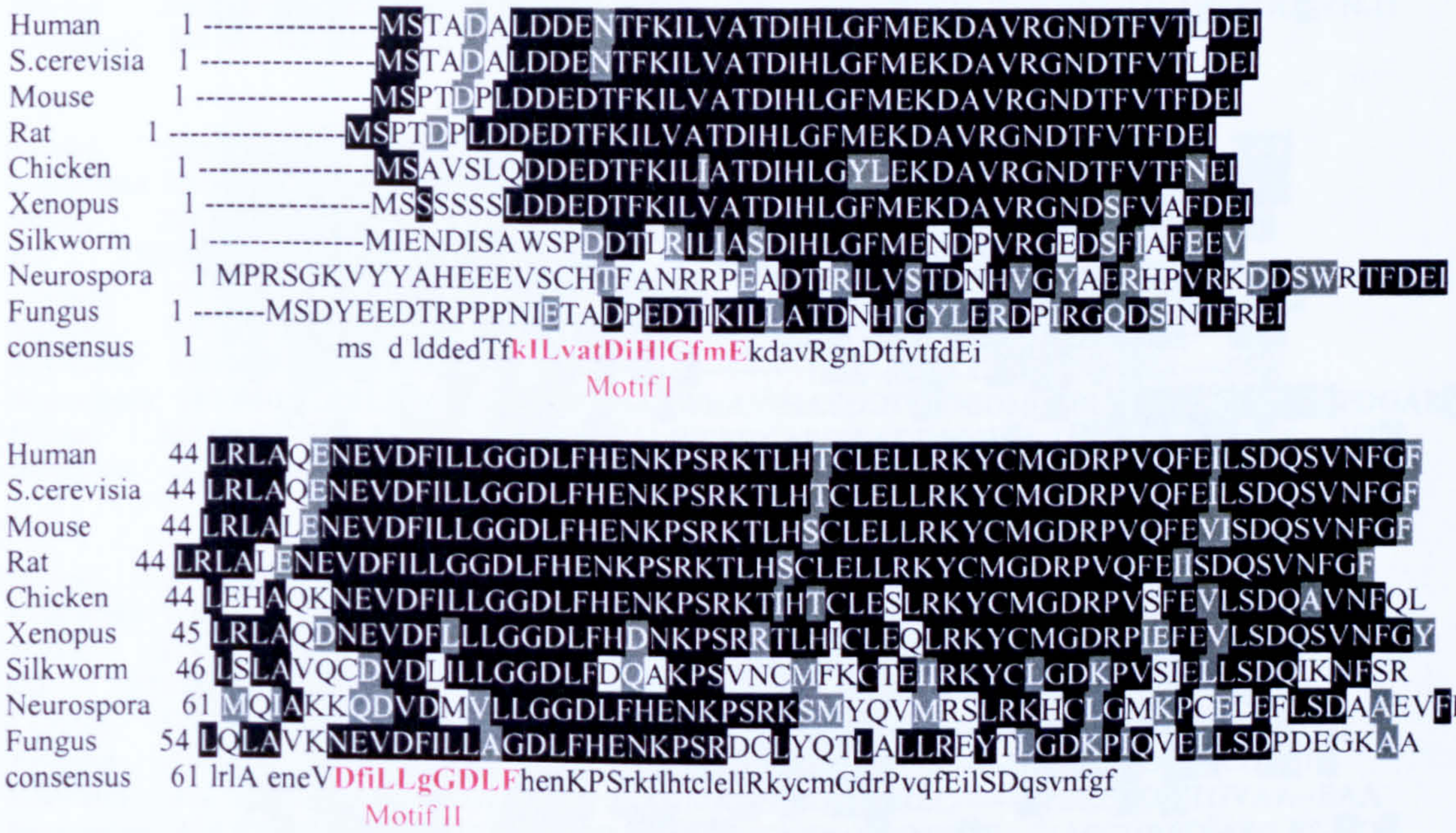

```
Human        269 SVVTSLSPGEAVKKHVGLLRIKGRKMNMHKIPLHTVRQFFMEDIVLANHPDIFNPDNPKV
S.cerevisia  269 SVVTSLSPGEAVKKHVGLLRIKGRKMNMHKIPLHTVRQFFMEDIVLANHPDIFNPDNPKV
Mouse        269 SVVTSLSPGEAVKKHVGLLRIKGRKMNMQKLPLRTVRRFFIEDVVLANHPNLFNPDNPKV
Rat          269 SVVTALSPGETVKKHVGLLRVKGRKMNMQKLPLRTVRQFFMEDVVLANHPSLFNPDNPKV
Chicken      269 SVVTSLSPGEAVKKHIGLLRVKGKKMKMQRIALETVRTFYMEDVVLADHPELFNPDNPKV
Xenopus      270 SVATSLSPGEAEKKHVGLLRIKGKKMNMQKIPLQTVRQFFIEDLVLSDYPDIFNPDNPRV
Silkworm     268 TVATSLAAGEALPKHCGLLEIHKGNFKLTPLPLQTVRPFIFKTIVLS--EENIGSDDVNE
Neurospora   285 SVATSLVPGEAVPKHVAILNITGRKFEVDKIPLKTVRPFVTREIVLASDKRFKGLDKQNN
Fungus       290 SVATSLADGEAIEKHVALLEIKGKEFQLTPIPLRTVRPFVISEVVLEDAAEEEGLDVN-D
consensus    301 sVvTsLspGEavkKHvglLrikgrkmnm kipLhTVR FfmediVLa hpdifnpDnpkv

Human        329 TQAIQSFCLEKIEEMLENAERER----------LGNSHQPEKPLVRLRVDYSG----GFE
S.cerevisia  329 TQAIQSFCLEKIEEMLENAERER----------LGNSHQPEKPLVRLRVDYSG----GFE
Mouse        329 TQAIQSFCLEKIEEMLDSAERER----------LGNPQQPGKPLIRLRVDYSG----GFE
Rat          329 TQAIQSFCLEKIEEMLDSAERER----------LGNPQQPEKPLIRLRVDYSG----GFE
Chicken      329 TQAIQAFCMEKVEEMMLDNAERER----------LGNPRQPQKPLIILRVDYTG----GFE
Xenopus      330 TQEIETFCIEKVEEAMLDTAERER----------LGNPRQPDKPLIRLRVDYTG----GFE
Silkworm     326 NEKVQEFLKNRVNEAIDEASKLK----------TADLRQPLLPLIRLSIFYER----ESQ
Neurospora   345 RHEITKRLMVIVNEMIEEANAFWRAV-HAEDDDMDEDMEPPLPLVRLKVDYTAPDGARYE
Fungus       349 QMEITKYLKQKVNDLIDQAQALWEERNARSIEAGDEEIPPMLPLVRLKVDTTN----VTQ
consensus    361 tqaiqsfclekveemld Aerer          lgn hqP kPLirLrvdysg    gfe

Human        375 PFSVLRFSQKFVDRVANPKDIIHFFRHREQKEKTG-------EEINFGKLITKPS-EGTT
S.cerevisia  375 PFSVLRFSQKFVDRVANPKDIIHFFRHREQKEKTG-------EEINFGKLITKPS-EGTT
Mouse        375 PFNVLRFSQKFVDRVANPKDVIHFFRHREQKGKTG-------EEINFGMLITKPASEGAT
Rat          375 PFNVLRFSQKFVDRVANPKDVIHFFRHREQKGKTG-------EEINFGKLIIKPASEGTT
Chicken      375 PFIVHRFSQKYMDRVANPKDIIHFFRHREQKEKND-------NDINFGKLLSRPASEEVT
Xenopus      376 PFNTLRFSQKFVDRTANPKDIIHFFRHKEQKDKKDS------ITINFGKIDSKPLLEGTT
Silkworm     372 NFNRIRFGQNFNGLVANPNDLLIMKKEKKIREKREC------DPEEEGDMTGVAA--EAA
Neurospora   404 VENPHRFSNRFTGKVANHNDVVRFHCNTKGKKNVAT------APGVREDIAEILES-ADT
Fungus       405 TSNPIRFGQEFQGRVANPRDLLVFHRSKKAGKRGAGKVDIDQPELSIDDPDLTVSEKLAK
consensus    421 pfnvlRFsqkfvdrvANpkDiihffrhreqkek g       eeinfgklitkp  eg t

Human        427 LRVEDLVKQYFQTAEKNVQLSLLTERGMGEAVQEFVDKEEKDAIEELVKYQLEKTQRFLK
S.cerevisia  427 LRVEDLVKQYFQTAEKNVQLSLLTERGMGEAVQEFVDKEEKDAIEELVKYQLEKTQRFLK
Mouse        428 LRVEDLVKQYFQTAEKNVQLSLLTERGMGEAVQEFVDKEEKDAIEELVKYQLEKTQRFLK
Rat          428 LRVEDLVKQYFQTAEKNVQLSLLTERGMGEAVQEFVDKEEKDAIEELVKYQLEKTQRFLK
Chicken      428 LRVEDLVKQYFQTAEKKVQLSLLTERRMGEAVQEFVDKEEKDAIEELVKFQLEKTQRFLK
Xenopus      430 LRVEDLVKEYFKTAEKNVQLSLLTERGMGEAVQEFVDKEEKDALEELVKFQLEKTQRFLK
Silkworm     424 D-VESLLRAYYEAQPKDKRLSVLSVRVITDAVRDFTLKHNEDVLRRAFDAHKRRCIAALL
Neurospora   457 IKVDNLVQEFFAQQS----LKILPQAPFSDAVNQFVSKDDKHAVEMFVIESLSTQVKELL
Fungus       465 VRVKTLVREYLAAQE----LQLLGENGMSDAIQMFVEKDDIHAIQTHVNKSLKTMLKNIK
consensus    481 lrVedLvkqyfqtaeknvqLslLtergmgeAvqeFvdKeekdaieelvkyqlektqrflk

Human        487 ERHIDALEDKIDEEVRRFRETRQKNTNE----------EDDEVREAMTRAR
S.cerevisia  487 ERHIDALEDKIDEEVRRFRETRQKNTNE----------EDDEVREAMTRAR
Mouse        488 ERHIDALEDKIDEEVRRFRESRQRNTNE----------EDDEVREAMSRAR
Rat          488 ERHIDALEDKIDEEVRRFRESRQRNTNE----------EDDEVREAMSRAR
Chicken      488 ERHIDAEEEKIDEEVRKFRESRRKNTEE----------EDEEVREAMTRAR
Xenopus      490 ERHIDAEEEKIDEEVRKFRETRKTNTNE----------EDEEVREAIQRAR
Silkworm     483 ESTAET-----EKEIAEQLEVCKRELDE----------ADDEKLHTLVDAS
Neurospora   513 QLDDDK-IVDLDAHIQDFRQVMEKSFDAGQHKQAQRTKRFKRKPDGWDSDLDGHWINQPQ
Fungus       521 SDEVDE--DDLDDLLAKAKQRQEEEYLEAT----------RAGESAKGKGKAK
consensus    541 erhida edkideevrrfretr kntne                eddevreamtrar
```

```
Human          528 ALRSQSEESASAFSADDLMSIDLAEQMANDSDDSISAATNKGRGRGRGRRGGRGQNSASR
S.cerevisia    528 ALRSQSEESASAFSADDLMSIDLAEQMANDSDDSISAATNKGRGRGRGRRGGRGQNSASR
Mouse          529 ALRSQSETSTSAFSAEDLS-FDTSEQTANDSDDSLSAVPSRGRGRGRGRRGARGQSSAPR
Rat            529 ALRSQSENAASAFSADDLS-FDITEQTADDSDDSQSAVPSRGRGRGRGRRGGRGQSTAPR
Chicken        529 AHRSEGVVLDSASSDEGLM--DTGMKASGDSDDDIPTTLSRGRGRGRAR-GARGQNSAAR
Xenopus        531 THRSQAPDVEMSDEDDDAL---LRKVSLSDDEDVRASMPARGRGRGRAR-GGRGQSTTTR
Silkworm       519 ARPSAPAAQLIVPVVKLPN-TVGKRTIVVLSSDEEELSTRS----GRGR-----TTRASR
Neurospora     572 ALEDIPAEVEPKGNDRPTKRVPTSGVTFSDEDEDMDMDNQPVPIRAAPKRGAAAKTTAAA
Fungus         562 ATDDDGGAASDDSMLMDIDTGGGATFNMSDDDDDDEPPPPP------KRRAATSRATTTK
consensus      601 alrsq    sa s ddl  d     dsdd i    kgrgrgrgrrggrgqssasr

Human          588 GGSQRGR----ADTGLETSTRSRNSKTAVSA-SRNMSIIDAFK-STRQQPSRNVTTKNYS
S.cerevisia    588 GGSQRGR----ADTGLETSTRSRNSKTAVSA-SRNMSIIDAFK-STRQQPSRNVTTKNYS
Mouse          588 GGSQRG-----RDTGLEITTRGRSSKATSST-SRNMSIIDAFR-STRQQPSRNVAPKNYS
Rat            588 GGSQRG-----RDTGLGISTRGRSSKATAST-SRNMSIIDAFR-STRQQPSRNVATKNYS
Chicken        586 GSSRRGR----GNTSQGSSTSSRTYKSVP---DKNSSIMDAFR-SLKPEPSQSTSKFFSE
Xenopus        587 GTSRRGR----GSASADQPSSGRATKATG----KNMSILDAFKPSSRQPTARNVAKKTYS
Silkworm       569 GKSPRG-----------KSTRATKASAP----------APSPPERRTPRRSAAQKSTS
Neurospora     632 KKAAPGKKAAPAKKAAPAKKAAPAKKAPARGRKKKTPFVDSDEEEEEDYPEDDDEEEEEA
Fungus         616 KAPAKAP----AKKATTTTARGRGKKAAPPSSDDEVIELDDDEDEISEEEVVAKPVKRTS
consensus      661 ggs rgr    a tg   strgr sKa     rnmsiidafk strq psrnv  k ys

Human          642 EVIEVDESDVEEDIFPTTSKTDQRWSSTSSSKIMS-----QSQVSKGVDFESSEDD-DDD
S.cerevisia    642 EVIEVDESDVEEDIFPTTSKTDQRWSSTSSSKIMS-----QSQVSKGVDFESSEDD-DDD
Mouse          641 ETIEVDDS-DEDDIFPTNSRADQRWSGTTSSKRMS-----QSQTAKGVDFESDEDD-DDD
Rat            641 ETIEVDES-DDDDSFPTSSRADQRWSGTAPSKRMS-----QSQTAKGVDFESDEDD-DDD
Chicken        638 DIIDDEMDLEESPISLSSKTNQRSSAMSSFSKRGS-----QSQMSRGVDFESDE----DD
Xenopus        639 EDIEDDDSDLEEVSFTPSSVIESRRTSSTSTSYSRKSTQPQSQATKAHFFDDDDDEEDFD
Silkworm       606 CFRIS-----------------------------------------------------
Neurospora     692 DEEEEDVIMEDDEEDPPAPPPKPKAISRVASTRASAR---ATPVRATPARATQARLRLRR
Fungus         672 RAAVLSQSQAPAKKAPAKKKTPARQTQTQLSFAPAGRSSRAAASKARSKMVFDDDDDDDD
consensus      721 e ievdes  eed fpttsk d r s ts sk  s     qsq  kgvdfesdedd ddd

Human          696 PFMNTSSLRRNRR
S.cerevisia    696 PFMNTSSLRRNRR
Mouse          694 PFMSSSCPRRNRR
Rat            694 PFMSGSCPRRNRR
Chicken        689 PFKNTATSRR---
Xenopus        699 PFKKSGPSRRGRR
Silkworm       ------------
Neurospora     749 PPKPGLLARRLG-
Fungus         732 ------------
consensus      781 pf  t   rr rr
```

Appendix VI

Cancer Sample Details

Sample	Sex	Age	T	N	Dukes'	MSI
1	f	76	3	0	b	MSS
2	f	83	4	1	c	MSS
3	m	72	3	1	c	MSS
4	f	87	3	0	b	MSS
5	m	61	3	1	c	MSS
6	m	87	3	0	b	MSS
7	f	91	2	0	a	MSI-L
8	m	54	2	0	a	MSS
9	m	73	4	2	c	MSS
10	m	62	4	2	c	MSS
11	f	68	3	2	c	MSS
12	m	65	3	2	c	MSS
13	m	60	2	0	a	MSS
14	m	77	3	0	b	MSS
15	f	40	3	2	c	MSS
16	f	65	3	1	c	MSS
17	f	46	3	0	b	MSS
18	f	93	3	0	b	MSS
19	m	78	3	0	b	MSS
20	f	84	3	1	c	MSS
21	m	63	3	0	b	MSS
22	m	71	3	0	b	MSS
23	f	61	3	2	c	MSS
24	f	31	3	0	b	MSS
25	m	57	4	2	c	MSS
26	m	94	3	2	c	MSS
27	m	86	3	1	c	MSS
28	f	93	4	1	c	MSS
29	m	50	3	1	c	MSS
30	m	70	3	0	b	MSS
31	m	51	4	1	c	MSS
32	m	41	3	1	c	MSS
33	m	57	3	1	c	MSS
34	m	38	3	0	b	MSS
35	m	56	2	0	b	MSS
36	f	79	3	1	c	MSS
37	f	54	4	1	c	MSS
38	m	79	4	0	b	MSS
39	f	78	4	0	b	MSS
40	m	52	3	0	b	MSI-L
41	f	88	3	0	b	MSS
42	m	90	3	0	b	MSI-H
43	f	76	3	0	b	MSI-H
44	f	79	3	1	c	MSS
45	f	66	4	1	c	MSS
46	f	58	3	2	c	MSS
47	m	71	4	2	c	MSS
48	f	51	3	0	b	MSS
49	m	53	4	0	b	MSS
50	f	76	4	2	c	MSS
51	m	90	3	1	c	MSS
52	f	40	2	1	c	MSS
53	m	79	3	2	c	MSS
54	m	62	3	2	c	MSS
55	m	73	3	0	b	MSS

Sample	Sex	Age	T	N	Dukes'	MSI
56	f	66	3	2	c	MSS
57	m	84	3	0	b	MSS
58	f	68	3	0	b	MSI-H
59	m	72	3	2	c	MSI-L
60	f	62	3	0	b	MSS
61	m	79	3	2	c	MSS
62	m	67	3	1	c	MSS
63	f	79	3	2	c	MSS
64	f	86	4	1	c	MSS
65	m	81	3	0	b	MSS
66	f	72	2	0	b	MSS
67	m	60	3	2	c	MSS
68	f	69	3	0	b	MSI-H
69	m	68	3	0	b	MSS
70	m	68	3	0	b	MSS
71	f	78	4	0	b	MSS
72	m	78	3	2	c	MSS
73	m	72	2	0	b	MSS
74	m	86	4	2	c	MSS
75	m	74	2	0	b	MSS
76	f	72	4	0	b	MSS
77	f	84	3	1	c	MSS
78	m	69	3	2	c	MSS
79	m	67	3	1	c	MSS
80	m	61	3	1	c	MSS
81	f	59	4	1	c	MSS
82	m	66	2	0	a	MSS
83	m	73	4	0	b	MSS
84	f	66	3	0	b	MSS
85	m	84	3	0	b	MSS
86	m	63	3	2	c	MSS
87	m	54	3	2	c	MSS
88	f	91	2	2	c	MSS
89	m	63	3	0	b	MSS
90	m	29	2	0	b	MSS
91	f	73	4	2	c	MSS
92	m	73	2	1	c	MSS
93	f	76	2	1	c	MSS
94	m	64	2	0	b	MSS
95	f	79	2	0	b	MSS
96	f	79	3	0	b	MSS
97	f	69	3	0	b	MSS
98	m	67	3	1	c	MSS
99	m	60	3	1	c	MSS
100	f	85	3	0	b	MSS
101	f	65	3	0	b	MSS
102	m	68	3	0	b	MSS
103	m	58	3	2	c	MSS
104	f	58	2	1	c	MSS
105	f	89	2	0	a	MSS
106	m	85	2	2	c	MSS
107	unknown	82	4	2	c	MSS
108	unknown	56	3	0	b	MSI-H
109	unknown	73	3	1	c	MSS
110	m	80	2	0	b	MSI-H
111	f	53	3	0	b	MSI-H
112	unknown	75	2	0	a	MSS
113	unknown	71	4	1	c	MSI-L
114	unknown	62	3	0	b	MSI-H

Sample	Sex	Age	T	N	Dukes'	MSI
115	m	70	3	1	c	MSS
116	m	42	3	0	b	MSI-L
117	unknown	82	3	0	b	MSI-H
118	unknown	66	3	1	c	MSI-H
119	unknown	50	3	2	c	MSS
120	unknown	90	3	0	b	MSS
121	unknown	66	3	2	c	MSS
122	unknown	39	3	1	c	MSS
123	unknown	59	2	0	b	MSS
124	unknown	68	3	0	b	MSI-H
125	unknown	57	3	1	c	MSI-H
126	unknown	66	3	1	c	MSI-L
127	unknown	78	3	1	c	MSS
128	unknown	81	4	2	c	MSI-H
129	unknown	74	3	0	b	MSS
131	unknown	61	3	2	c	MSS
132	unknown	82	2	0	b	MSS
134	unknown	68	3	0	b	MSI-H
136	unknown	69	4	2	c	MSS

Appendix VII

Suppliers Addresses

ABgene,
Blenheim Road, Epsom, Surrey, KT19 9AP

American Type Culture Collection (ATCC)
P.O. Box 1549, Manassas, VA 20108 USA

Amersham Pharmacia Biotech UK Limited.
Amersham Place, Little Chalfont, Buckinghamshire, HP7 9NA

Ananchem, Ltd,
Anachem House, Charles Street, Luton, Bedfordshire, LU2 0EB

Becton Dickinson,
Between Twons Road, Cowley, Oxford, OX4 3LY

Bethyl Laboratories Inc,
25043 West FM 1097, Montgomery, TX 77356

Bennet Scientific Ltd.,
1 Tenterk Close, Bleadon, Weston-supe-Mare, Somerset, BS24 0PJ

Bibby Sterilin Ltd,
Tilling Drive, Staffordshire, ST15 0SA

Bioline Ltd.
16 The Edge Business Centre, Humber Road, London NW2 6EW

Bio-Rad Laboratories Ltd.
Bio-Rad House, Maylands Avenue, Hemel Hemstead, Herts, HP2 7TP

Britannia Pharmaceuticals,
41-51 Brighton Road, Redhill, Surrey, RH1 6YS

Calbiochem,
10394 Pacific Center Court, San Diego, California 92121 USA

Cambrex Bioscience Inc. (formerly BioWhittaker),
8830 Biggs Ford Road, Walkersville, MD 21793-0127, USA

Cancer Research UK,
P.O. Box 123, Lincoln's Inn Fields, London WC2A 3PX

Professor Carl Smythe,
Centre for Developmental Genetics, University of Sheffield, Firth Court, Sheffield.

Cell Signaling Technology, Inc.
166B Cummings Center, Beverly, MA 01915

CIS Biointernational,
RN306-91400 Saday, BP32, F-91132, Gif/Yvette, Cedex, France.

Continental Lab Products (CLP),
5648 Copley Drive, San Diego, CA 92111, USA

Corning Inc.,
HP-AB-03, Corning, NY 14831, USA

Denver Instrument Company,
1855 Blake Street, Suite 201, Denver, CO 80202, USA

Epicentre,
726 Post Road, Madison, WI 53713, USA

Eppendorf AG,
Barkhausenweg 1, 22331 Hamberg, Germany.

Eurogentec,
Parc scientifique du Sart Tilman, 4102 Seraing, Belgium
Gene Codes Corporation,
640 Avis Drive, Ann Arbor, MI 48108, USA

Gilson Medical Electronics,
BP45, F95400, Villiers-le-Bel, France.

Grant Instruments (Cambridge) Ltd,
Shepreth, Cambridge, SG8 6GB

Greiner Labs,
Maybach Strasse 2, Postfach 1162, D-7M3, Frickenhausen, Germany.

GRI Ltd,
Gene House, Queensborough Lane, Rayne, Braintree, Essex, CM77 6TZ

Harvard Apparatus Inc.,
Fircroft Way, Edenbridge, Kent, TN8 6HE

Hirschmann Laboratory,
D-72606, Nuertingen, Germany.

ILFORD Imaging UK Limited
Town Lane, Mobberley, Knutsford, Cheshire WA16 7JL

International Equipment Company,
300 Second Avenue, Needham Heights, MA 02494, USA

Invitrogen Life Technologies,
3 Fountain Drive, Inchinnan Business Park, Paisley, UK.

Kodak Scientific Imaging Systems,
LabTech International, 1 Acorn House, The Broyle, Rigmer, East Sussex, BN8 5NW

MediCell International Ltd.,
239 Liverpool Road, London, N1 1LX

Mettler-Toledo Ltd,
64 Boston Road, Beaumont Leys, Leicester, LE4 1AW

MWG-Biotech AG,
Anzinger Strasse 7, D-85560, Edersberg, Germany.

Nalgene,
Unit 1a, Thorn Business Park, Hereford, HR2 6JT

New England Biolabs, Inc. (NEB),
32 Tozer Road, Beverly, MA 01915-5599

Nikon,
Nikon House, 380 Richmond Rd, Kingston-Upon Thames, Surrey, KT2 5PR

Oncogene Research Products,
10394 Pacific Center Court, San Diego, California 92121 USA

Perbio,
Knutpunkten 34, SE-252 78 Helsingborg, Sweden

Philip Harris Scientific,
Lynn Lane, Shenstone, Lichfield, Stafford.

Promega UK,
Delta House, Chilworth Science Park, Southampton SO16 7NS

QIAGEN Ltd.
Boundary Court, Gatwick Road, Crawley, West Sussex, RH10 9AX

Roche,
F. Hoffmann-La Roche Ltd, Grenzacherstrasse 124, CH-4070 Basel, Switzerland

Sanyo Gallenkamp,
Monarch Way, Belton Park, Loughborough, LE11 5XG

Sanyo Scientific,
1062 Thorndale Avenue, Bensenville, IL 60106, USA

Scaleman,
10 Peabody Street, Bradford, MA 01835, USA

Scientific Industries,
70 Orville Drive, Bohemia, NY 11716, USA

Scotsman Ice System Ltd,
20010 Bettonlino di Pogliano, Milan, Italy.

Sigma-Aldrich Company Ltd.,
Fancy Road, Poole, Dorset, BH12 4QH

SLS Ltd.,
Wilford Industrial Estate, Nottingham, NG11 7EP

Starstedt Ltd.,
68 Boston Road, Beaumont Leys, Leicester, LE4 1AW

Stata Corporation,
702 University Drive East, College Station, TX 77840, USA

Stratagene,
11011 N. Torrey Pines Road, La Jolla, CA 92037

Stuart Scientific,
21 Holmethorpe Avenue, Redhill, Surrey, RH1 2NB

Thermo Forma Scientific,
401 Millcreek Road, PO Box 649, Marietta, OH 45750, USA

UVP Inc,
Upland, CA, USA

Volac International Ltd.,
Orwell, Royston, Herts, SG8 5QZ

VWR International Ltd.,
Merck House, Poole, Dorset, BH15 1TD

Whatmann Biometra,
Rudolf-Wissel-Strasse 30, 37079, Gottingen

Publications and Presentations Arising from this Study

Papers:

Scorah, J., Bolderson, E., Helleday, T., Smythe, C., Meuth, M. (2003). The ATM-NBS1-MRE11 pathway is essential for the homologous recombination repair mediated rescue of DNA replication forks impaired by thymidine. *Submitted for Publication.*

Poster Presentations:

Yorkshire Cancer Research Annual Scientific Meeting, 2001-2003

American Association of Cancer Research 94th Annual Scientific Meeting, 2003